



WESTINGHOUSE PROPRIETARY CLASS 3

VERIFICATION TESTING AND ANALYSES
OF THE 17 x 17 OPTIMIZED FUEL
ASSEMBLY

ORIGINAL VERSION: MARCH 1979

EDITED BY:

M. D. BEAUMONT
J. SKARITKA

APPROVED VERSION: AUGUST 1981

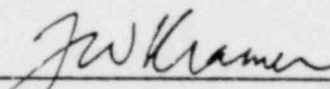
EDITED BY:

S. L. DAVIDSON
J. A. IORII

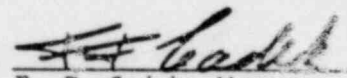
CONTRIBUTORS:

S. L. DAVIDSON
F. E. WOTLEY
Y. C. LEE
T. BOGARD
W. J. BRYAN

Approved:


F. W. Kramer, NFD
Engineering Manager

Approved:

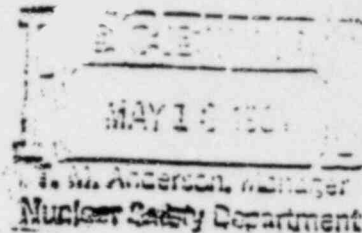

F. F. Cadek, Manager
Major Programs
NFD Fuel Projects

Approved:


T. M. Anderson, Manager
Nuclear Safety Dept.,
Nuclear Technology Division



UNITED STATES
NUCLEAR REGULATORY COMMISSION
WASHINGTON, D. C. 20555



Westinghouse Electrical Corporation
ATTN: T. A. Anderson, Manager
Nuclear Safety Department
P. O. Box 355
Pittsburgh, Pennsylvania 15230

Dear Mr. Anderson:

SUBJECT: ACCEPTANCE FOR REFERENCING TOPICAL REPORT WCAP 9401(P)/WCAP 9402(NP)

The Nuclear Regulatory Commission has completed its review of the Westinghouse Electric Corporation Licensing Topical Report Number WCAP 9401/WCAP 9402 (the nonproprietary version) entitled "Verification Testing and Analyses of the 17 x 17 Optimized Fuel Assembly". The topical report documents the results of the tests and analyses performed by Westinghouse intended to verify the design adequacy of the new Westinghouse 17 x 17 Optimized Fuel Assembly (OFA). It includes the results of hydraulic flow testing and critical heat flux (CHF) testing and analyses. In addition, the reactor vessel and core models used for seismic and loss of coolant accident analyses are described and the results of the analyses are presented. The summary of our safety evaluation is attached.

As a result of our review, we have concluded that the topical report WCAP 9401/WCAP 9402, as modified to appropriately reflect responses to staff questions, is acceptable for referencing in license applications to the extent specified and under the limitations in the topical report itself and in our safety evaluation of the topical report. In this regard, this acceptance does not constitute acceptance of a "mixed" core reload. The staff review of a mixed core reload will be performed in conjunction with our review of topical report WCAP 9272 entitled "Westinghouse Reload Safety Evaluation Methodology".

We do not intend to repeat the review of the safety features described in the topical report and found acceptable in the attachment. Our acceptance applies only to the features described in the topical report and under the conditions discussed in the attachment.

Mr. T. M. Anderson

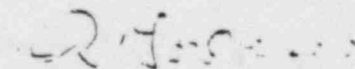
-2-

MAY 7 1967

In accordance with established procedure, it is requested that Westinghouse Electric Corporation publish an approved version of this report, incorporating the information provided in your responses to staff questions, within three months of receipt of this letter. The revision is to incorporate this letter and the attached topical report safety evaluation following the title page and thus just in front of the abstract. The report identifications of the approved reports are to have a -A suffix.

Should Nuclear Regulatory Commission criteria or regulations change such that our conclusions as to the acceptability of the report are invalidated, Westinghouse Electric Corporation and/or the applicants referencing the topical report will be expected to revise and resubmit their respective documentation or submit justification for the continued effective applicability of the topical report without revision of their respective documentation.

Sincerely,



Robert L. Tedesco, Assistant Director
for Licensing
Division of Licensing

Enclosure:
Topical Report Evaluation

cc: Mr. Bruce Lorenz
Westinghouse Electric Corporation
Nuclear Safety Department
P. O. Box 355
Pittsburgh, Pennsylvania 15230

SAFETY EVALUATION
OF THE
WESTINGHOUSE ELECTRIC CORPORATION
TOPICAL REPORT WCAP-9401

"VERIFICATION TESTING AND ANALYSIS OF THE 17 X 17
OPTIMIZED FUEL ASSEMBLY"



April, 1981

Core Performance Branch

UNITED STATES
NUCLEAR REGULATORY COMMISSION
WASHINGTON, D. C. 20585

Table of Contents

<u>Section</u>	<u>Page No.</u>
1.0 Introduction.....	1
2.0 Summary of Report and Test Procedures.....	2
2.1 Hydraulic Flow Tests.....	2
2.1.1 Assembly Lift Forces.....	2
2.1.2 Assembly Pressure Drop.....	3
2.1.3 Cladding Fretting Wear.....	4
2.2 Critical Heat Flux Tests.....	4
2.3 Seismic and LOCA Analyses.....	6
3.0 Summary of Staff Evaluation.....	7
3.1 Hydraulic Flow Tests.....	7
3.1.1 Assembly Lift Forces.....	7
3.1.2 Assembly Pressure Drop.....	8
3.1.3 Cladding Fretting Wear.....	11
3.2 Critical Heat Flux Tests.....	11
3.3 Seismic and LOCA Analyses.....	14
3.3.1 Applied Forces.....	15
3.3.2 Structural Models.....	16
3.3.3 Component Evaluations.....	18
3.3.3.1 Components Other Than Grids.....	18
3.3.3.2 Grids.....	19
4.0 Regulatory Position.....	20
5.0 References.....	22

1.0 Introduction

When Westinghouse proposed the 17 x 17 optimized fuel assembly (OFA) design, the licensing topical report wCAP-9401, "Verification Testing and Analyses of the 17 x 17 Optimized Fuel Assembly" (Ref. 1), was submitted in support of the design. The report documents the results of (a) full-sized assembly hydraulic flow tests that provided information on fuel assembly lift forces, fuel assembly pressure drop, and cladding fretting wear, (b) critical heat flux tests of electrically heated fuel rod simulator bundles, and (c) seismic and LOCA mechanical response analyses on Westinghouse 4-loop plants that included static and dynamic structural testing of the OFA.

2.0 Summary of Report and Test Procedures

The report describes the verification testing performed on the Westinghouse 17 x 17 OFA and the interpretation of the test results. The 17 x 17 OFA is comprised of 8 grids, 264 fuel rods, 24 thimbles, and 1 instrumentation tube. The thimble and instrumentation tubes, cladding, and 6 inner grids are made from Zircaloy-4, while the top and bottom nozzles and end grids are made from Inconel. The Zircaloy grids contain mixing vanes and each grid is constructed of thicker and taller grid straps compared with the Inconel design. The outside diameters (ODs) of the OFA cladding and the thimble tubes are, respectively, slightly smaller than those of the standard 17 x 17 design.

The fuel rods in the OFA test assemblies were filled with depleted UO_2 fuel pellets, prepressurized with helium, and positioned off the bottom nozzle. During the flow tests, thimble plugging devices restricted bypass flow.

2.1 Hydraulic Flow Tests

Full-scale hydraulic flow tests were performed in the Fuel Assembly Test System (FATS) facility. The FATS facility is capable of testing two full-sized fuel assemblies side-by-side. The flow tests were conducted in three different phases. These phases were:

- Phase 1: A standard 17 x 17 fuel assembly adjacent to a 17 x 17 OFA.
- Phase 2: Two 17 x 17 OFAs side-by-side.
- Phase 3: Same as Phase 1 but included a 1000-hour wear test.

2.1.1 Assembly Lift Forces

Fuel assembly lift force measurements were made using four load cells. The load cells were mounted through the lower core plate (two cells per assembly) and the lift forces were measured by recording the off loading of the load cells.

The load cells were calibrated before the baffle was assembled and during the loading of fuel assemblies. Calibrations were also performed at all test temperatures. As flow was increased, the lift forces were measured as a function of flow rate.

2.1.2 Assembly Pressure Drop

Static pressure taps were located on the baffle enclosure within the test vessel and used to measure the fuel assembly pressure drops. The overall fuel assembly ΔP s were measured by ΔP transducers having an accuracy of $\pm 0.5\%$ and a minimum frequency response of 50 Hz.

Pressure drop data were obtained by first achieving the desired loop temperature, stopping flow, zeroing the pressure transducers, and restarting flow. Once the flow stabilized, ΔP data were taken.

Based on the data, Westinghouse concluded that the difference in pressure drop between the optimized fuel assembly and the standard fuel assembly was shown to be negligible.

2.1.3 Cladding Fretting Wear

One purpose of the verification testing for the OFA was to assess the susceptibility to fretting wear at grid-to-cladding contact points.

Following Phase 1 and 2 testing, all fuel rods were inspected at each grid location and no wear was observed.

The OFA assembly that was used in the 1000-hour Phase 3 test employed two modifications: (a) some fuel rods were preoxidized and (b) three outer rows of grid cells were initially sized to conservatively represent EOL spacing. After completing the test, 131 fuel rods from the OFA assembly were inspected for wear at each grid location. The average wear depth, at a 95% confidence and 95% probability level, were determined for both the unoxidized and preoxidized fuel rods. From the pre-oxidized 95/95 wear depth, a conservative extrapolation was made to determine the magnitude of wear depth corresponding to EOL.

2.2 Critical Heat Flux Tests

The purpose of Section 2.0 of WCAP-9401 is to show that the thermal-hydraulic characteristics of the 17 x 17 OFA are

not significantly different from those of the standard 17 x 17 design. In this section of the report CHF data are reported and analyzed.

The CHF tests were run in the high-pressure loop at the Chemical Engineering Laboratory of Columbia University. The test sections were composed of 25 rods which were 14 feet long arranged in a 5 x 5 square array. Two series of tests were run. In the first series all the rods were heated. This simulated a region in the fuel assembly where there would be all fuel rods. The second series left the center rod of the bundle unheated. This represented a region in the fuel assembly where an instrument tube would be located.

The axial heat flux had a cosine shape with the peak in the center. Data were obtained using thermocouples located at various distances along the heated length.

It was concluded that:

1. The CHF characteristics of the 17 x 17 OFA can be described by the "R" grid form of the WRB-1 CHF correlation.
2. The new data can be incorporated into the "R" grid data base without changing the Departure from Nucleate Boiling Ratio (DNBR) design criterion of 1.17.

2.3 Seismic and LOCA Analyses

The general scope of a structural analysis is to define the applied forces, develop a mathematical representation of the physical structure (model), and obtain the response of the structure to the applied forces. The structural responses obtained are either used as input to a substructure analysis or compared to accepted limiting values. Analysis highlights of each component of this analysis procedure are presented in subsequent paragraphs.

The applied forces described in the submittal are for the postulated combined-seismic-LOCA transient event. These forces include the effects of seismic ground motion, internal thermal-hydraulic depressurization, and cavity pressurization. The loading conditions chosen are indicated to be generically applicable and bounding for a number of Westinghouse 17 x 17 twelve-foot fuel assembly plants.

Essentially four mathematical models are discussed in the submittal. A SYSTEMS MODEL is described, which is used to develop input for a DETAILED CORE MODEL. The response of this core model is then used as input to a LATERAL FUEL ASSEMBLY MODEL from which component stresses are determined. An AXIAL FUEL ASSEMBLY MODEL is also described. This axial model is used to determine component stresses based on the fuel assembly

response from a referenced vertical systems internals model.

The described systems model, when used to obtain the structural responses to seismic disturbances, introduces modeling concepts to represent the fluid environment existing within the reactor vessel. This modeling includes both a horizontal and vertical implementation. The horizontal modeling uses established modeling procedures while the vertical model is based upon a novel approach. These modeling techniques are not used when determining the structural response to LOCA excitations.

The responses derived from the vertical and lateral fuel assembly models are compared with accepted limiting values. The limit values chosen are based on NRC acceptance criteria in Reference 2.

3.0 Summary of Staff Evaluation

3.1 Hydraulic Flow Tests

3.1.1 Assembly Lift Forces

The lift force data presented in Figure -6 of WCAP-9401 show good agreement between the load cell measurements and the lift forces calculated from measured ΔP s.

3.1.2 Assembly Pressure Drop

Westinghouse conclusion: The difference in pressure drop between the optimized fuel assembly and the standard fuel assembly was shown to be negligible.

The results from Phase 1 and 2 of the pressure drop test were presented in a plot of ΔP -versus-flow rate. Westinghouse stated that the figure could provide a direct comparison of the hydraulic characteristics of the two fuel assemblies. However, a reader of WCAP-9401 could not make such a comparison based on this figure. The only comparison that can be made is one of the hydraulic characteristics of Phase 1 and 2 of the test series. The data from Phase 3 were not presented in the figure. The reason for this, as stated by Westinghouse, is that Phase 1 and 3 data were virtually identical.

The staff questioned Westinghouse on the validity of running the pressure drop tests at conditions below steady state and anticipated transient conditions. Westinghouse stated that pressure drop, ΔP , is given by:

$$\Delta P = K (\rho V^2 / 2g),$$

Where ρ is density, V is flow velocity, K is component loss coefficient, and g is the gravitational constant.

The variable K is a function of Reynolds number and a log-log plot of K-versus-Reynolds number is linear. Therefore, extrapolations to reactor operating conditions can be made with confidence. The flow rates were 10% above mechanical design flow rates and the testing is representative of flows during anticipated transients. The staff concurs that the test data that Westinghouse has can be analytically extrapolated to reactor operating conditions with a high degree of confidence.

In response to another staff question, Westinghouse provided a figure of the standard assembly and OFA side-by-side. The figure shows that the standard and OFA grid centerlines are matched up over the length of the assemblies. The grid material and length for the six middle grids are not the same for the standard and optimized design. The staff had questions concerning the compatibility of these grids. Westinghouse stated that the grids were compatible for the following reasons:

1. The height of the grid has a negligible effect on hydraulic compatibility. The major hydraulic mismatch is due to the expansion and contraction losses through the grid and not the additional frictional loss from grid height.
2. There are no elevation mismatches of grids.

3. Compatibility is justified by the negligible ΔP difference between the flow-tested OFA and standard fuel assemblies.

The staff has reviewed the flow test data and has concluded that this type of testing (standard and OFA side-by-side) is insufficient to draw the conclusion that the OFA and standard assembly are compatible. These tests did not address the effects of different grid heights and different fuel pin diameters on diversion cross flow between fuel assemblies. The compatibility of the two different types of grids should be demonstrated in a more quantified manner before operation with a mixed core can be evaluated. In Section 18.3.2 of WCAP-9500 (Ref. 4), Westinghouse indicated the possibility of flow tests to verify the hydraulic compatibility of the two types of assemblies. They also stated that for a mixed core reload, the methodology described in WCAP-9272, "Westinghouse Reload Safety Evaluation Methodology," (Ref. 16) will be used to perform the reload safety analysis. Based on the commitment to address our concerns on mixed assembly compatibility in WCAP-9272, our review of a mixed core reload will be in conjunction with our review of WCAP-9272.

3.1.3 Cladding Fretting Wear

The testing and subsequent analyses of cladding wear anticipated in the OFA design are consistent with those previously performed (Ref. 3) for the standard 17 x 17 fuel assembly design. The EOL wear depth has been predicted conservatively and this value is less than the design wear depth as described in a Westinghouse response to a staff question on WCAP-9500 (Ref. 4). We believe that there is no operating experience from Westinghouse-NSSS plants that would indicate a fuel failure problem arising from cladding fretting wear. Therefore, we find the cladding fretting wear analysis to be acceptable.

3.2 Critical Heat Flux Tests

Westinghouse conclusion: The CHF characteristics of the 17 x 17 OFA can be described by the "R" grid form of the WRB-1 CHF correlation.

The results from the CHF testing were presented in the form of tables containing the run number, inlet pressure, temperature, velocity, the local quality and heat flux (predicted and measured), the ratio of the measured-to-predicted CHF for the optimized fuel assembly, $(M/P)_{opt}$, the predicted and measured

elevation from the inlet where CHF occurs, the original 17 x 17 matching run number, the $(M/P)_{org}$, and the repeatability parameter. Also, there were plots of the repeatability parameter-versus-inlet pressure, flow, and local quality. Each of these presentations were given for both a typical and thimble subchannel. The repeatability parameter is defined as:

$$S_R = 1 - [(M/P)_{opt} / (M/P)_{org}] = [(M/P)_{org} - (M/P)_{opt}] / (M/P)_{org}.$$

The values of $(\frac{M}{P})_{opt}$ and $(\frac{M}{P})_{org}$ are taken from tests run at the same flow conditions. Westinghouse stated that the use of the repeatability parameter to compare data effectively eliminates correlation uncertainties. The uncertainties that remain are due to errors in the loop operating condition measurements and genuine differences between the two test sections. The staff has reviewed this type of analysis and concluded that it is acceptable for estimating DNV test repeatability.

Based on the results of the CHF tests, the staff concluded that the WRB-1 CHF correlation in its present form is an acceptable means of predicting CHF in the OFA.

Westinghouse conclusion: The new data can be incorporated into the "R" grid data base without changing the DNBR design criterion of 1.17.

In order for the above statement to be true, it must be shown that the OFA belongs to the population which is used to determine the limit or that 1.17 is a conservative limit relative to any limit based on OFA data.

Westinghouse has performed F-tests and an analysis of means to show that the OFA data belong to the total population. Of the five F-tests performed, the OFA passed three. For the two F-tests that the OFA failed, Westinghouse determined the DNBR limit using only the bad or rejected OFA data. It was shown that a DNBR limit of 1.17 would be conservative when applied to the rejected data. The analysis of means showed that the data (standard, thimble, and typical OFA) were within the limits on the means.

In determining the DNBR limit for the OFA, Westinghouse used the variance within the test series about the mean (σ^2). For the data presented in WCAP-9401, there are three variances; the variance within the test series about the mean, the variance among the test series means, and the total variance. These variances are related to each other by the following equation (Ref. 14):

$$\sigma_{\text{total}}^2 = \sigma_w^2 + \sigma_A^2,$$

where σ_w^2 is the variance within the test series about the mean, σ_A^2 is the variance among test series means, and σ_{total}^2 is the total variance.

The total variance (σ_{total}^2) should be used to determine the DNBR limit and not the variance within the test series about the mean (σ_w^2). The staff has computed the DNBR limit using the total variance. The DNBR limit calculated by the staff was 1.1685 while the DNBR limit reported in WCAP-9401 was 1.165. Therefore, the staff concludes that the DNBR limit of 1.17 is acceptable.

3.3 Seismic and LOCA Analyses

The technical evaluation contained in this section considers the effects of seismic and LOCA combined loading. The Westinghouse analysis procedure including analytical models, computer methods, and acceptance criteria have been evaluated. The evaluation was accomplished by reviewing the Westinghouse submittal and using independent audit calculations. In general, the Westinghouse assessment of the seismic-LOCA loads problem is acceptable. Detailed evaluations of each phase of the structural analysis procedure are presented in subsequent paragraphs.

3.3.1 Applied Forces

The loading conditions assumed in the submittal for determining applied forces are not well defined. Although additional loading condition definition was supplied in response to requests for additional information (Refs. 6 and 7), significant expansion of the information supplied would be necessary to justify this applicability to all Westinghouse-NSSS plants. Our conclusions concerning the results presented in WCAP-9401 therefore apply only to these loading conditions.

Insufficient information was supplied to justify an in-depth review of the internal hydraulic or cavity pressure load development; however, a previous 4-loop Westinghouse plant audit (Ref. 5) indicated that the Westinghouse approach used for developing these applied loads is acceptable. The additional data (supplied in References 6 and 7) for several parametric studies in the submittal indicated that little change in fuel system response is likely to occur for the parameters varied.

The applied loads, although not found applicable to all cases, provide useful cases that may be used for comparison in some plant-specific reviews. In certain cases, a comparison of plant specific applied loads to those in the present submittal in conjunction with the parametric study results will constitute a basis for plant-specific fuel system acceptability.

3.3.2 Structural Models

The four mathematical models presented in the submittal were reviewed. The review encompassed methods, structural representations, and analytical-experimental correlations associated with the models. Each of the four model reviews is discussed in the subsequent paragraphs.

The system model was reviewed without the aid of audit calculations. The detail associated with the model was noted and was judged to be sufficient to determine core plate motions. This judgment was based on the audit calculations and comparisons presented in Reference 5. Although the WECAN computer code used in the systems analysis was not directly audited, the code has been benchmarked against hand calculations and problems in the open literature and is presently under review by the NRC staff and projected to have a favorable safety evaluation.

Two new modeling concepts associated with the systems model were reviewed. Based on the responses (Refs. 5, 6, and 7) designed to clarify various aspects of the vertical and lateral fluid models, the methods used to incorporate this effect are considered acceptable for seismic analyses. This determination was supported by the experimental-analytical correlations supplied.

The remaining three analytical models are essentially the same as those presented in WCAP-8236 (Ref. 8). The methods and models in Reference 8 are considered acceptable to the NRC staff based on a previous review. However, because of the basic design changes documented in the submittal, additional experimental-analytical correlations were requested and supplied in References 3, 6, and 7. Based on this experimental verification (and previous acceptance by the NRC of Reference 8), the structural representations are considered acceptable.

The computer code WEGAP used to determine the core region response is not the code previously accepted by the NRC. The solution of a standard problem was, therefore, required before accepting this calculational procedure. The identical standard problem originally accepted for the previous code verification was solved and transmitted in Reference 9. A comparison of the results in Reference 9 with those in References 10 and 11 demonstrates the applicability of the WEGAP code for solving this type of problem. In conclusion, the WEGAP computer code is acceptable for determining core region model response.

3.3.3 Component Evaluations

The basic criteria for acceptability for the postulated seismic-LOCA condition is to provide assurance that the reactor can be brought safely to a cold shutdown condition (see Appendix E of Reference 2). To demonstrate acceptability, the following six components were evaluated:

1. Fuel rods.
2. Guide thimbles.
3. End boxes.
4. Inserts.
5. Sleeves.
6. Spacer grids.

These component evaluations are discussed in subsequent paragraphs.

3.3.3.1 Components Other Than Grids

Fuel assembly components (other than grids) are evaluated based on the stress criteria outlined in Reference 4. These criteria are consistent with the NRC guidelines presented in Reference 2. The material properties used in the evaluation are taken from Reference 12. Lateral analysis stresses are obtained using the maximum fuel assembly deflection based on the physical deflection limits imposed by the core region baffle. The axial stresses are

obtained by matching vertical (LOCA) system model nozzle impact loads to drop analysis results on the axial fuel assembly model.

A combination of seismic and LOCA fuel assembly component stresses was not performed. The stresses due to vertical excitation are almost totally LOCA while the lateral stresses are deflection limited for both the seismic and LOCA conditions.

These fuel assembly component stresses are considerably below the allowable limit values. Therefore, these fuel assembly components are considered acceptable for the defined loading conditions.

3.3.3.2 Grids

Fuel assembly spacer grid evaluations are based on the limiting value of crushing load P_{crit} as defined in Reference 2. The development of the value of P_{crit} was not discussed in the original submittals; however, this information is presented in Reference 7. This information has been reviewed in conjunction with Reference 2 and is considered acceptable.

Response grid loads were not combined in an appropriate fashion in the original WCAP-9401 report. However, in response to our questions (Reference 7), seismic and LOCA response loads are combined using the SRSS method with a 1.3 factor for steam flashing applied to the LOCA loads. No sensitivity adjustment is considered necessary based on the parametric study results documented in Reference 7 and previous sensitivity studies.

The combined-factored spacer grid response loads are below the limiting value of P_{crit} . Therefore, the spacer grid design is considered acceptable for the defined loading conditions.

4.0 Regulatory Position

We have reviewed WCAP-9401 and additional supporting material (Refs. 4, 6, 7, 9, 10, 13, and 15). As a result of our review, we conclude the following:

1. The WRB-1 CHF correlation is an acceptable correlation for use in the thermal-hydraulic analysis of the OFA.

2. The DNBR limit of 1.17 is an acceptable thermal margin limit for the OFA.
3. The analyses of assembly lift forces and cladding fretting wear for the OFA design are acceptable.
4. Reasonable evidence demonstrated that the OFA design can withstand the effects of the defined seismic-LOCA event for the cases studied. A determination will be required on a plant-by-plant basis to show that the applied forces fall within the envelope of these cases; otherwise, additional analyses will be required.
5. Before the staff can approve a mixed core reload, Westinghouse must provide additional submittals which demonstrate in a more quantified manner the effects on diversion crossflow of the different grid heights and different fuel pin diameters and the consequential effects on DNB. Also, the review of a mixed core reload will be in conjunction with the review of WCAP-9272.

Therefore, the staff finds WCAP-9401 an acceptable and referential report with the exception noted above.

5.0 References

1. "Verification Testing and Analyses of the 17 x 17 Optimized Fuel Assembly," Westinghouse report WCAP-9401 (non-proprietary version WCAP-9402), dated March 1, 1979, attached to letter from T. M. Anderson (Westinghouse) to J. F. Stoliz (USNRC), NS-TMA-2057, dated March 30, 1979.
2. S. B. Hosford, et al., "Asymmetric Blowdown Loads on PWR Systems," USNRC report NUREG-0609, dated January 1981.
3. "Hydraulic Flow Test of the 17 x 17 Fuel Assembly," Westinghouse report WCAP-8278, dated February 1974.
4. "Reference Core Report 17 x 17 Optimized Fuel Assembly." Westinghouse report WCAP-9500, dated July 1979.
5. R. W. Macek (EG&G), "Nonlinear LOCA Dynamic Analysis of the Indian Point Unit 3 Primary Coolant System," RE-A-77-106, Rev. 1, dated May 1978.
6. T. M. Anderson (Westinghouse) letter to J. R. Miller (USNRC), NS-TMA-2293, "Verification Testing and Analysis of the Westinghouse 17 x 17 Optimized Fuel Assembly-WCAP-9401 (Response to Partial Question Set 1)," dated August 22, 1980.
7. T. M. Anderson (Westinghouse) letter to J. R. Miller (USNRC), NS-TMA-2384, "Response to Request Number 3 for Additional Information on WCAP-9401, (NRC letter from R. L. Tedesco to T. M. Anderson, dated January 22, 1981)," dated February 13, 1981.
8. L. Gasinski, et al., "Safety Analysis of the 17 x 17 Fuel Assembly for Combined Seismic and Loss-of-Coolant Accident," Westinghouse report WCAP-8236 (including WCAP-8236 Addendum No. 1. Additional Question Response Set 1 and Additional Question Response Set 2)," dated December 1973.
9. T. M. Anderson (Westinghouse) letter to J. R. Miller (USNRC), NS-TMA-2310, "Verification Testing and Analysis of the Westinghouse 17 x 17 Optimized Fuel Assembly," (WEGAP Standard Problem Solution)," dated September 17, 1980.
10. T. M. Anderson (Westinghouse) letter to D. F. Ross Jr. (USNRC), "WEGAP Standard Problem Solution," NS-TMA-1772, dated May 1, 1978.
11. J. A. Dearien (EG&G) letters to R. E. Tiller (DOE), "Fuel Assembly Mechanical Response Standard Problem," JAD-57-78 and JAD-80-78, dated March 16 and April 21, 1978.
12. M. D. Beaumont and J. A. Iorii, "Properties of Fuel and Core Component Material," Westinghouse report WCAP-9179, Rev. 1, dated July 1978.

ABSTRACT

This report documents the results of the tests and analyses performed by Westinghouse to verify the design adequacy of the new Westinghouse 17x17 Optimized Fuel Assembly (OFA). It includes the results of hydraulic flow testing and critical heat flux (CHF) testing and analyses. In addition, the reactor vessel and core models used for seismic and loss of coolant accident analyses are described, and the results of the analyses are presented.

Full-scale hydraulic flow tests were performed for two side-by-side 17x17 OFAs as well as a current standard Westinghouse 17x17 fuel assembly adjacent to a 17x17 OFA. The test results showed a negligible difference in fuel assembly pressure drop, when comparing an OFA and a standard assembly. Clad fretting wear results for the OFA fuel rod were found to be acceptable when extrapolated to end-of-life reactor conditions.

Critical heat flux tests were conducted with electrically heated rod bundle sections which model the OFA. Analysis of the data shows no substantial difference in CHF between the OFA and the current standard 17x17 fuel assembly design.

The seismic and loss of coolant accident analyses were performed encompassing a number of Westinghouse four loop, twelve foot plants. Static and dynamic structural test results of an OFA compared with analytical predictions indicate that the fuel assembly lateral and axial structural behavior can be fully determined with finite element models. It was concluded that these analytical models are appropriate for investigation of fuel assembly responses under the lateral seismic, lateral blowdown and vertical blowdown accidents. Analysis of the 17x17 OFA component stresses and grid impact forces due to a postulated, faulted condition accident has indicated that the design is structurally acceptable based upon the established allowable design limits.

TABLE OF CONTENTS

<u>Section</u>	<u>Title</u>	<u>Page</u>
NRC Acceptance Letter		A-1
Safety Evaluation Report		B-1
1.0	HYDRAULIC FLOW TESTING	1-1
1.1	Introduction	1-1
1.2	Hardware Description	1-2
1.2.1	Fuel Assemblies	1-2
1.2.2	Fuel Assembly Test System (FATS) Facility	1-5
1.2.2.1	Facility Description	1-5
1.2.2.2	FATS Test Vessel and Test Assemblies	1-5
1.3	Pre-Test Preparations and Instrumentation	1-8
1.3.1	Pressure Drop Measurements	1-8
1.3.2	Fuel Assembly Lift Force Measurements	1-8
1.3.3	Preoxidized Fuel Rods and Grids	1-8
1.4	Flow Testing Plan and Results	1-11
1.4.1	Test Operations	1-11
1.4.2	Fuel Assembly Lift Forces	1-11
1.4.3	Pressure Drop	1-15
1.4.4	Fuel Rod Fretting Wear	1-15
1.4.4.1	Wear Results - Phases 1 and 2	1-15
1.4.4.2	Wear Results - Phase 3	1-17
1.5	Test Conclusions	1-19
1.5.1	Lift Forces	1-19
1.5.2	Pressure Drop	1-19
1.5.3	Wear	1-19
2.0	CRITICAL HEAT FLUX TESTING AND ANALYSES	2-1
2.1	Introduction	2-1
2.2	Test Facilities and Test Sections	2-2
2.2.1	Facilities	2-2
2.2.2	Test Sections	2-2

TABLE OF CONTENTS (Continued)

<u>Section</u>	<u>Title</u>	<u>Page</u>
2.3	Data Reduction and Analysis	2-7
2.3.1	Data Reduction	2-7
2.3.2	Data Analysis	2-7
2.4	Criterion for Design	2-16
2.5	Conclusions	2-18
2.6	References	2-19
	Letter from T. M. Anderson to J. F. Stolz, NS-TMA-2232, dated April 16, 1980	C-1
3.0	SAFETY ANALYSES OF THE EIGHT GRID 17x17 OPTIMIZED FUEL ASSEMBLY FOR SEISMIC AND LOSS OF COOLANT ACCIDENTS IN WESTINGHOUSE FOUR LOOP PLANTS	3-1
3.1	Introduction	3-1
3.2	Fuel Assembly Lateral Seismic Analysis	3-1
3.2.1	Analytical Procedure	3-3
3.2.2	Fuel Assembly Lateral Model	3-3
3.2.3	Reactor Pressure Vessel Model	3-9
	3.2.3.1 Seismic Evaluation	3-19
	3.2.3.2 Loss of Coolant Accident Evaluation	3-20
3.2.4	Reactor Core Model (Horizontal)	3-22
3.2.5	Fuel Assembly Dynamic Properties	3-25
3.2.6	Core Seismic Responses	3-31
3.2.7	Fuel Assembly Seismic Stresses	3-36
3.3	Lateral Blowdown Analysis	3-39
3.3.1	Analytical Procedure	3-39
3.3.2	Analytical Method and Modeling	3-43
3.3.3	Lateral Blowdown Analysis Results	3-43
3.4	Vertical Blowdown Analysis	3-47
3.4.1	Fuel Assembly Axial Model	3-47
3.4.2	Fuel Assembly Model Verification	3-55
	3.4.2.1 Static Deflection Analysis	3-55
	3.4.2.2 Dynamic Analysis	3-55
3.4.3	Fuel Assembly Response	3-55
3.4.4	Fuel Assembly Component Stresses	3-58

TABLE OF CONTENTS (Continued)

<u>Section</u>	<u>Title</u>	<u>Page</u>
3.5	Summary and Conclusions	3-62
3.5.1	Seismic Analysis	3-62
3.5.2	Lateral Blowdown Analysis	3-65
3.5.3	Vertical Blowdown Analysis	3-65
3.5.4	Conclusion	3-66
3.6	References	3-66
	Letter from T. M. Anderson to J. P. Miller, NS-TMA-2310, dated September 17, 1980	D-1
	Letter from R. A. Wiesemann to J. R. Miller, AW-80-58, dated September 18, 1980	E-1
	Letter from R. A. Wiesemann to J. F. Stolz, AW-78-23, dated March 21, 1978	F-1
	Appendix A, WEGAP Verification with the USNRC Sample Problems	G-1
	Letter from T. M. Anderson to J. F. Stolz, NS-TMA-2057, March 30, 1979	H-1
	Letter from T. M. Anderson to J. R. Miller, NS-TMA-2293, dated August 22, 1980	I-1
	Letter from L. S. Rubenstein to R. L. Tedesco dated June 23, 1980 (NRC Internal Letter)	J-1
	Letter from R. L. Tedesco to T. M. Anderson dated January 22, 1981	K-1
	Letter from T. M. Anderson to J. R. Miller, NS-TMA-2384, dated February 13, 1981	L-1
	Letter from R. L. Tedesco to T. M. Anderson dated February 12, 1981	M-1
	Letter from T. M. Anderson to J. R. Miller, NS-TMA-2400, dated March 2, 1981	N-1

LIST OF FIGURES

<u>Figure</u>	<u>Title</u>	<u>Page</u>
1-1	17x17 Optimized Fuel Assembly	1-3
1-2	Schematic of Fuel Assembly Test System (FATS)	1-6
1-3	FATS Test System and Baffled Assemblies	1-7
1-4	Location of Fuel Assembly Pressure Drop Measurement	1-9
1-5	Location of Preoxidized Rods	1-10
1-6	Fuel Assembly Lift Force Versus Assembly Flow at 300°F	1-14
1-7	Measured Fuel Assembly ΔP Versus Assembly Flow Rate	1-16
1-8	Wear Volume Versus Wear Depth for an OFA Fuel Rod	1-18
2-1	5x5 Rod Bundle Cross Section - Typical Cell	2-3
2-2	5x5 Rod Bundle Cross Section - Thimble Cell	2-4
2-3	Grid, Thermocouple and Pressure Tap Locations	2-5
2-4	Axial Heat Flux Distribution	2-6
2-5	Variation of Repeatability Parameter, δ_R , with Test Variables - Thimble Cell	2-14
2-6	Variation of Repeatability Parameter, δ_R , with Test Variables - Typical Cell	2-15
3-1	Plant Frequency Response Envelope at Reactor Vessel Supports	3-2
3-2	Response Spectrum at Reactor Vessel Support	3-4
3-3	Fuel Assembly Seismic Analysis Procedure	3-5
3-4	Fuel Assembly Finite Element Model	3-6
3-5	17x17 8-Grid OFA Lateral Stiffness	3-8
3-6	Typical Reactor Pressure Vessel and Internal Components	3-10
3-7a	Core Barrel Internals Model	3-11
3-7b	Reactor Core Barrel Model	3-12
3-7c	RPV Shell Model	3-13
3-7d	Vertical Hydrodynamics Model	3-14
3-8	Upper Core Plate, Lower Core Plate, and Upper Core Barrel Motions - SSE	3-23
3-9	Upper to Lower Core Plate Motions - 17x17 8-Grid OFA	3-24
3-10	Schematic Representation of Computer Model Used to Analyze Core Dynamic Response	3-28

LIST OF FIGURES

<u>Figure</u>	<u>Title</u>	<u>Page</u>
3-11	Fuel Assembly Finite Element Model	3-29
3-12	412 17x17 8-Grid OFA Normalized Vibrational Modal Shapes	3-30
3-13	Displacement Responses of Fuel Assembly No. 1 - Grid No. 5 and Grid No. 4	3-32
3-14	Displacement Responses of Fuel Assembly No. 10 - Grid No. 5 and Grid No. 4	3-33
3-15	Displacement Responses of Fuel Assembly No. 15 - Grid No. 5 and Grid No. 4	3-34
3-16	Impact Force Responses Between Fuel Assembly No. 1 and Baffle Plate - Grid No. 5 and Grid No. 4	3-35
3-17	Impact Force Responses Between Fuel Assembly No. 15 and Baffle Plate - Grid No. 5 and Grid No. 4	3-38
3-18	Core Lateral Blowdown Analysis Procedure	3-42
3-19	Upper Core Plate, Lower Core Plate and Core Barrel Motions	3-44
3-20	Schematic Representation of Computer Model Used to Analyze Core Dynamic Response	3-45
3-21	OFA Fuel Assembly No. 1 Relative Displacement Response	3-46
3-22	Grid Impact Force Responses Fuel Assembly No. 1	3-51
3-23	OFA Grid No. 4 Impact Force Responses Between Peripheral Assemblies and Baffle Plate	3-52
3-24	Fuel Assembly Finite Element Model for Axial Analysis	3-53
3-25	Fuel Assembly Axial Load Deflection Characteristics	3-56
3-26	Impact Force at Bottom Nozzle	3-60
3-27	Holddown Spring Force at Top Nozzle	3-61

LIST OF TABLES

<u>Table</u>	<u>Title</u>	<u>Page</u>
1-1	Comparison of 17x17 Optimized Test Assembly and 17x17 Standard Assembly Design Parameters	i-4
1-2	FATS Flow Test Plan - Phase 1 and Phase 2	1-12
1-3	FATS Flow Test Plan - Phase 3	1-13
2-1	Critical Heat Flux Test Results for OFA Typical Cell	2-8
2-2	Critical Heat Flux Test Results for OFA Thimble Cell	2-11
2-3	WRB-1 CHF Correlation - Statistical Results	2-17
3-1	Mechanical Constants for 17x17 8-Grid OFA Model (Full)	3-27
3-2	17x17 8-Grid OFA Seismic Analysis Results Summary	3-37
3-3	Fuel Assembly Stresses for SSE	3-40
3-4	Fuel Assembly Maximum Seismic Stresses and Limits at Reactor Operating Condition (600°F)	3-41
3-5	17x17 8-Grid OFA []+ Analysis Results	3-48 (a,c)
3-6	Fuel Assembly Stresses for []+	3-49 (a,c)
3-7	Fuel Assembly Component Stresses and Limits, LOCA	3-50
3-8	Fuel Assembly Impact Forces for Various Break Locations	3-59
3-9	Fuel Rod and Thimble Blowdown Forces and Stresses []+	3-63 (a,c)
3-10	Fuel Assembly Component Blowdown Stresses and Limits (KSI)	3-64

1.0 HYDRAULIC FLOW TESTING

1.1 INTRODUCTION

As a part of the verification tests of the Westinghouse 17x17 Optimized Fuel Assembly (OFA) design, full-scale hydraulic flow tests were performed in the Fuel Assembly Test System (FATS) facility. This facility has the capability to test two full size fuel assemblies side-by-side. Two OFAs were tested, side-by-side, to simulate reactor hydraulic conditions. Likewise an OFA and a current standard 17x17 fuel assembly were tested, side-by-side, to verify the hydraulic compatibility of the two assembly designs for use in "mixed core" designs. The fuel assembly and FAT facility descriptions are given in Section 1.2.

The flow tests were performed in the following phases:

- Phase 1 - consisted of a standard 17x17 fuel assembly adjacent to a 17x17 OFA.
- Phase 2 - consisted of two 17x17 OFAs, side-by-side.
- Phase 3 - Same as Phase 1 but also includes a 1000 hour wear test.

Section 1.2 and 1.3 describe the test set-up. The results of the pressure drop, assembly hydraulic lift force and the fuel rod fretting wear data are given in Section 1.4, and the test plant description is presented in Figure 1-1.

1.2 HARDWARE DESCRIPTION

1.2.1 FUEL ASSEMBLIES

The two 17x17 OFAs had 8 grids, 264 fuel rods, 24 thimbles and a center instrumentation tube, as shown in Figure 1-1. The fuel rod cladding, thimble and instrumentation tubes, and six inner grids were made of Zircaloy-4. The top and bottom grids were made of Inconel. The six inner Zircaloy mixing vane grids had the same basic mechanical configuration as the standard Inconel grids, but the strap dimensions (thickness and height) were increased compared to the Inconel design. The OFAs contained slightly smaller fuel rod and thimble tube diameters than the standard assembly. One OFA test assembly was not instrumented and had the 264 fuel rods filled with depleted UO_2 pellets. The instrumented OFA test assembly contained 254 fuel rods filled with depleted UO_2 and 10 empty rods to carry instrument leads.

The standard 17x17 assembly (8 Inconel grids) had the same reference dimensions as the OFA assembly shown in Figure 1-1. This assembly contained fuel rods filled with lead in order to simulate the weight of fuel rods filled with UO_2 pellets.

For all fuel assemblies tested, thimble plugging devices were used to restrict flow through the thimble tubes. All fuel rods were positioned above the bottom nozzle the same distance as used in current production fuel assemblies. Fuel rods were pressurized with He to levels currently in use. The test assemblies were hydraulically and structurally representative of assemblies fabricated for reactor use.

A comparison between the OFA and standard assembly designs is given in Table 1-1.

1.2.2 FUEL ASSEMBLY TEST SYSTEM (FATS) FACILITY

1.2.2.1 Facility Description

Figure 1-2 shows a schematic of the fuel assembly test system. Water was supplied from the storage tank, pumped into the test vessel bottom and out the vessel top, and passed through a heat exchanger to maintain the desired fluid test temperature. Flow was controlled by a pneumatically operated proportional control valve (No. 1) and continuously recirculated back through the pumps via the line bypass valve (No. 2). The loop flow rate was measured with a 10-inch Varco Venturi located on the outlet side of the test vessel. The two identical pumps are capable of delivering up to 5500 gpm when operating together. There are two heat exchanger units, a water-water (W/W) unit to control system temperature between 105-150°F, and an air-water (A/W) unit to control temperatures between 150-300°F. The filter removes particulate matter from the test water as may be required. During normal test operations the filter isolation valve (No. 3) is closed.

1.2.2.2 FATS Test Vessel and Test Assemblies

Figure 1-3 shows the placement of the test assemblies into the baffle enclosure and test vessel. Water enters the bottom of the rectangular baffle enclosure, flows up through the lower core plate simulator and test assemblies, and exits through the upper baffle enclosure and test vessel outlet pipe.

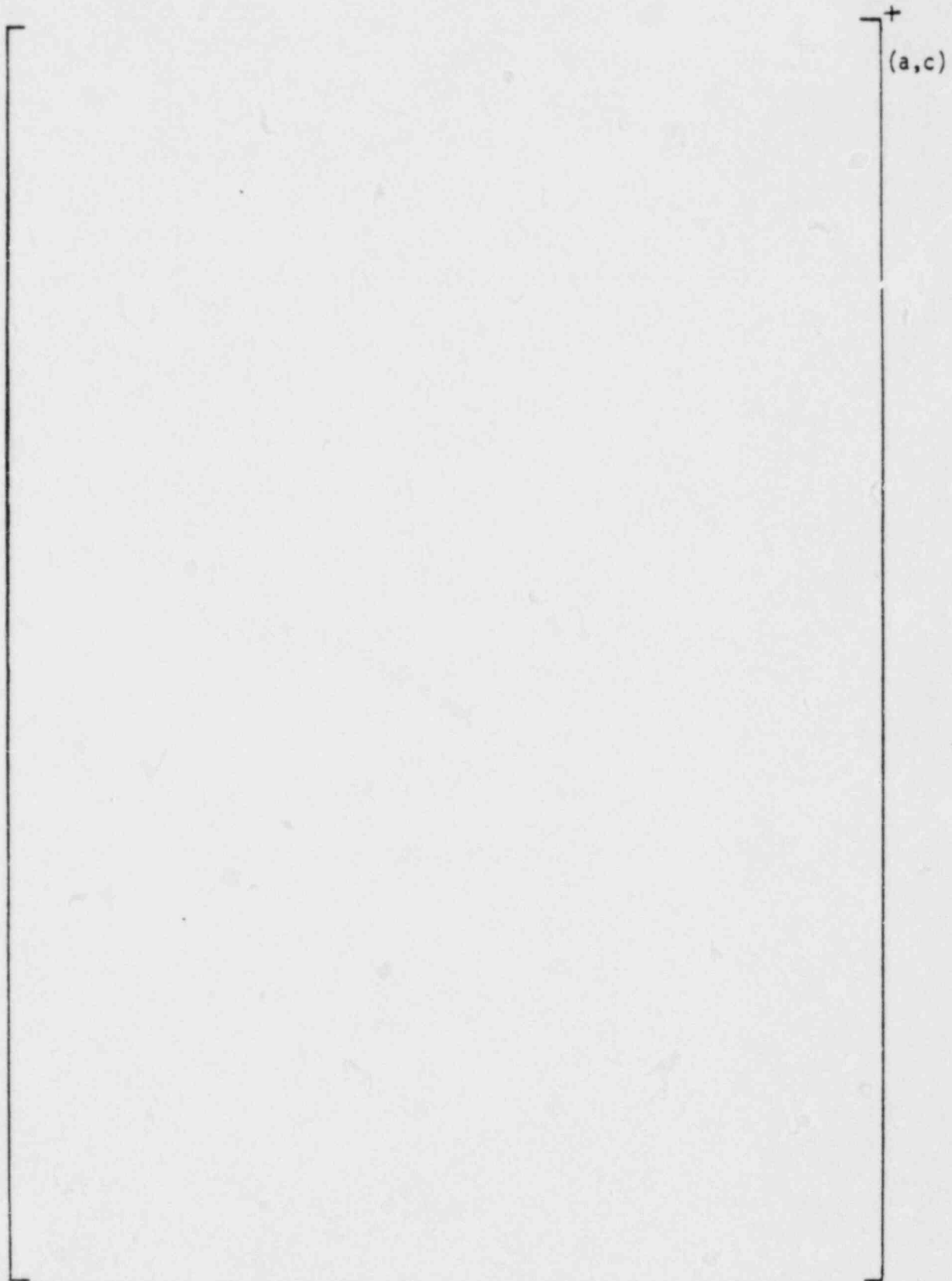


Figure 1-2 Schematic of Fuel Assembly Test System (FATS)

14.038-1 (a,c)

+

Figure 1-3. FATS Test Vessel and Baffled Assemblies

1.3 PRE-TEST PREPARATIONS AND INSTRUMENTATION

1.3.1 PRESSURE DROP MEASUREMENTS

Static pressure taps were used to measure the fuel assembly pressure drops. These were located on the baffle enclosure within the test vessel as shown on Figure 1-4. Each pressure measurement tap had a redundant tap located at the same elevation on a perpendicular baffle wall (90° apart). A data acquisition system was used to collect and condition the data, which consisted of approximately 100 ΔP readings for each set of flow and temperature conditions.

Using the pressure tap locations in Figure 1-4, ΔP transducers were used to measure the overall fuel assembly ΔP s. The ΔP transducers had an accuracy of $\pm 0.5\%$ and a minimum frequency response of 50 Hz.

1.3.2 FUEL ASSEMBLY LIFT FORCE MEASUREMENTS

Fuel assembly lift forces were measured by recording the off-loading of four load cells, (two load cells per assembly), mounted through the lower core plate. As flow was increased, the data provided the lift forces as a function of flow.

Load cells were calibrated in the lower core plate before the baffle was assembled and during the loading of the fuel assemblies into the barrel at room temperature. Calibrations were the performed at all test temperatures. The transducer test measurement capability is given in Section 1.4.1.

1.3.3 PREOXIDIZED FUEL RODS AND GRIDS

In order to determine fuel rod fretting wear, sixty-two fuel rods were preoxidized to simulate in-reactor conditions. The oxidized fuel rods were randomly located as shown in Figure 1-5. For Phases 1 and 2 the grid cells were adjusted to investigate the effect of cell size on wear.

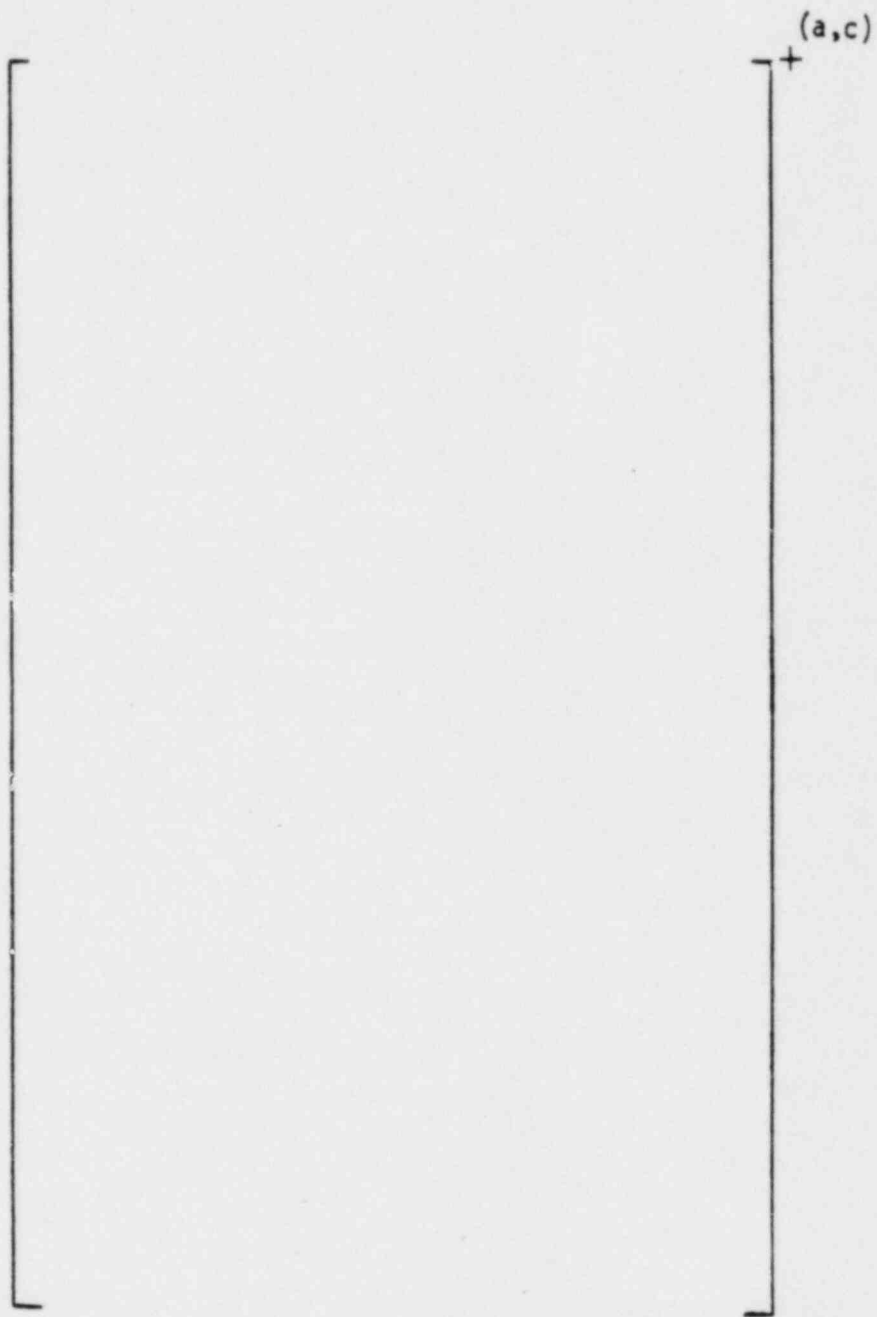


Figure 1-4 Location of Fuel Assembly Pressure Drop Measurement

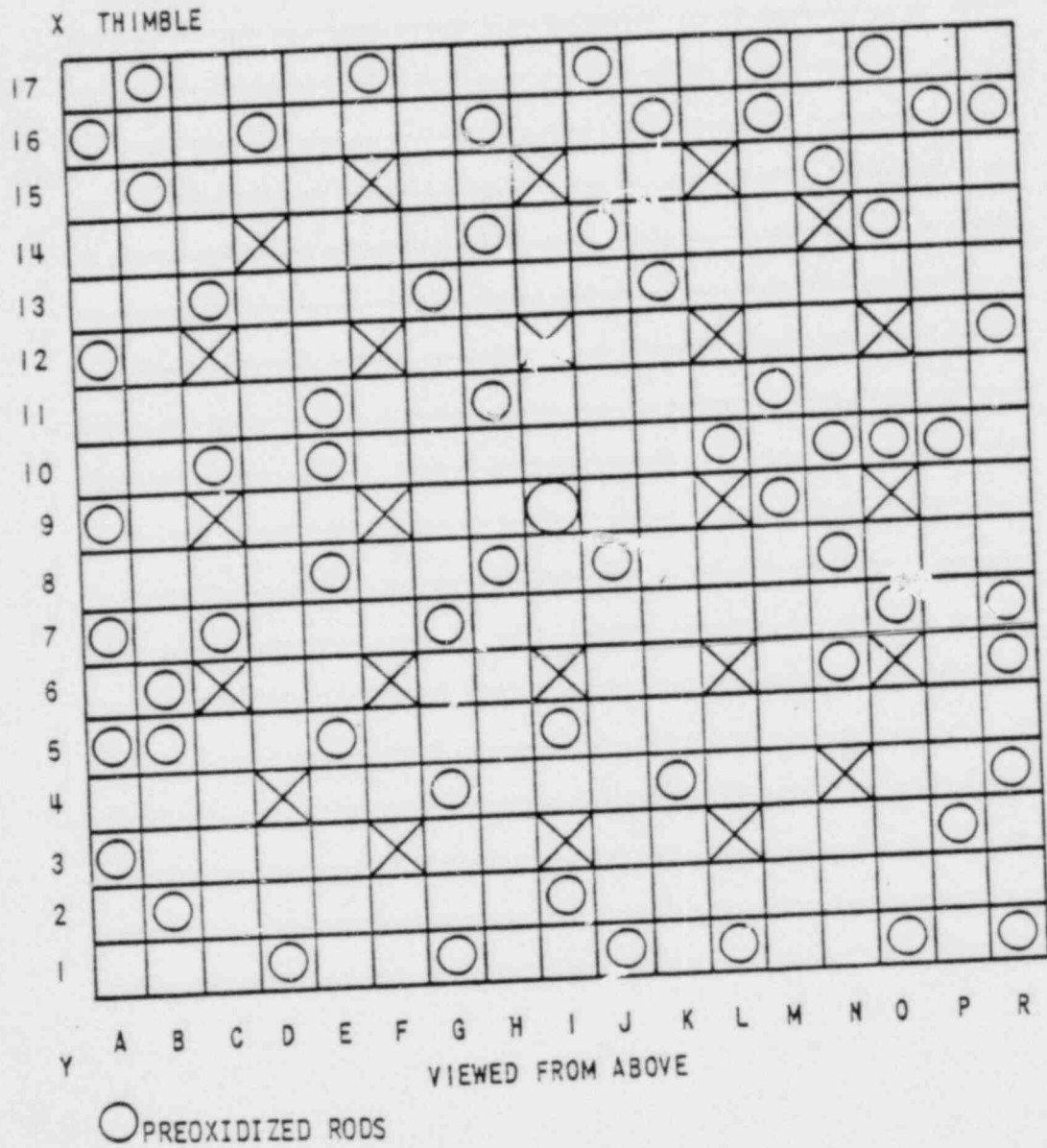


Figure 1-5. LOCATION OF PREOXIDIZED RODS

1.4 FLOW TESTING PLAN AND RESULTS

1.4.1 TEST OPERATIONS

Test operations were maintained at the conditions described in Tables 1-1 and 1-2 for Phases 1, 2 and 3. These tables specify the information sought, temperature, pressure and flow rates for each of the tests performed.

The following measurement capabilities were maintained during testing:

<u>Parameter</u>	<u>Ranges</u>	<u>Required Accuracy (%)</u>
Loop Temperature	50-300 ^o F	+ 0.25
Loop Pressure	0-200 psig	+ 2.0
Loop Flow Rate	1000-5500 gpm	+ 0.5
Nominal Fuel Rod Bundle Flow	2400 gpm	+ 0.5
All ΔP Measurements	Varies-psid	+ 0.5
Assembly Lift	0-2000 lbs	+ 0.5

1.4.2 FUEL ASSEMBLY LIFT FORCES

Lift force data were obtained during Phases 1, 2 and 3 with the test conditions given in Tables 1-1 and 1-2. Results given in Figure 1-6 show lift forces calculated from measured assembly ΔP and measured from load cells. The load cell measurements were in good agreement with the lift forces calculated from the measured assembly pressure drops. At a given flow rate the measured lift forces are slightly greater (about 10%) at 100^oF coolant temperature compared to a 300^oF coolant temperature.

TABLE 1-2

FATS FLOW TEST PLAN - PHASE 1* AND PHASE 2⁺

<u>Test Phase/ (Number of Tests)</u>	<u>Information Sought</u>	<u>Data Recorded</u>	<u>Temperature (°F)</u>	<u>Pressure (psig)</u>	<u>Flow per Assy (gpm)</u>
1(4); 2(4)	Pressure Drop determinations	ΔP (psi)	100	220	500, 700 1000, 1500
1(4); 2(4)	Same as above	Same	200	Same	Same
1(4); 2(4)	Same as above	Same	250	Same	Same
1(7); 2(7)	Same as above	Same	300	Same	500, 700 1000, 1500 2000, 2400 2570
1(4); 2(4)	Assembly lift force	Lift force (lbs)	100	220	500, 700 1000, 1500
1(4); 2(4)	Same as above	Same	200	Same	Same
1(4), 2(4)	Same as above	Same	250	Same	Same
1(7); 2(7)	Same as above	Same	300	Same	500, 700 1000, 1500 2000, 2400 2570

*Test Assemblies - Instrumented 17x17 OFA And Standard 17x17 Inconel Grid Assembly.

+Test Assemblies - Instrumented and Non-Instrumented 17x17 OFAs.

TABLE 1-3

FATS FLOW TEST PLAN - PHASE 3⁺

<u>Number of Tests</u>	<u>Information Sought</u>	<u>Data Recorded</u>	<u>Temperature (°F)</u>	<u>Pressure (psig)</u>	<u>Flow per Assy (gpm)</u>
2	Assembly lift forces	Lift force (lbs)	100	220	1000, 1500
2	Same as above	Same	200	Same	Same
2	Same as above	Same	250	Same	Same
5	Same as above	Same	300	Same	1000, 1500 2000, 2200 2400
1	Wear - 1000 hour test	-	300	220	2360*

+Test Assemblies - Instrumented 17x17 OFA And 17x17 Inconel Grid.

*Represents []⁺ of Mechanical Design Flow (MDF).

(b,c)

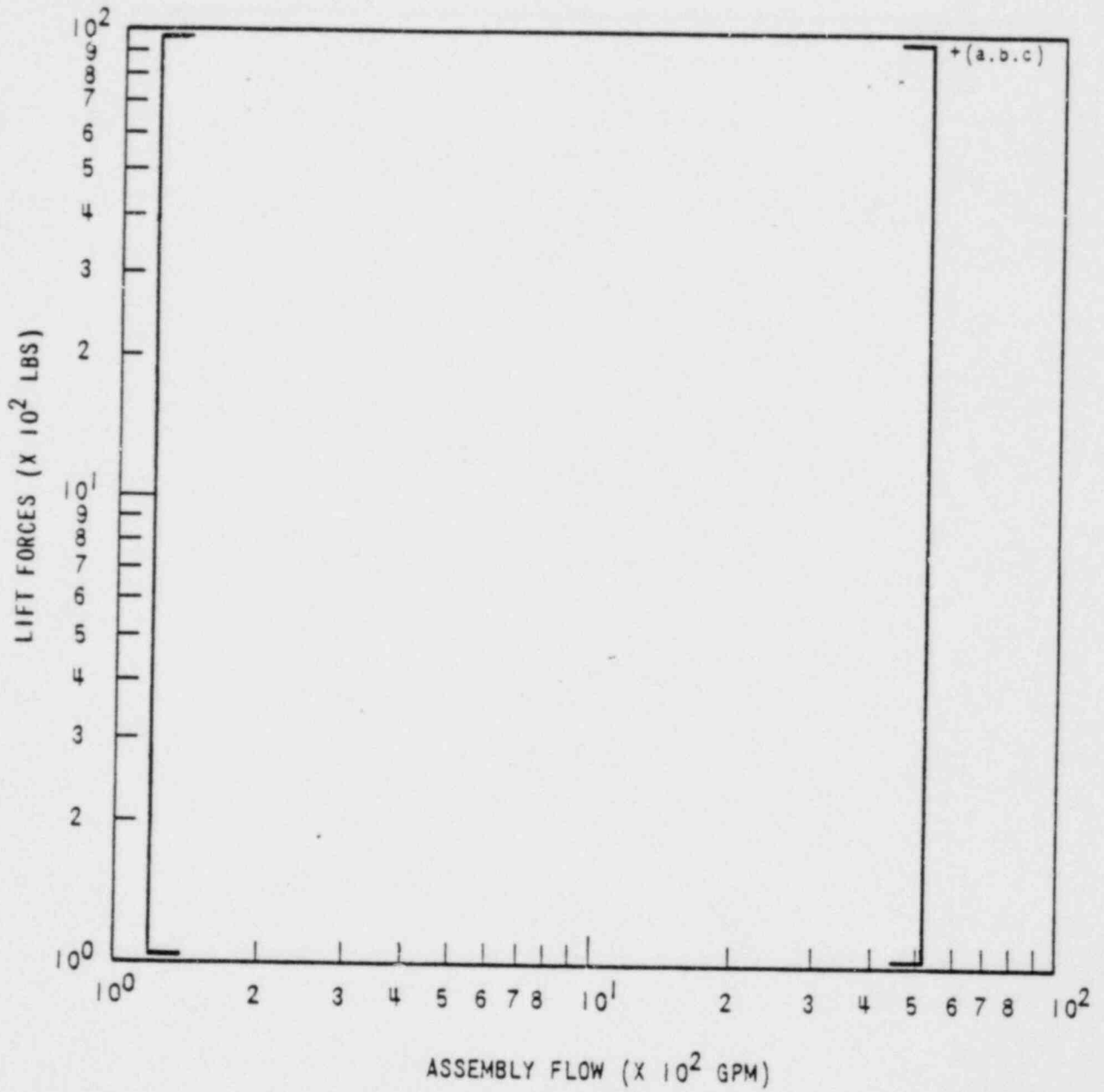


Figure 1-6. Fuel Assembly Lift Force vs Assembly Flow at 300°F

1.4.3 PRESSURE DROP

Pressure drop data were obtained from the static pressure taps shown in Figure 1-4. For a given test condition, once the desired loop temperature was achieved, the test procedure was to stop the flow, zero the pressure transducers, restart the flow, and take the data when the flow stabilized. The data consisted of approximately 100 ΔP readings for each set of flow and temperature conditions.

The fuel assembly static pressure drop measurements for both Phase 1 and Phase 2 are presented in Figure 1-7 to provide a direct comparison of the hydraulic characteristics between the two fuel assemblies. Additional data taken during Phase 3 (not shown) were virtually identical to that obtained during Phase 1.

The best fits of the two sets of data indicated [

] + To determine the significance of this (b,c)
difference, a statistical analysis was performed on the two sets of data. A treatment coefficient was calculated from a combined fit of the two sets of data. This coefficient was tested for significance at a 95% tolerance limit and it was found that the statistical difference in the pressure losses between the two phases of testing was [(a,c)

] + Therefore, the overall fuel assembly pressure drop (a,c)
[] + for both the 17x17 OFA and standard
Inconel assembly.

1.4.4 FUEL ROD FRETTING WEAR

1.4.4.1 Wear Results - Phases 1 and 2

At the completion of Phase 1 and 2 testing all fuel rods were inspected at each grid location and each support point for fretting wear. Each fuel rod was rotated 45° and removed from the fuel assembly. The rotation of the fuel rods assured that unloading scratches did not interfere with the fretting evaluation.

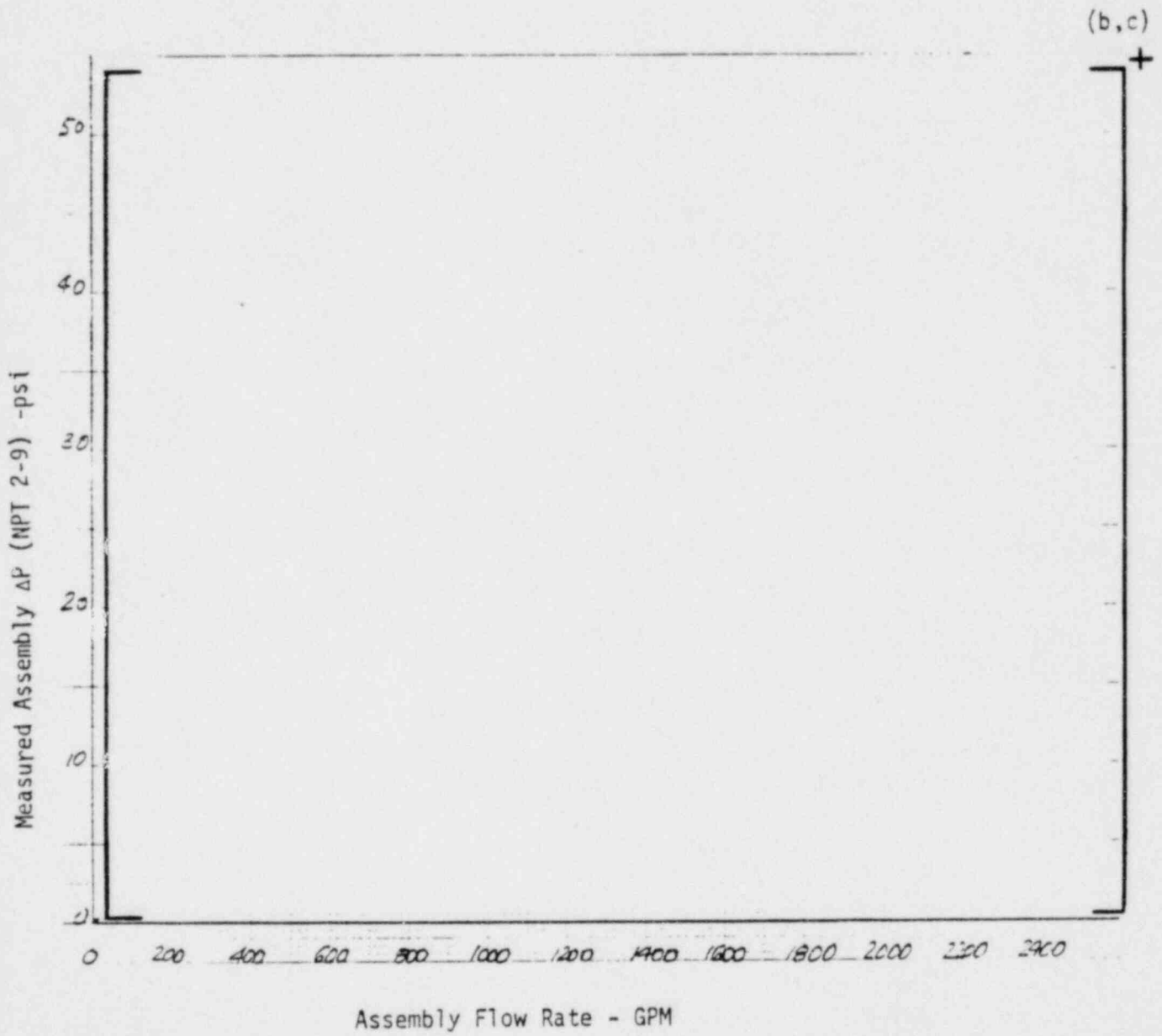


Figure 1-7 Measured Fuel Assembly Static ΔP vs. Assembly Flow Rate

During Phase 1 and 2 testing a total of 166.8 hours of running time was logged. No wear was detected by visual examination for any rods.

1.4.4.2 Wear Results - Phase 3

A new fuel assembly structure was incorporated into the 1000 hours Phase 3 test program. The outer three rows of grid cells were initially sized to conservatively represent the worst end-of-life conditions expected in reactor operation. At the completion of the 1000 hour test, 131 rods (36 preoxidized) were inspected. All eight grid locations were examined for rod fretting wear. From the data obtained, it was determined the 1000 hour average wear depth, at a 95% confidence and 95% probability level, is []⁺ uils for the preoxidized rods and []⁺ mils for the unoxidized rods. It is conservatively assumed that the wear volume at the end-of-life (EOL) in reactor operation (approximately 35,000 hours) is proportional to the wear volume obtained at 1000 hour testing for the preoxidized rods. Therefore the EOL wear volume for reactor operation is estimated to be approximately 35 times that of the 1000 hours test. Using Figure 1-8 and the []⁺ mil wear depth of the 1000 hour test preoxidized rods, the wear depth for oxidized rods at EOL (48 months of full flow) in a reactor is approximately []⁺ mils.

(a,b,c)

(a,b,c)

(a,c)

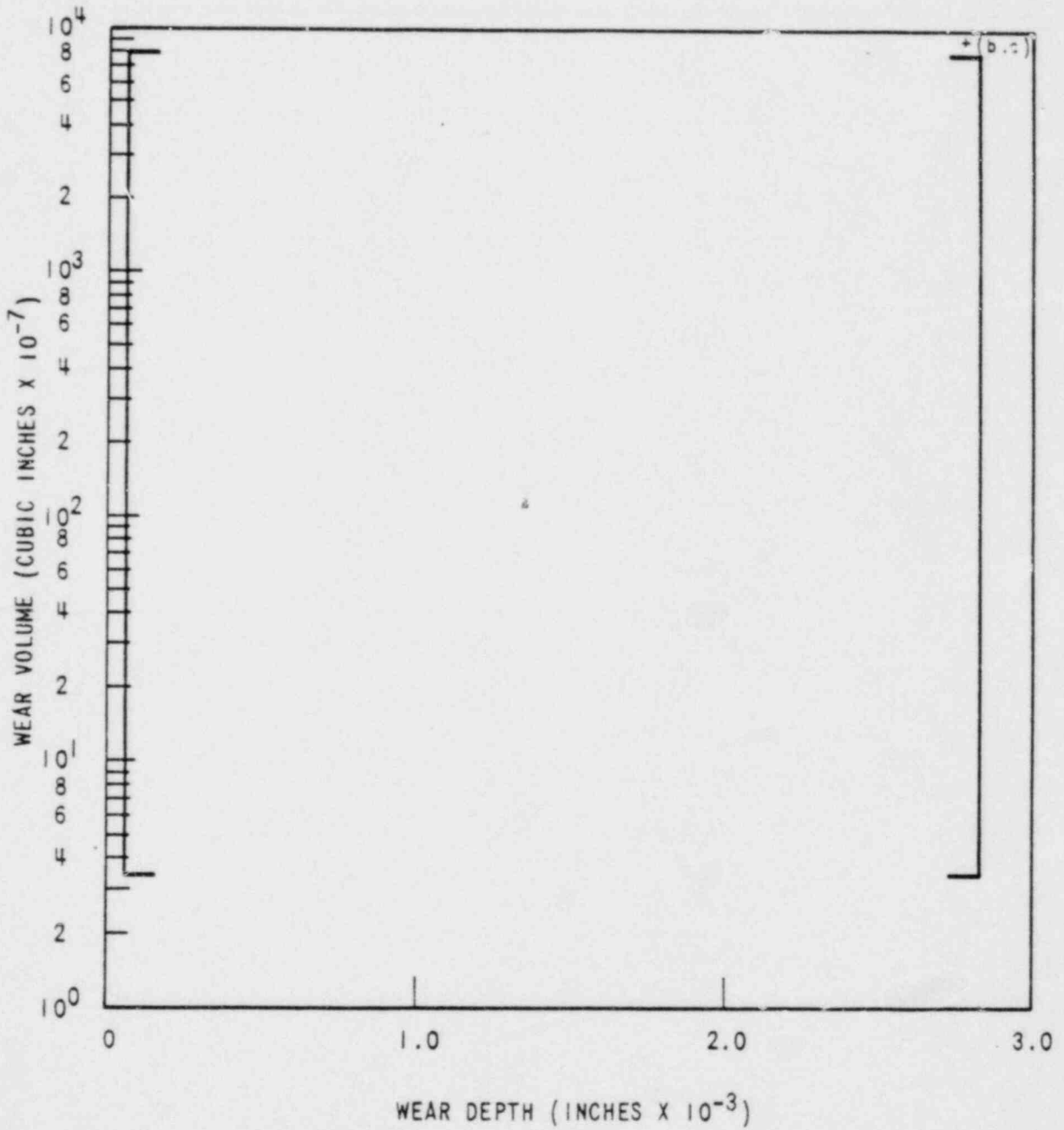


Figure 1-8 Wear Volume Versus Wear Depth for a OFA Fuel Rod

1.5 TEST CONCLUSIONS

1.5.1 LIFT FORCES

Fuel assembly lift forces determined directly from load cell measurements are consistent with lift forces calculated from pressure drop measurements.

1.5.2 PRESSURE DROP

The difference in fuel assembly pressure drop between the optimized fuel assembly and the standard (Inconel) fuel assembly was shown []⁺ (a,b,c)

1.5.3 WEAR

For the 1000 hour test, the average wear depth for the preoxidized fuel rods was []⁺ mils at a 95% confidence level. From this result, the extrapolated fuel rod clad fretting wear of []⁺ mils at end-of-life in a reactor is acceptable. (a,b,c) (a,c)

2.0 CRITICAL HEAT FLUX TESTING AND ANALYSIS

2.1 INTRODUCTION

References 1 and 2 describe the results of extensive Critical Heat Flux (CHF) tests conducted with electrically heated rod bundle test sections built to model the current Westinghouse 17x17 fuel assembly design. This chapter describes similar CHF tests which model the optimized 17x17 fuel assembly. From a CHF standpoint, the optimized 17x17 design differs from the current 17x17 design in two respects:

1. The dimensions of the type "R" mixing vane grid have been altered due to a material change.
2. The fuel rod diameter has been reduced to []⁺ inch (from (a,c)
0.374 inch).

CHF tests were conducted with two test sections -- typical cell and thimble cell - each of which was 14 feet long and was composed of 25 rods in a 5x5 square array. The center rod was unheated for the thimble cell test.

2.2 TEST FACILITIES AND TEST SECTIONS

2.2.1 FACILITIES

The test facilities and procedures have been described in detail in References 1 and 2. No significant changes were made for the optimized 17x17 fuel assembly CHF tests.

2.2.2 TEST SECTIONS

The two test sections utilized for these tests were quite similar to those described in References 1 and 2 except for the following differences.

The mixing vane grid design was modified because a new material (Zircaloy) was used which has different mechanical properties than an Inconel grid. This necessitated slight changes in various grid dimensions, but there was no significant departure from type "R" grid characteristics.

The heater rod diameter has been reduced to []⁺ inch. Figure 2-1 is a sketch of the rod bundle cross-section of the typical cell test section. Figure 2-2 shows the corresponding cross-section for the thimble cell

(a,c)

The axial positions of the grids, pressure taps and thermocouples are shown in Figure 2-3. Figure 2-4 shows the axial cosine heat flux profile used in these tests.

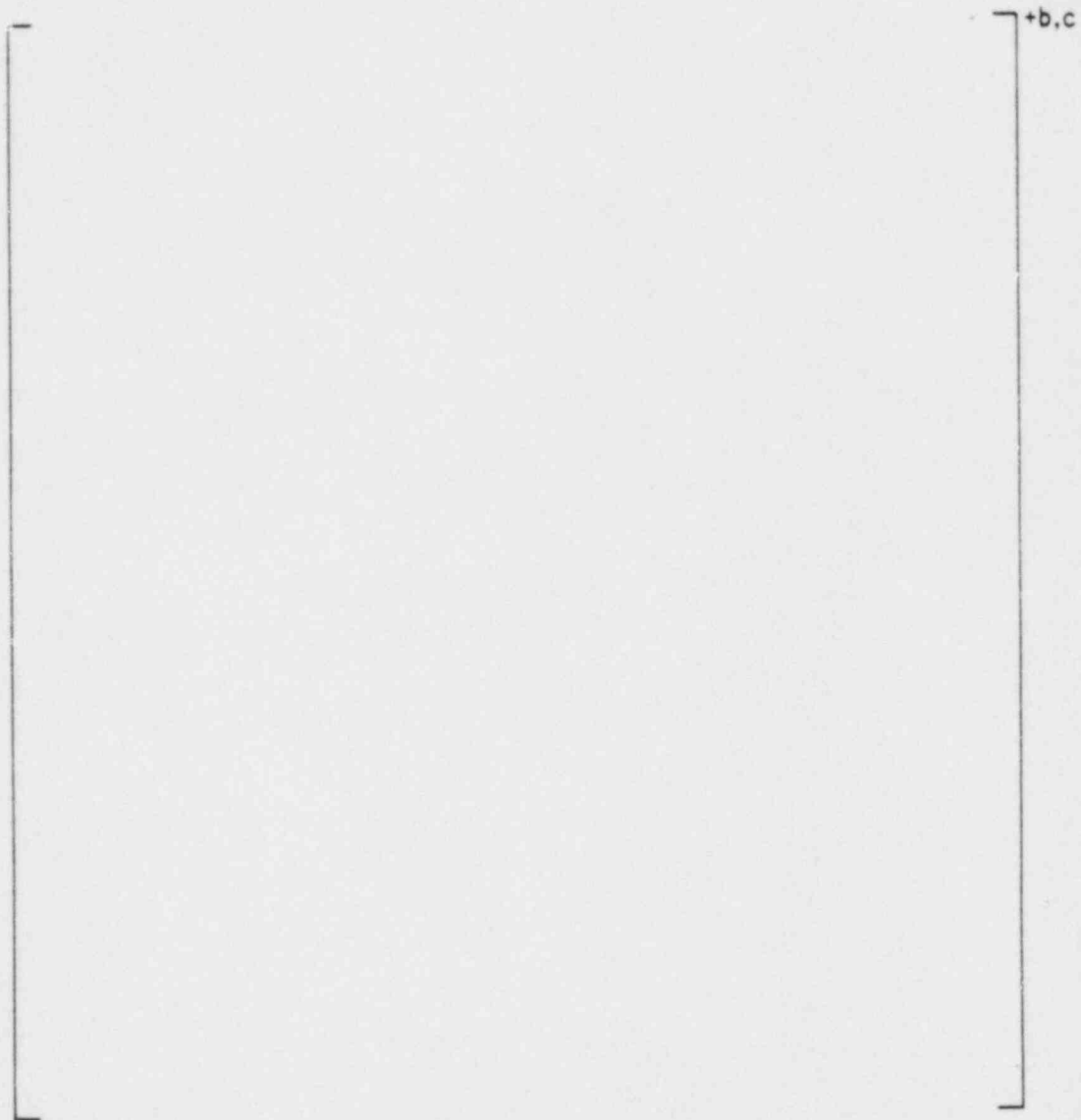


Figure 2-1. 5x5 Rod Bundle Cross Section Typical Cell

13.987-4

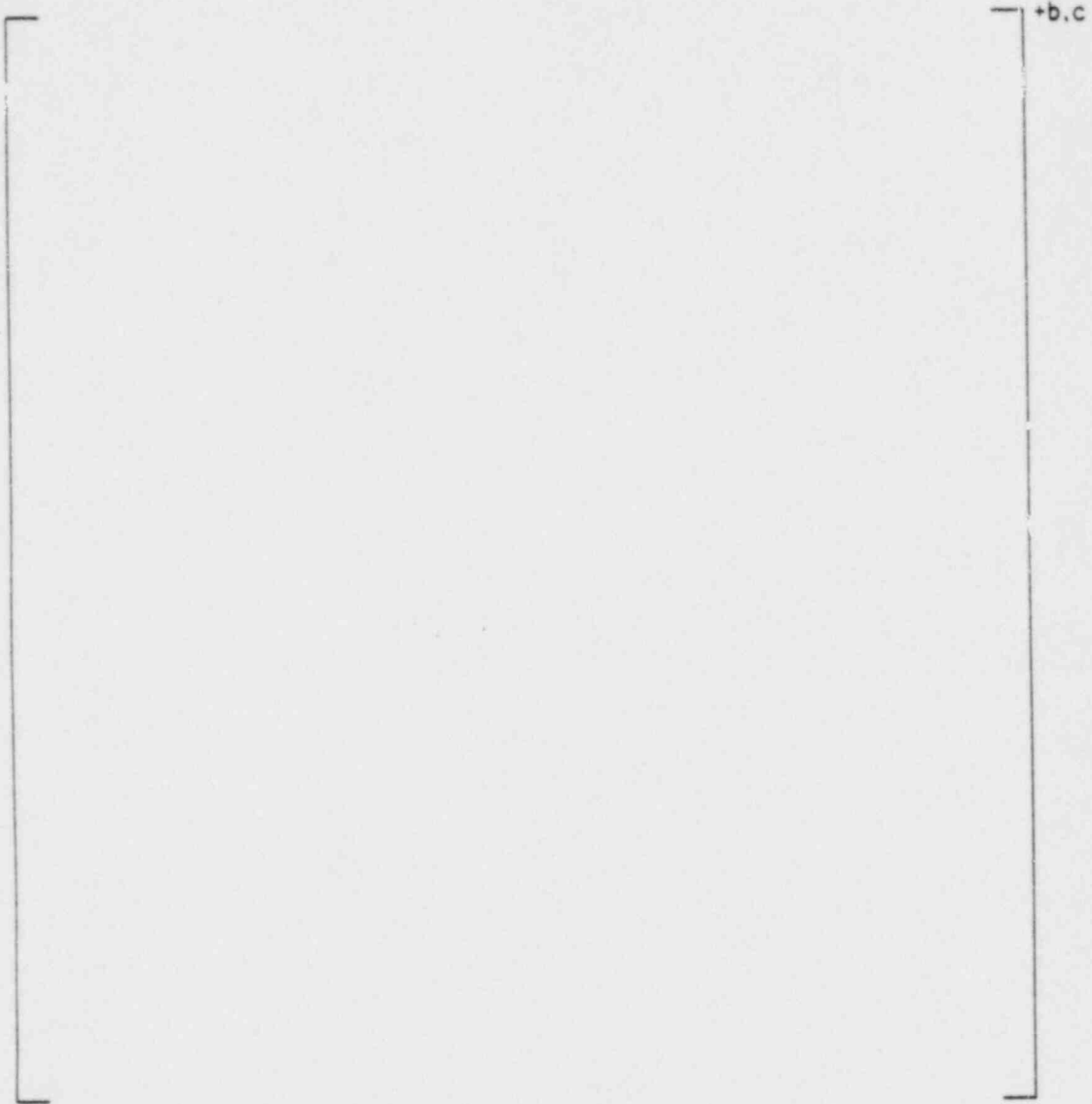


Figure 2-2. 5x5 Rod Bundle Cross Section Thimble Cell

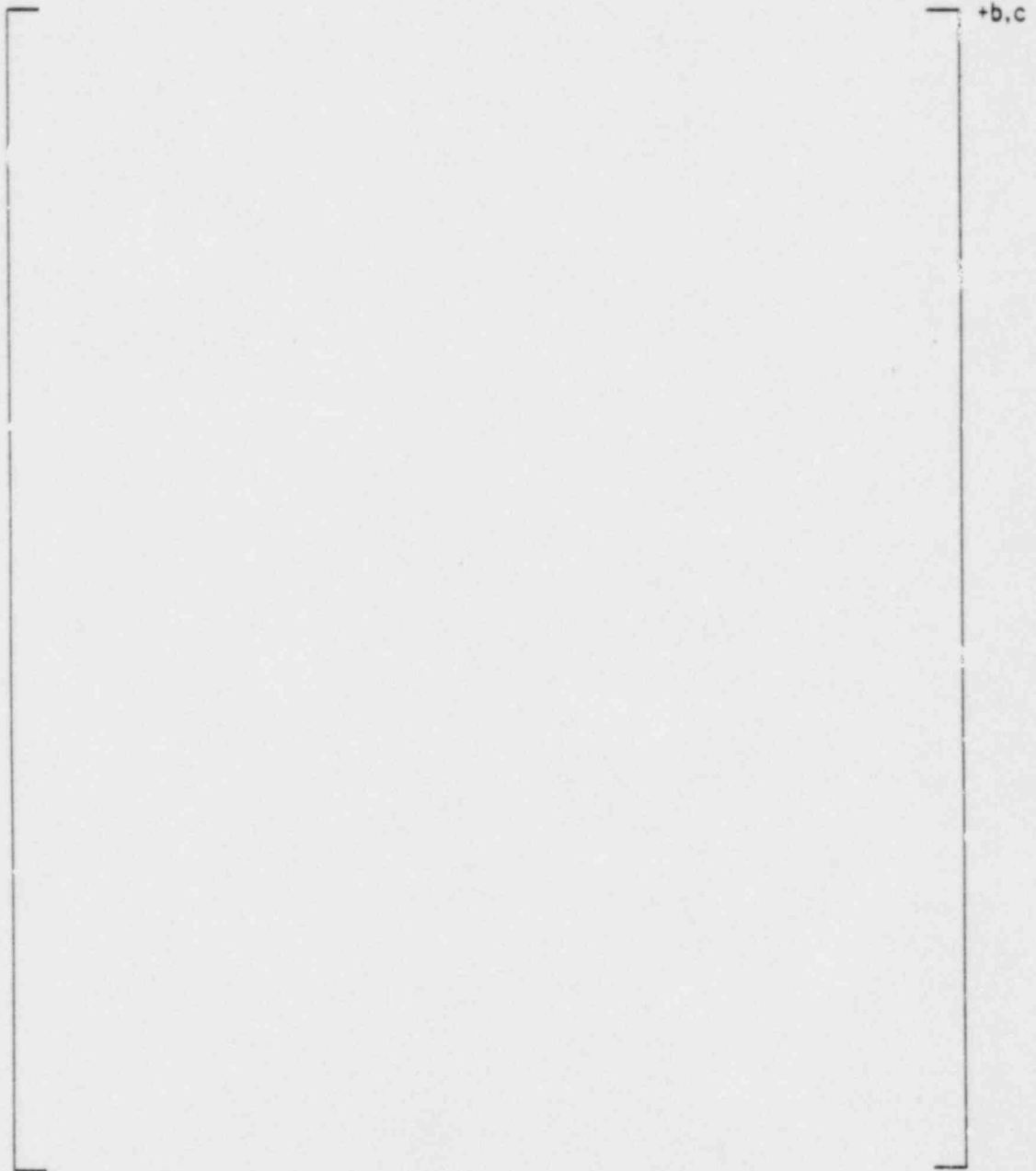
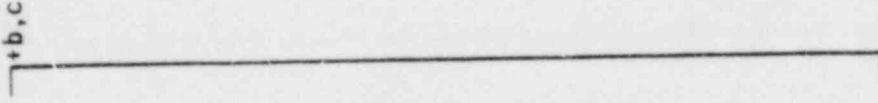


Figure 2-3. Grid, Thermocouple and Pressure Tap Locations

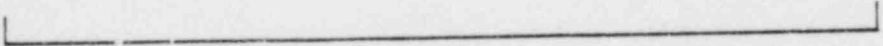
b, c



Z, AXIAL DISTANCE FROM BEGINNING OF HEATED LENGTH (INCHES)

Figure 2.4. Axial Heat Flux Distribution

$q''_{\text{LOCAL}} / q''_{\text{AVG}}$ LOCAL-TO-AVERAGE HEAT FLUX RATIO



2.3 DATA REDUCTION AND ANALYSIS

2.3.1 DATA REDUCTION

Data reduction was carried out in the same manner as that described in References 1 and 2, except that a new CHF correlation, the WRB-1 of Reference 3, was used to predict CHF. A performance factor of []⁺ was used. This is the same value which was used for the original 17x17 geometry data, Reference 3.

(a,c)

2.3.2 DATA ANALYSIS

The results of these tests are tabulated in Table 2-1 for the typical cell and in Table 2-2 (for the thimble cell). Most of the runs in this test program were carried out at inlet conditions which match those of the original 17x17 (0.374 inch rod diameter) data set. These matching runs, together with their M/P values, are also given in Tables 2-1 and 2-2*.

In order to reveal any differences in CHF characteristics which might exist between the optimized and the original 17x17 design, a repeatability parameter, δ_R , is defined for each matched pair of the optimized design and the original 17x17 geometry runs:

$$\delta_R = 1 - \frac{\left(\frac{M}{P}\right)_{opt}}{\left(\frac{M}{P}\right)_{orig}} = \frac{\left(\frac{M}{P}\right)_{orig} - \left(\frac{M}{P}\right)_{opt}}{\left(\frac{M}{P}\right)_{orig}}$$

where $\left(\frac{M}{P}\right)_{opt}$ is the measured-to-predicted CHF ratio for the optimized 17x17 fuel assembly design.,

$\left(\frac{M}{P}\right)_{orig}$ is the measured-to-predicted CHF ratio for the original 17x17 fuel assembly design of References 1 and 2.

*Complete tabulations of these original 17x17 data are given in Tables A-5 and A-18 of Reference 3.

TABLE 2-1

CRITICAL HEAT FLUX TEST RESULTS FOR OFA TYPICAL CELL

RUN NO.	INLET PRESSURE (PSIA)	INLET TEMP (°F)	INLET MASS VELOCITY (10 ⁻⁶ LBM/HR-SQ FT)	LOCAL QUALITY (10 ⁻⁶ BTU/HR-SQ FT)		(M/P) _{OPT} (HR ⁻¹)	ELEVATION FROM INLET (INCHES)		ORIGINAL 17A17 MATCHING RUN NO.	(M/P) _{ORIG}	δ _R *
				MEAS.	PRED.		PRED.	MEAS.			
W2178						(b,c) .8144			W1990	.8245	.0123
W2179						.8747			W1986	.9151	.0442
W2180						.8624			W1991	.8584	-.0046
W2181						.9263			W1987	.9196	-.0072
W2182						.8728			W1992	.9519	.0831
W2183						.9272			W1988	1.0330	.1025
W2184						.9295			W1993	.9352	.0061
W2185						.9621			W1994	.9521	-0.0105
W2186						.8189			W1999	.9291	.1187
W2187						.7834			W1995	.7923	.0113
W2188						.8295			W1996	.8689	.0454
W2190						.8940			W1997	.8721	-.0251
W2191						.8440			W2001	1.0264	.1778
W2192						.9281			W1998	.8589	-.0805
W2193						.5024			W2002	.9466	.0461
W2194						.8659			W2000	1.0031	.1368
W2195						.9774			W1985	.8683	-.1256
W2196						.9740			W1979/1989	1.0218	.0468
W2197						.9646			W1986	.9151	-.0540
W2198						1.0070			W1990	.8245	-.2213
W2199						1.0039			W1984/1987	.9635	-.0207
W2200						1.0384			W1981/1991	.9275	-.1195
W2201						1.1258			W2011	1.0584	-.0636
W2202						1.1123			W2012	1.0731	-0.0365
W2203						1.0373			W2013	1.0539	.0158
W2204						.9825			W1981/1991	.9275	-0.0592
W2205						1.0323			W1992/2021	.9116	-.1324

TABLE 2-1 (Cont inued)

CRITICAL HEAT FLUX TEST RESULTS FOR OFA TYPICAL CELL

RUN NO.	INLET PRESSURE (PSIA)	INLET TEMP (°F)	INLET MASS VELOCITY (10 ⁻⁶ LBM/HR-SQ FT)	LOCAL QUALITY (Z)	LOCAL HEAT FLUX (10 ⁻⁶ BTU/HR-SQ FT)		(M/P) _{OPT} CHF (WRB-1)	ELEVATION FROM INLET (INCHES)		ORIGINAL MATCHING RUN NO.	(M/P) _{ORIG}	δ _R *
					PRED.	MEAS.		PRED.	MEAS.			
W2206							(b,c) .9943			(b) W1979/2052	1.0082	-.0138
W2207							.9440			W1982	.9088	-.0387
W2208							1.0628			W1983	1.0449	-.0171
W2209							.9690			W1980/2050	.9374	-.0337
W2210							1.0381			W1981	.9967	-.0415
W2211							.8840			W2034	.9474	.0670
W2212							1.0444			W2038	.9688	-.0780
W2213							1.2279			W2023	1.0492	-.1703
W2214							1.1325			W2074	1.1220	-.0093
W2215							1.0474			W2025	1.0774	.0279
W2216							.9833			W2026	1.0470	.0609
W2217							1.0650			W2040	1.0574	-.0071
W2218							1.2024			W2023/2042	1.0767	-.1167
W2219							1.1603			W2924/2044	1.1496	-.0093
W2220							1.1420					
W2221							1.0795			W2030	1.1231	.0389
W2222							1.0576			W2031	1.2024	.1205
W2223							1.1171			W2027	1.0134	-.1023
W2224							1.0404			W2077	1.0134	.0266
W2225							.9622			W2028	1.1229	.1432
W2226							.9784			W20-8/2029	.9887	.0095
W2227							1.0089			W2016	1.0036	.0052
W2228							.9727			W2017	1.0546	.0777
W2229							.9529			W2018	1.0203	.0661
W2230							.9941			W2019	1.0005	.0064
W2231							1.0056			W2014	1.0332	.0268

TABLE 2-1 (Continued)

CRITICAL HEAT FLUX TEST RESULTS FOR OFA TYPICAL CELL

RUN NO.	INLET PRESSURE (PSIA)	INLET TEMP (°F)	INLET MASS VELOCITY (10 ⁻⁶ LBM/HR-SQ FT)	LOCAL HEAT FLUX QUALITY (10 ⁻⁶ BTU/HR-SQ FT)		(M/P) OPT CHF (WRB-1)	ELEVATION FROM INLET (INCHES)		ORIGINAL MATURING RUN NO.	(M/P) ORIG	δ _R *
				(Z, MEAS.)	PRED.		PRED.	MEAS.			
W2232	[]	[]	[]	(b,c)	0.9955	[]	[]	[]	(b,c) W2015	0.9760	-0.0199
W2233				0.9563	W2020				0.8955	-0.0678	
W2234				0.9933	W2003				0.9909	-0.0024	
W2235				1.1509	W2008				1.1099	-0.0369	
W2236				0.9610	W2004				0.9577	-0.0034	
W2237				1.0815	W2009				1.0822	0.0007	
W2238				0.9111	W2005				0.9592	0.0502	
W2239				1.0655	W2010				1.0689	-0.0158	
W2240				0.9348	W2006				1.0119	0.0762	
W2241				1.0761	W2007				0.9703	-0.1090	

$$\delta_R = 1 - \frac{\left(\frac{M}{P}\right)_{OPT}}{\left(\frac{M}{P}\right)_{ORIG}}$$

Test Section Length, L = 14 Ft
 Equivalent Hydraulic Dia. DE = .5071 IN
 9 RODS 100;
 16 RODS 82;
 ROD O.D. = []
 ZIRC SPRING MW GRIDS 20 IN SPACING
 INNER ROD/OUTER ROD POWER = 1.2195

TABLE 2-2

CRITICAL HEAT FLUX TEST RESULTS FOR OFA THIMBLE CELL

RUN NO.	INLET PRESSURE (PSIA)	INLET TEMP (°F)	INLET MASS VELOCITY (10 ⁻⁶ LBH/HR-SQ FT)	LOCAL HEAT FLUX		(H/P) _{OPT} CHF (MRB-1)	ELEVATION FROM INLET (INCHES)		ORIGINAL MATCHING RUN NO.	(H/P) _{ORIG}	δ _R *
				QUALITY (Z)	LOCAL (10 ⁻⁶ BTU/HR-SQ FT)		PRED.	MEAS.			
W2110						(b,c) .9000			(b,c) W1906	.8614	-.0448
W2111						.8913			W1875/1907	.8992	.0088
W2112						1.0301			W1903	.8811	-.1691
W2113						1.0121			W1904	1.0208	.0086
W2114						.9763			W1874/1902	.9399	-.0387
W2115						.9987			W1905	1.0165	.0176
W2116						1.0894			W1904	1.0208	-.0672
W2117						1.0203			W1902	.9246	-.1035
W2118						.9655			W1877	.9574	-.0084
W2119						.8769			W1909	1.0250	.1354
W2120						.9748			W1886	1.1506	.1528
W2121						1.0177			W1889	1.1773	.1356
W2122						.8989			W1895	.9935	.0953
W2123						.9325			W1896	.9510	.0195
W2124						.9568			W1897	1.0187	.0608
W2125						.9952			W1899	.8875	-.1213
W2126						.9563			W1901	.9236	-.0354
W2127						.9827			W1912	.9180	-.0704
W2128						1.0054			W1913	.9492	-.0592
W2159						.9259			W1904	1.0208	.0930
W2160						.9512			W1902	.9246	-.0287
W2161						.9711			W1904	1.0208	.0487
W2162						1.0110			W1903	.8811	-.1474
W2163						.9931			W1905	1.0165	.0231
W2164						1.0550			W1880	.8547	-.2343
W2165						.9628				1.0072	.0441
W2166						.9382			W1882	.9943	.0565
W2167						.9510			W1883	1.0614	.1041

TABLE 2-2 (Continued)

CRITICAL HEAT FLUX TEST RESULTS FOR OFA THIMBLE CELL

RUN NO.	INLET PRESSURE (PSIA)	INLET TEMP (°F)	INLET MASS VELOCITY (10 ⁻⁶ LBM/HR-SQ FT)	LOCAL QUALITY (X)	LOCAL HEAT FLUX (10 ⁻⁶ BTU/HR-SQ FT)		(M/P) _{OPT} CHF (WRB-1)	ELEVATION FROM INLET (INCHES)		ORIGINAL 17x17 MATCHING	(M/P) _{ORIG}	δ _R [*]
					MEAS.	PRED.		PRED.	MEAS.	RUN NO.		
W2168	[] (b,c) 1.0145] +		(b,c) W1884	1.0948	.0734
W2169										W1885	.9909	.0803
W2170										W1919	.9805	-.1085
W2171										W1920/1921	.9738	-.0043
W2172										W1867/1876	.9333	-.0099
W2173										W1868/1875	.9797	-.0414
W2174										W1869/1872	1.0305	.0115
W2175										W1870/1871	.9580	-.0032
W2176										W1904	1.0208	.0387
W2177										W1902	.9246	.0112

13

$$\delta_R^* = 1 - \frac{\left(\frac{M}{P}\right)_{OPT}}{\left(\frac{M}{P}\right)_{ORIG}}$$

Test Section Length,
Equivalent Hydraulic Dia.

L = 14 Ft
DE = .4079 IN
8 RODS 100:
16 RODS 82:

ROD O.D. = []⁺ (a,c)
ZIRC SPRING MV GRIDS 20 IN SPACING
INNER ROD/OUTER ROD POWER = 1.2195

Values of δ_R are tabulated in Tables 2-1 and 2-2 and are shown plotted against fluid parameters in Figures 2-5 and 2-6. These plots display random scatter about zero and show no apparent trends with the principal test parameters. This is a clear indication that there are no substantial differences in CHF between the optimized and the original 17x17 designs.

13.987-5

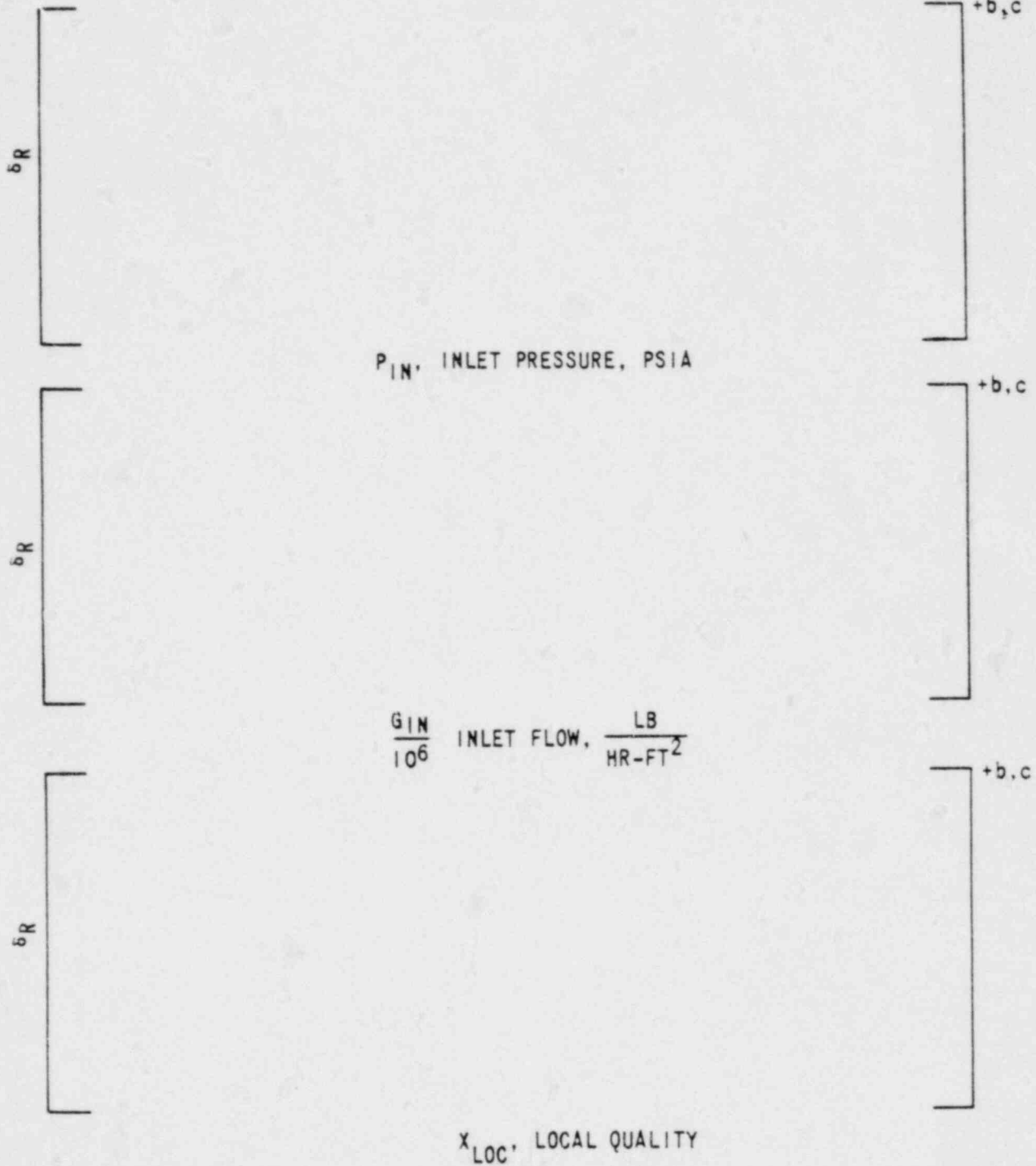


Figure 2-5. Variation of Repeatability Parameter, δ_R , with Test Variables - Thimble Cell

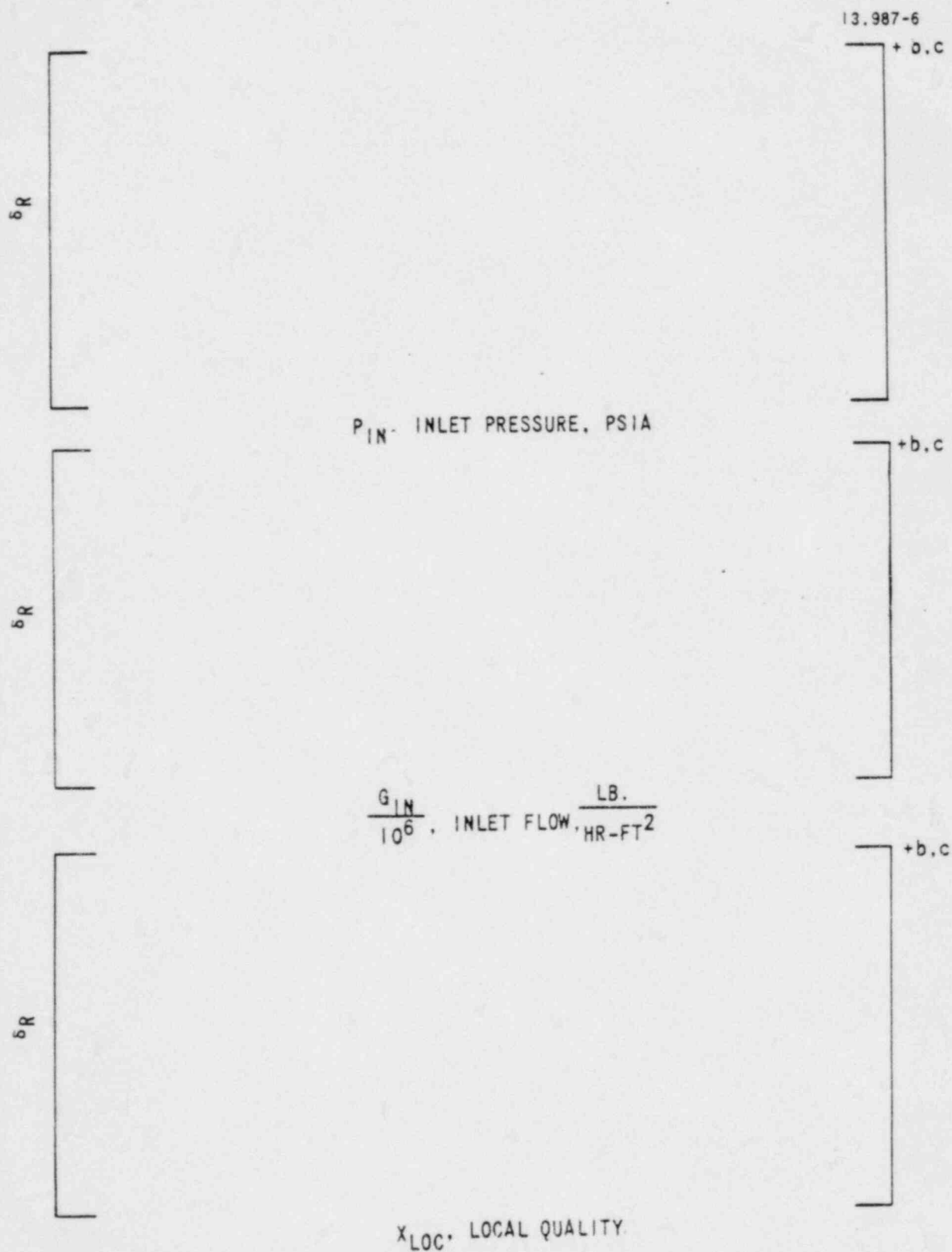


Figure 2-6. Variation of Repeatability Parameter, δ_R , with Test Variables - Typical Cell

2.4 CRITERION FOR DESIGN

Because the optimized design 17x17 data are indistinguishable from the other 17x17 data sets, these new sets can be incorporated into the data base of the WRB-1 correlation of Reference 3. This is done in Table 2-3 which includes all the "R" grid data of Reference 3 plus the two new data sets of this study.

As shown in Table 2-3, this expanded "R" grid data base yields statistics for the WRB-1 correlation which are essentially the same as those given in Reference 3. When values of $(M/P)_{avg}$ and sample standard deviation, S, are used to calculate the 95/95 value of DNBR using the method of Owen (Reference 4), the result is:

$$(DNBR)_{95/95} = \frac{1}{\left(\frac{M}{P}\right)_{avg} - KS} = \frac{1}{1.0062 - (1.7243)(0.0857)}$$

Where K is a statistical factor (Reference 4)

$$(DNBR)_{95/95} = 1.165$$

This is essentially the same value (1.17) found for the "R" grid data of Reference 3. Hence, the design $(DNBR)_{95/95} = 1.17$ recommended in Reference 3 is not changed by the incorporation of the new optimized fuel 17x17 data into the "R" grid data base of the WRB-1 correlation.

TABLE 2-3

WRB-1 CHF CORRELATION - STATISTICAL RESULTS

Rod O. D. Inch	Heated Length L _H Ft	Grid Spacing S _{gp} Inch	Heat Flux Profile	Configuration *	Number of Data Pcs. N	(M/F) _{avg}	Sample Standard Deviation, S	Reference
0.374	14	22	UNIF	TYP - 5x5	71	0.9964	0.0655	(3)
0.374	14	26	UNIF	TYP - 5x5	73	1.0041	0.0805	
0.374	8	22	UNIF	TYP - 5x5	67	1.0502	0.1020	
0.374	8	26	UNIF	TYP - 5x5	78	1.0136	0.0848	
0.374	14	22	COSINE	TYP - 5x5	74	1.0022	0.0852	
0.422	8	20	COSINE	TYP - 4x4	33	1.0042	0.0528	
0.422	8	20	USINU	TYP - 4x4	33	0.9937	0.0649	
0.422	8	26	USINU	TYP - 4x4	36	0.9846	0.0922	
0.422	14	26	USINU	TYP - 4x4	35	1.0584	0.0816	
0.422	14	20	USINU	TYP - 4x4	36	1.0100	0.0915	
0.422	14	13	USINU	TYP - 4x4	38	0.9737	0.0781	
0.422	14	32	USINU	TYP - 4x4	38	1.0238	0.0752	
0.422	8	32	USINU	TYP - 4x4	31	0.9913	0.0724	
0.422	14	26	USINU	TYP - 4x4	71	1.0466	0.0829	
0.422	14	26	UNIF	TYP - 4x4	42	0.9321	0.0595	
0.422	14	26	USINU	TH - 4x4	39	1.0141	0.0579	
0.422	14	32	USINU	TH - 4x4	37	0.9738	0.0887	
0.374 ^(b,c)	14	22	COSINE	TH - 5x5	70	1.0002	0.0796	
0.374 ^(b,c)	8	26	UNIF	TH - 5x5	68	1.0303	0.1048	
[] [†]	14	20	COSINE	TYP - 5x5	63	0.9918	0.0970	This study
[] [†]	14	20	COSINE	TH - 5x5	38	0.9755	0.0504	This study
ALL DATA				1071	1.0062	0.0857		

† Results use all "R" grid data, including new optimized 17x17 data

* TYP - Typical Cell
TH - Thimble Cell

2.5 CONCLUSIONS

The CHF characteristics of the optimized 17x17 fuel assembly design are not significantly different from those of the original design, and can be adequately described by the "R" grid form of the WRB-1 CHF correlation with a performance factor of []⁺. Furthermore, the new data can be incorporated into the "R" grid data base without changing the DNBR design criterion of 1.17.

(a,c)

2.6 REFERENCES

1. K. W. Hill, F. E. Motley, F. F. Cadek, A. H. Wenzel, "Effect of 17x17 Fuel Assembly Geometry on DNB," WCAP-8926-P-A (Westinghouse Proprietary) and WCAP-8297-A (Non-proprietary), February 1975.
2. F. E. Motley, A. H. Wenzel, F. F. Cadek, "Critical Heat Flux Testing of 17x17 Fuel Assembly Geometry with 22-Inch Grid Spacing," WCAP-8536, (Westinghouse Proprietary) and WCAP-8537 (Non-proprietary), May 1975.
3. Motley, F. E., Hill, K. W., Cadek, F. F., Shefcheck, J., "New Westinghouse Correlation WPB-1 for Predicting Critical Heat Flux in Rod Bundles with Mixing Vane Grids," WCAP-8762, (Westinghouse Proprietary), July 1976.
4. D. B. Owen, "Factors for One-Sided Tolerance Limits and for Variable Sampling Plans," SCR-607, March, 1963.

Westinghouse
Electric Corporation

Water Reactor
Divisions

Nuclear Technology Division
Box 355
Pittsburgh Pennsylvania 15230

April 16, 1980
NS-TMA-2232

Mr. John F. Stolz, Chief
Light Water Reactors Branch #1
Division of Project Management
Office of Nuclear Reactor Regulation
U. S. Nuclear Regulatory Commission
Washington, D. C. 20555

SUBJECT: "Verification Testing and Analyses of the Westinghouse 17 X 17
Optimized Fuel Assembly" - WCAP-9401 (Proprietary) and WCAP-9402
(Non-Proprietary)

Dear Mr. Stolz:

Enclosed are:

1. Twenty (20) copies of Revision 1 to Section 3.0 of Westinghouse Topical Report, "Verification Testing and Analyses of the Westinghouse 17 X 17 Optimized Fuel Assembly" (WCAP-9401 Proprietary).
2. Forty (40) copies of Revision 1 to Section 3.0 of Westinghouse Topical Report, "Verification Testing and Analyses of the Westinghouse 17 X 17 Optimized Fuel Assembly" (WCAP-9402 Non-Proprietary).

Also enclosed are:

1. One (1) copy of Application for Withholding (Non-Proprietary).
2. One (1) copy of original Affidavit (Non-Proprietary).

As discussed with members of the NRC's Core Performance Branch, this revision was necessitated to reflect changes made to the system representation and modeling of the reactor pressure vessel, reactor internals, reactor core, and reactor support mechanism. Also incorporated into the text of this revision are responses to NRC questions discussed during a meeting between Westinghouse and the NRC held in March 1980.

To facilitate Staff review of this topical report, the revised portions of Section 3.0 are denoted by bars in the right margin of the text. We will reissue the entire topical report, including the revised Section 3.0 and all related correspondence, once the Staff's review is completed and the report approved.

Mr. John F. Stolz

-2-

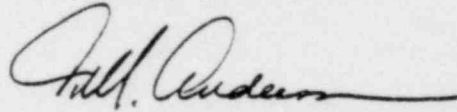
April 16, 1980
NS-TMA-2232

It is our understanding that this revision will not adversely affect the Staff's review schedule which calls for an SER by August 15, 1980. We are available to answer any questions or concerns you may have on this subject.

This submittal contains proprietary information of Westinghouse Electric Corporation. In conformance with the requirements of 10CFR2.790, as amended, of the Commission's regulations, we are enclosing with this submittal an application for withholding from public disclosure and an affidavit. The affidavit sets forth the basis on which the information may be withheld from public disclosure by the Commission.

Correspondence with respect to the affidavit or application for withholding should reference AW-80-18 and should be addressed to R. A. Wiesemann, Manager of Regulatory and Legislative Affairs, Westinghouse Electric Corporation, P. O. Box 355, Pittsburgh, Pennsylvania 15230.

Very truly yours,



T. M. Anderson, Manager
Nuclear Safety Department

/bek
Enclosure

3.0 SAFETY ANALYSES OF THE EIGHT GRID 17x17
OPTIMIZED FUEL ASSEMBLY FOR SEISMIC AND LOSS
OF COOLANT ACCIDENTS IN WESTINGHOUSE
FOUR LOOP PLANTS

3.1 INTRODUCTION

The safety analysis for the 17x17 8-grid optimized fuel assembly (OFA) design has been performed to assess the structural adequacy under faulted condition loads.

The faulted condition loads considered in the design evaluation are derived from the maximum responses obtained from the lateral safe shut-down earthquake, SSE, and the loss-of-coolant blowdown accident, LOCA. The detailed analyses including general analytical procedures, model development, and the results of both postulated accidents are presented in the subsequent sections of this report.

The analysis presented are applicable to a number of Westinghouse 4-Loop 17x17 twelve foot fuel assembly plants. These plants have a similar reactor internals design, permitting generic analyses with consideration of variations in RPV support stiffnesses and an umbrella of the LOCA and SSE excitations. This procedure of umbrella analyses produces structural response which are conservatively larger than those realistically expected from plant specific analyses.

3.2 FUEL ASSEMBLY LATERAL SEISMIC ANALYSIS

The 17x17 8-grid OFA was analyzed for maximum seismic deflection and grid impact forces using the time history method. The dynamic characteristics of a 17x17 8-grid OFA were modeled and analyzed using the general purpose finite element computer codes. The artificial seismic wave was developed with its response spectrum enveloping a number of Westinghouse four loop, twelve foot fuel assembly plants (Figure 3-1).

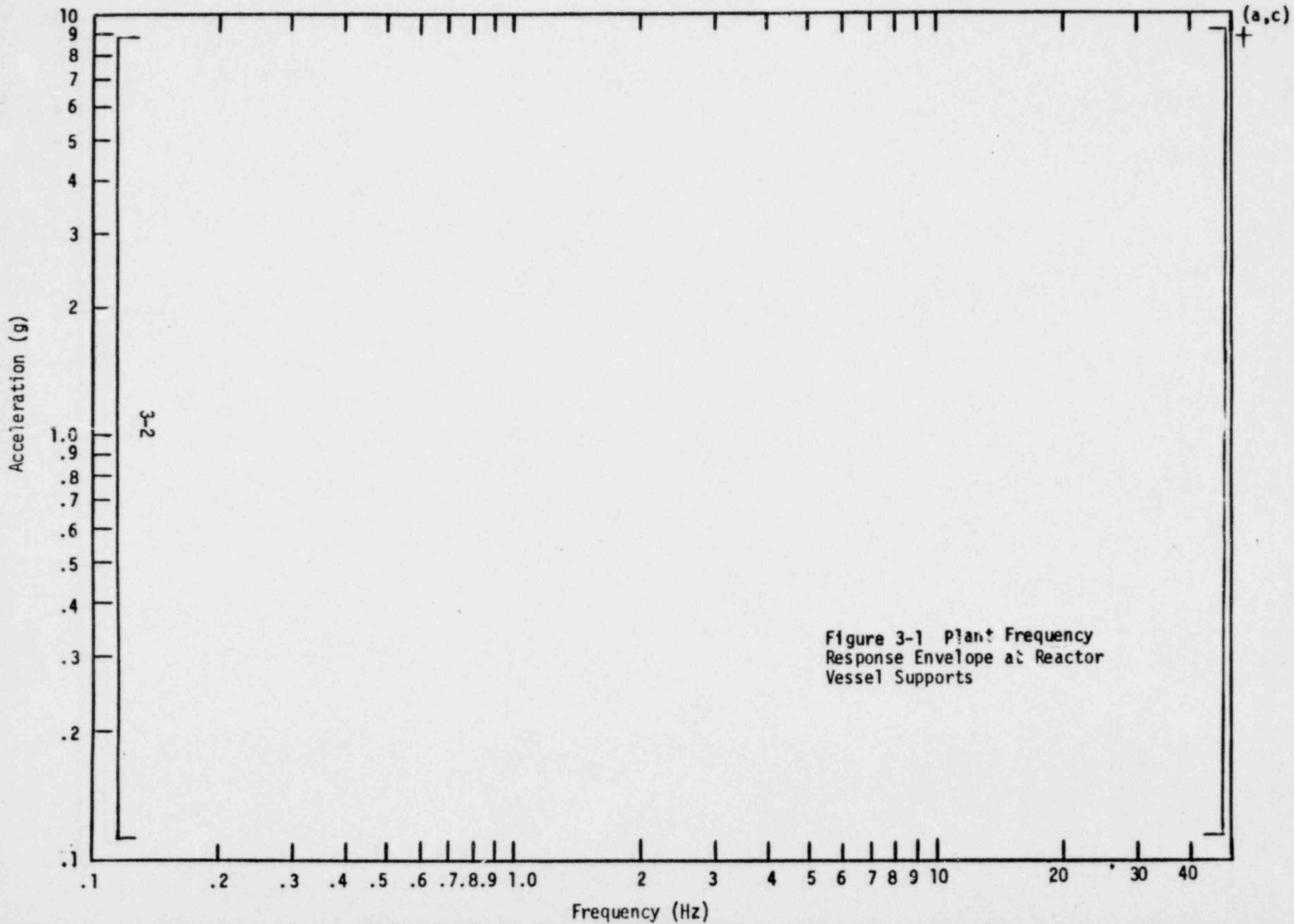


Figure 3-1 Plant Frequency Response Envelope at Reactor Vessel Supports

The core plate motions were generated based on the value of the vessel []⁺ used in the reactor vessel model. The worst case of core plate motion was determined by using the []⁺ (a,c)

[]⁺ Figure 3-2 indicates that the response spectrum of the seismic wave at reactor vessel support []⁺ (a,c)

[]⁺ (a,c)

The fuel assembly was modeled using a discrete mass and far-coupled spring system in order to reduce the number of dynamic degrees-of-freedom and to fully preserve the essential fuel assembly dynamic properties such as mass distribution, fundamental frequencies, mode shapes and orthogonality relationships among distinct vibrational modes.

The general purpose computer code was programmed using the maximum number of 15 fuel assemblies in an array of a reactor core in a four loop plant.

3.2.1 ANALYTICAL PROCEDURE

For sufficiently large horizontal forces, the fuel assemblies will deflect and impact the core barrel or an adjacent assembly. Since the reactor core exhibits a geometrically nonlinear behavior due to core component discontinuities, a time history method was used to obtain the fuel assembly seismic response.

The general analytical procedure for evaluating the fuel assembly seismically induced stresses and deflections is outlined in Figure 3-3.

3.2.2 FUEL ASSEMBLY LATERAL MODEL

The analytical model used is shown in Figure 3-4 and is the same as that used in the standard Westinghouse fuel assembly analysis⁽²⁾ with appropriate changes for 17x17 8-grid OFA characteristics. The fuel assembly skeleton is represented by the central beam lattice structure;

4806A

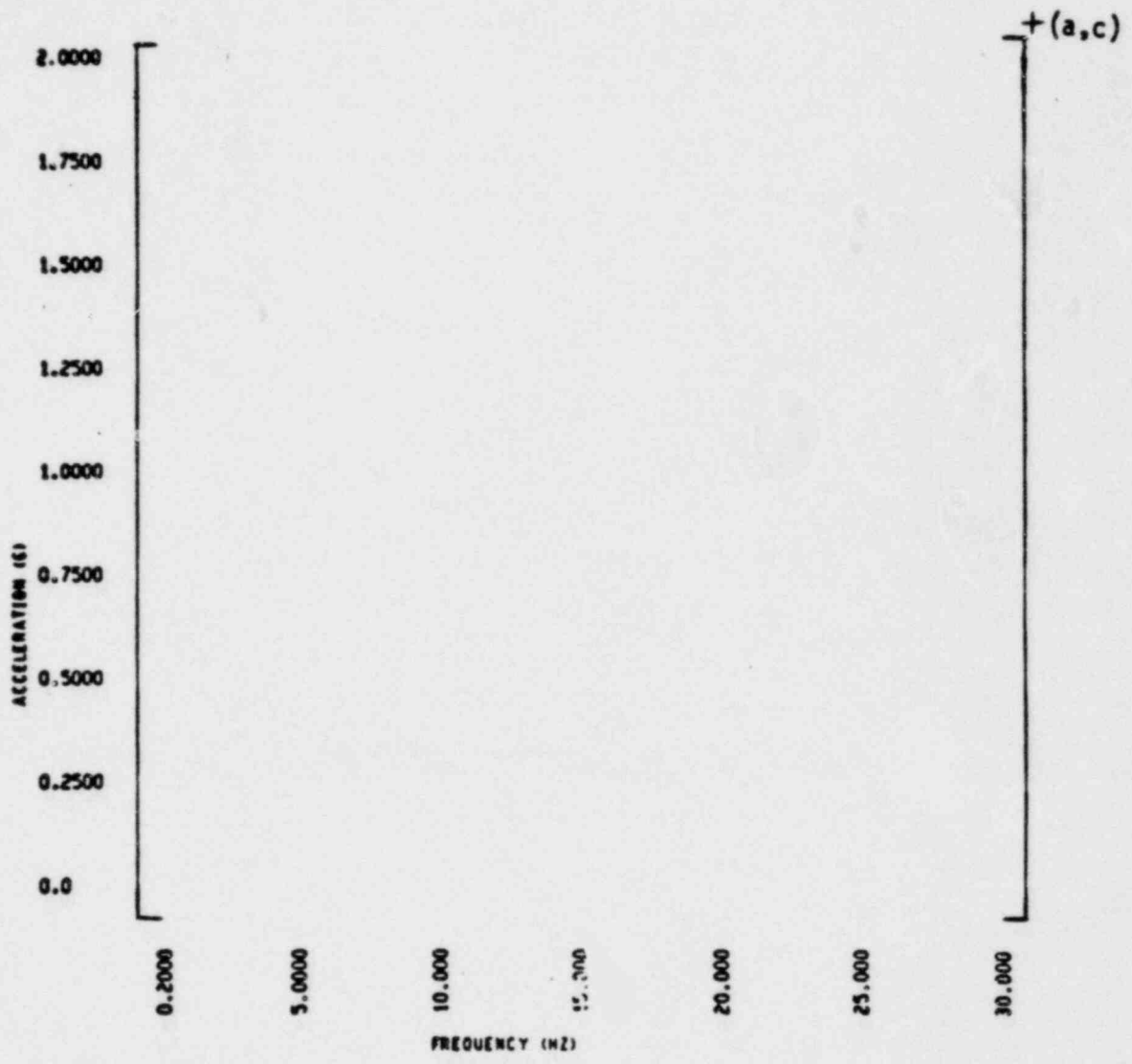


Figure 3-2
 Response Spectrum
 at
 Reactor Vessel Support

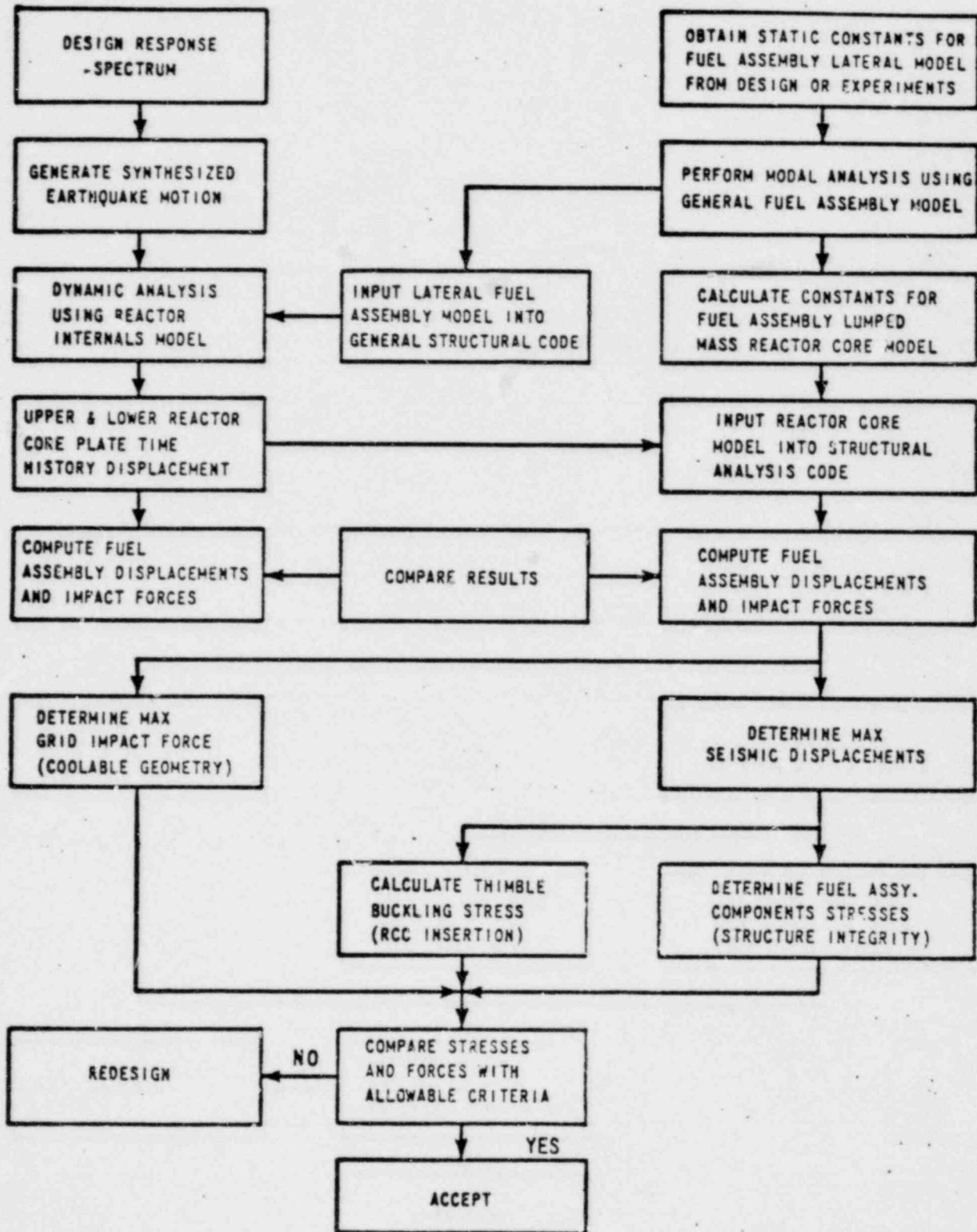


Figure 3-3
 Fuel Assembly Seismic
 Analysis Procedure

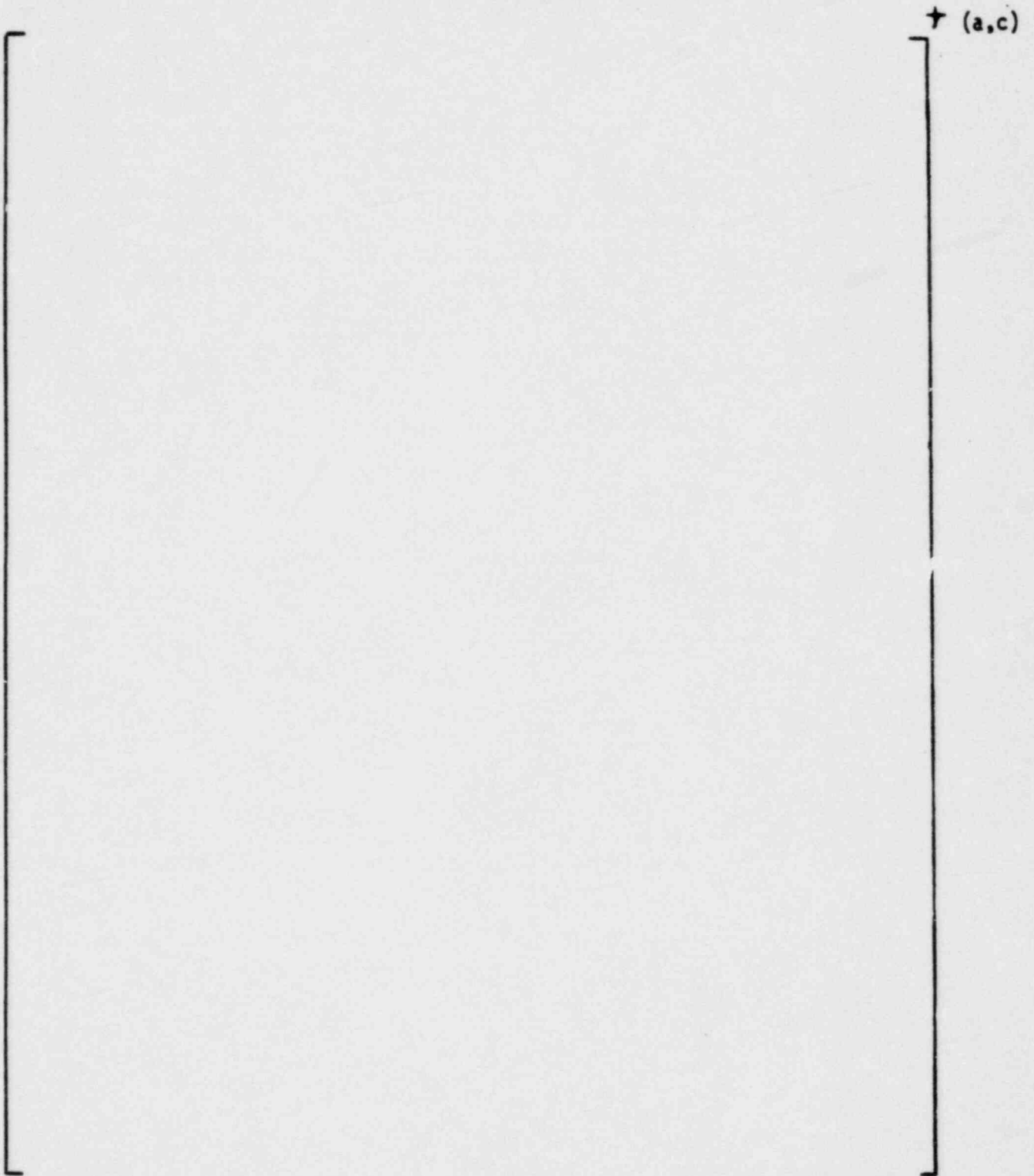


Figure 3-4
Fuel Assembly Finite Element Model

elements 3 to 101 and 4 to 102 for thimble tube including dashpots, inserts and sleeves; elements 1-2, 3-4, 1-3, and 2-4 for the top nozzle; and elements 101-102, 101-103, 102-104, and 103-104 for the bottom nozzle. A pair of thimble tubes are used to represent twenty-five thimbles. The location of the thimble tubes in the analytical model are recalculated in order to preserve the assembly flexural rigidity during lateral loading analysis.

Fuel tube elements 7 to 99 and 8 to 100 are attached to the skeleton model and constrained by the friction elements such as 5 to 7 and 9 to 11 etc., which simulate the grid spring, dimple and various other components necessary for analysis. | 1

The assembly characteristics and basic assumptions are based on:

- Nominal fuel rod and thimble dimensions
- Nominal axial dimensions
- Material properties at temperature condition
- Nominal grid spring unloading stiffness and dimple stiffness
- Best estimate grid spring force and dimple forces
- Best estimate fuel rod to grid coefficient of friction.

The fuel assembly was constrained with core plate pins at both ends to simulate reactor support conditions. Incremental lateral loads were applied at the fifth grid of the model, and the load deflection characteristics were obtained. Figure 3-5 gives the analytical results for the lateral stiffness of the OFA.

As a result of the lateral finite element model analysis, the following fuel assembly characteristics were noted:

[] ^{+(a,c)}

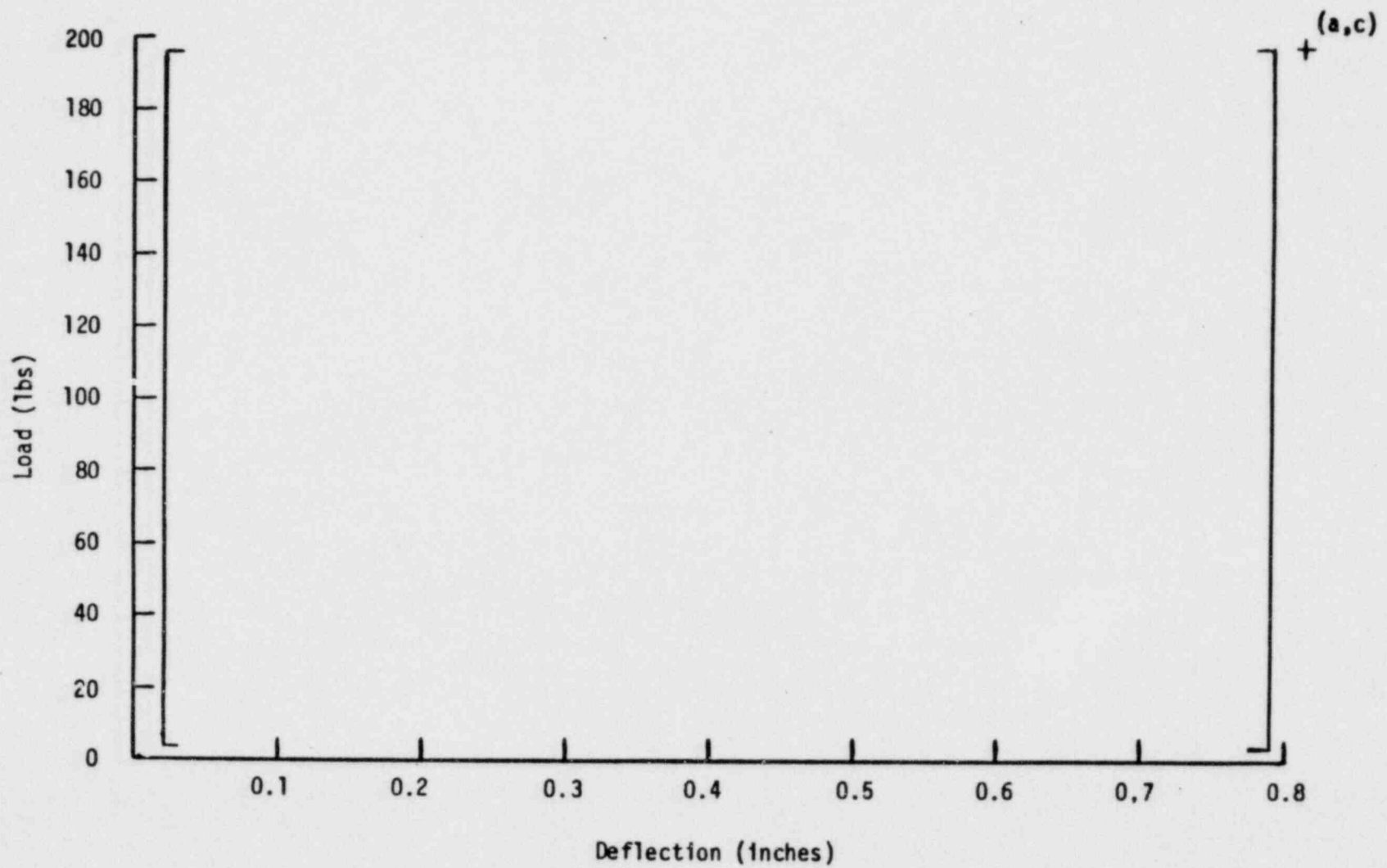


Figure 3-5 17x17 8 grid OFA Lateral Stiffness

3.2.3 REACTOR PRESSURE VESSEL MODEL

The components of a typical reactor pressure vessel (RPV) are shown in Figure 3-6. To obtain the proper dynamic input for the reactor core analysis, it is necessary to develop and analyze a complete system representative of the reactor pressure vessel, reactor internals, reactor core and reactor support mechanism. A model was developed including []⁺ behavior, effects of []⁺ (a,c)

[]⁺ Decoupling the RPV model from the remainder of the nuclear steam supply system is accomplished by []⁺ (a,c)

[]⁺ (a,c)

A finite element representation using the WECAN⁽¹⁾ computer code is used to solve the transient response for postulated seismic and loss-of-coolant-accident (LOCA) excitations. A schematic of the model is shown in Figure 3-7. The model is []⁺

[]⁺ Elements input to the model (a,c)
include []⁺

[]⁺ The model is best described (a,c)
as []⁺

[]⁺ (a,c)

Note that the segments of the model shown in Figure 3-7 are combined properly in the total RPV model and are discussed separately only for the purpose of clarification. First, the structural portion of the model shown in Figure 3-7, a through c, will be discussed, presenting the model from the innermost segment outward, and then discussing the coupling of the []⁺ Following the (a,c)

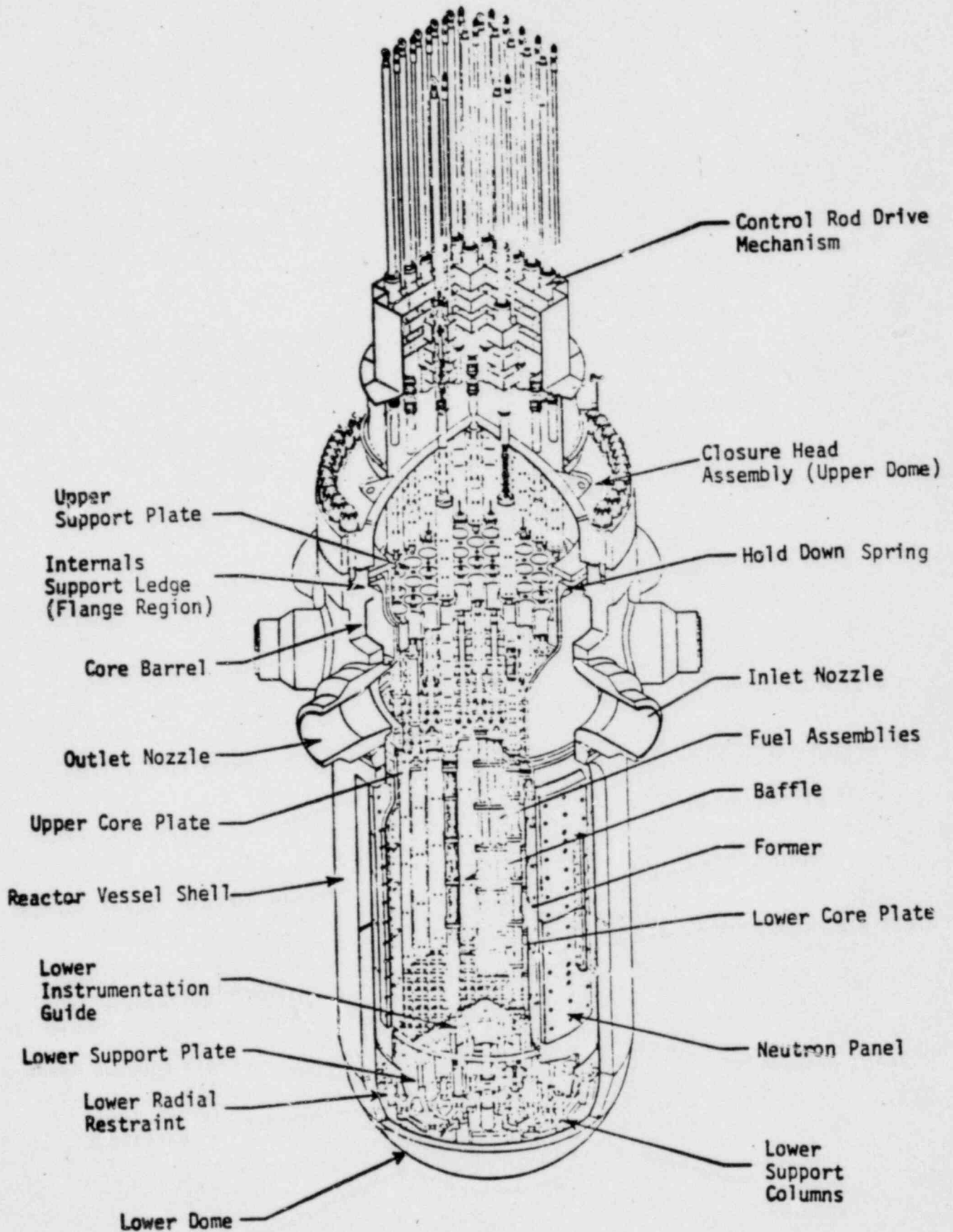


FIGURE 3-6 TYPICAL REACTOR PRESSURE VESSEL AND INTERNAL COMPONENTS

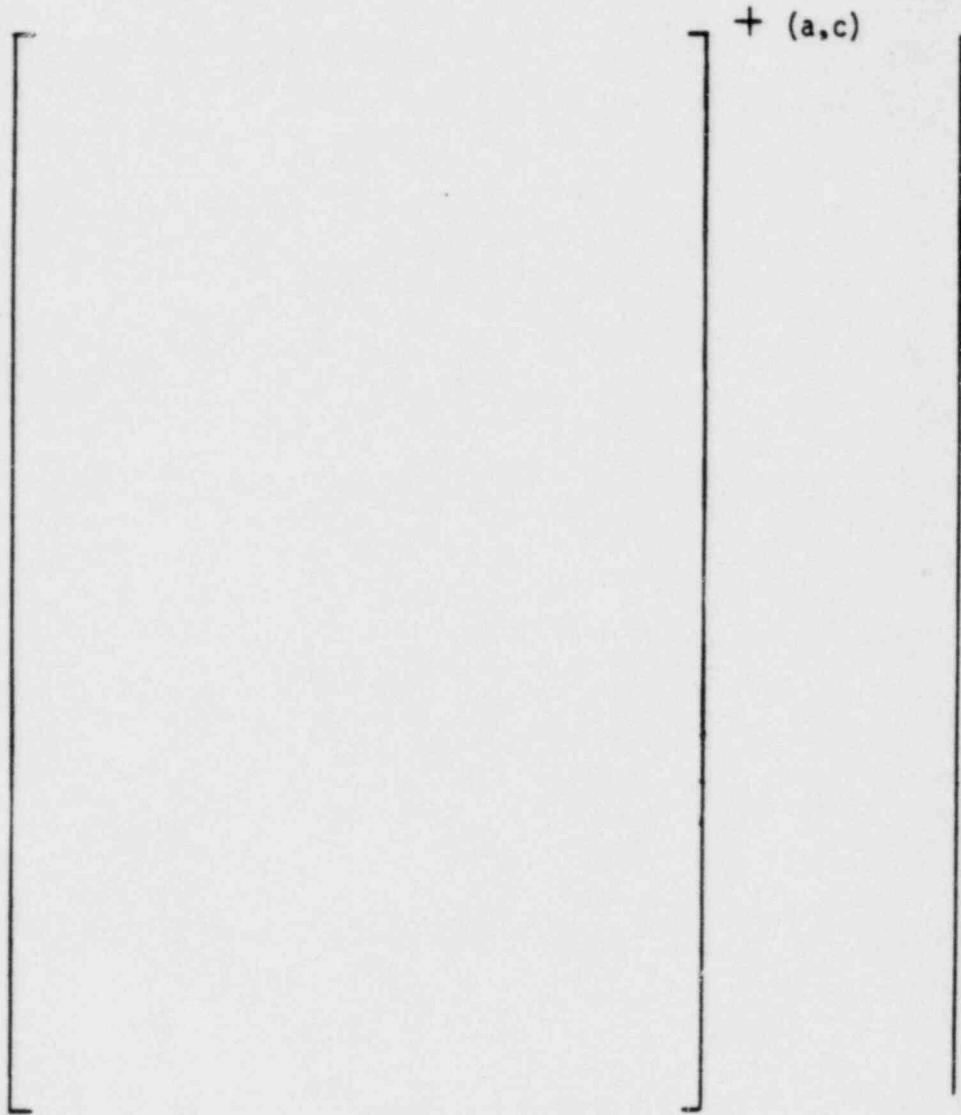


Figure 3-7(a) Core Barrel Internals' Model

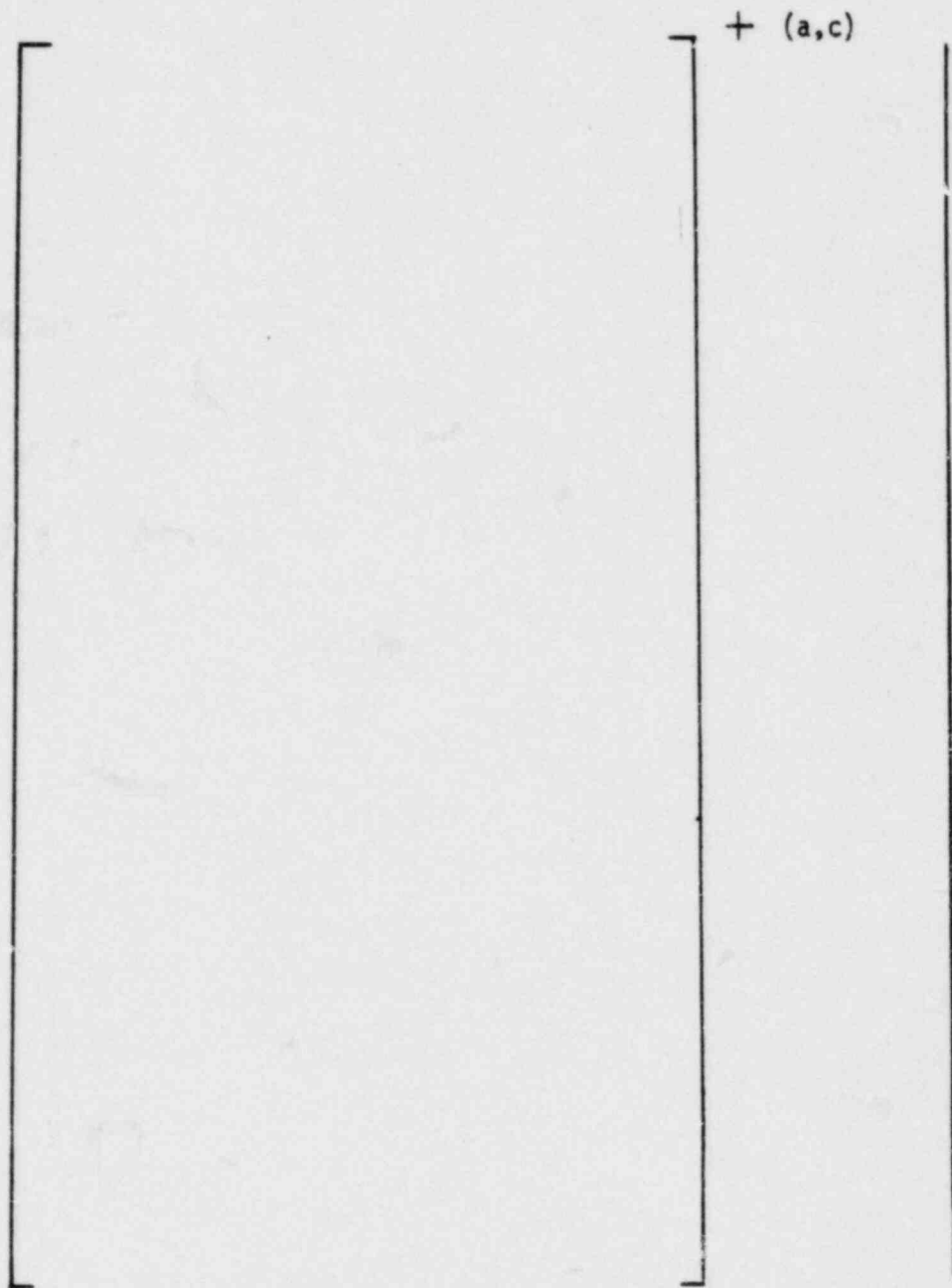


Figure 3-7(b) Reactor Core Barrel Model

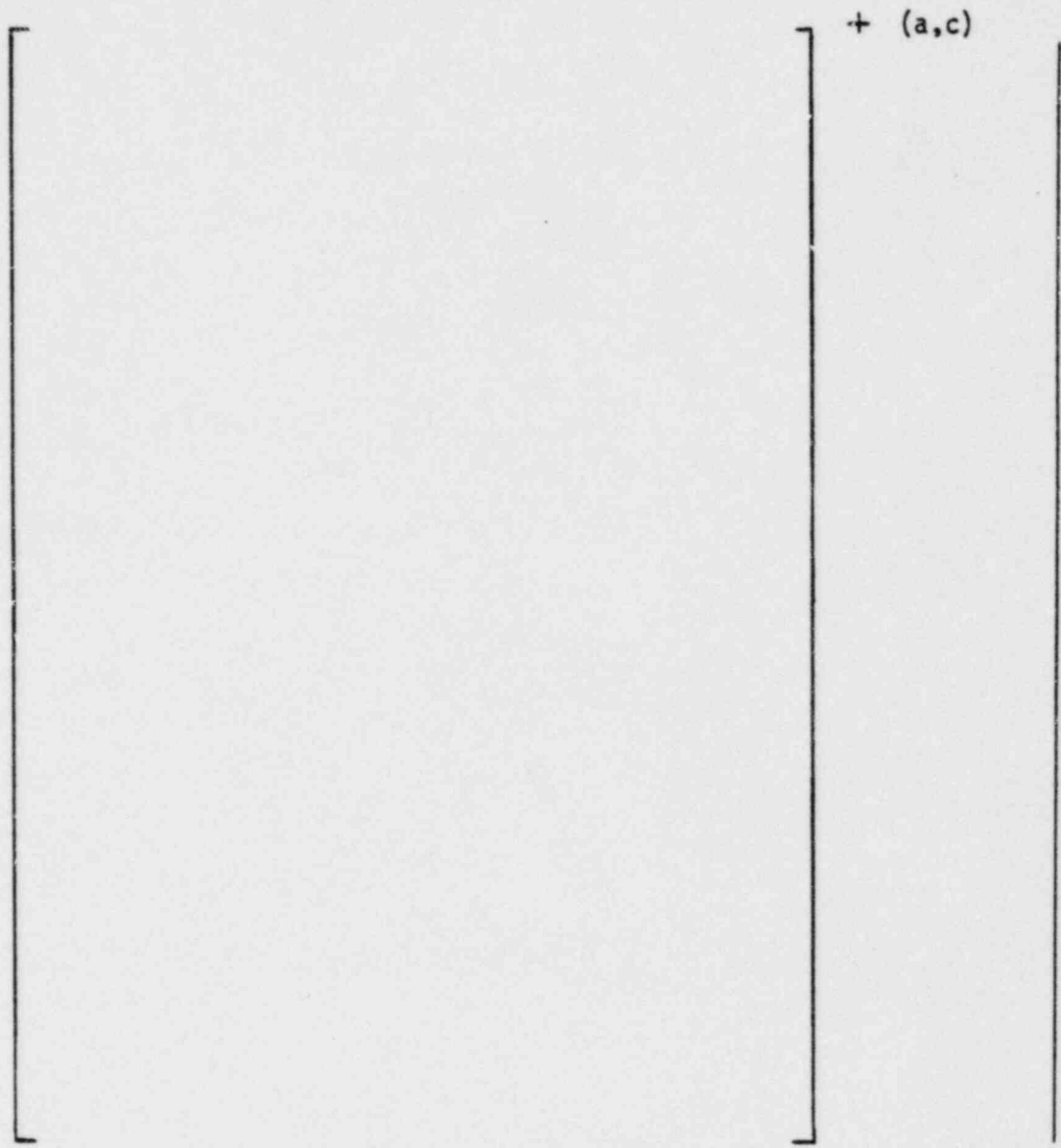


Figure 3-7(c) RPV Shell Model

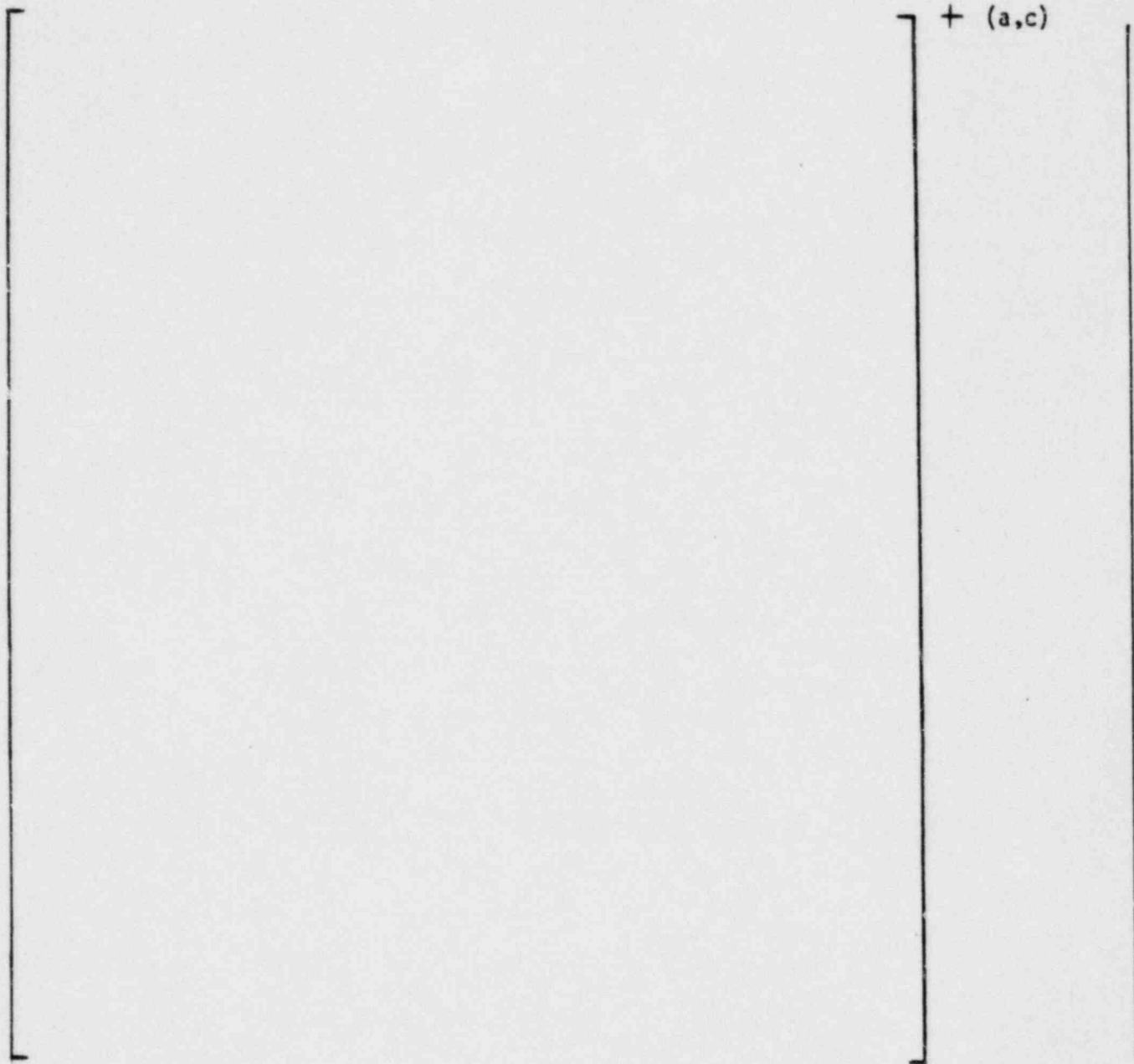


Figure 3-7(d) Vertical Hydrodynamics Model

structural discussion, the [described.

] + model will be

(a,c)

+ (a,c)

+(a,c)

Fluid-structure or hydroelastic interaction is included in the reactor pressure vessel model for seismic evaluation. For purposes of discussion, the hydroelastic interaction can be conveniently divided into horizontal and vertical phenomena. The horizontal hydroelastic interaction is significant in the cylindrical fluid flow region between the core barrel and reactor vessel (the downcomer). [

]† For LOCA considerations, the downcomer fluid-structure interaction is included in the thermal-hydraulic loads from the MULTIFLEX⁽⁵⁾ program.

(a,c)

+(a,c)

[] + (a,c)

The portion of the model representing the vertical fluid-structure interaction is shown in Figure 3-7(d). This fluid model represents the fluid forces (inertia, stiffness and buoyancy) that act on the bounding structures and couples these forces to the structures' vertical movements. Incorporating this []⁺ model provides a realistic method for including vertical fluid-structure interaction phenomena. The model includes the actual water mass in the reactor vessel and no virtual water mass is employed, i.e., the reactor vessel weight corresponds to the physical value. The []⁺ model is removed for LOCA evaluation.

+ (a,c)

[]

+ (a,c)

[] + (a,c)

+(a,c)

3.2.3.1 Seismic Evaluation

A nonlinear, time-history seismic analysis of the reactor pressure vessel model was performed. The seismic excitation was applied at the RPV support location and was synthesized to contain a wide range of frequency components. The excitation was developed such that the

[

]† The (a,c)

response spectra from the synthesized and umbrella spectra are shown in Figure 3-1. As a result of the RPV transient analysis, the motion of the nodal points in the model were obtained including [

]†

(a,c)

A number of RPV seismic time-history analyses were performed for the effect of [

]† Because the core seismic analysis indicated that the fuel assembly response is in general dependent upon the [

1 (a,c)

]† The worst case time-history response of the core plates and the relative upper to lower core plates are shown in Figures 3-8 and 3-9 respectively. The displacements were digitized and used as input to the core model.

(a,c)

3.2.3.2 Loss-of-Coolant-Accident Evaluation

The RPV model was analyzed for the effect of worse case loss-of-coolant-accidents (LOCA). LOCA excitation results from the release of the pressurized primary system's coolant and, for guillotine pipe breaks, from the disturbance of the mechanical equilibrium in the piping which is present prior to the rupture. The release of coolant leads to depressurization waves traveling internal to the primary coolant system and, for ruptures postulated at the RPV safe ends, pressurization occurs rapidly in the cavity surrounding the vessel. The RPV cavity pressurization can exert an asymmetric force on the outside of the RPV. Thus, the loads induced on the RPV and internals for LOCA may be characterized as: (1) reactor coolant loop mechanical loads (for guillotine ruptures), (2) reactor internal hydraulic loads and (3) RPV cavity pressurization loads (only for breaks at the reactor vessel safe end locations). The reactor internals hydraulic loads were calculated using the MULTIFLEX⁽⁵⁾ thermal hydraulic code which considers the fluid-structure interaction in the downcomer. Loop mechanical loads were obtained from loop normal operating condition analyses of typical four loop plants. Reactor cavity pressurization loads were obtained from typical cavity loads calculations.

There are eleven postulated break locations in the primary coolant system⁽⁶⁾: five in the hot leg pipe, three in the cross-over leg pipe and three in the cold leg pipe. Break locations were chosen from these to produce the worse case response of the reactor core with respect to grid lateral impact loads and fuel assembly to core plate interface loads. Analyses were performed for three worse case pipe ruptures: [

]⁺ (a,c)

These break locations have been shown to be worse case based upon the results of previous structural analyses of Westinghouse supplied reactor coolant systems. Cold leg pipe ruptures produce more severe lateral impact loads than hot leg pipe ruptures. Cross-over leg ruptures do not induce significant loads on the RPV. Thus, for lateral response, the breaks at the [

]⁺ Review of break opening areas as determined from LOCA analyses of primary coolant systems revealed that break opening areas did not exceed []⁺ for ruptures (a,c)

at the vessel inlet safe end and pump outlet safe end, respectively. A vessel inlet nozzle rupture with a break opening area of [

]⁺ was chosen as a conservative analytical basis for cold leg pipe ruptures. Additional break locations must be considered to assure that the maximum fuel nozzle vertical loads are determined. For the purposes of conservatism, the maximum break opening area postulated in the hot leg was analyzed: [(a,c)

]⁺ An RPV outlet nozzle rupture was also considered to determine the effect of a hot leg break with cavity pressure. A [(a,c)

]⁺ was analyzed since break opening areas for RPV outlet nozzle safe end ruptures do not exceed []⁺ (a,c)

Thus, considering the []⁺ leads to determination of the worse case vertical fuel assembly nozzle loads. Several analyses were conducted for each of (a,c)

the postulated break locations for the effect of [

]⁺ The results include transient core plate and core barrel displacements for input into the reactor core LOCA model. In addition, fuel assembly vertical nozzle loads were obtained. (a,c)

3.2.4 REACTOR CORE MODEL (HORIZONTAL)

The analytical reactor core model, shown in Figure 3-10 was used to simulate the fuel assembly interaction during seismic excitation. A total of 15 fuel assemblies was used to analyze the core response. The fuel assembly contains eight grids, two of which are near the end supports and can be considered as an integral part of the end supports, therefore, a six mass model was selected to represent the dynamic response of the fuel assembly's six interior Zircaloy grids. A spring mass system was used to simulate the dynamic characteristics of the fuel assemblies. The values for the spring rates and mass distribution for the model were calculated based on fuel assembly analytically determined mode shapes and corresponding frequencies. The model used far-coupling⁽³⁾ techniques to obtain the proper fuel assembly dynamic characteristics, consequently, an accurate representation of the fuel assembly modal shapes and natural frequencies were obtained.

The analysis of the upper and lower reactor core plate motions indicated that the relative horizontal displacement was small in comparison with the translational motion (Figures 3-8 and 3-9). The core plates together with the core barrel translate horizontally as a rigid body.

The lower core plate, upper core plate and the core barrel motions at upper core plate elevations $F_1(t)$, $F_2(t)$, and $F_3(t)$ respectively were simultaneously applied to the complete core model. The core barrel motions at each individual grid elevation were then linearly interpolated between the motions of the upper core barrel and the lower core plate at every particular time instant.

The core finite element model containing gaps was used to simulate the geometric non-linearities between the fuel assemblies as well as the clearance between the peripheral fuel assemblies and baffle plate. The nominal hot gap sizes of []⁺ inch were used for baffle plate peripheral and fuel assembly gap respectively.

(a,c)

The equation of motion for the structural system is given by:

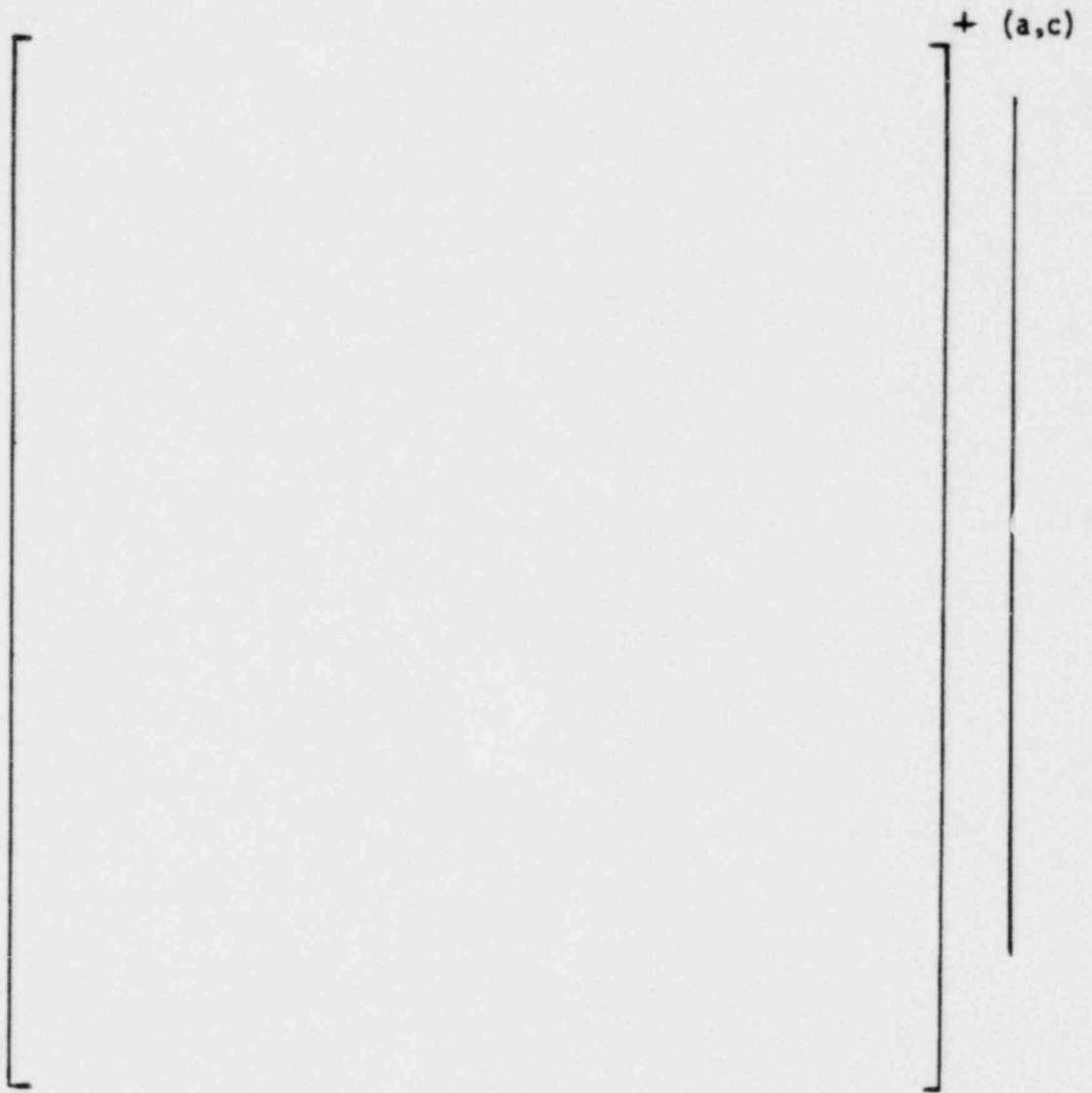


Figure 3-8 Upper Core Plate, Lower Core Plate,
and Upper Core Barrel Motions - SSE

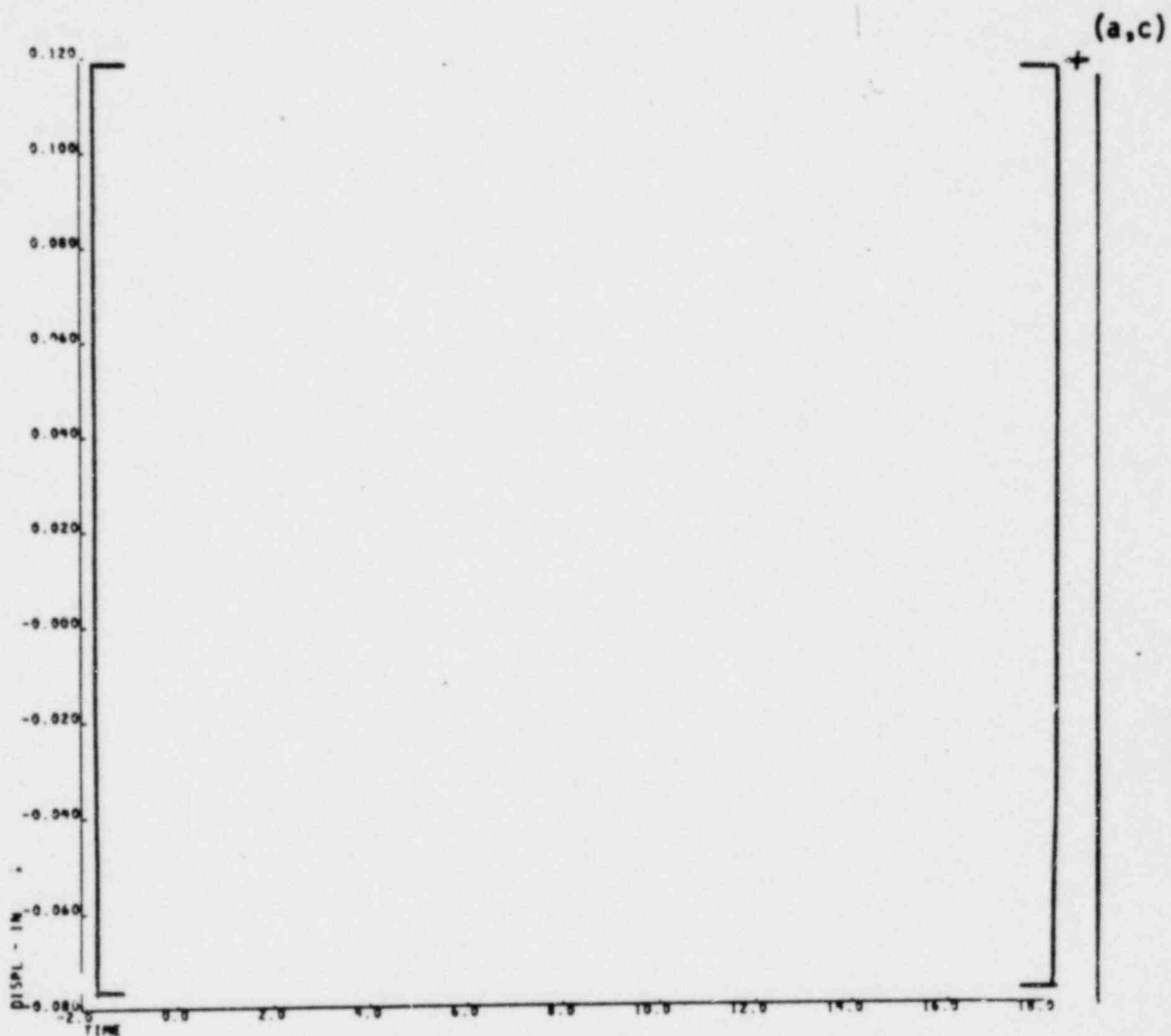


Figure 3-9 Upper to Lower Core Plate Motions-17x17 8-Grid OFA

$$[M] \{\ddot{X}\} + [C] \{\dot{X}\} + [K] \{X\} = \{F(t)\}$$

where:

- [M] = the total mass matrix of the structure
- [C] = the total viscous damping matrix of the structure
- [K] = the total stiffness matrix of the structure
- {X} = the nodal point displacement vector
- { \dot{X} } = the nodal point velocity vector
- { \ddot{X} } = the nodal point acceleration vector
- F(t) = the vector of applied nodal forces

A general finite element code using the Newmark-Beta multistep direct integration method⁽⁸⁾ was used to calculate the displacement response solutions at each successive time step by iterating the impact force.

The time increment of []⁺ msec. was chosen for the transient analyses to assure the proper solution convergence. The selected time increment is approximately []⁺ of the shortest period of the core system.

(a,c)

(a,c)

3.2.5 FUEL ASSEMBLY DYNAMIC PROPERTIES

The analytical techniques to determine the fuel assembly response to a seismic wave discussed in the previous section requires fuel assembly dynamic properties as input information.

The lateral natural frequencies and mode shapes of the 8-grid assembly were calculated by use of a general finite element fuel assembly model which included the major components such as skeleton, fuel rods, grid springs, dimples, etc., their geometric configuration, and physical properties. These values were verified by test results, and a plot of

the fuel assembly mode shapes is presented in Figure 3-12. Based on the mode shapes and natural frequencies, an equivalent spring mass finite element system was constructed preserving the fuel assembly dynamic characteristics such as fundamental frequencies, mode shapes, masses and the orthogonality relation of the principal modes.

In the reactor core model, the fuel assembly was represented by a series of springs and masses as shown in Figure 3-11. The mechanical constants used for the 8-grid fuel assembly design analysis are presented in Table 3-1. The spring stiffnesses given in Table 3-1 have been adjusted to include the water mass and temperature condition.

The impact damping and stiffness elements designated as C_S , C_G , and K_S , K_G in the reactor core model (Figure 3-10) were also determined experimentally. The stiffness, K_S , which represents the combined fuel rod and dimple stiffness constraint within the grid and characteristic rod motion relative to the grid, was obtained from fuel assembly tests. In these tests, the general procedure was to displace the fuel assembly center grid a prescribed amount relative to the ends and suddenly remove the restraint. The fuel assembly was then free to vibrate and impact with a lateral constraint which was positioned approximately 0.04 inches from the rest position in the opposite direction to the midspan initial displacement. A load cell was placed in series with the grid constraints to measure the impact force as a function of time. Displacement transducers were located at various grid locations along the fuel assembly to determine its response during the impact. Based on the results of these tests, appropriate impact stiffness, K_S , and damping, C_S , constraints were obtained.

The physical values for K_G , C_G , K_S and C_S are given as the following:

$$\begin{array}{ll}
 K_G = [\quad]^+ \text{ lb/in} & K_S = [\quad]^+ \text{ lb/in} \\
 C_G = [\quad]^+ \text{ lb-sec/in} & C_S = [\quad]^+ \text{ lb-sec/in}
 \end{array}
 \quad \left| \begin{array}{l} (b,c) \\ (b,c) \end{array} \right.$$

The value, K_G , represents the grid dynamic stiffness and was determined experimentally from grid impact tests. These tests were conducted

TABLE 3-1

MECHANICAL CONSTANTS FOR 17x17 8-GRID
OPTIMIZED FUEL ASSEMBLY MODEL (FULL)

No.	Mass lb-sec ² /in	Spring Stiffness lb/in.	Damping Coefficient lb-sec/in.
1	[]]
2			
3			
4			
5			
6			
7			
8			
9			
10			
11			
12			
13			
14			
15			
16			
17			
18			
19			
20			
21			

+(a,b,c)

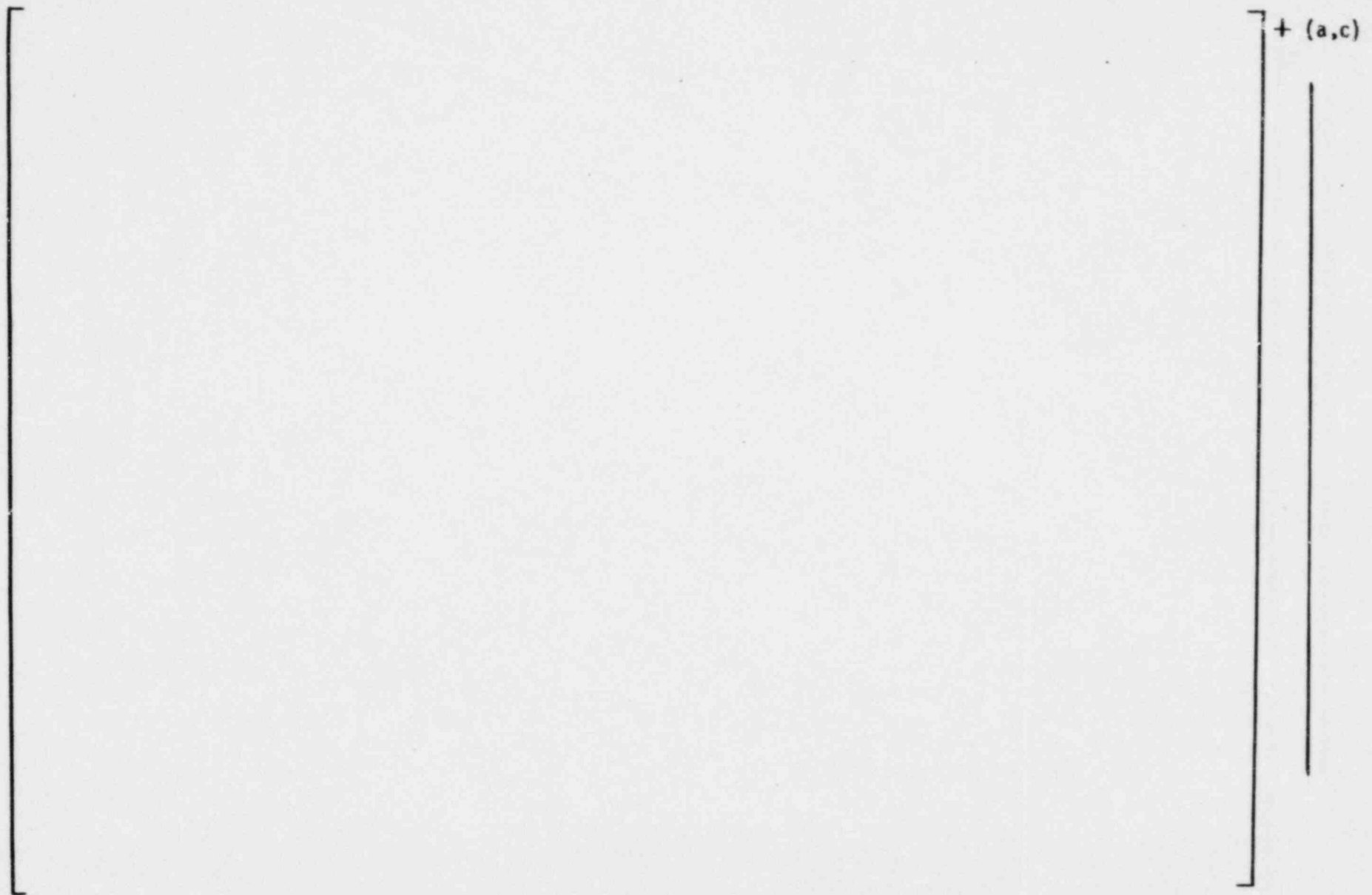


Figure 3-10 Schematic Representation of Computer Model used to Analyze Core Dynamic Response

(a,c)

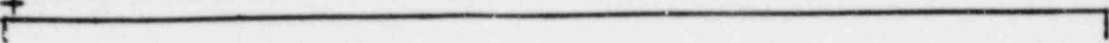


Figure 3-11 Fuel Assembly Finite Element Model

1

1

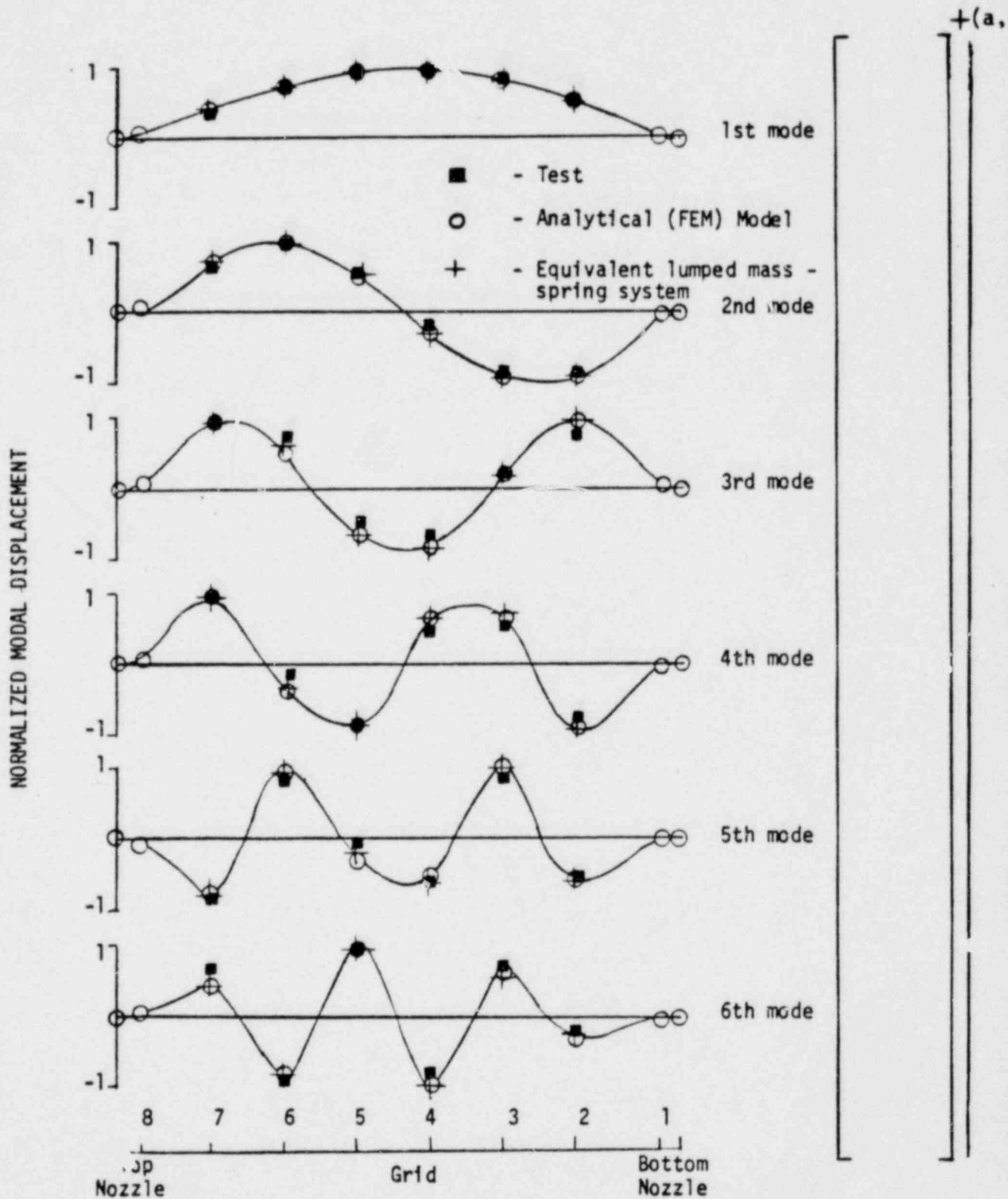


Figure 3-12 412 17x17 8-Grid Optimized Fuel Assembly Normalized Vibrational Modal Shapes

both at ambient temperature and operating temperature using prototype grids. Partial length fuel tubes were inserted in the grids to simulate reactor structural support conditions. A pendulum type impact fixture was used which simulated the impact loads predicted by seismic analysis. The impact hammer weight was predetermined based on the fuel assembly grid span weight. A load cell was mounted in series with the grid to measure the impact force and duration. The grid dynamic buckling strength, impact duration, and the restitution (impact damping, C_G) were obtained from these tests and incorporated into the reactor core (seismic) model. The grid typical buckling failure mode obtained from the dynamic impact tests indicated local deformation of two inner rows of cells. This type of failure mode is advantageous since the thimble tube locations are not distorted. The buckling strength obtained from the grid dynamic tests are compared with fuel assembly grid impact forces obtained from the seismic analyses of the reactor core model.

3.2.6 CORE SEISMIC RESPONSES

The reactor vessel model was analyzed using the synthesized time history applied at the reactor support. The responses of the upper core plate, lower core plate, and the baffle plate obtained from this model were used as the input to the reactor core model. The maximum responses of an optimized fuel assembly are used to assess the fuel assembly seismic capability.

The central grids (grid No. 4 and No. 5) relative displacement responses for the 17x17 8-grid optimized fuel assemblies No. 1, No. 10, and No. 15 are plotted and shown in Figures 3-13 through 3-15, respectively. Figure 3-14 shows that fuel assembly No. 10 has a maximum fuel assembly deflection of []⁺ inches at t=5.3090 seconds.

(a,c)

Figures 3-13 and 3-16 show the fuel assembly central grid responses for the peripheral fuel assemblies. The displacement plots indicated that the fuel assembly motion was limited by the core barrel restraints which in turn resulted in grid impact forces.

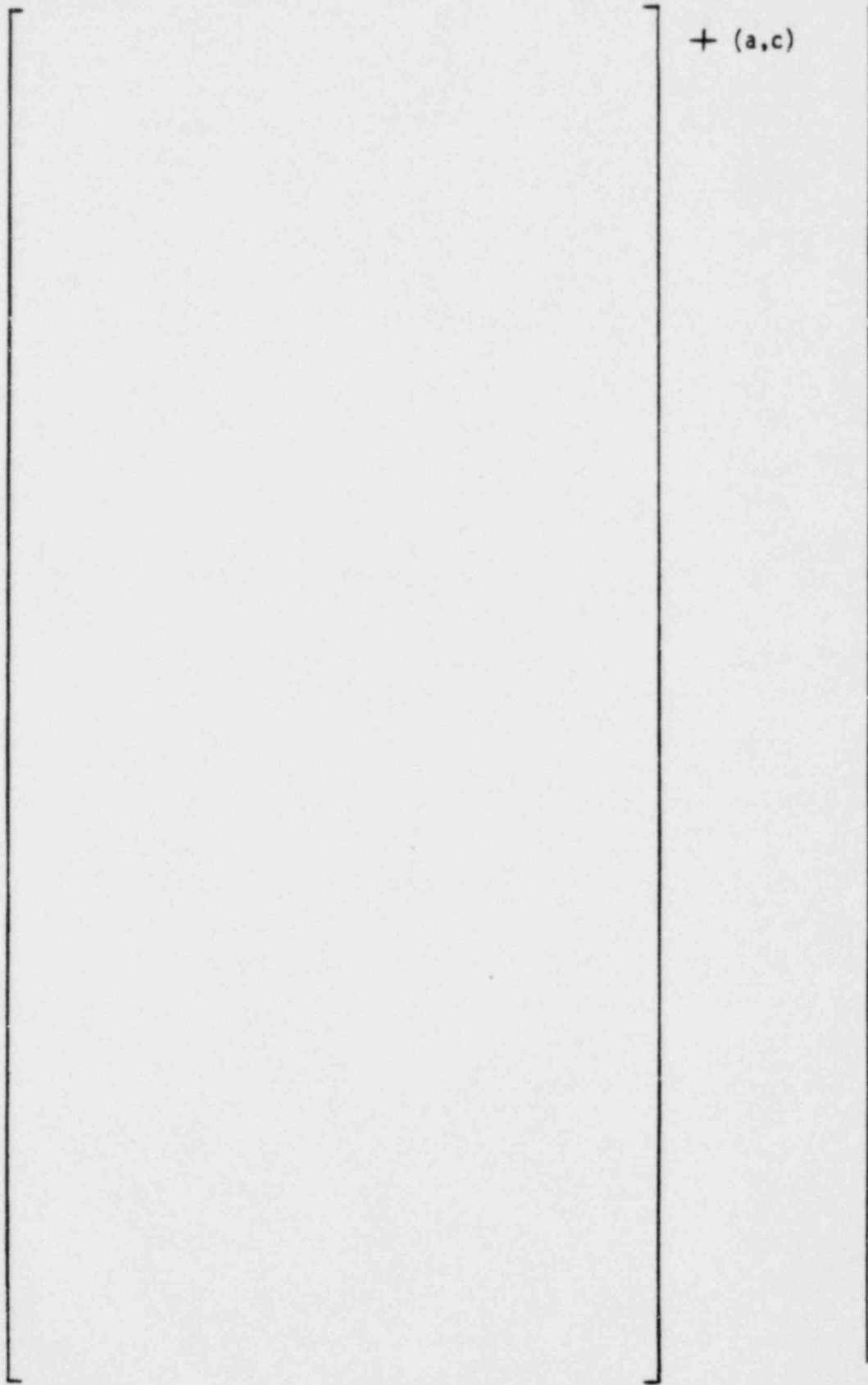


Figure 3-13 - Displacement Responses of Fuel Assembly
No. 1 - Grid No. 5 and Grid No. 4

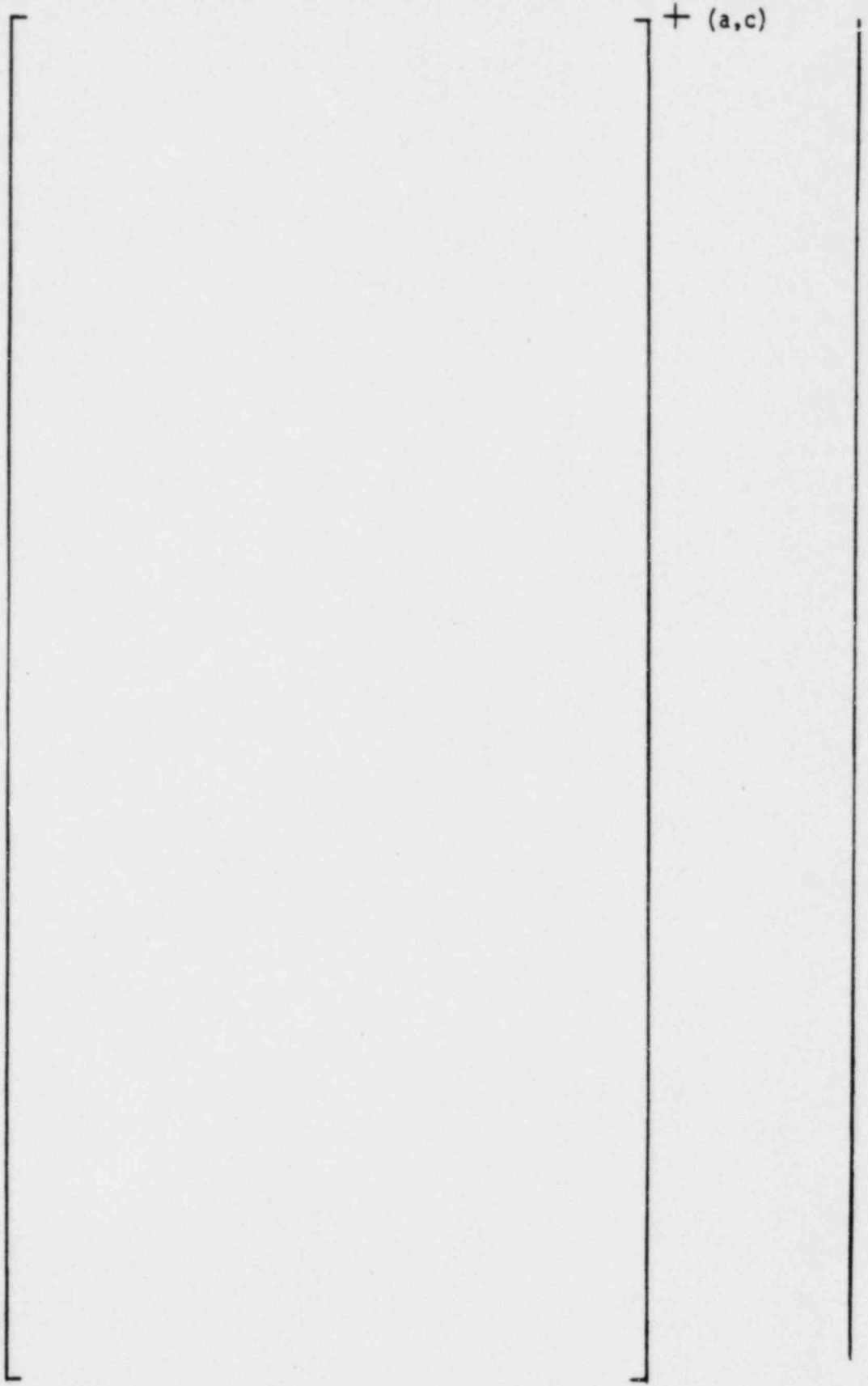


Figure 3-14 Displacement Response of Fuel Assembly
No. 10 - Grid No. 5 and Grid No. 4

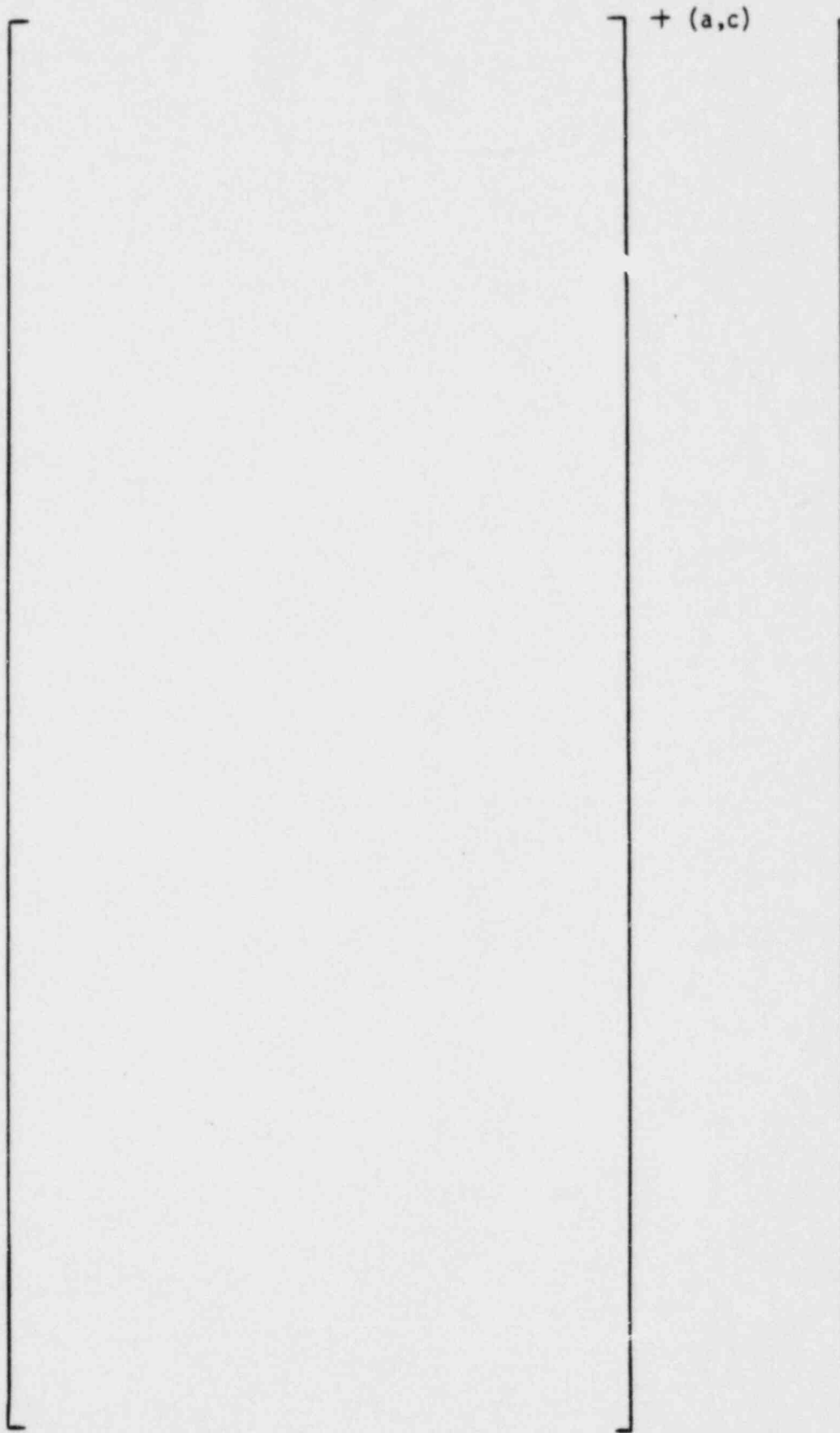


Figure 3-15 Displacement Responses of Fuel Assembly
No. 15 - Grid No. 5 and Grid No. 4

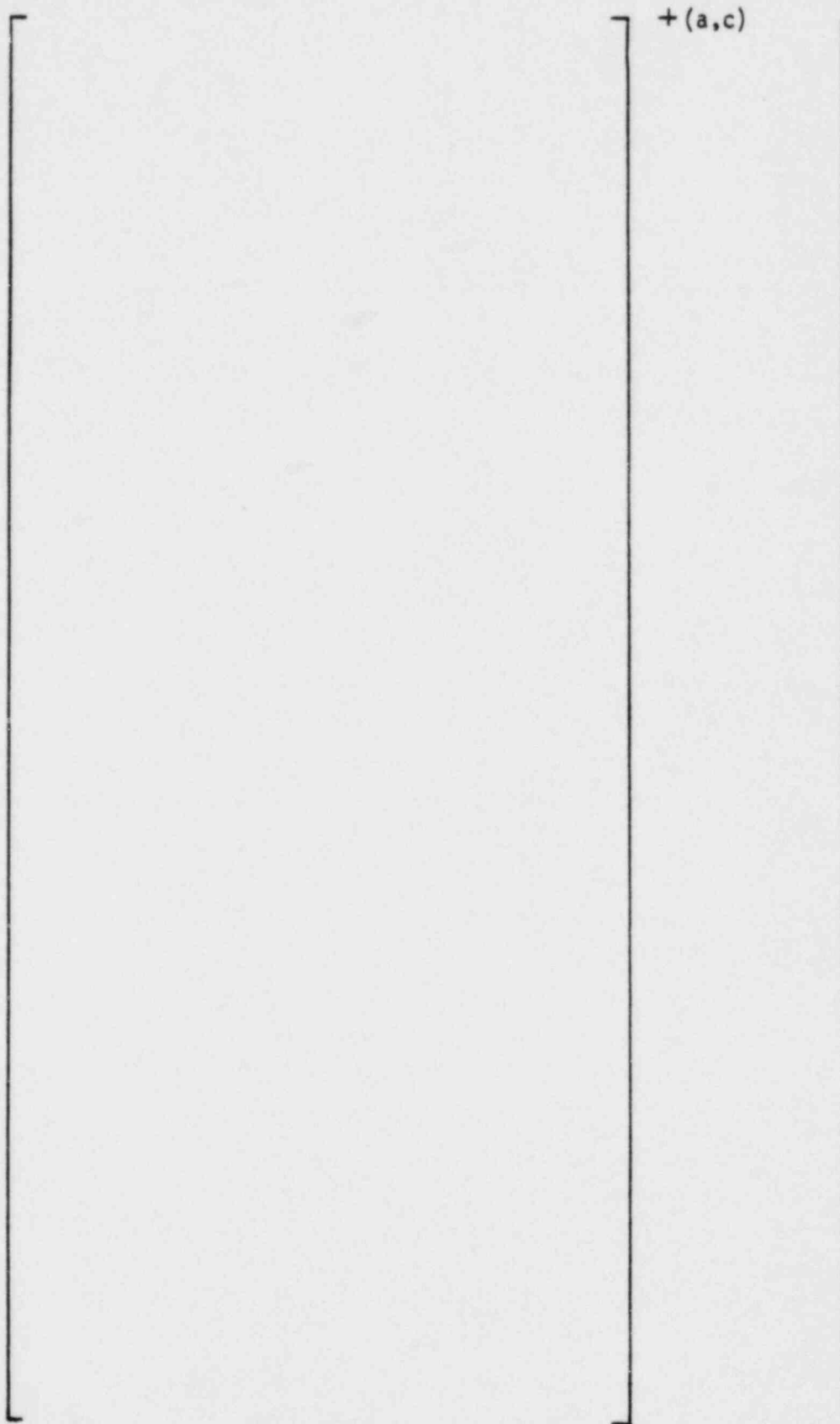


Figure 3-16 Impact Force Responses Between Fuel Assembly No. 1 and Baffle Plate - Grid No. 5 and Grid No. 4

The central grid impact force response for the peripheral fuel assemblies (No. 1 and 15) during a ten second seismic analysis are shown in Figures 3-16 and 3-17. A maximum impact force of []⁺ lbs between grid No. 4 of the first fuel assembly and the baffle plate restraints occurred at t=5.2365 seconds after initiation of the postulated seismic events.

(a,c)

The seismic results of a reactor core comprised of 193 17x17 8-grid optimized fuel assemblies are summarized in Table 3-2. The tabulated values are the absolute maxima at each of the designated grid elevations. Based upon the maximum relative displacement response, the fuel assembly component stress distributions were then calculated using a general fuel assembly model as described in Section 3.2.2.

The maximum grid impact force of []⁺ lbs. is well below the experimentally established lower 95 percent confidence limit of the true mean Zircaloy grid dynamic crush strength of []⁺ lb at operating temperature, 600°F. It is thus concluded that a coolable geometry is maintained during the postulated conservative seismic event.

(a,c)

(a,c)

The results of the full core seismic analysis indicated that the grid impact force and the fuel assembly relative displacement responses were approximately symmetric with respect to the middle elevation of the reactor core. The symmetric responses were due to the core geometric configuration and the seismic forcing functions. The relative horizontal displacement between the upper core plate (including the upper core barrel) and the lower core plate is small in comparison with the amplitude of the horizontal oscillation. The input forcing functions can be considered as approximately symmetric. Thus, a symmetric model could be used as an alternate system for core seismic analysis.

3.2.7 FUEL ASSEMBLY SEISMIC STRESSES

The results of the analysis using the synthesized seismic wave indicated a maximum fuel assembly center grid displacement of []⁺ inch, which was equivalent to the physical limit imposed by the accumulated interfuel assembly gaps plus grid flexibility.

(a,c)

TABLE 3-2

17x17 8-GRID OPTIMIZED FUEL ASSEMBLY
SEISMIC ANALYSIS RESULTS SUMMARY

Grid Impact Force				Max. Peripheral FA* Relative Displacement		
Grid No.	FA No.	Value (lbs)	Time	FA No.	Value (inches)	Time
7	[
6						
5						
4						
3						
2						

+(a,c)

*The relative displacement with respect to the fuel assembly centerline.

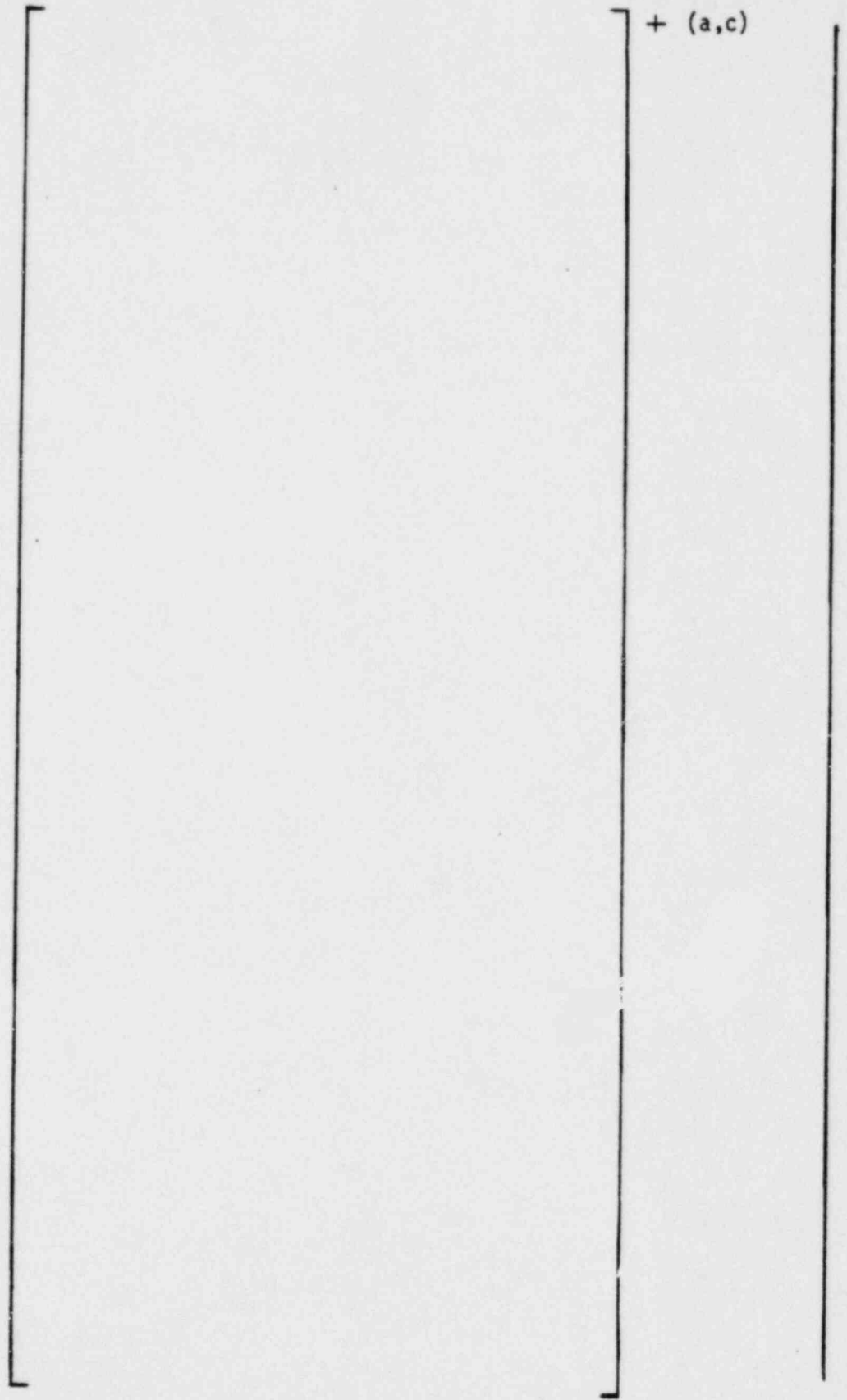


Figure 3-17 Impact Force Responses Between Fuel Assembly No. 15 and Baffle Plate - Grid No. 5 and Grid No. 4

Based on the maximum displacement response, the fuel assembly stress distributions were calculated using the fuel assembly lateral model. The calculated thimble and fuel tube stresses corresponding to a standard fuel assembly are tabulated in Table 3-3. The tabulated stresses were the maximum values obtained between grids for the particular span.

The maximum stresses for various fuel assembly components were compared with the allowable limits and are tabulated in Table 3-4. All the calculated seismic stresses are well below the acceptable limits.

The critical thimble tube buckling stress due to combined bending moment and axial compression would result in substantially higher stress than the material yield strength. As shown in Table 3-4, the combined stress is well below the yield strength, thus the thimble tube will not buckle elastically.

3.3 LATERAL BLOWDOWN ANALYSIS

3.3.1 ANALYTICAL PROCEDURE

The fuel assembly responses resulting from a limiting pipe break accident were analyzed using the time history method. The limiting LOCA accident was established based on the results of a series of parametric studies on various pipe break locations and sizes for a typical Westinghouse four loop reactor design.

The forcing function used in the analysis was an asymmetric transient loading with respect to the reactor core model. It was developed from the time dependent hydraulic cavity pressure, loop mechanical loads and lateral loads as a result of a pipe rupture. The dynamic characteristics of the complete fuel assembly at operating temperature conditions were fully preserved in a reactor core modeling consideration. The reactor core finite element model, which is similar to the seismic core model as described in Section 3.2 was used to obtain the fuel assembly deflection and grid impact loads. The general analytical procedure for obtaining the grid impact forces and fuel assembly deflection responses is outlined in Figure 3-18

TABLE 3-3

FUEL ASSEMBLY STRESSES FOR SSE

Thimble Stresses (ksi)				Fuel Tube Stresses (ksi)			
Span Location	Max Direct	Max Bending	Max Combined	Max Direct	Max Bending	Max Combined	
Top 9							+(a,c)
8							
7							
6							
5							
4							
3							
2							
Bottom 1							

TABLE 3-4

FUEL ASSEMBLY MAXIMUM SEISMIC STRESSES AND LIMITS AT
REACTOR OPERATING CONDITION (600°F)

Component	Primary Stresses (ksi)			Combined Stresses (ksi)
	Max. Direct	Max. Bending	Allowable ^[a]	Max Direct and Bending Allowable ^[a]
Thimble	[] + (a,c)
Sleeve				
Insert				
Fuel Rod ^[b]				
Top and Bottom Nozzles				

a. Westinghouse WCAP 9500 Sec. 4.2.1.5.

b. The primary operating stresses due to the pressure differential across the cladding of 1250 psia at BOL zero burnup, hot operating temperature, are $\sigma_L = []^+$ ksi and $\sigma_{Hoop} = []^+$ ksi. The resulting combined stresses in (a,c) comparing with allowable limits indicate that all stresses are well below the acceptable limits.

c. Small Value.

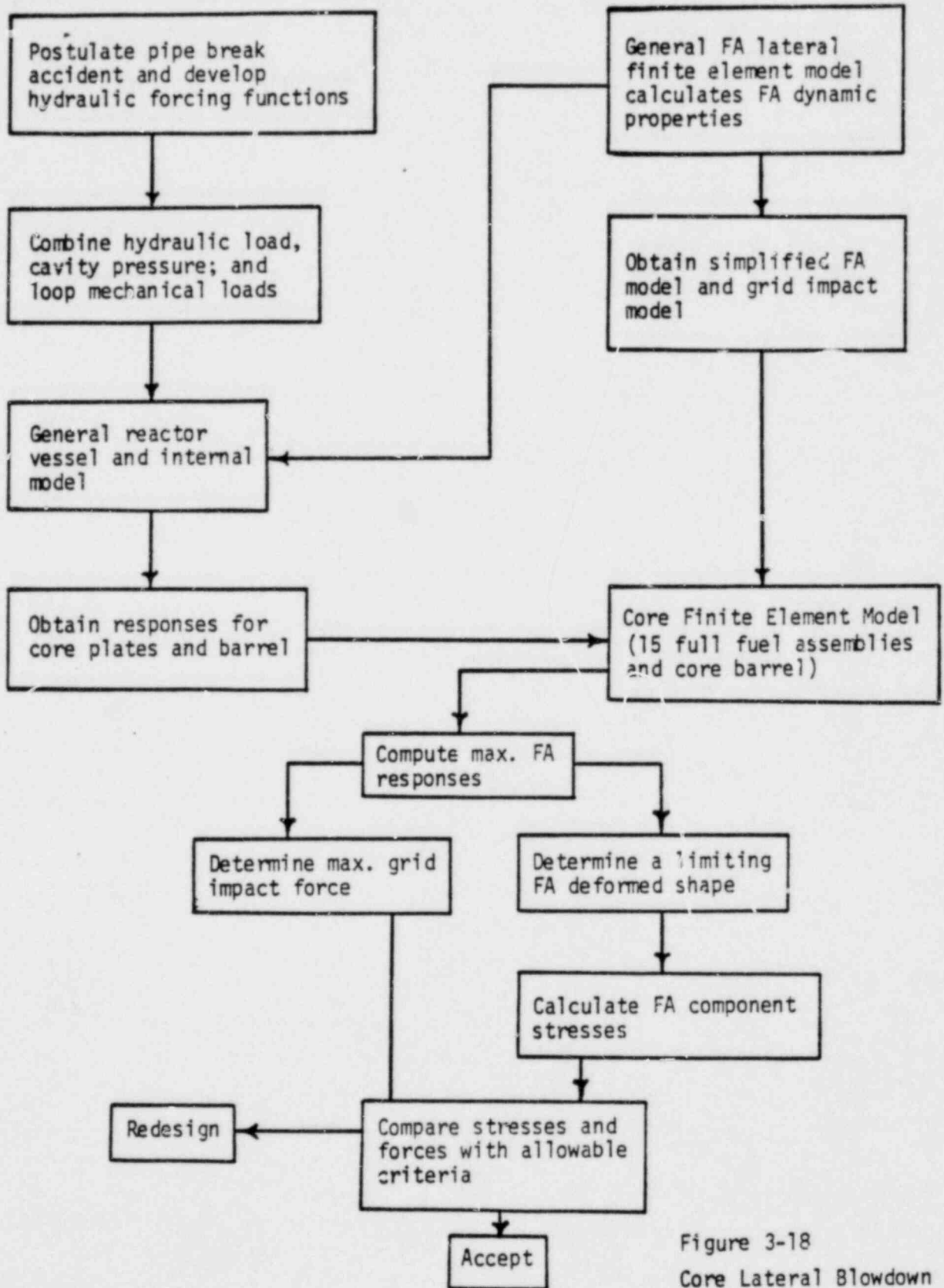


Figure 3-18
Core Lateral Blowdown
Analysis Procedure

3.3.2 ANALYTICAL METHOD AND MODELING

The vessel motion induces primary lateral loads on the reactor core. The seismic model described in Section 3.2 was used to obtain the fuel assembly deflection and grid impact responses. The upper core plate, lower core plate, and upper core barrel motions (Figure 3-19) resulting from the reactor vessel movement indicated significant differences. These differences were noticed at any instant after the initiation of the pipe rupture. A complete core finite element model consisting of the maximum number of fuel assemblies across the core diameter was used to analyze the fuel assembly responses.

Figure 3-19 shows the plots of typical transient motions for the upper core plate, lower core plate and core barrel. These motions are obtained from the time history analysis of the general reactor vessel and internals finite element model as described in Section 3.2.3.

The complete core model is schematically shown in Figure 3-20. The lower core plate, upper core plate, and the core barrel motions at each individual grid elevations designated as $F_1(t)$, $F_2(t)$, $F_3(t)$, ..., and $F_8(t)$, respectively were then simultaneously applied to the complete core model.

3.3.3 LATERAL BLOWDOWN ANALYSIS RESULTS

The fuel assembly response, namely, displacements and grid impact forces, was obtained from the reactor core model using the core plates and core barrel motions. A typical displacement response for a peripheral fuel assembly position at each individual grid elevation relative to the fuel assembly centerline is given in Figure 3-21. Examination of the fuel assembly response curves indicate that the initial relative motion is in the opposite direction with respect to the excitation motion. The fuel assembly motion then reverses resulting in impacting at the baffle wall opposite the pipe break. The maximum fuel assembly deflection which occurs in the peripheral fuel assembly was approximately []⁺ inches at grid No. 4 of fuel assembly No. 2 at $t=0.3936$ second.

(a,c)

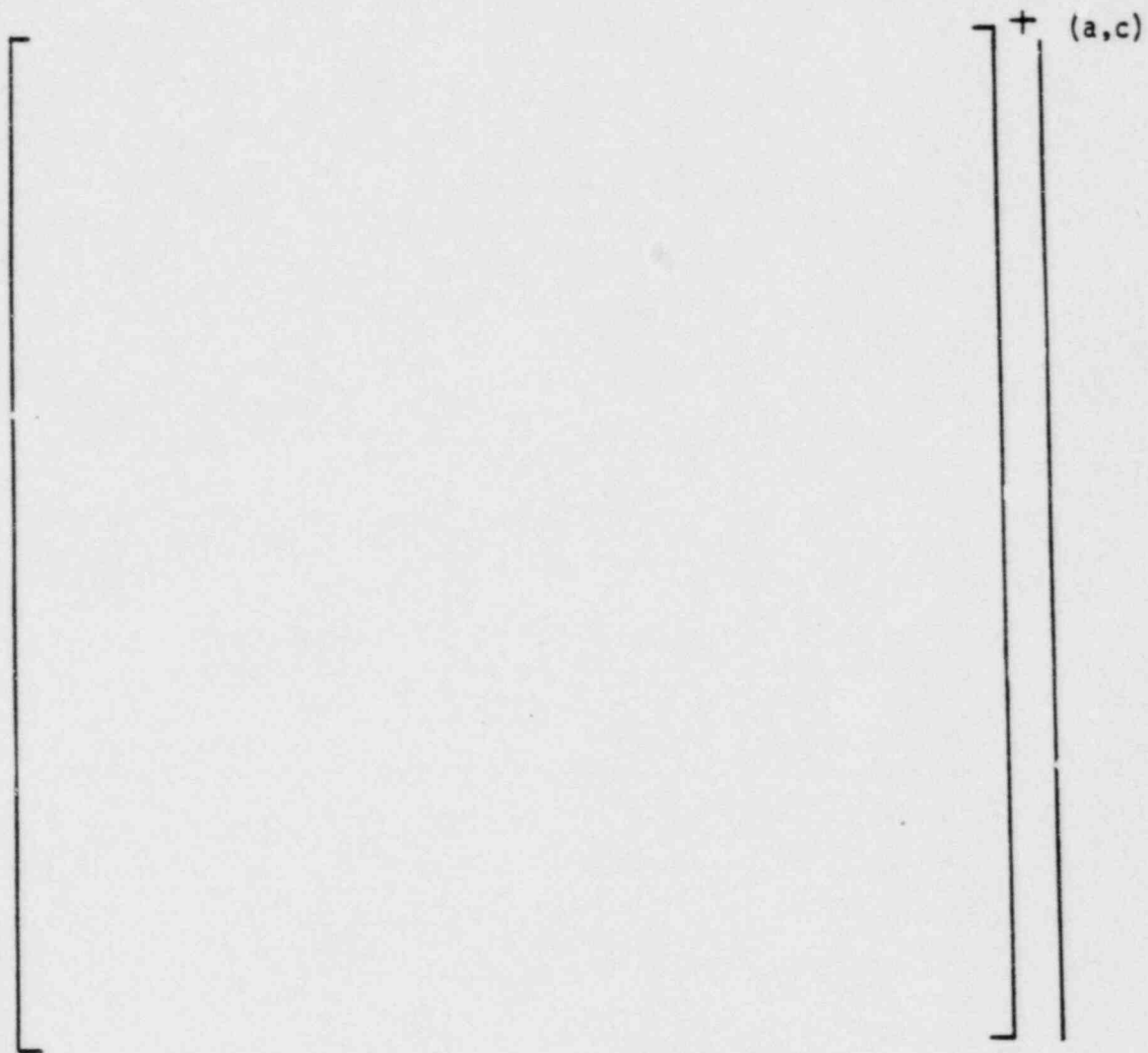


Figure 3-19 Upper Core Plate, Lower Core Plate and Core Barrel Motions

3-45

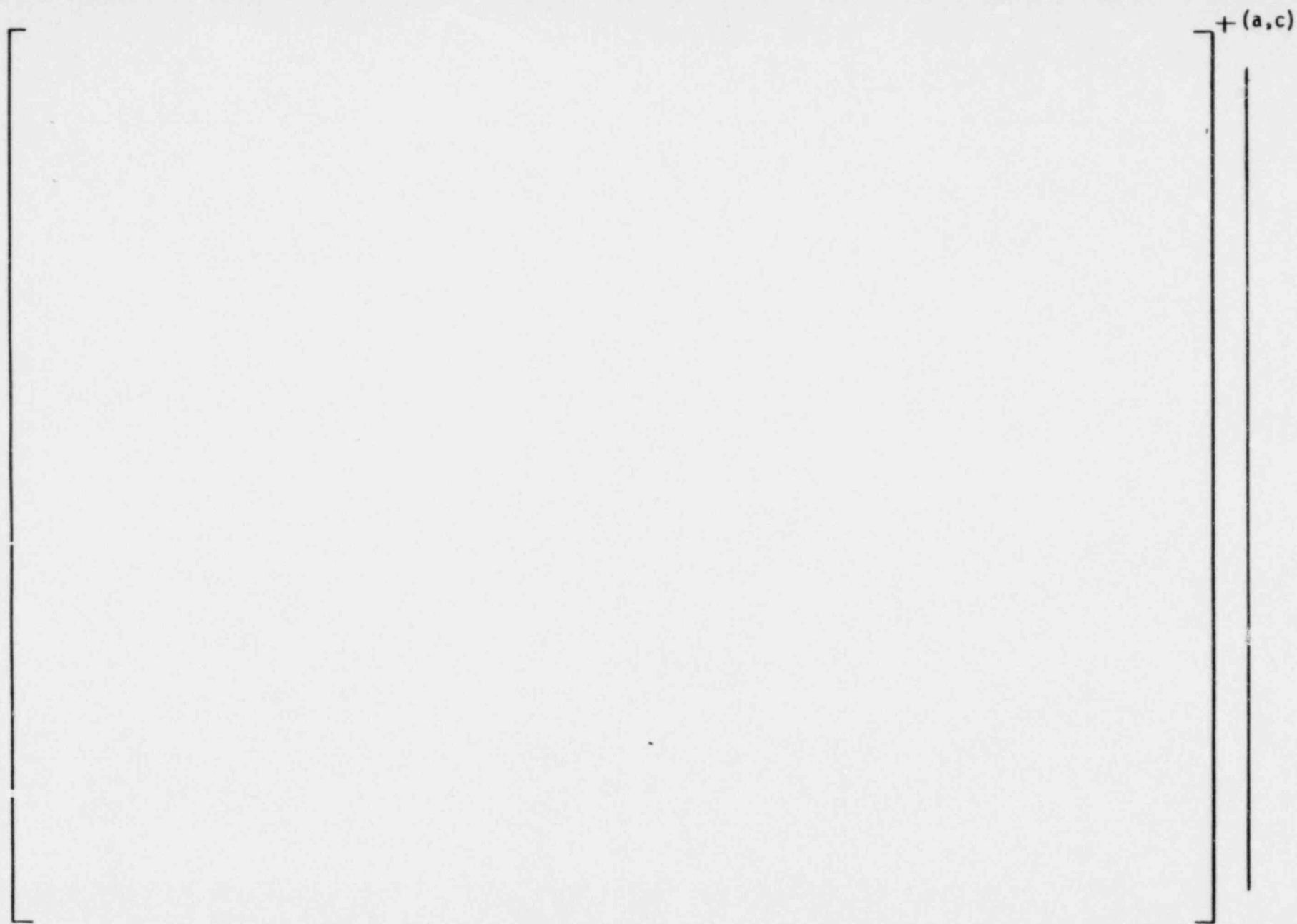


Figure 3-20 Schematic Representation of Computer Model used to Analyze Core Dynamic Response

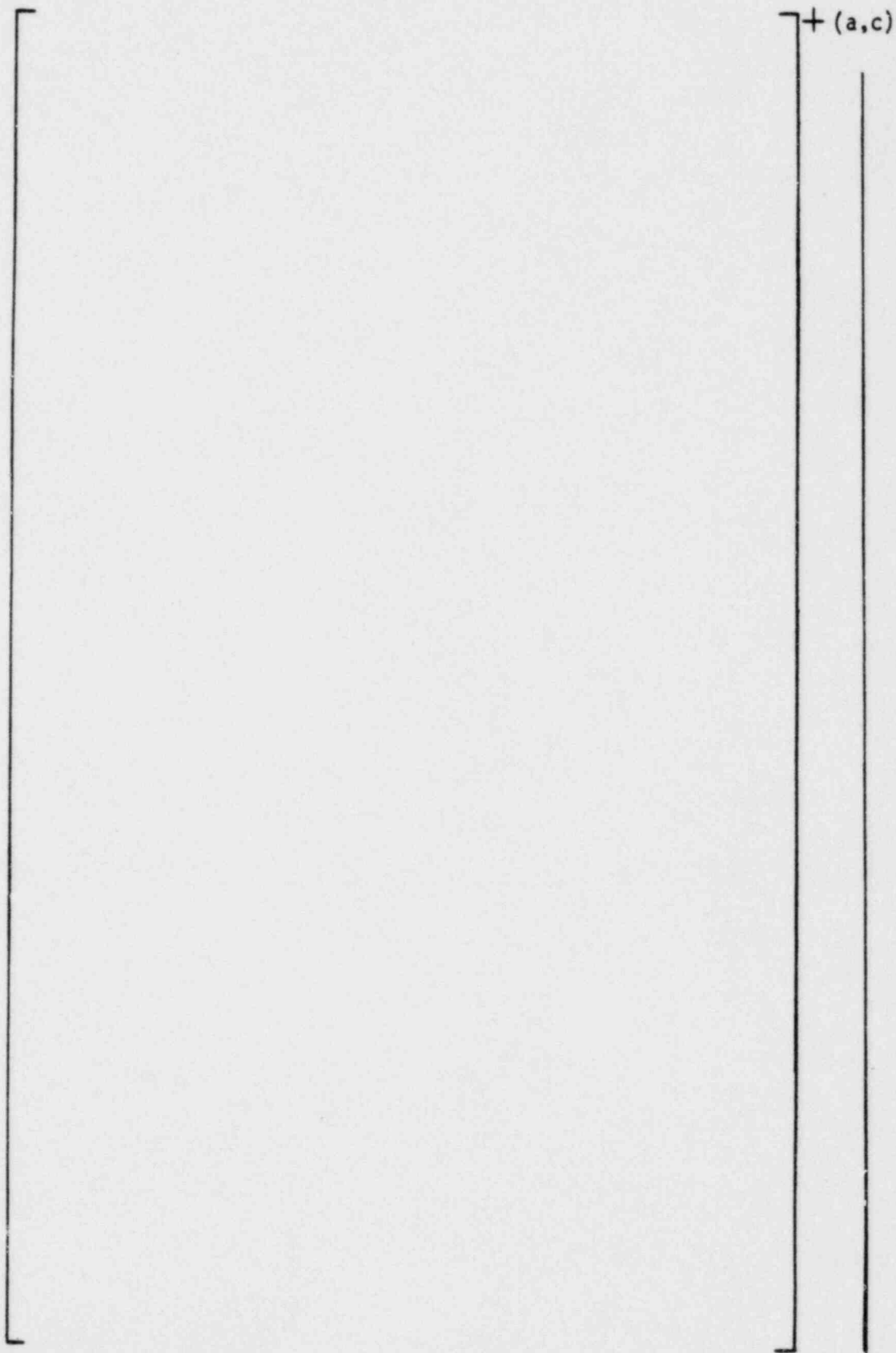


Figure 3-21 Optimized Fuel Assembly No. 1 Relative Displacement Response

The fuel assembly grid impact forces were also obtained from the reactor core time history response. The maximum impact force occurs at the peripheral fuel assembly location adjacent to the baffle wall. The peak impact force occurs at the 4th grid elevation. The grid impact forces are also rapidly attenuated for fuel assembly positions inward from the peripheral fuel. The grid impact force for the peripheral fuel assembly adjacent to the baffle on the opposite side of the reactor were substantially lower. Consequently, only a small portion of the core experiences substantial grid impact forces. The maximum grid impact force of [. . .]⁺ lbs occurred at grid location No. 4 at t=0.2841 seconds after initiation of a postulated RPV inlet nozzle break accident. Figure 3-22 shows the typical impact force plots for peripheral fuel assembly No. 1. The impact force responses at grid No. 4 between the peripheral fuel assemblies and baffle plates are given in Figure 3-23.

(a,c)

The maximum responses for the various grids of a 17x17 8-grid optimized fuel assembly are summarized in Table 3-5. The stress distribution for all optimized fuel assemblies is tabulated in Table 3-6. The maximum fuel assembly component stresses together with their allowable limits are given in Table 3-7. As seen from the tabulated values from this table, the fuel assembly stresses resulting from the maximum fuel assembly deflection indicated substantial safety margins compared to the allowable values.

3.4 VERTICAL BLOWDOWN ANALYSIS

The blowdown accident is postulated as a sudden rupture of a primary coolant pipe. This accident causes waves to propagate through the reactor pressure vessel and excite the various internal components. The mathematical modeling and techniques used to determine the component dynamic response of the reactor internals model are discussed in Reference 7.

3.4.1 FUEL ASSEMBLY AXIAL MODEL

The fuel assembly model shown in Figure 3-24, a one-dimensional (axial) finite element model, was used to represent the fuel assembly structure

TABLE 3-5

17x17 8-GRID OPTIMIZED FUEL ASSEMBLY

[]⁺ ANALYSIS RESULTS

(a,c)

Grid Impact Force				Max. Peripheral FA* Relative Displacement		
Grid No.	FA No.	Value (lbs)	Time	FA No.	Value (inches)	Time
7						
6						
5						
4						
3						
2						

+(a,c)

*The relative displacement with respect to the fuel assembly centerline.

TABLE 3-6

FUEL ASSEMBLY STRESSES FOR

[]⁺

(a,c)

[]⁺

(a,c)

Thimble Stresses (ksi)				Fuel Tube Stresses (ksi)		
Span Location	Max Direct	Max Bending	Max Combined	Max Direct	Max Bending	Max Combined
Top 9						
8						
7						
6						
5						
4						
3						
2						
Bottom 1						

+(a,c)

TABLE 3-7

FUEL ASSEMBLY COMPONENT STRESSES AND LIMITS, LOCA

Component	Max. Direct Stress Intensity (Ksi)	Max. Bending Stress Intensity (Ksi)	Allowable Stress Limit (Ksi)	Max. Combined Stress Intensity (Ksi)	Allowable Stress Intensity (Ksi)
Fuel Rod	[]
Thimble					
Sleeve					
Insert					

+(a,
| 1

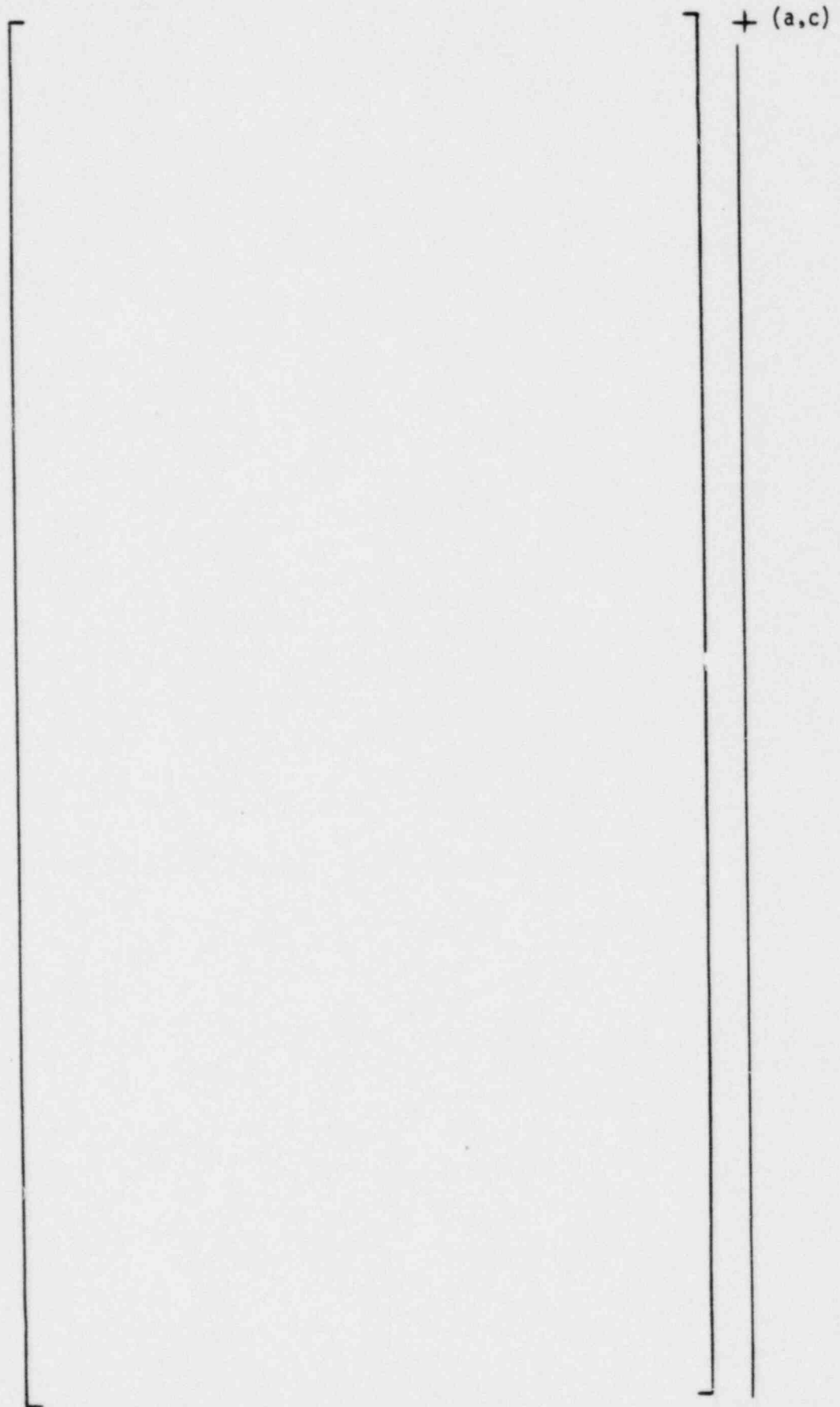


Figure 3-22 OFA Grid Impact Force Responses
Fuel Assembly No. 1

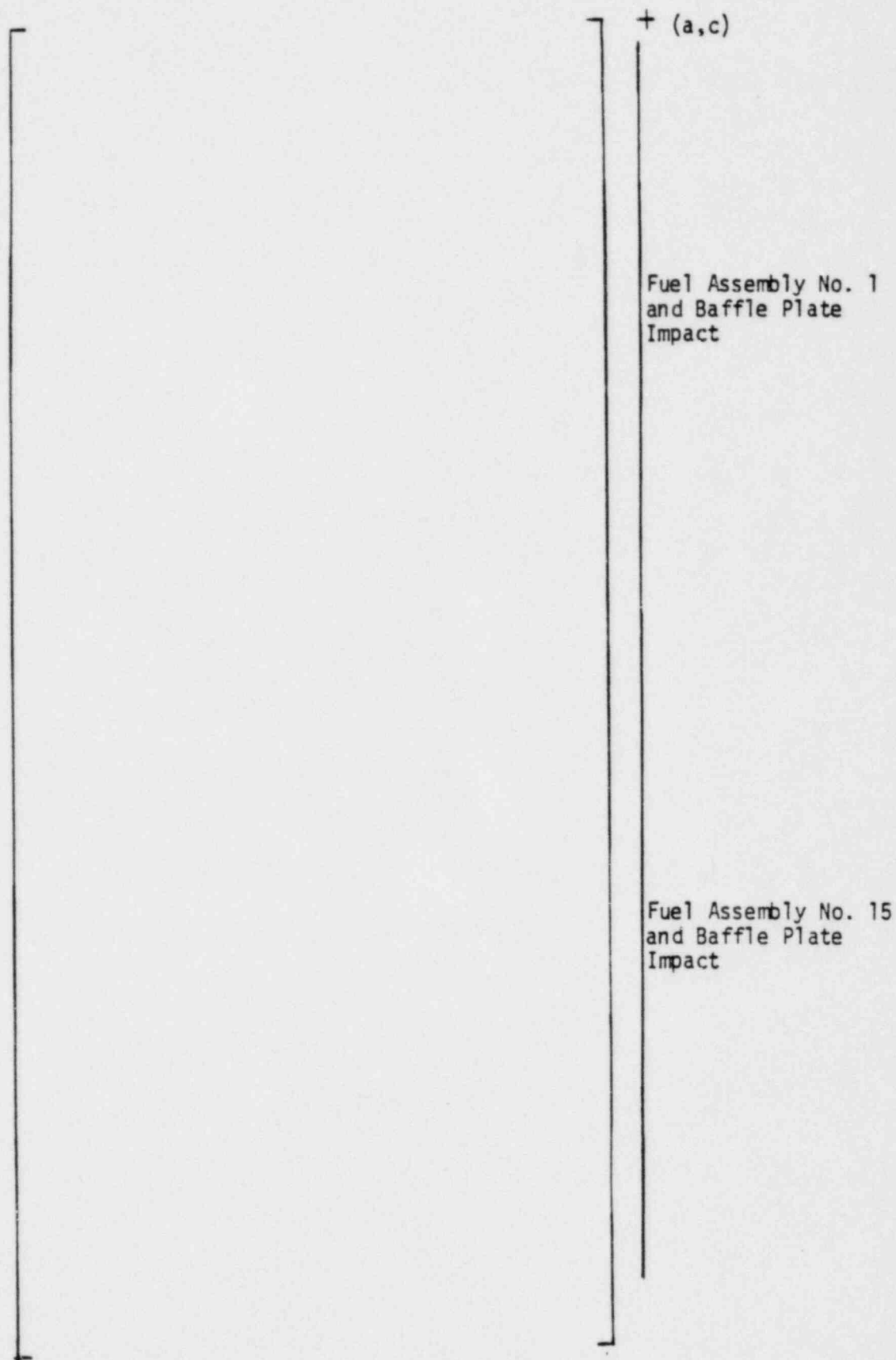


Figure 3-23 Optimized Fuel Assembly Grid No. 4 Impact Force Responses Between Peripheral Assemblies and Baffle Plate

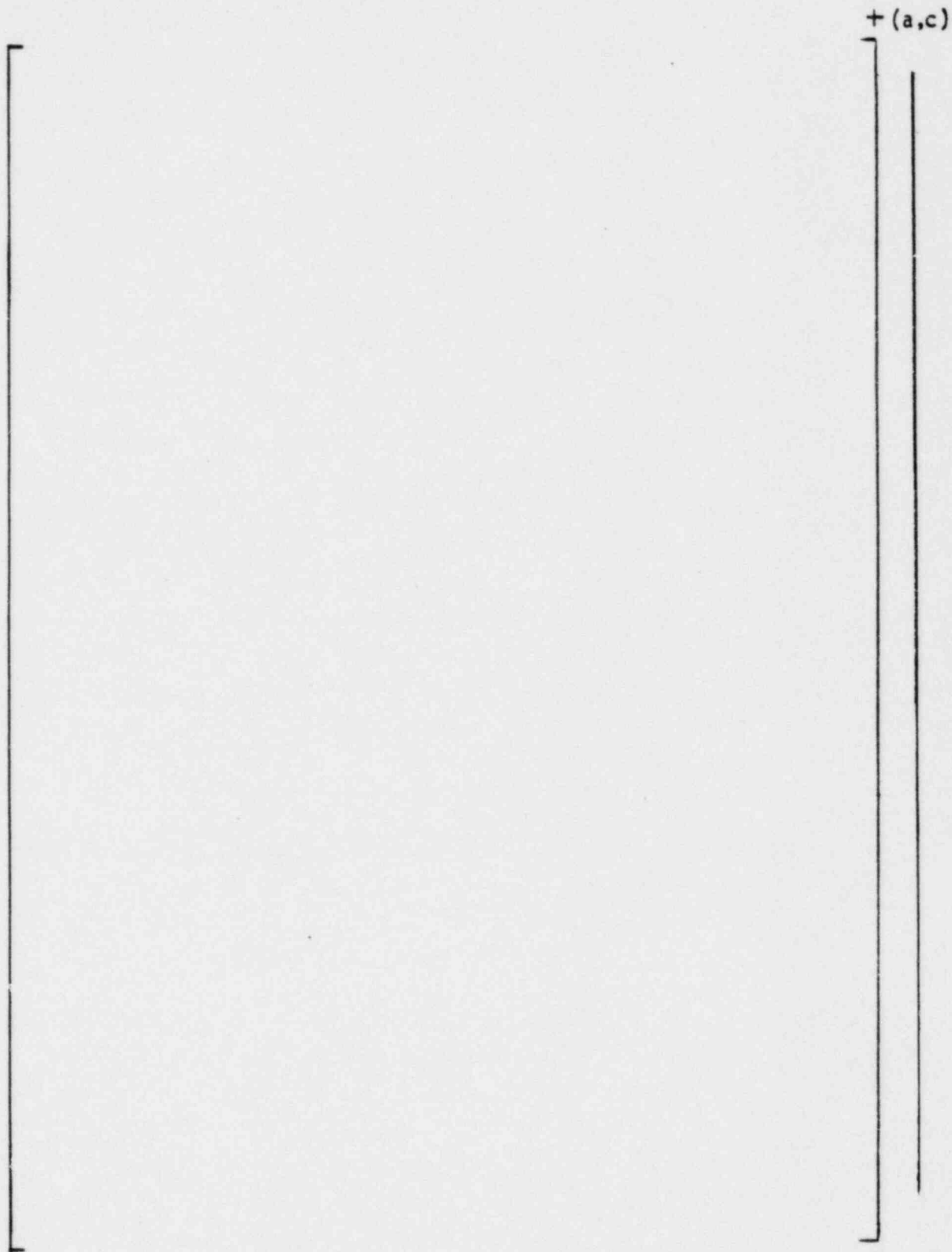


Figure 3-24 Fuel Assembly Finite Element Model for Axial Analysis

and was analyzed using a general finite element code. The model is the same as that used in standard Westinghouse fuel assembly analyses⁽²⁾ with appropriate changes for 17x17 OFA mechanical properties. The top and bottom nozzles are represented by the one dimensional spring elements 1-3 and 19-23, respectively. The one-dimensional spring elements shown between nodal points 3 and 19 inclusively represent the total (24) thimble stiffness. The stiffness of fuel rods is modeled with the 1-D spring elements between nodes 4, 6, etc. to 18. The fuel rod-grid friction is simulated by the sliding elements 4-5, 6-7, etc. The linear spring 21-19 represents the stainless steel inserts.

The 1-D spring finite element used in the analytical model, depending on the mechanical response desired, can be chosen as a single or double acting spring, with or without an initial preload. In addition, a parallel viscous damper with a concentrated nodal mass can be added to the spring elements for dynamic analysis. The sliding elements are primarily shear transmitting members which produce relative motion or slip between adjacent elements when the shear load exceeds the maximum predetermined frictional value.

The spring rate for the various spring elements was determined as follows:

a) For the thimble elements

$$k_i = \frac{nAE}{L_i}$$

where

- L_i = length of span i
- A = thimble cross-sectional area
- n = number of thimbles

b) For the fuel rod elements, the above equation is reevaluated using fuel rod properties

The model constants were obtained using the following assumptions:

- Nominal fuel rod and thimble dimensions
- Axial loads equally distributed (i.e., each of the thimbles or fuel rods carry the same loads respectively).
- All the fuel rods at each grid elevation slip as a unit when the force exceeds the total drag force of all the rods per grid.
- The fuel rod-grid friction forces were obtained experimentally for the cold BOL conditions. The friction forces at operating conditions were determined based on the fuel rod normal forces.
- The spring stiffness values were based on the material properties at operating temperatures.

3.4.2 FUEL ASSEMBLY MODEL VERIFICATION

3.4.2.1 Static Deflection Analysis

An analytical study of the fuel assembly axial model, shown in Figure 3-24, was performed in which the sensitivity and effects of the various model physical parameters were determined. The fuel assembly axial load deflection characteristics were calculated for the normal operating conditions. Plots of the load deflection characteristics for the hot (600°F) and cold conditions are presented in Figure 3-25. The nonlinear behavior is a result for fuel rod slippage in the grids as the rod to grid forces reach the friction force limit. The fuel rod slippage occurs initially at the exterior grid elevations (i.e., the grids adjacent to the nozzles) and continues, successively, toward the fuel assembly interior grid locations for increasing axial loads.

3.4.2.2 Dynamic Analysis

During a blowdown accident, the hydraulic forces produced by a main coolant pipe rupture cause the fuel assemblies to translate vertically

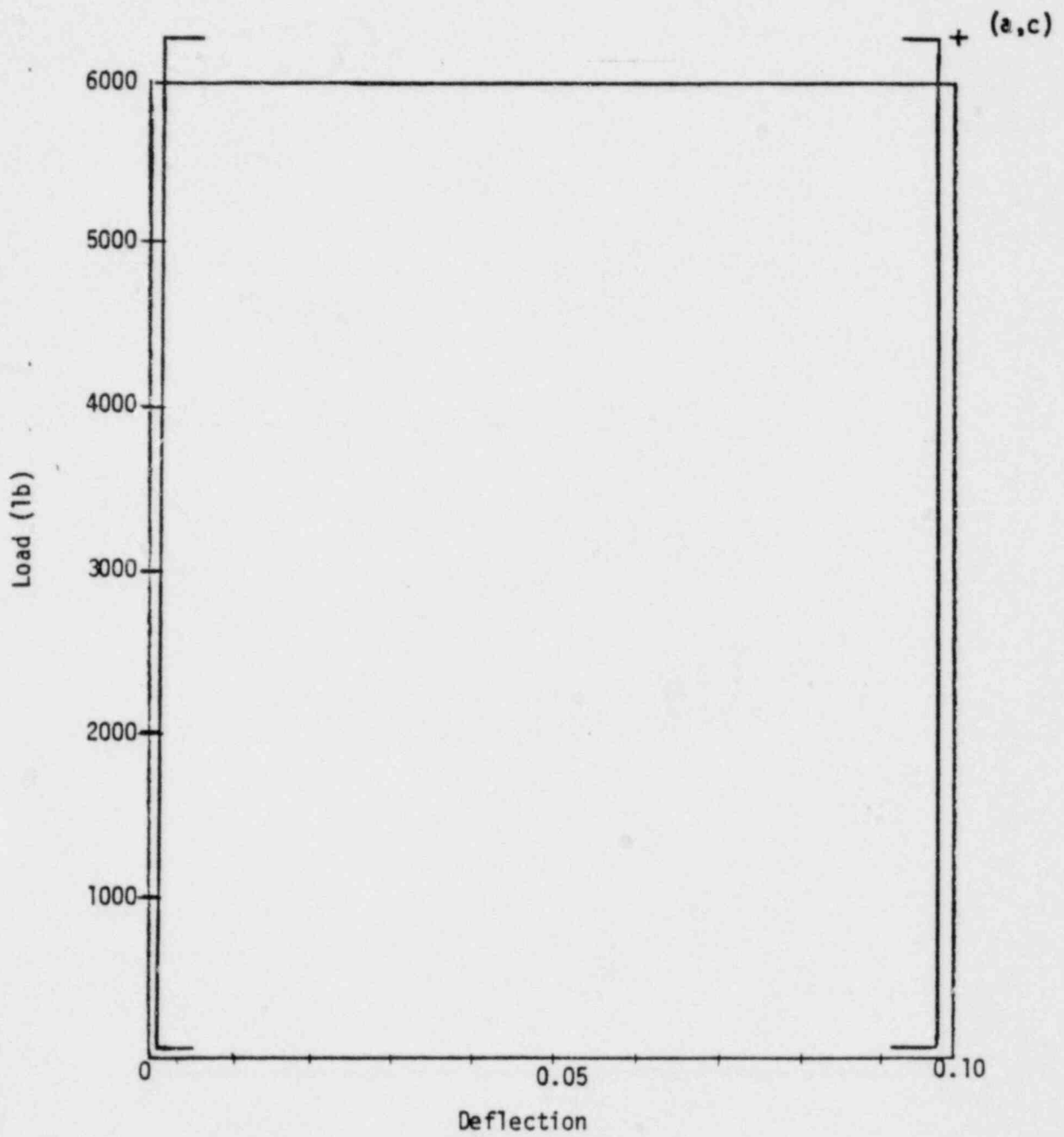


Figure 3-25 FUEL ASSEMBLY AXIAL LOAD DEFLECTION CHARACTERISTICS

and impact with the upper and lower core plates resulting in rapidly applied axial loads. To ascertain the fuel assembly impact force accurately under these conditions, an experimental and analytical study of the fuel assembly was performed in which the fuel assembly was dropped vertically from a predetermined height onto a rigid constraint. The primary objective of the study was to simulate analytically the external forces generated by an axial impact and to determine the internal force and stress distribution within the fuel assembly of the various major components.

The finite element model formulated for the static axial stiffness study was used in the impact analysis to obtain the fuel assembly dynamic characteristics.

The viscous damper was modeled in parallel with the bottom nozzle to simulate the impact damping. The value for the damping coefficient was obtained from the following relation:

$$\text{Impact Damping Coefficient} = D \sqrt{4K_n M_f}$$

where:

K_n = bottom nozzle stiffness

M_f = fuel assembly mass

D = experimentally determined constant

The value for the impact damping coefficient was determined from experimental and analytic study. The fuel assembly impact loads were generated analytically by applying gravitational forces to the finite element model, suddenly releasing the constraints and allowing it to translate axially and impact with a rigid surface. This procedure was used to determine the fuel assembly impact force response versus impact velocity. The analytical prediction using the finite element model was compared with experimental data from fuel assembly axial impact tests.

A series of impact tests were performed in which a prototype 17x17 8-grid fuel assembly was dropped from predetermined heights of [

]⁺ inch. These drop heights were chosen so as to complement the values predicted analytically for a blowdown accident. The data obtained from these tests included fuel assembly external impact force (measured at the bottom nozzle), internal strain distribution, fuel assembly grid deflection, impact time, and coefficient of restitution. The tested fuel assembly was pregapped for the zircaloy grids to simulate the grid spring relaxation.

(a,c)

The test setup consisted of a full-length prototype fuel assembly, a rigid impact surface connected in series with a load cell, a magnetic quick release mechanism, and displacement transducers. The fuel assembly impact force and rebound versus drop heights were recorded. A parametric study was performed to determine the appropriate damping coefficients for the finite element model.

3.4.3 FUEL ASSEMBLY RESPONSE

An analysis of the reactor internals was performed for three break locations as defined in reference (6). The general locations and size of the break areas are as follows: [

]⁺ A summary of the fuel assembly maximum impact forces for the various cases considered are presented in Table 3-8. The fuel assembly displacement response for the various hot leg breaks showed no impacting of the top nozzle with the upper core plate. The []⁺ resulted in the largest fuel assembly impact force and, therefore, was used as a conservative value to assess the fuel assembly component stresses.

(a,c)

(a,c)

Figures 3-26 and 3-27 show the typical impact force responses at the fuel assembly bottom nozzle and top nozzle holdown spring, respectively.

3.4.4 FUEL ASSEMBLY COMPONENT STRESSES

The fuel assembly component forces are a nonlinear function of the assembly impact force. Consequently, an iterative process in which the

TABLE 3-8

FUEL ASSEMBLY IMPACT FORCES FOR VARIOUS BREAK LOCATIONS

Case	Break Location	Break Size (in ²)	Vertical Impact Forces Soft Support (lb)	Vertical Impact Forces Stiff Support (lb)
1 2 3				

+(a,c)

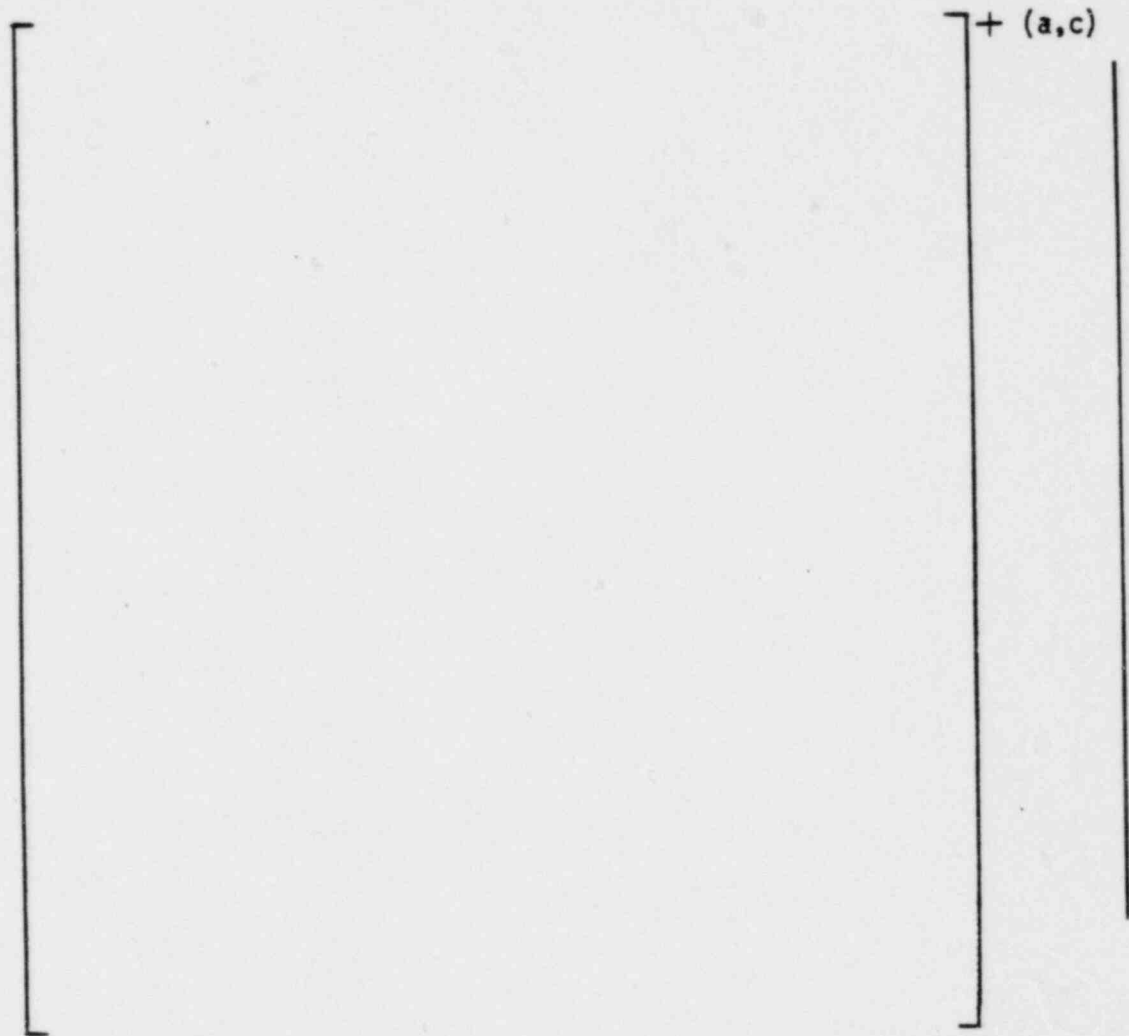


Figure 3-26 Impact Force at Bottom Nozzle

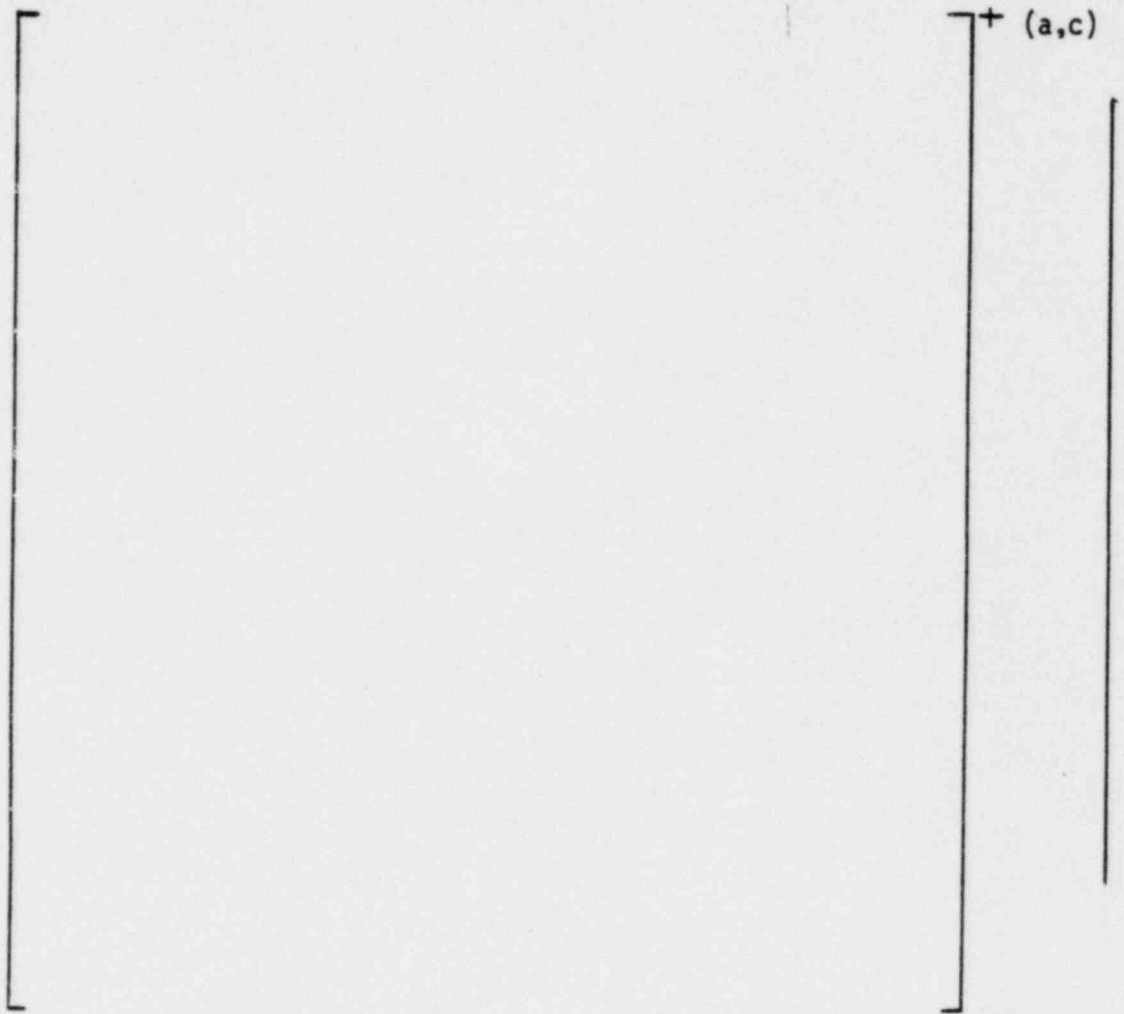


Figure 3-27 Holddown Spring Force at Top Nozzle

fuel assembly was impacted from various drop heights was used to obtain the desired impact force. The fuel assembly component forces and corresponding stresses resulting from a fuel assembly simulated drop impact analysis in which the impact force was []⁺ lbs. are presented in Table 3-9. The maximum component stresses obtained from the limiting cases are presented in Table 3-10.

(a,c)

3.5 SUMMARY AND CONCLUSION

The analytical results of the faulted condition evaluation are briefly summarized in the following paragraphs.

3.5.1 SEISMIC ANALYSIS

The time history method was used to obtain the maximum fuel assembly relative deflection and grid impact force responses. The synthesized seismic wave with its own response spectrum envelops the design floor, response spectrum at the reactor vessel support for a number of Westinghouse four loop, twelve foot fuel assembly plants. The core plate motions were obtained using the reactor vessel model with various combinations of reactor support stiffnesses. The most severe transient was selected as an input for the core model. The reactor core was evaluated using a discrete mass and spring finite element model and the time history motions as excitation input. The results of the analysis indicated that the maximum grid impact force was approximately []⁺ percent of the allowable grid load strength. The fuel assembly maximum deflection response was []⁺ inches, resulting in fuel rod and thimble stresses well below the established allowable values.

(a,c)

(a,c)

Based on the maximum responses obtained from the seismic analysis, component buckling strength, and allowable stress values, it is concluded that the 17x17 8-grid optimized fuel assembly is adequately designed to remain functional, i.e., the core coolable geometry will be maintained in the event of a Safe Shutdown Earthquake (SSE).

TABLE 3-9

FUEL ROD AND THIMBLE BLOWDOWN FORCES AND STRESSES

[]⁺

(a,c)

Location	Thimble		Fuel Tube	
	Load/ Thimble (lbs)	Direct Stress (ksi)	Load/ Tube (lbs)	Direct Stress (ksi)
1st span (bottom)	[]		[]	
2nd span				
3rd span				
4th span				
5th span				
6th span				
7th span				
8th span				
9th span (top)				

+(a,c)

*Inserts

**Sleeve

TABLE 3-10

FUEL ASSEMBLY COMPONENT BLOWDOWN STRESS AND LIMITS (KSI)

Component	Max. Uniform Stress Intensity	Allowable Stress Limit (P_M, P_L)	Combined Stress $\sigma_m + \sigma_B$	Allowable Stress Limits ($P_M + P_B, P_L$)
Thimble	[]
Fuel Rod				
Inserts				
Top Sleeves				
Top Nozzle Plate				
Bottom Nozzle Plate				

+(a,c)

[]^{+(a,c)}

3-64

3.5.2 LATERAL BLOWDOWN ANALYSIS

The lateral blowdown analysis was also performed to obtain the grid impact forces and fuel assembly deflection responses resulting from the most limiting main coolant pipe break. Since the resulting vessel motion was primarily an asymmetric transient, the finite element model representation of a full core was analyzed using the time history method. The most limiting break was identified as the [

] + break based on a series of fuel assembly responses.

(a,c)

The maximum fuel assembly relative deflection was approximately [] + inches. The fuel assembly component stresses resulting from this deflection indicate substantial margins compared to the allowable values. The maximum grid impact force was approximately [] + percent of the allowable grid load at temperature. The allowable grid impact load is established as the lower 95 percent confidence limit on the true mean of the experimentally determined grid crush strength at 600°F. It is concluded that the 17x17 8-grid optimized fuel assembly is structurally capable of resisting the hypothetical pipe break accident and also able to maintain the coolable geometry for all fuel assemblies throughout the transient.

(a,c)

(a,c)

3.5.3 VERTICAL BLOWDOWN ANALYSIS

Three major primary coolant pipe break sizes and locations, as specified in Reference 6, were used in the vertical blowdown analysis to establish the maximum impact force response. The fuel assembly response and impact forces were obtained for each of the three aforementioned pipe locations to determine the limiting breaks.

The vertical blowdown analyses of various break locations indicated the response obtained from a [

] + in a four loop plant would result in a maximum impact force, in this case an impact load, of [] + lbs at the bottom nozzle legs of the fuel assembly. The maximum fuel assembly component stresses corresponding to the maximum impact force indicated that they are well below the allowable stress values established for faulted condition loads.

(a,c)

(a,c)

3.5.4 CONCLUSION

The analytical model representation of a reactor core adequately characterizes the core response under seismic and LOCA excitations. Static and dynamic structural test results of a fuel assembly compared with analytical predictions indicate that the fuel assembly lateral and axial structural behavior can be fully determined with finite element models. It was concluded that these analytical models could be used to investigate fuel assembly responses under the lateral seismic, lateral blowdown and vertical blowdown accidents. Analysis of the 17x17 8-grid optimized fuel assembly component stresses and grid impact forces due to a postulated faulted condition accident has indicated that the design is structurally acceptable based on the established allowable design limits.

3.6 REFERENCES

1. "Benchmark Problem Solutions Employed for Verification of the WECAN Computer Program," WCAP-8929, April 1977.
2. Gesinski, L. T. and Chiang, D., "Safety Analysis of the 17x17 Fuel Assembly for Combined Seismic and Loss-of-Coolant Accident," WCAP-8236, December 1973.
3. Biggs, J. M., "Introduction to Structural Dynamics," McGraw-Hill Book Co., Inc. New York, 1964.
4. Fritz, R. J. "The Effects of Liquids on the Dynamic Motion of Immersed Solids," Trans. Am. Soc. Mech. Eng. 94, Series B 167-163 (1972).
5. "MULTIFLEX, A Fortran-IV Computer Program for Analyzing Thermal-Hydraulic-Structure System Dynamics," WCAP-8708 P/A, Vol. I and II, September 1977.

6. "Pipe Breaks for the LOCA Analysis of Westinghouse Primary Coolant Loop," WCAP-8172-A, January 1975.
7. Bohm, G. and LaFaille, J., "Reactor Internals Response Under a Blow-down Accident," First International Conf. on Structural Mechanics in Reactor Technology, Berlin, Germany, September 20-24, 1971.
8. ASME Boiler and Pressure Vessel Code, Section III Division 1, Appendix N, Winter 1978 Addenda.



Westinghouse
Electric Corporation

Water Reactor
Divisions

Nuclear Technology Division

Box 355
Pittsburgh Pennsylvania 15230

September 17, 1980

NS-TMA-2310

Mr. James R. Miller, Chief
Special Projects Branch
Division of Project Management
U.S. Nuclear Regulatory Commission
Phillips Building
7920 Norfolk Avenue
Bethesda, Maryland 20014

Subject: "Verification Testing and Analyses of the Westinghouse 17x17
Optimized Fuel Assembly" - WCAP-9401 (Proprietary) and
WCAP-9402 (Non-Proprietary)

Dear Mr. Miller,

Enclosed are:

1. Forty (40) copies of Appendix A, "WEGAP Verification with the U.S. NRC Sample Problems" to the subject topical report (WCAP 9401 Proprietary)
2. Thirty-five (35) copies of Appendix A, "WEGAP Verification with the U.S. NRC Sample Problems" to the subject topical report (WCAP 9402 Non-Proprietary).

Also enclosed are:

1. One (1) copy of Application for Withholding (Non-Proprietary).
2. One (1) copy of original Affidavit (Non-Proprietary).

The enclosed report fulfills a Westinghouse commitment made via telephone conversation of April 16, 1980 with the Staff's Mr. G. Alberthal to supply the necessary documentation to verify the general finite element computer code WEGAP, which was used in the supporting analysis to WCAP 9401, Section 3.0 to calculate the dynamic structural response of the reactor core.

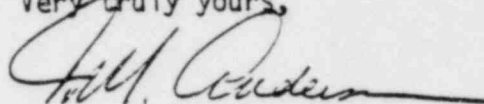
It is Westinghouse's understanding that submittal of this appendix will not adversely impact the NRC's review schedule for WCAP 9401.

Once WCAP 9401/9402 receives NRC approval, Westinghouse plans to incorporate this appendix into the approved, or "A" versions of this topical report.

This submittal contains proprietary information of Westinghouse Electric Corporation. In conformance with the requirements of 10CFR2.790, as amended, of the Commission's regulations, we are enclosing with this submittal an application for withholding from public disclosure and an affidavit. The affidavit sets forth the basis on which the information may be withheld from public disclosure by the Commission.

Correspondence with respect to the affidavit or application for withholding should reference AW-80-58, and should be addressed to R. A. Wiesemann, Manager of Regulatory and Legislative Affairs, Westinghouse Electric Corporation, P.O. Box 355, Pittsburgh, Pennsylvania 15230

Very truly yours,

A handwritten signature in cursive script, appearing to read "T. M. Anderson", with a long horizontal flourish extending to the right.

T. M. Anderson, Manager
Nuclear Safety Department



Westinghouse
Electric Corporation

Water Reactor
Divisions

Nuclear Technology Division

Box 355
Pittsburgh Pennsylvania 15230

September 18, 1980
AW-80-58

Mr. James R. Miller, Chief
Special Projects Branch
Division of Project Management
U. S. Nuclear Regulatory Commission
Phillips Building
7920 Norfolk Avenue
Bethesda, Maryland 20014

APPLICATION FOR WITHHOLDING
INFORMATION FROM PUBLIC DISCLOSURE

SUBJECT: WCAP-9401, "Verification Testing and Analyses of the Westinghouse
17X17 Optimized Fuel Assembly"

REF: Westinghouse Letter No. NS-TMA-2310, Anderson to Miller, dated
September 17, 1980

Dear Mr. Miller:

The proprietary material transmitted by the referenced letter supplements the proprietary material previously submitted concerning the Westinghouse Optimized Fuel Assembly Testing/Analyses Program (Reference: NS-TMA-2057 dated March 30, 1979). Further, the affidavits submitted to justify the material previously submitted, AW-78-23 and AW-78-61, are equally applicable to this material.

Accordingly, withholding the subject information from public disclosure is requested in accordance with the previously submitted affidavit and application for withholding, AW-78-23, dated March 21, 1978, a copy of which is attached.

Correspondence with respect to this application for withholding or the accompanying affidavit should reference AW-80-58, and should be addressed to the undersigned.

Very truly yours,

A handwritten signature in cursive script that reads "Robert A. Wiesemann".

Robert A. Wiesemann, Manager
Regulatory & Legislative Affairs

/bek
Attachment

cc: E. C. Shomaker, Esq.
Office of the Executive Legal Director, NRC



Westinghouse
Electric Corporation

Water Reactor
Divisions

Box 355
Pittsburgh Pennsylvania 15230

March 21, 1978
AW-78-23

Mr. John F. Stolz, Chief
Light Water Reactors Branch No. 1
Division of Project Management
Office of Nuclear Reactor Regulation
U.S. Nuclear Regulatory Commission
Washington, D.C. 20555

APPLICATION FOR WITHHOLDING PROPRIETARY

INFORMATION FROM PUBLIC DISCLOSURE

SUBJECT: Copies of Slides Used in Westinghouse Optimized Fuel
Assembly Presentation to NRC on March 21, 1978

REF: Westinghouse Letter No. NS-CE-1729, Eichelinger to Stolz,
dated March 21, 1978

Dear Mr. Stolz:

This application for withholding is submitted by Westinghouse Electric Corporation ("Westinghouse") pursuant to the provision of paragraph (b)(1) of Section 2.790 of the Commission's regulations.

The undersigned has reviewed the information sought to be withheld and is authorized to apply for its withholding on behalf of Westinghouse, WRD, notification of which was sent to the Secretary of the Commission on April 19, 1976.

The affidavit accompanying this application sets forth the basis on which the information may be withheld from public disclosure by the Commission and addresses with specificity the considerations listed in paragraph (b)(4) of Section 2.790 of the Commission's regulations.

Accordingly, it is respectfully requested that the subject information which is proprietary to Westinghouse be withheld from public disclosure in accordance with 10 CFR Section 2.790 of the Commission's regulations.

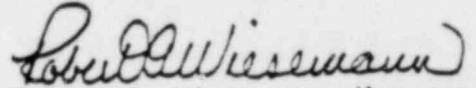
Mr. J. F. Stolz

-2-

AW-78-23
March 21, 1978

Correspondence with respect to this application for withholding or the accompanying affidavit should reference AW-78-23, and should be addressed to the undersigned.

Very truly yours,


Robert A. Wiesemann, Manager
Licensing Programs

cc: J. A. Cooke, Esq.
Office of the Executive Legal Director

/rd

enclosure

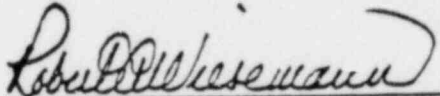
AFFIDAVIT

COMMONWEALTH OF PENNSYLVANIA:

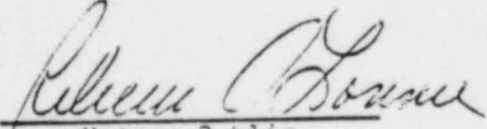
SS

COUNTY OF ALLEGHENY:

Before me, the undersigned authority, personally appeared Robert A. Wiesemann, who, being by me duly sworn according to law, deposes and says that he is authorized to execute this Affidavit on behalf of Westinghouse Electric Corporation ("Westinghouse") and that the averments of fact set forth in this Affidavit are true and correct to the best of his knowledge, information, and belief:


Robert A. Wiesemann, Manager
Licensing Programs

Sworn to and subscribed
before me this 10 day
of March 1978.


Notary Public

AW-78-23

- (1) I am Manager, Licensing Programs, in the Pressurized Water Reactor Systems Division, of Westinghouse Electric Corporation and as such, I have been specifically delegated the function of reviewing the proprietary information sought to be withheld from public disclosure in connection with nuclear power plant licensing or rulemaking proceedings, and am authorized to apply for its withholding on behalf of the Westinghouse Water Reactor Divisions.
- (2) I am making this affidavit in conformance with the provisions of 10 CFR Section 2.790 of the Commission's regulations and in conjunction with the Westinghouse application for withholding accompanying this Affidavit.
- (3) I have personal knowledge of the criteria and procedures utilized by Westinghouse Nuclear Energy Systems in designating information as a trade secret, privileged or as confidential commercial or financial information.
- (4) Pursuant to the provisions of paragraph (b)(4) of Section 2.790 of the Commission's regulations, the following is furnished for consideration by the Commission in determining whether the information sought to be withheld from public disclosure should be withheld.
 - (i) The information sought to be withheld from public disclosure is owned and has been held in confidence by Westinghouse.
 - (ii) The information is of a type customarily held in confidence by Westinghouse and not customarily disclosed to the public. Westinghouse has a rational basis for determining the types of information customarily held in confidence by it and, in that connection, utilizes a system to determine when and

whether to hold certain types of information in confidence. The application of that system and the substance of that system constitutes Westinghouse policy and provides the rational basis required.

Criteria and Standards Utilized

In determining whether information in a document or report is proprietary, the following criteria and standards are utilized by Westinghouse. Information is proprietary if any one of the following are met:

- (a) The information reveals the distinguishing aspects of a process (or component, structure, tool, method, etc.) where prevention of its use by any of Westinghouse's competitors without license from Westinghouse constitutes a competitive economic advantage over other companies.
- (b) It consists of supporting data, including test data, relative to a process (or component, structure, tool, method, etc.), the application of which data secures a competitive economic advantage, e.g., by optimization or improved marketability.
- (c) Its use by a competitor would reduce his expenditure of resources or improve his competitive position in the design, manufacture, shipment, installation, assurance of quality, or licensing of a similar product.
- (d) It reveals cost or price information, production capacities, budget levels, or commercial strategies of Westinghouse, its customers or suppliers.

AW-78-23

- (e) It reveals aspects of past, present, or future Westinghouse or customer funded development plans and programs of potential commercial value to Westinghouse.
 - (f) It contains patentable ideas, for which patent protection may be desirable.
 - (g) It is not the property of Westinghouse, but must be treated as proprietary by Westinghouse according to agreements with the owner.
- (iii) The information is being transmitted to the Commission in confidence and, under the provisions of 10 CFR Section 2.790, it is to be received in confidence by the Commission.
- (iv) The information is not available in public sources to the best of our knowledge and belief.
- (v) The proprietary information sought to be withheld in this submittal are the copies of slides utilized by Westinghouse in its presentation to the NRC at the March 21, 1978 meeting concerning the Westinghouse optimized fuel assembly. The letter and the copies of slides are being submitted in preliminary form to the Commission for review and comment on the Westinghouse optimized fuel assembly in advance of a formal submittal for NRC approval.

Public disclosure of this information is likely to cause substantial harm to the competitive position of Westinghouse as it would reveal the description of the approved design, the comparison of the improved design with the standard design, the nature of the tests conducted, the test conditions, the test results and the conclusions of the testing program,

all of which is recognized by the Staff to be of competitive value and because of the large amount of effort and money expended by Westinghouse over a period of several years in carrying out this particular development program. Further, it would enable competitors to use the information for commercial purposes and also to meet NRC requirements for licensing documentation, each without purchasing the right from Westinghouse to use the information.

Information regarding its development programs is valuable to Westinghouse because:

- (a) Information resulting from its development programs gives Westinghouse a competitive advantage over its competitors. It is, therefore, withheld from disclosure to protect the Westinghouse competitive position.
- (b) It is information which is marketable in many ways. The extent to which such information is available to competitors diminishes the Westinghouse ability to sell products and services involving the use of the information.
- (c) Use by our competitor would put Westinghouse at a competitive disadvantage by reducing his expenditure of resources at our expense.
- (d) Each component of proprietary information pertinent to a particular competitive advantage is potentially as valuable as the total competitive advantage. If competitors acquire components of proprietary information, any one component may be the key to the entire puzzle, thereby depriving Westinghouse of a competitive advantage.

- (e) The Westinghouse capacity to invest corporate assets in research and development depends upon the success in obtaining and maintaining a competitive advantage.

Being an innovative concept, this information might not be discovered by the competitors of Westinghouse independently. To duplicate this information, competitors would first have to be similarly inspired and would then have to expend an effort similar to that of Westinghouse to develop the design.

Further the deponent sayeth not.

Appendix A
to
WCAP 9401/9402, "Verification Testing
and Analyses of the Westinghouse
17x17 Optimized Fuel Assembly"

WEGAP VERIFICATION WITH THE
USNRC SAMPLE PROBLEMS

Westinghouse Electric Corporation
Nuclear Energy Systems
P.O. Box 355
Pittsburgh, Pennsylvania 15230

TABLE OF CONTENTS

<u>Title</u>	<u>Page</u>
Introduction	A-1
A specific Westinghouse Computer Code for Core Dynamic Response Analyses - WEGAP	A-1
Fuel Assembly Dynamic Responses for A Hypothetical Reactor Core Problem	A-3
- Statement of Sample Problem	A-3
- Assumptions and Analytical Modeling	A-3
- Analytical Results	A-4
Conclusions	A-5
References	A-6

INTRODUCTION

Currently, two Westinghouse computer codes, namely WECAN and WEGAP, are used for obtaining the dynamic response solution of the reactor core in pressurized water reactors. The purpose of this report is to describe the general analytical features of these computer codes and to present a comparison of the results as verification of the WEGAP Code.

The WECAN computer program is a Westinghouse general purpose finite element computer program for various types of structural analyses. The mathematical formulation, computational procedures, and the verification of various types of benchmark problems have been extensively discussed in the Westinghouse topical report (reference 1). The use of WECAN to solve the suggested sample problems was submitted to USNRC as given in reference 2.

This report is devoted to the discussion of the NRC sample problem solution using the WEGAP computer program. The WEGAP program is a special computer code for obtaining core dynamic responses.

A specific Westinghouse computer code for core dynamic response analysis-WEGAP

The WEGAP computer program is a specialized finite element computer program designed to solve the dynamic responses of the reactor core in pressurized water reactors. The program treats the interactions between the fuel assemblies as applied pseudo forces in order to eliminate the traditional approach of reformulating the structural stiffness matrix at each successive time step. An iterative procedure used to check the convergence of the impact force has been incorporated into the code to assure that the dynamic response solution is properly derived. The computer program also utilizes the individual fuel assembly properties throughout the analysis to reduce the computer core storage requirements.

These improvements in the method of solution and computation procedure enable us to obtain the dynamic response solution for a reactor core subjected to asymmetric boundary conditions with very efficient numerical techniques.

The governing differential equations of motion for a reactor core are:

+(a.c)

The Newmark-Beta multistep direct integration method as described in Reference 3 is used to obtain the displacement solution at each successive time step. The required time increment which is one-fourteenth or less of the shortest period is needed to assure solution convergence. Figure 1 shows the flow diagram of the overall procedure for analyzing the postulated SSE or LOCA transients. The flow diagram of WEGAP program structure is given in Figure 1A.

Fuel assembly dynamic response for a hypothetical reactor core problem

The dynamic response solutions to these problems were initially requested by the NRC in order to qualify the nuclear fuel vendors' computer code features as well as the analytical capability. The dynamic response solutions to the sample problems using the Westinghouse general purpose finite element, WECAN, were documented in Reference 2.

Statement of Sample Problems

The suggested NRC problems are summarized in Table 1. The first problem has a prescribed initial velocity input sine wave. The second problem has a combination of three sine waves with zero initial displacement and velocity for both upper and lower core plates. The motions for the lower core plate indicate a 0.006 sec time delay in reference to the upper core plate.

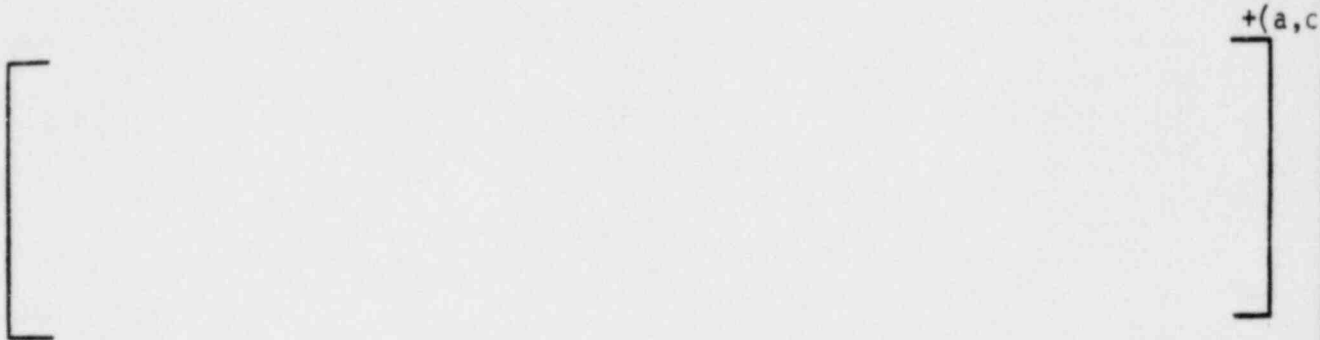
The simplified reactor core cross-section is illustrated in Figure 1. The core consists of five (5) assemblies on the longest diameter. The peripheral fuel assembly to baffle gap and the internal fuel assembly gap are 0.06 in. and 0.03 in. respectively. The fuel assembly mechanical properties such as a description of the fuel assembly lateral stiffness, mass distribution, material property and dynamic characteristics are given in Figure 3. The fuel assembly spacer grid mechanical properties are presented in Figure 4.

Assumptions and Analytical Modeling

The following assumptions were employed in the processes of obtaining the dynamic response solutions of the postulated core analyses.

1. The non-linear fuel assembly stiffness characteristics as illustrated in Figure 3 were not incorporated into the fuel assembly model (Figure 5).

2. []^{+(a,c)}



3. The lumped mass-spring system was used to simulate the fuel assembly dynamic characteristics.

Based on these assumptions, the simplified fuel assembly model as shown in Figure 5 was constructed using the discrete mass distribution, the first five fundamental resonant frequencies together with their mode shapes, and the orthogonality relationship among normalized mode shapes. This simplified fuel assembly finite element model preserves essentially all the fuel assembly important dynamic characteristics. The listing of the finite element model corresponding to the damping assumption (A) is given in Table 2. It should be noted that the discrete mass point corresponds to the first nodal point of the defined spring-damper element.

The bilinear elastic-plastic spacer grid models are also given in Table 2.

The reactor core model was represented by five (5) fuel assemblies as schematically shown in Figure 2. The summary of the core cross-section model, and the designation of fuel assembly and spacer grid models are given in Table 3. The baffle motions at each individual grid elevation were linearly interpolated as the input for the core model between the upper core plate and lower core plate.

Analytical Results

An analytical evaluation of the core model given in Table 3 was performed using the forcing function designated as case 2 in Table 1. The results of the grid maximum force and time of mid-grid impact are summarized in Tables 4 through 6. Table 4 presents the grid maximum impact force for each grid elevation for case 2A. The maximum response results correspond to a 0.5 sec. forcing function input. Both WEGAP and WECAN results were tabulated for the purpose of comparison. The transient responses obtained from the WEGAP core model compare extremely well

with that from WEGAN. The difference in peak grid force is well within 1%. The slight increase in impact force is attributed to the assumed grid weight of about 2 lbs.

The WEGAP results corresponding to the fuel assembly damping assumptions (A and B) are summarized in Table 5. The maximum impact force for each grid was screened from one second real time dynamic response results. The consideration of low damping coefficients at higher modes will slightly alter the dynamic response results.

However, the peak grid force does not show much difference for this particular example. The plots of the upper and lower core plate motions for Case 2A are shown as the dotted and solid lines respectively in Figure 6.

The dynamic response results of some selected fuel assembly positions - such as the fuel assembly relative displacements, total displacement, grid impact forces and fuel assembly support reaction forces are schematically shown in Figures 7 through 13.

A second analysis was performed using the forcing function designated as Case 2B as given in Table 1. This case was run to illustrate the non-linear feature of the WEGAP Code. The input upper and lower core plate motions are plotted as the dotted and solid curves respectively in Figure 14. The various dynamic response results are given in Figures 15 through 18. The maximum grid response results are summarized in Table 6. The grid impact force exceeding 2500 lb. would indicate that the bi-linear elastic feature of the grid model was utilized.

CONCLUSIONS

As a result of this comparison study, the following conclusions were noted:

1. The transient responses (grid impact forces, relative deflection, and support reaction force distribution) obtained from WEGAP core model compare extremely well with that from WEGAN. The differences in the peak responses are well within 1%.

2. The numerical techniques used in the WEGAP Code requires mass values at all nodal point locations. Consequently, some small differences in impact force predictions between the WECAN and WEGAP Codes are inherent due to the modeling differences. However, for severe dynamic transients, the analytical responses predicted by the two codes become insignificant.

REFERENCES

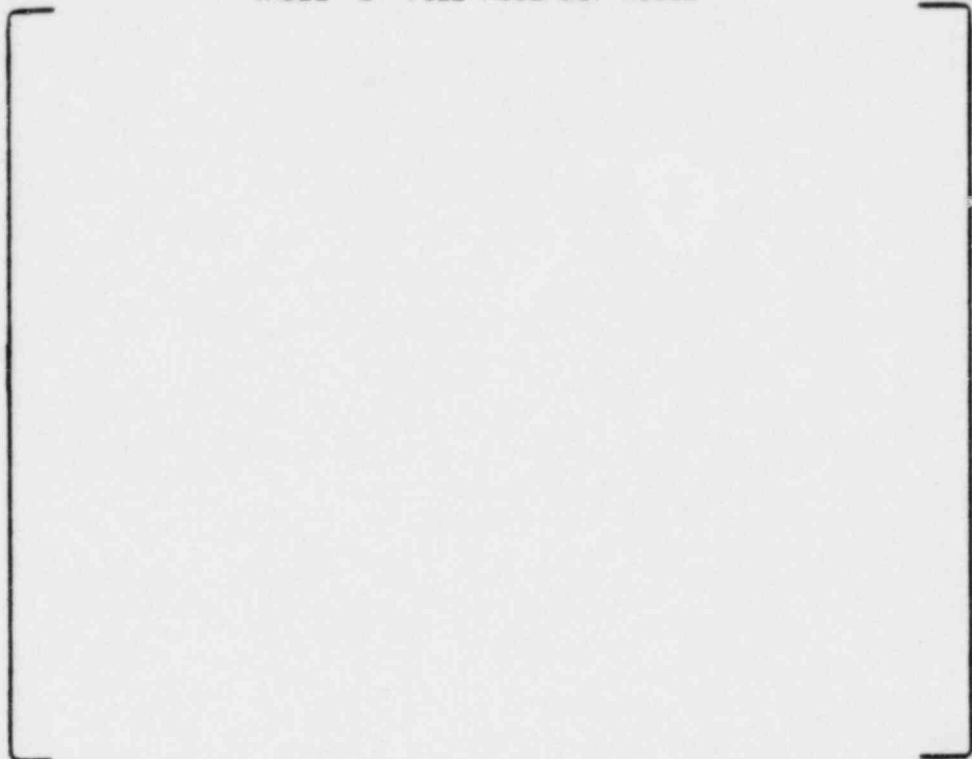
1. "Benchmark Problem Solutions Employed for Verification of the WECAN Computer Program", WCAP 8929, Westinghouse, 1977.
2. Letter, T.M. Anderson to Dr. D.F. Ross, Jr., dated May 1, 1978 (NS-TMA-1772).
3. ASME Boiler and Pressure Vessel Code, Section III Division 1, Appendix N, Winter 1978 Addenda.

TABLE 1
FORCING FUNCTIONS

CASE	FORCING FUNCTION	
1.	$x_U(t) = 0.5 \sin 18.85 t$ $x_L(t) = x_U(t)$	$\dot{x}_U(0) = 9.425 \text{ IN/SEC}$
6-9 2.	$x_U(t) = A (1.0 \sin 20.0 t + 0.5 \sin 100.0 t - 0.1296 \sin 540.0 t)$ $x_U(t) = 0$ $x_L(t) = x_U(t - \Delta t)$	$t \geq 0$ $t < 0$ $\Delta t = 0.006 \quad \text{ALL } t.$
	(A) $A = 1/20$	
	(B) $A = 1/5$	

TABLE 2 FUEL ASSEMBLY MODEL

+(a,c)



IMPACT PROPERTIES

PROPERTY SET NO. 1		STIF 1	DAMP 1	FMAX	STIF 2	DAMP 2
IMPACT EL	GAP					
5	.60000E-01	.25000E+06	220.00	2500.0	83300.	220.00
4	.60000E-01	.25000E+06	220.00	2500.0	83300.	220.00
3	.60000E-01	.25000E+06	220.00	2500.0	83300.	220.00
2	.60000E-01	.25000E+06	220.00	2500.0	83300.	220.00
1	.60000E-01	.25000E+06	220.00	2500.0	83300.	220.00

PROPERTY SET NO. 2		STIF 1	DAMP 1	FMAX	STIF 2	DAMP 2
IMPACT EL	GAP					
5	.30000E-01	.25000E+06	220.00	2500.0	83300.	220.00
4	.30000E-01	.25000E+06	220.00	2500.0	83300.	220.00
3	.30000E-01	.25000E+06	220.00	2500.0	83300.	220.00
2	.30000E-01	.25000E+06	220.00	2500.0	83300.	220.00
1	.30000E-01	.25000E+06	220.00	2500.0	83300.	220.00

TABLE 3 CORE MODEL

BAFFLE NBRRL=1 LINEAR INTER.	

	IMPACT PROPERTY SET 1
ASSEMBLY 1	* MODEL 1 *
	IMPACT PROPERTY SET 2
ASSEMBLY 2	* MODEL 1 *
	IMPACT PROPERTY SET 2
ASSEMBLY 3	* MODEL 1 *
	IMPACT PROPERTY SET 2
ASSEMBLY 4	* MODEL 1 *
	IMPACT PROPERTY SET 2
ASSEMBLY 5	* MODEL 1 *
	IMPACT PROPERTY SET 1

	BAFFLE

TABLE 4

WEGAP VERSUS WECAN GRID IMPACT FORCES - CASE 2A (0.5 sec. Response)

F/A Position	Max. Grid Load, Lbs					Time (Grid #3) Sec.
	Grid #1	Grid #2	Grid #3	Grid #4	Grid #5	
B-1	- (-)	390 (388)	563 (557)	424 (417)	- (-)	0.3195 (0.3198)
1-2	- (-)	185 (189)	381 (374)	261 (256)	- (-)	0.3200 (0.3200)
2-3	- (-)	48 (95)	174 (186)	103 (154)	- (+)	0.4262 (0.3143)
3-4	- (-)	94 (199)	172 (243)	143 (245)	- (-)	0.4260 (0.4198)
4-5	- (-)	218 (366)	375 (371)	356 (350)	- (-)	0.4250 (0.4250)
5-B	- (-)	420 (398)	582* (578)	576 (569)	41 (116,	0.4233 (0.4235)

() Values in parenthesis are from WECAN Analysis

* Maximum Grid Force

TABLE 5

WEGAP GRID IMPACT FORCE FOR F.A. DAMPING STUDY - CASE 2A (1 SEC RESPONSE)

F/A Position	Max. Grid Load, Lbs					Time (Grid #3) Sec.
	Grid #1	Grid #2	Grid #3	Grid #4	Grid #5	
B-1	61 (95)	545 (485)	569 (583)*	461 (444)	117 (146)	0.5755 (0.3195)
1-2	- (-)	243 (206)	381 (385)	261 (222)	- (-)	0.3200 (0.3200)
2-3	- (-)	82 (72)	174 (179)	103 (83)	- (-)	0.3210 (0.3210)
3-4	- (-)	94 (98)	172 (167)	143 (120)	- (-)	0.4260 (0.4260)
4-5	- (-)	218 (207)	375 (360)	356 (319)	- (-)	0.4250 (0.4250)
5-B	- (-)	449 (386)	582* (560)	576 (525)	69 (93)	0.4233 (0.4230)

F/A Damping: []⁺

Value in Parenthesis: 22% damping (1st mode), ~10% High Modes

(a,c)

* Maximum Grid Force

TABLE 6

WEGAP VERSUS WECAN GRID IMPACT FORCE - CASE 2B 0.5 SEC RESPONSE

F/A Position	Max. Grid Load, Lbs.					Time (Grid #3) Sec.
	Grid #5	Grid #4	Grid #3	Grid #2	Grid #1	
B-1	2044 (2020)	2405 (2417)	1921 (1922)	2722 (2712)	2170 (2290)	0.1433 (0.1435)
1-2	1315 (950)	1693 (1720)	1402 (1399)	2163 (2150)	1561 (1550)	0.1433 (0.1435)
2-3	751 (778)	1188 (1215)	926 (922)	1499 (1484)	1024 (1022)	0.1433 (0.1110)
3-4	1033 (1030)	1713 (1703)	1475 (1467)	1728 (1720)	1022 (1446)	0.1090 (0.1090)
4-5	1682 (1680)	2493 (2481)	2101 (2084)	2320 (2316)	1587 (1586)	0.1070 (0.1075)
5-B	2414 (2407)	3171* (3167)	2847 (2845)	2813 (2803)	2362 (2407)	0.1053 (0.1050)

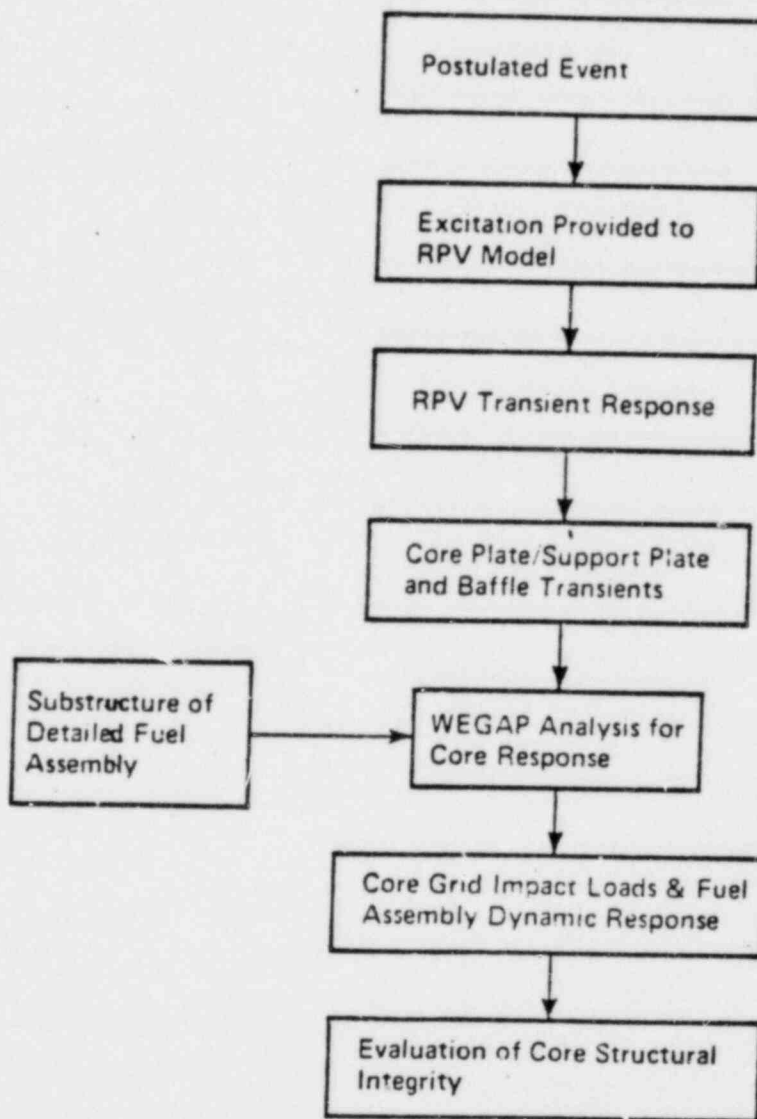
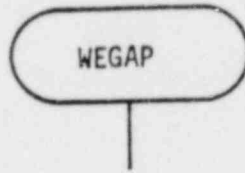
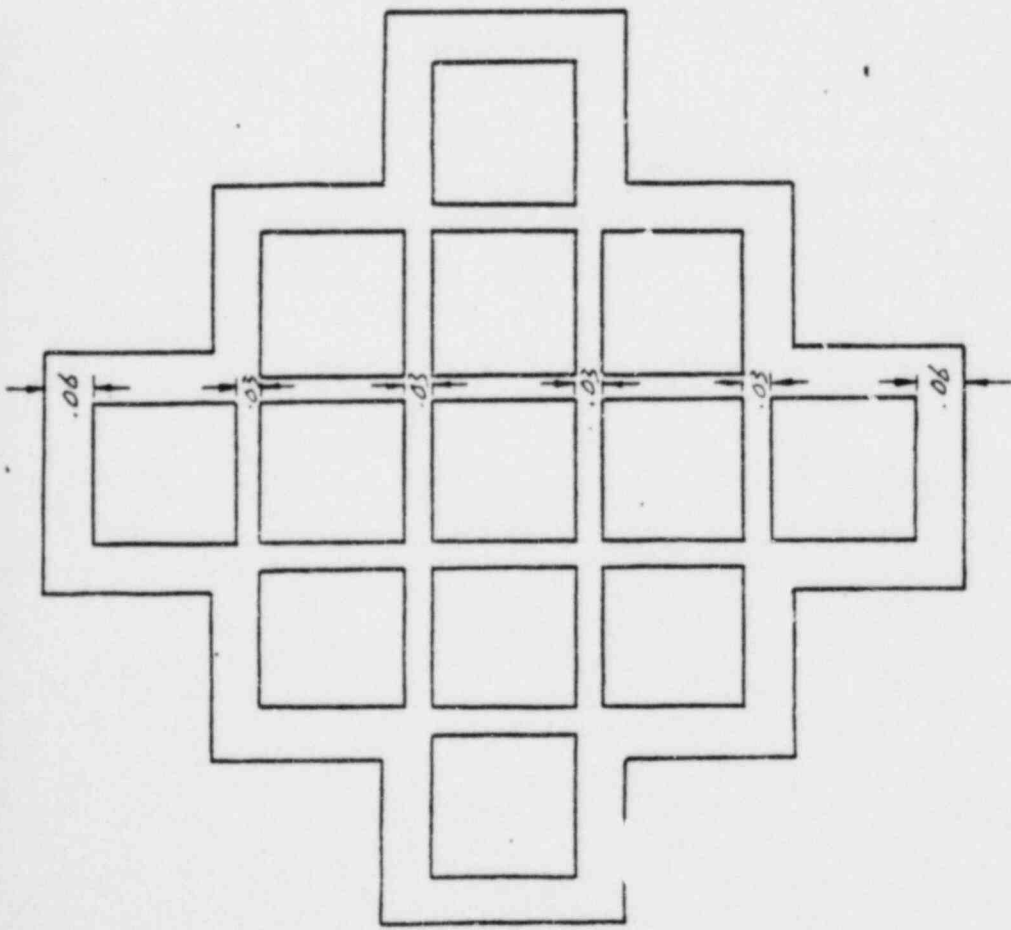
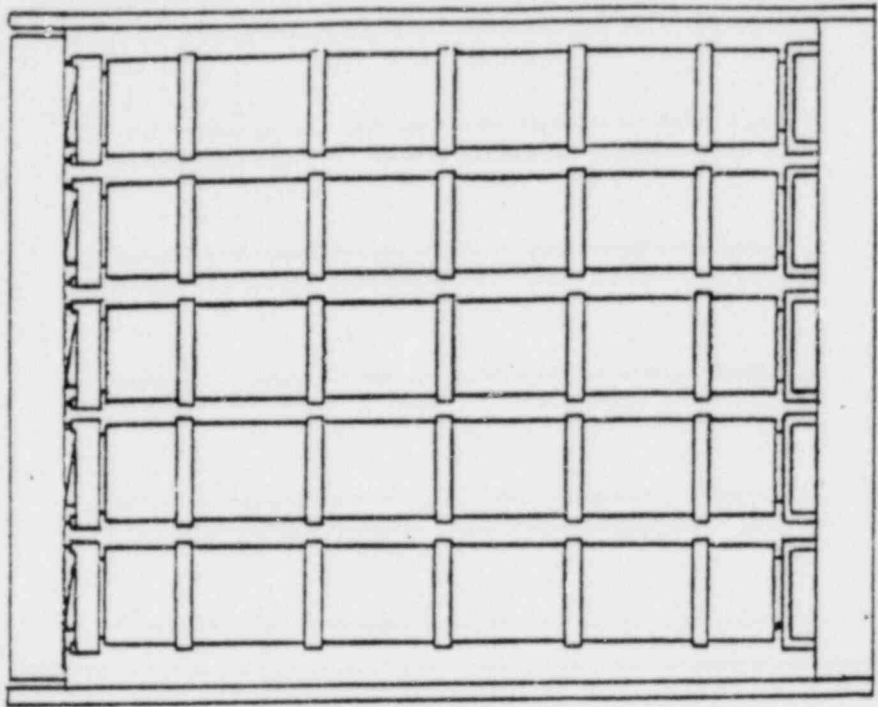


Figure 1 Overall Analysis Process



+ (a, c)

FIGURE 1A WEGAP FLOW DIAGRAM



13 Assemblies in all
 5 on largest diameter

FIGURE 2 REACTOR CORE CROSS SECTION

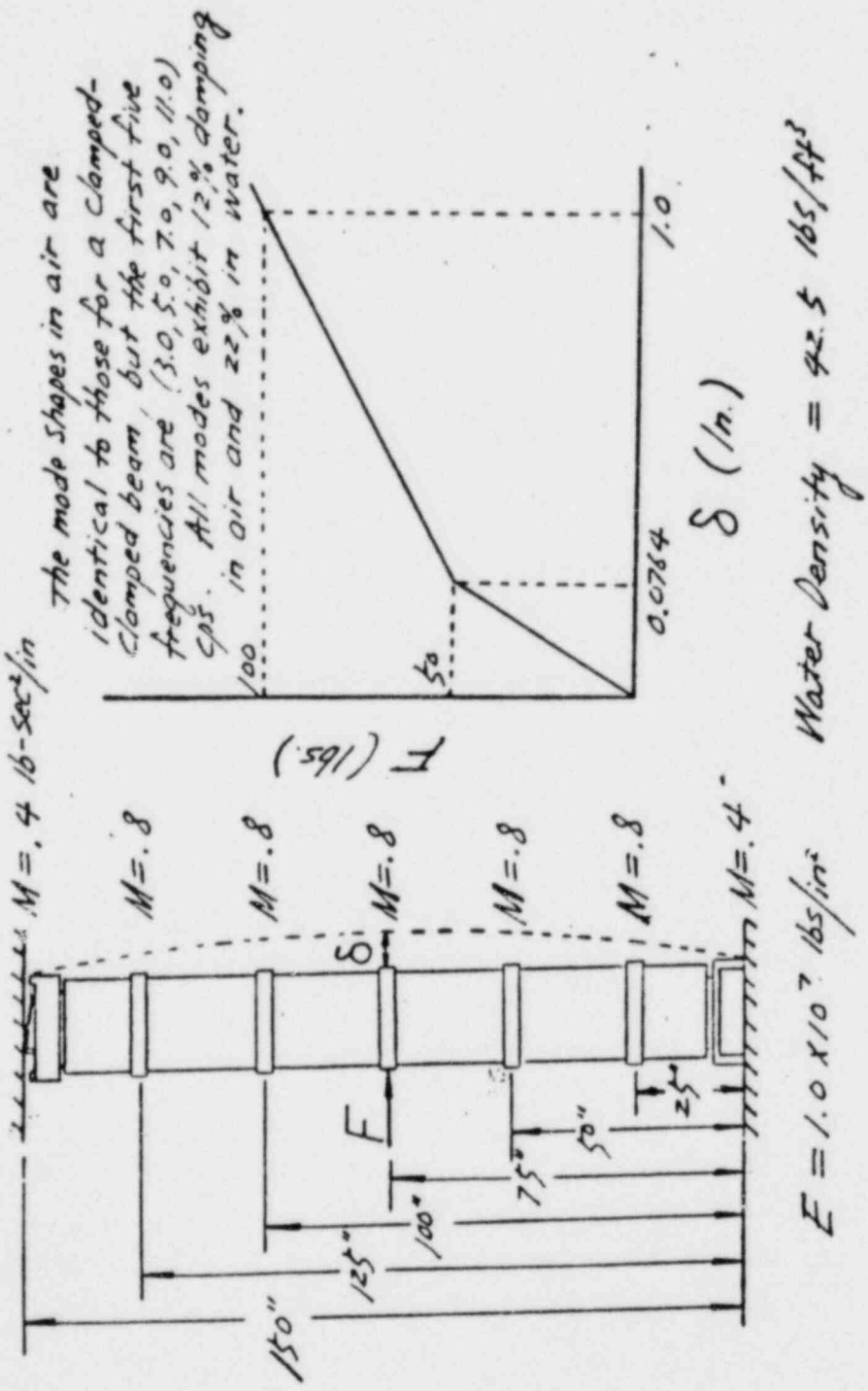


FIGURE 3 FUEL ASSEMBLY DESCRIPTION AND MECHANICAL PROPERTIES

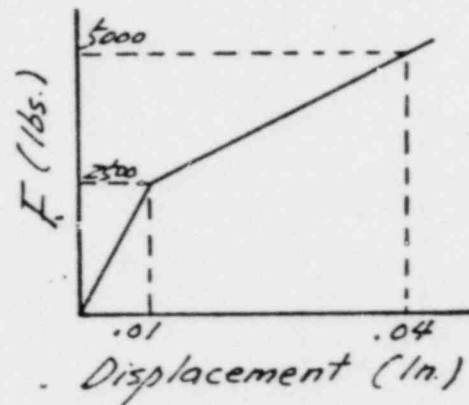
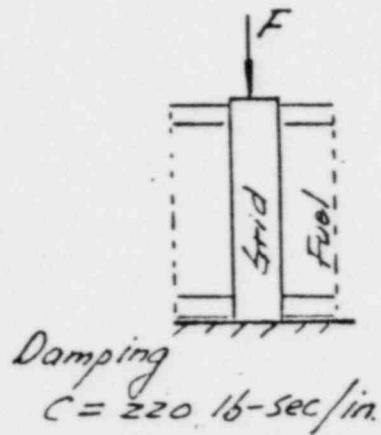
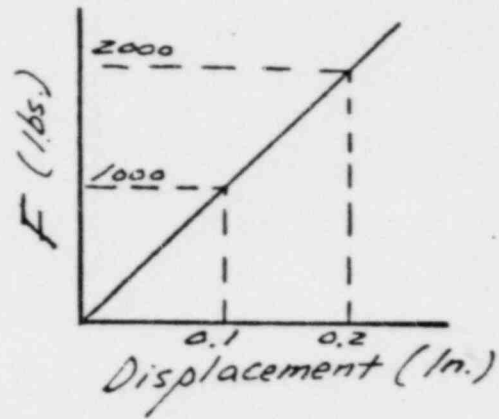
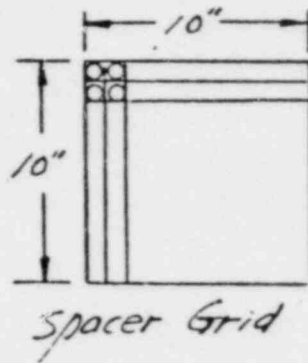
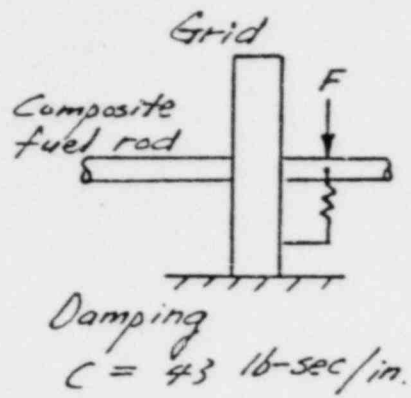


FIGURE 4 SAPCER GRID MECHANICAL PROPERTIES

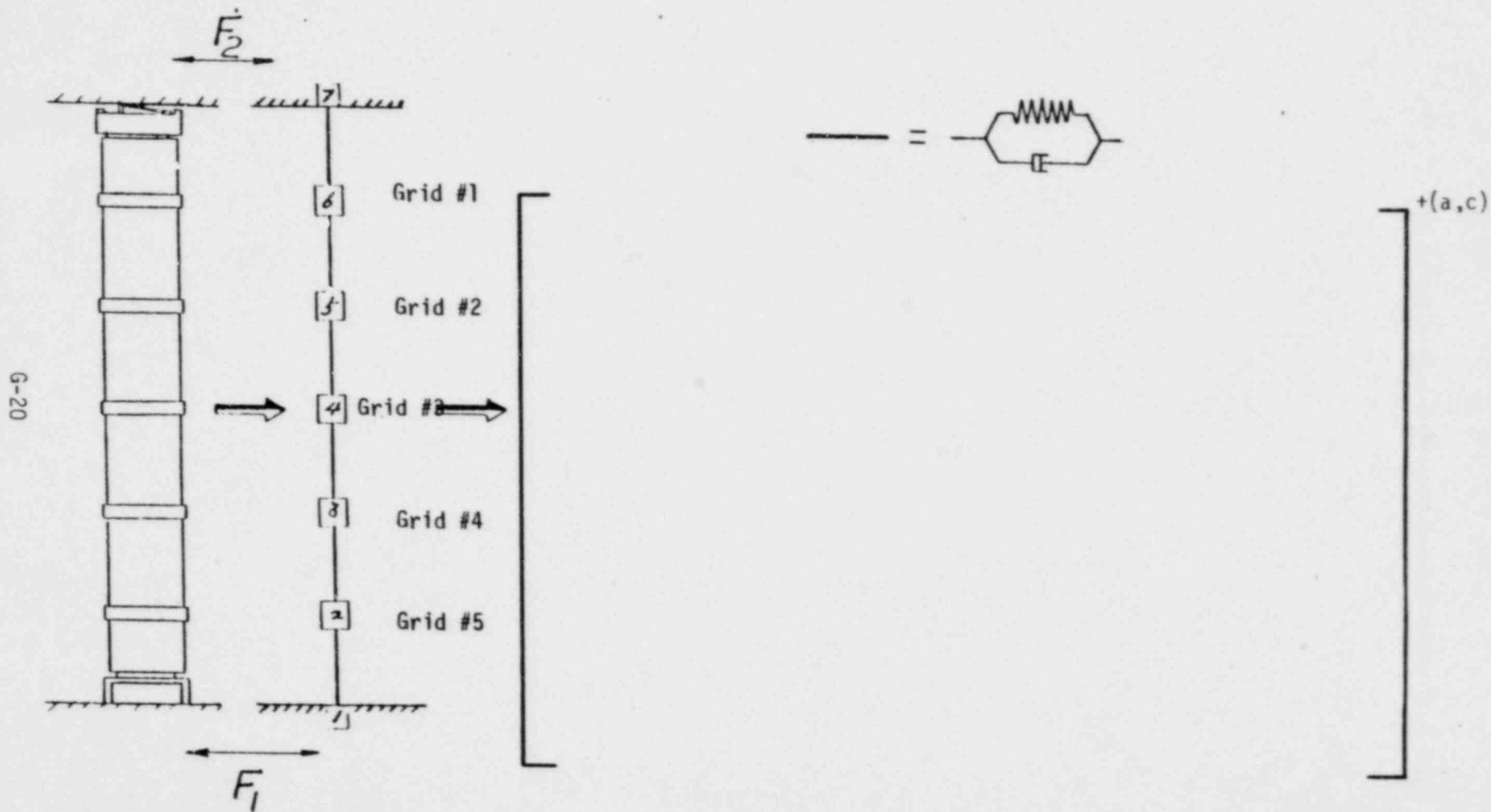


FIGURE 5 FUEL ASSEMBLY FINITE ELEMENT MODEL

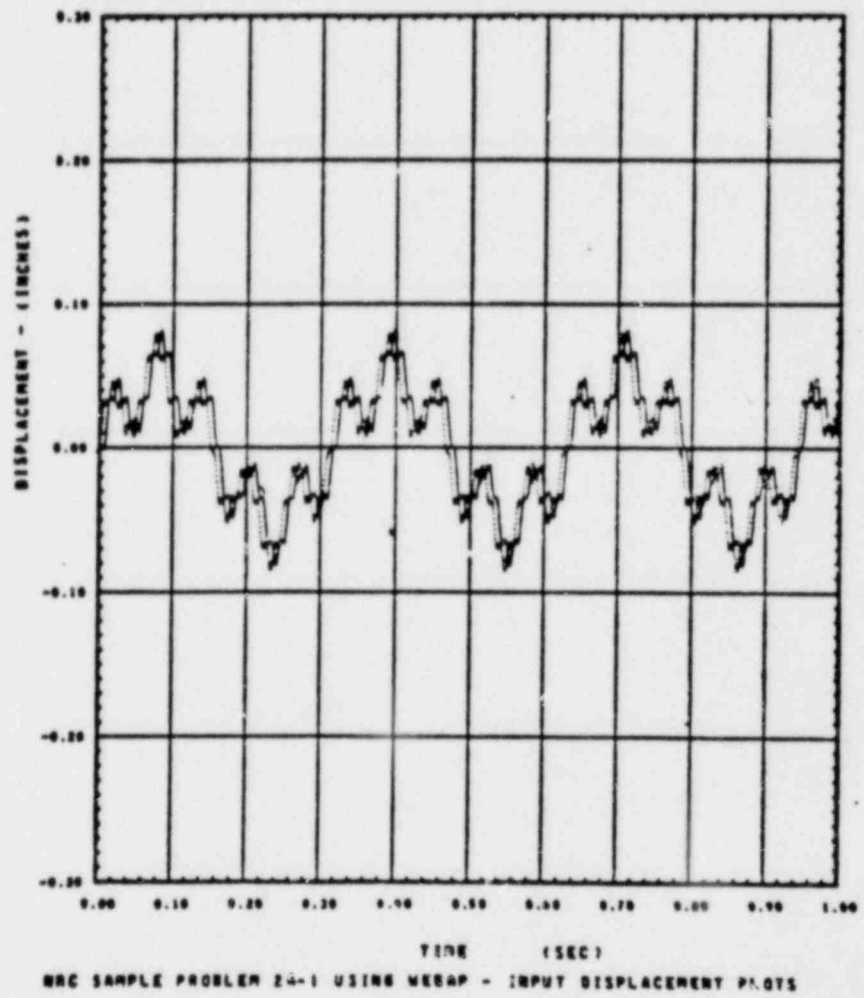


FIGURE 6 INPUT CORE PLATE DISPLACEMENT MOTIONS FOR CASE 2A

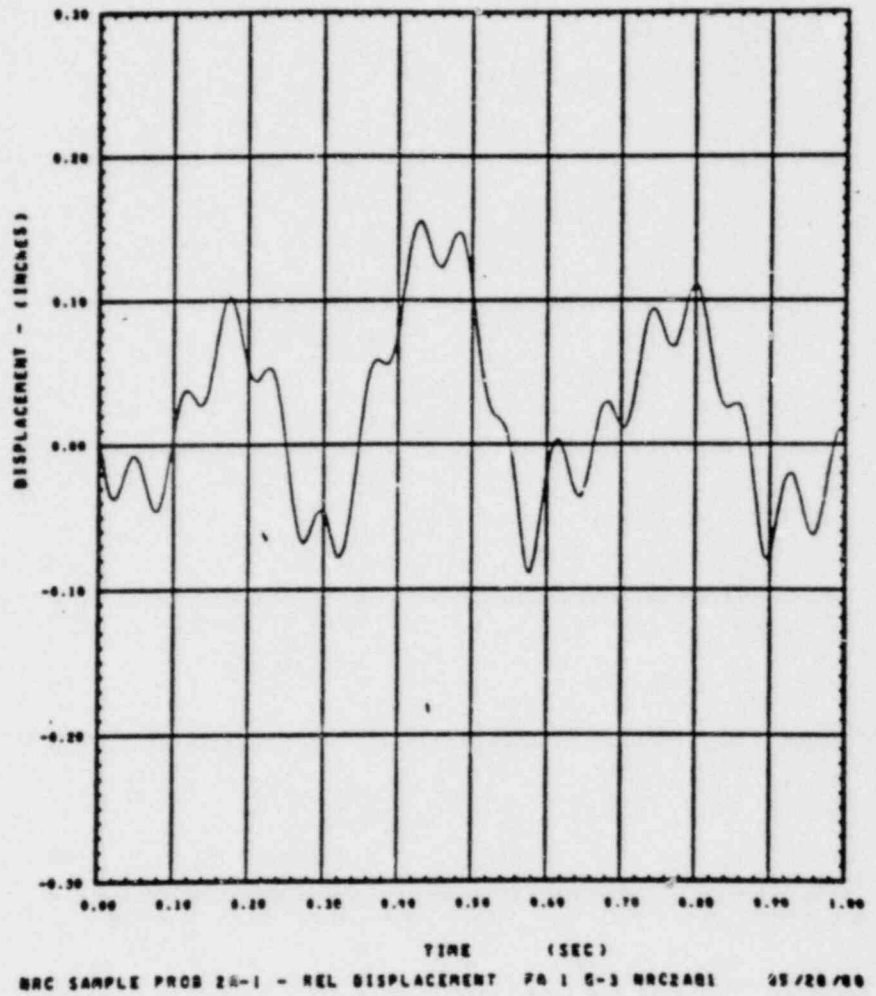


FIGURE 7 DISPLACEMENT RESPONSE OF FIRST FUEL ASSEMBLY GRID NO. 3
RELATIVE TO BAFFLE - CASE 2A

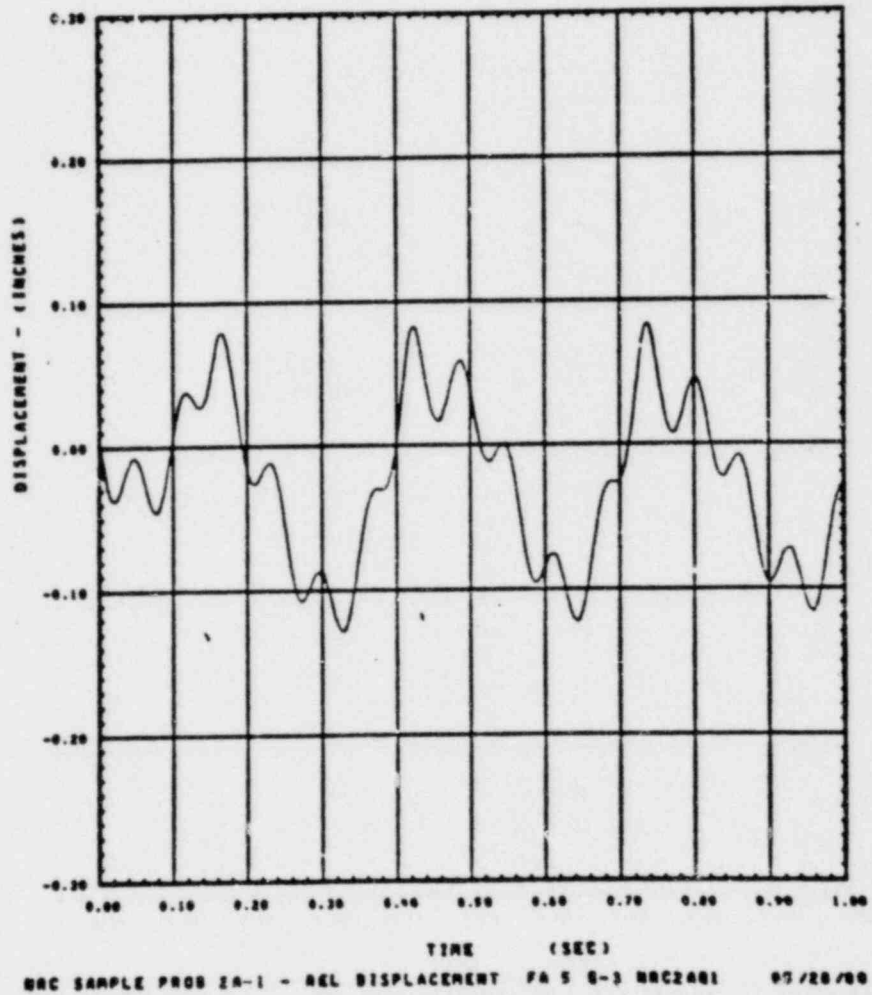


FIGURE 8 DISPLACEMENT RESPONSE OF FIFTH FUEL ASSEMBLY GRID NO. 3
RELATIVE TO BAFFLE - CASE 2A

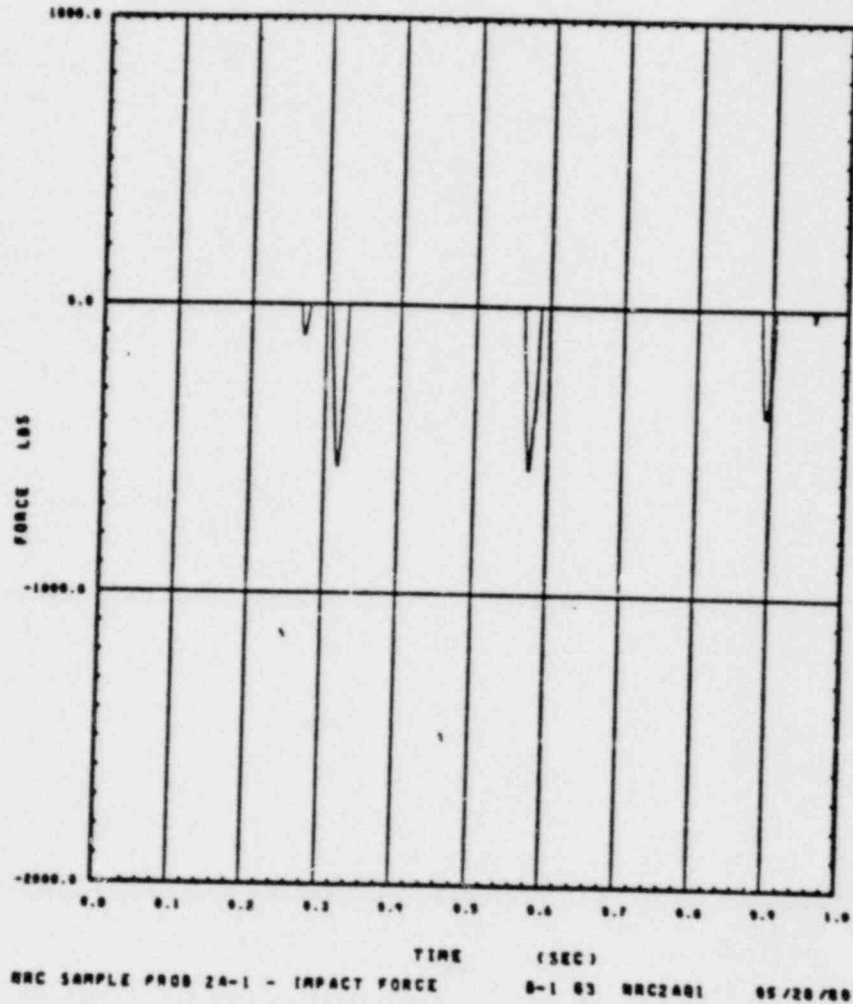


FIGURE 9 IMPACT FORCE RESPONSE BETWEEN BAFFLE AND FIRST FUEL ASSEMBLY AT GRID NO. 3 - CASE 2A

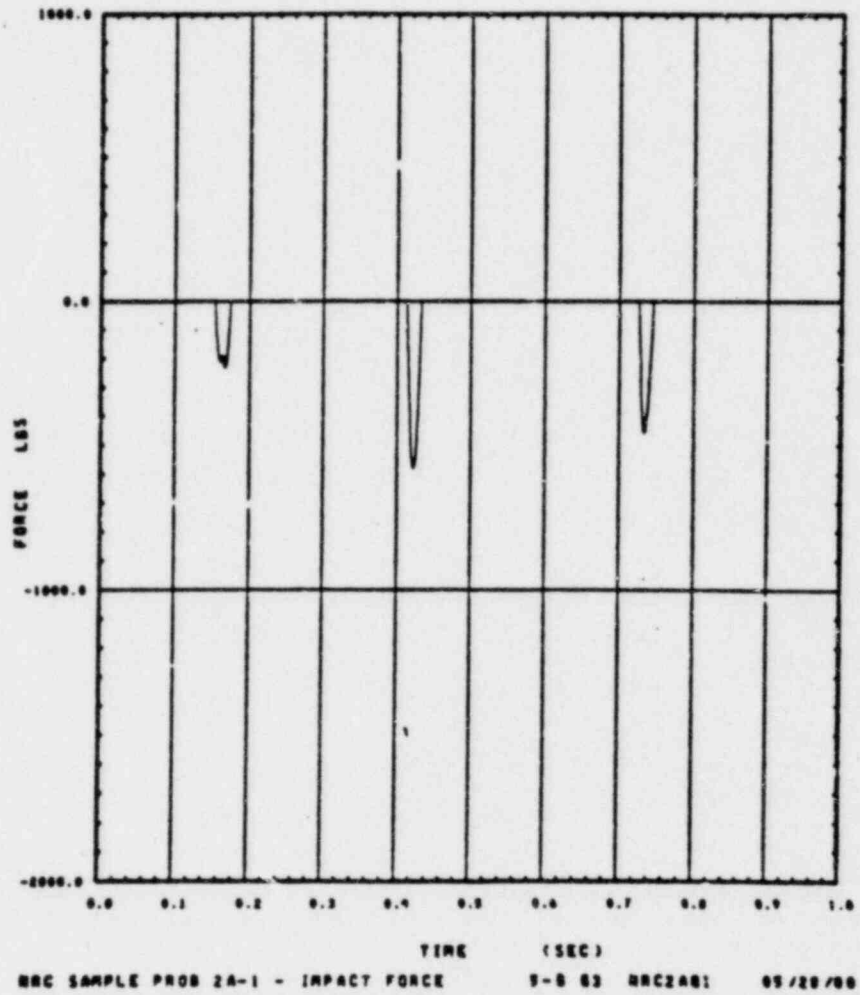


FIGURE 10 IMPACT FORCE RESPONSE BETWEEN FIFTH FUEL ASSEMBLY AND
 BAFFLE AT GRID NO. 3 - CASE 2A

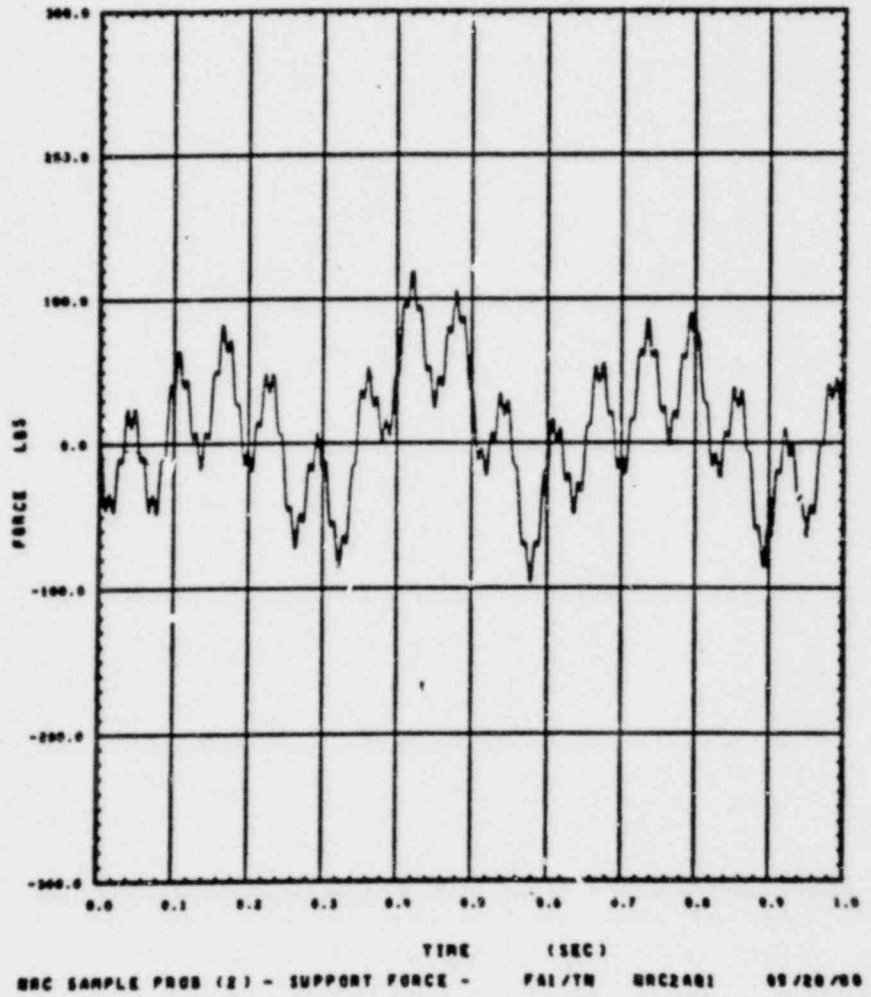


FIGURE 11 UPPER SUPPORT FORCE RESPONSE OF FIRST FUEL ASSEMBLY - CASE 2A

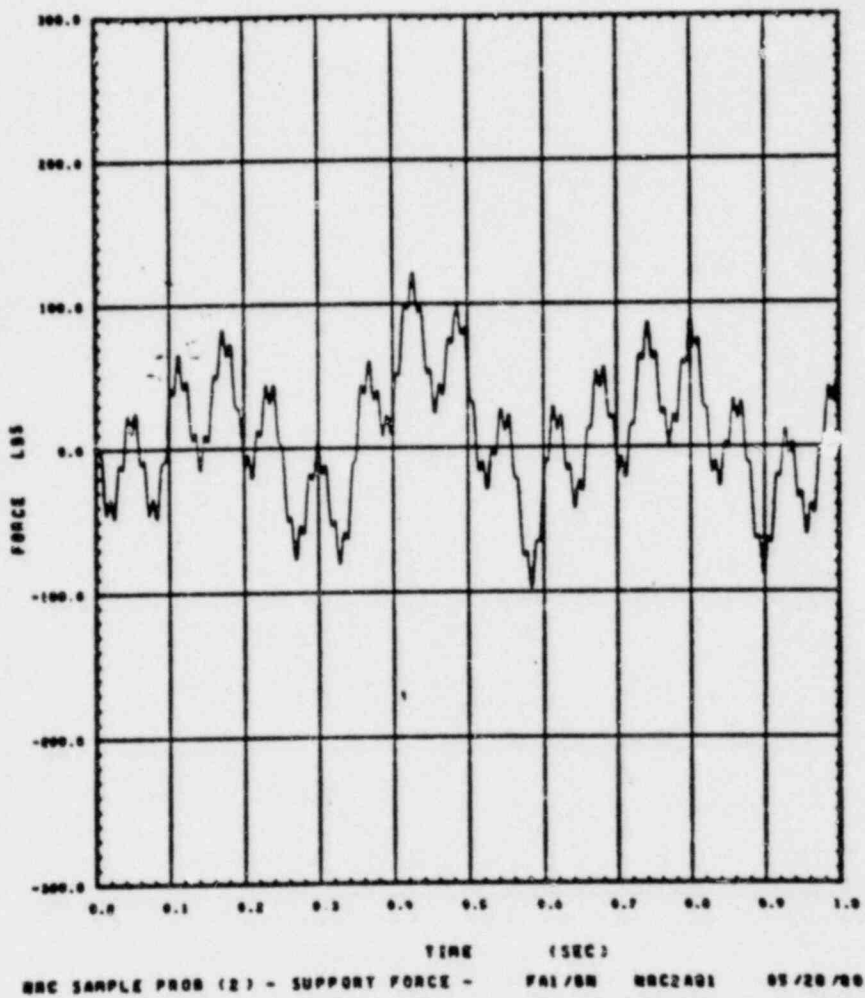


FIGURE 12 LOWER SUPPORT FORCE RESONSE OF FIRST FUEL ASSEMBLY - CASE 2A

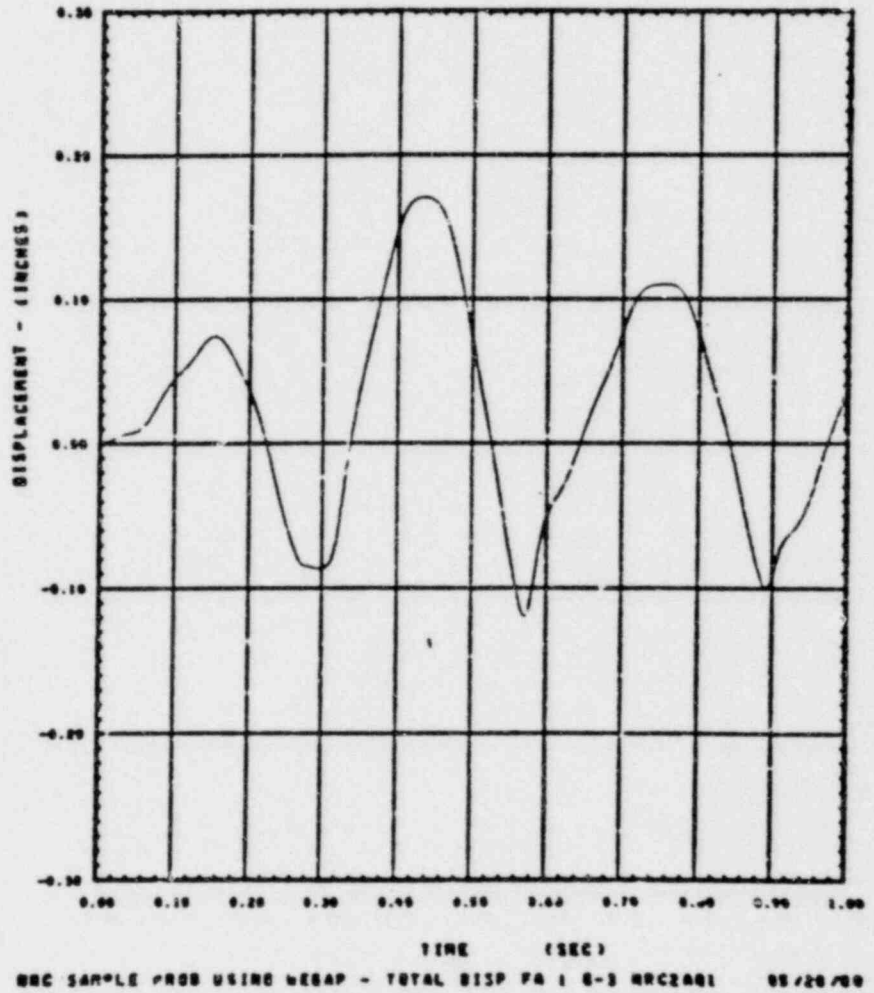
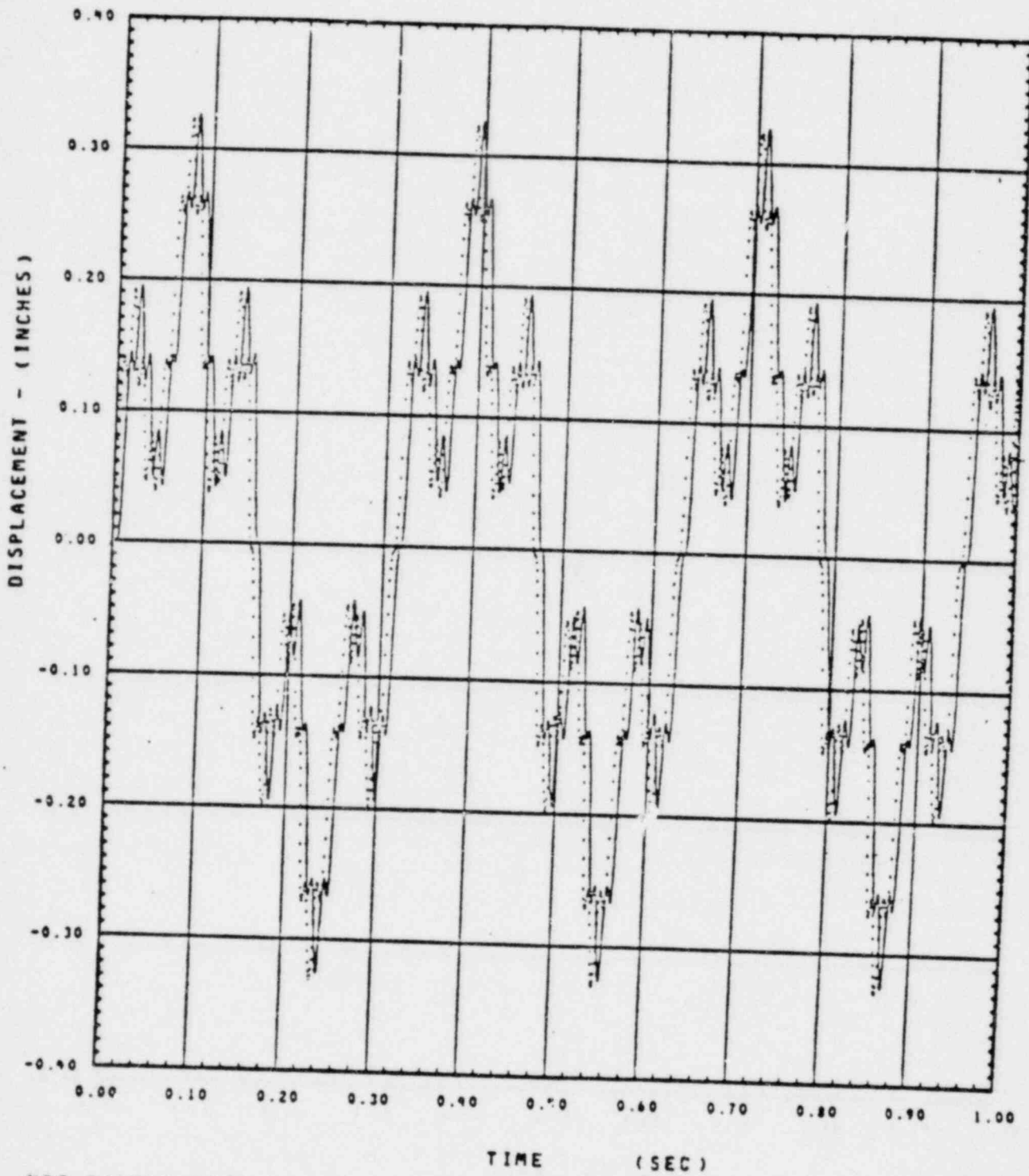


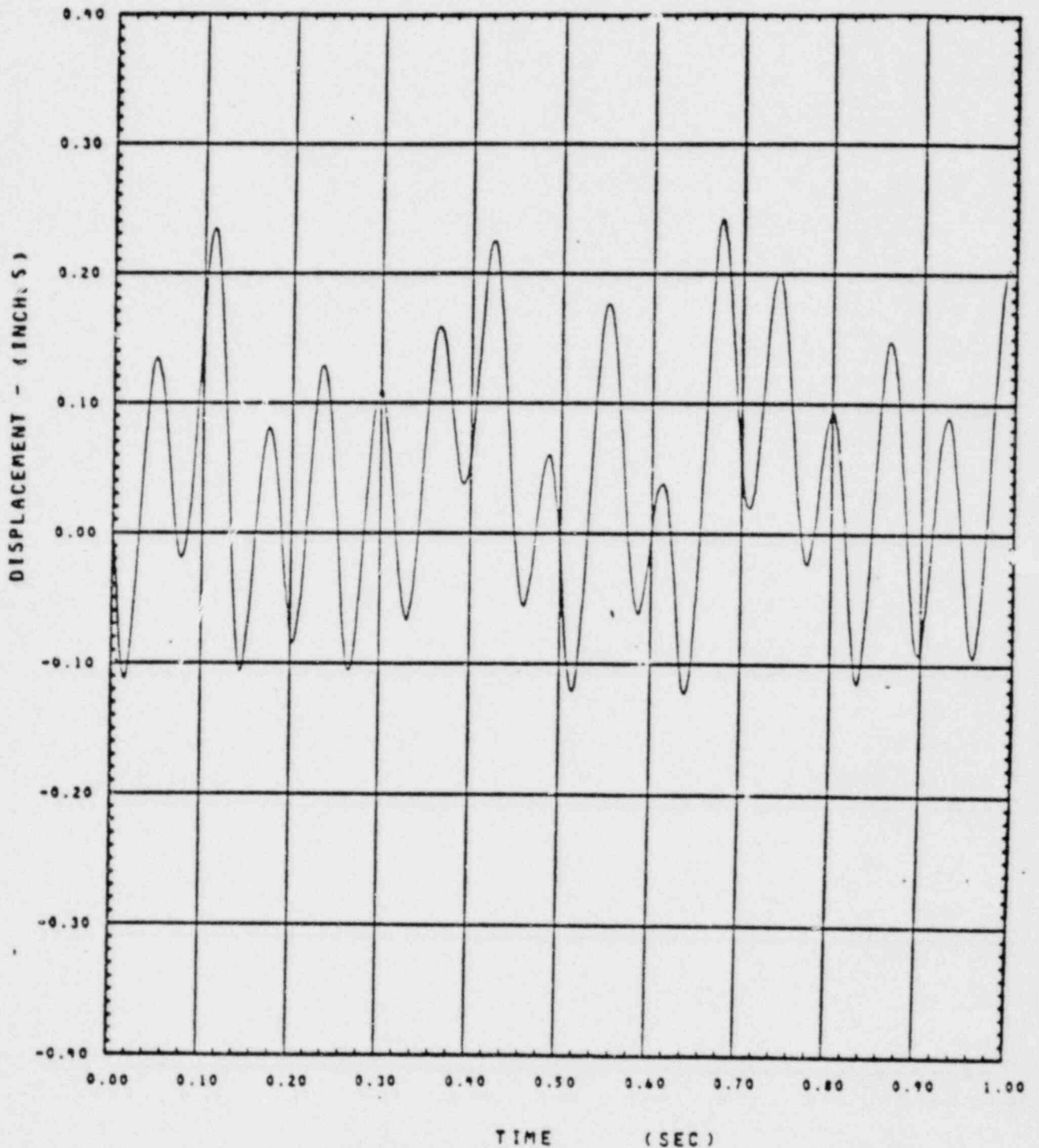
FIGURE 13 TOTAL DISPLACEMENT RESPONSE AT FIRST FUEL ASSEMBLY
AT GRID NO. 3 - CASE 2A



NRC SAMPLE PROBLEM 2B-1 USING WEGAP - INPUT DISPLACEMENT PLOTS

Figure 14

INPUT CORE PLATE DISPLACEMENT MOTIONS FOR CASE 2B

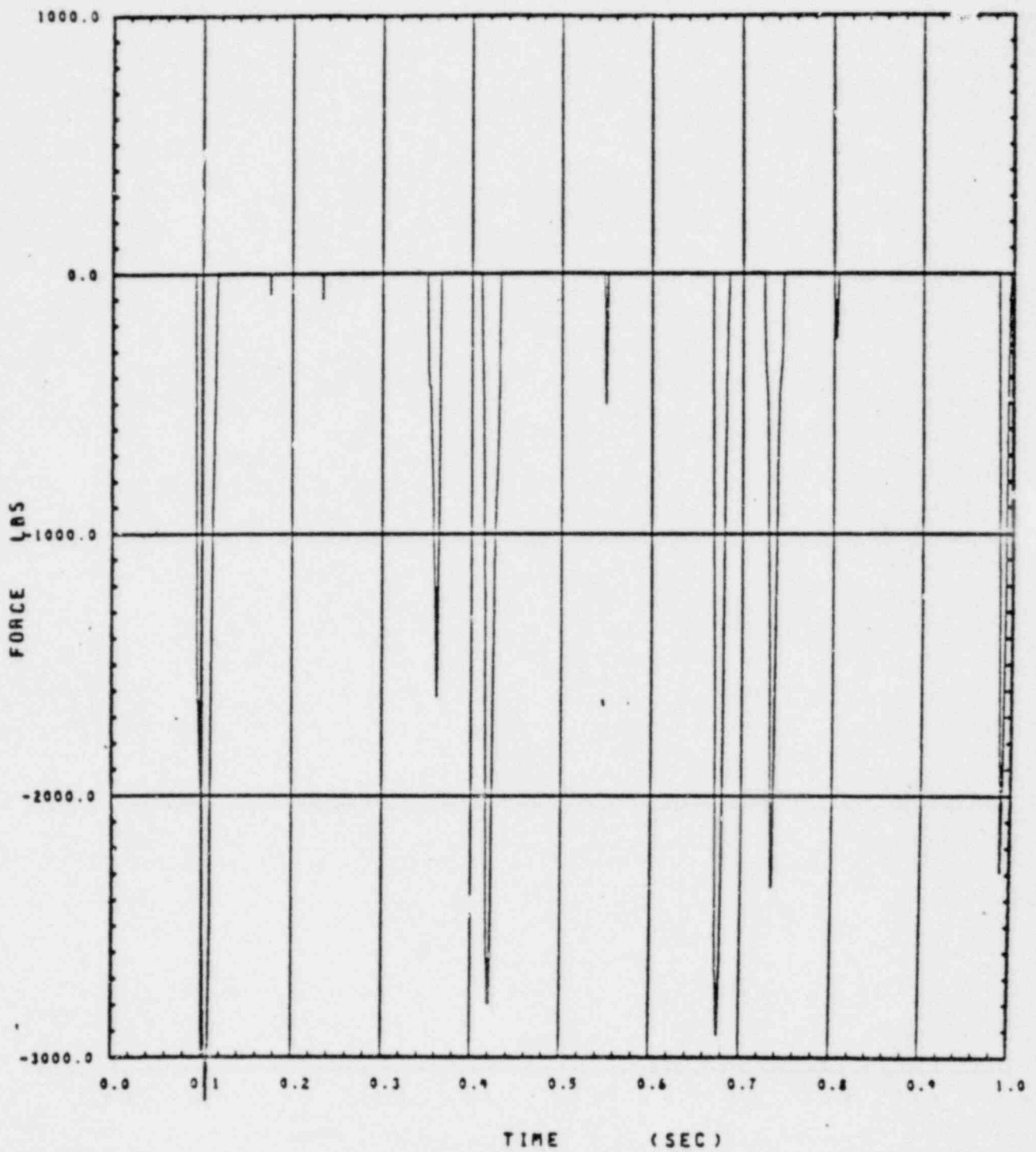


NRC SAMPLE PROB 2B-1 - REL DISPLACEMENT FA 1 G-3 NRC2B4F 05/30/80

Figure 15

DISPLACEMENT RESPONSE OF FIRST FUEL ASSEMBLY GRID NO. 3
 RELATIVE TO BAFFLE - CASE 2B

G-30



NRC SAMPLE PROB 2B-1 - IMPACT FORCE K-B G4 NRC284F 05/30/80

Figure 1.

IMPACT FORCE RESPONSE BETWEEN BAFFLE AND FIFTH FUEL ASSEMBLY
AT GRID NO. 4 - CASE 2B

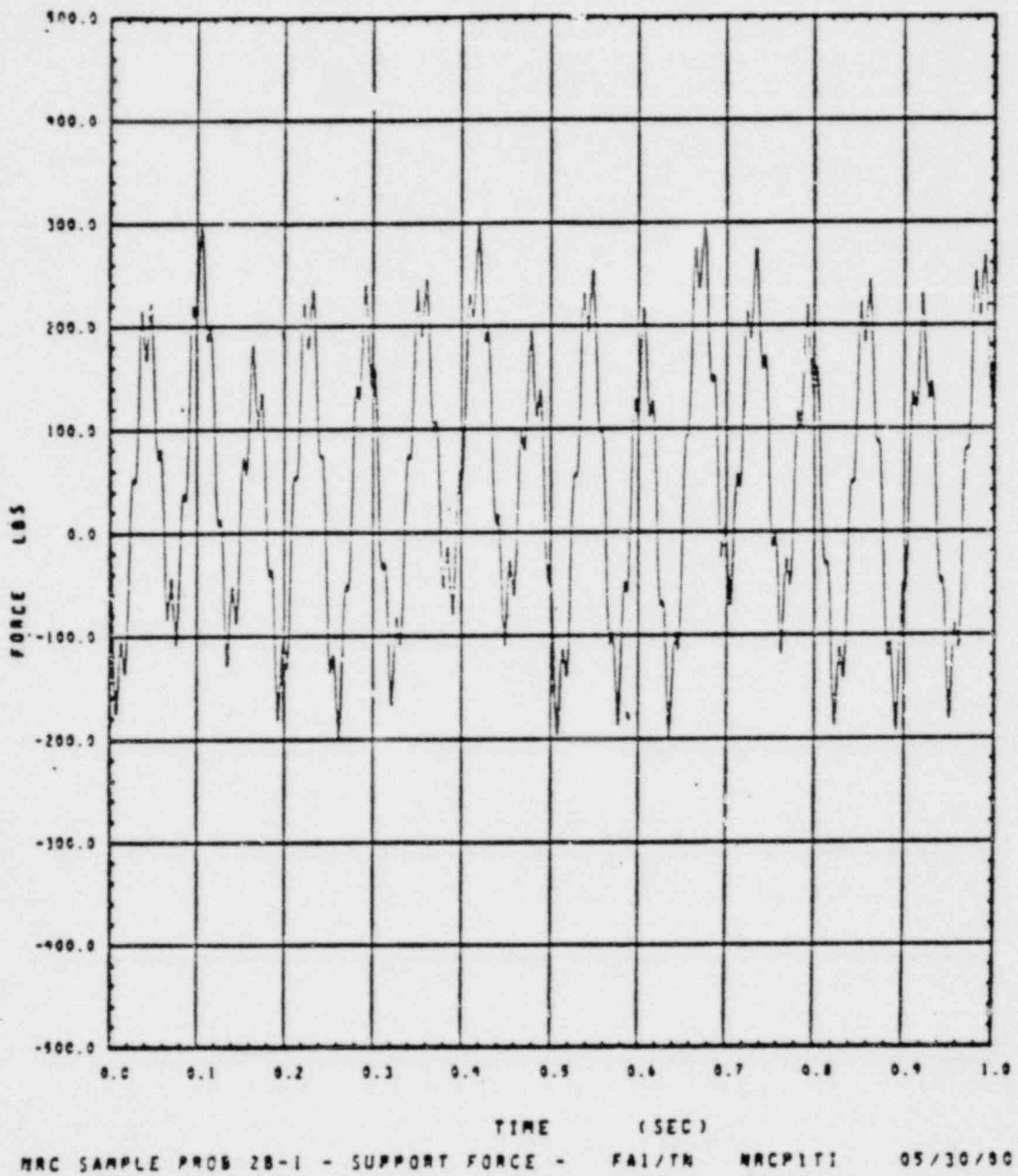
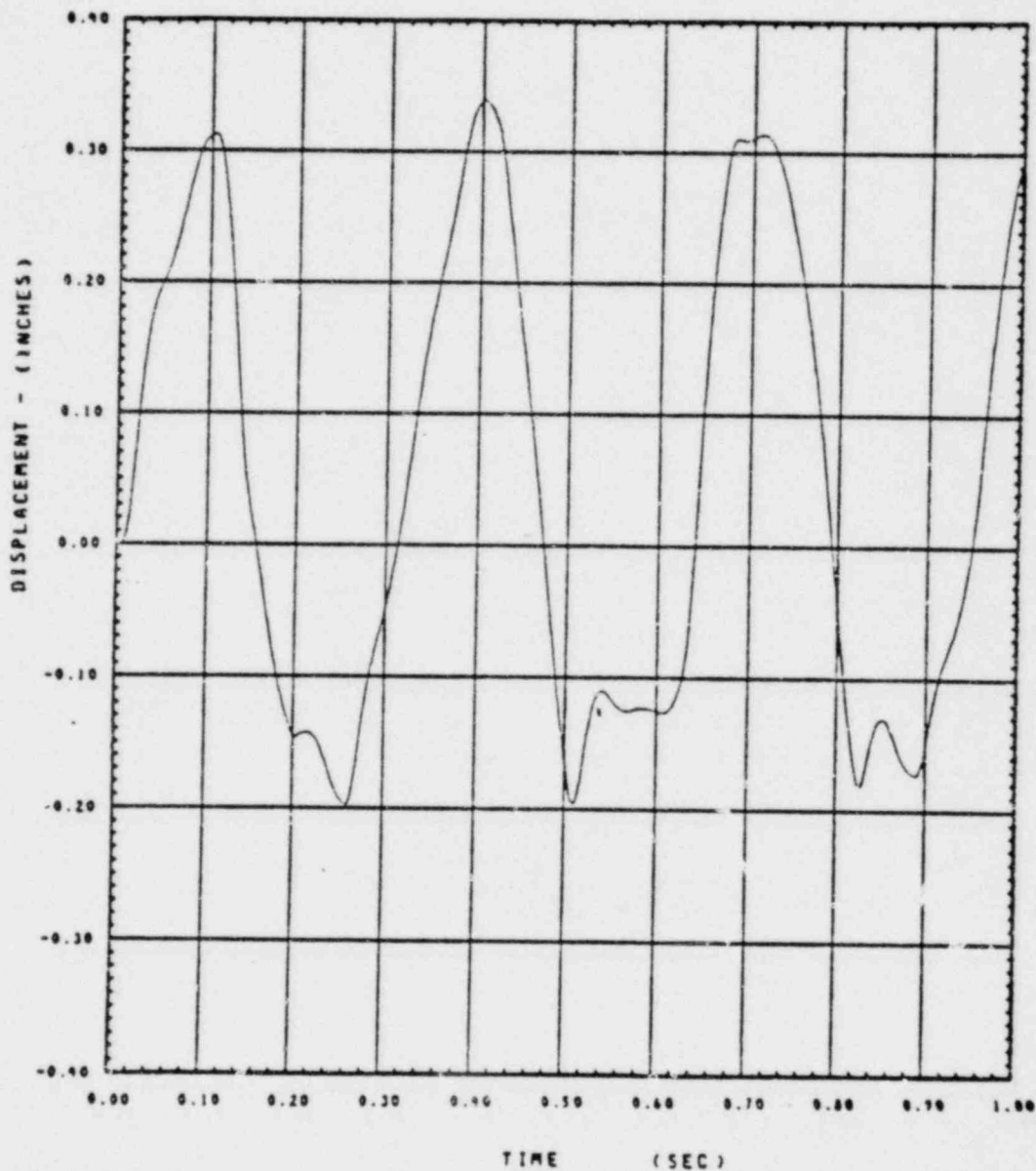


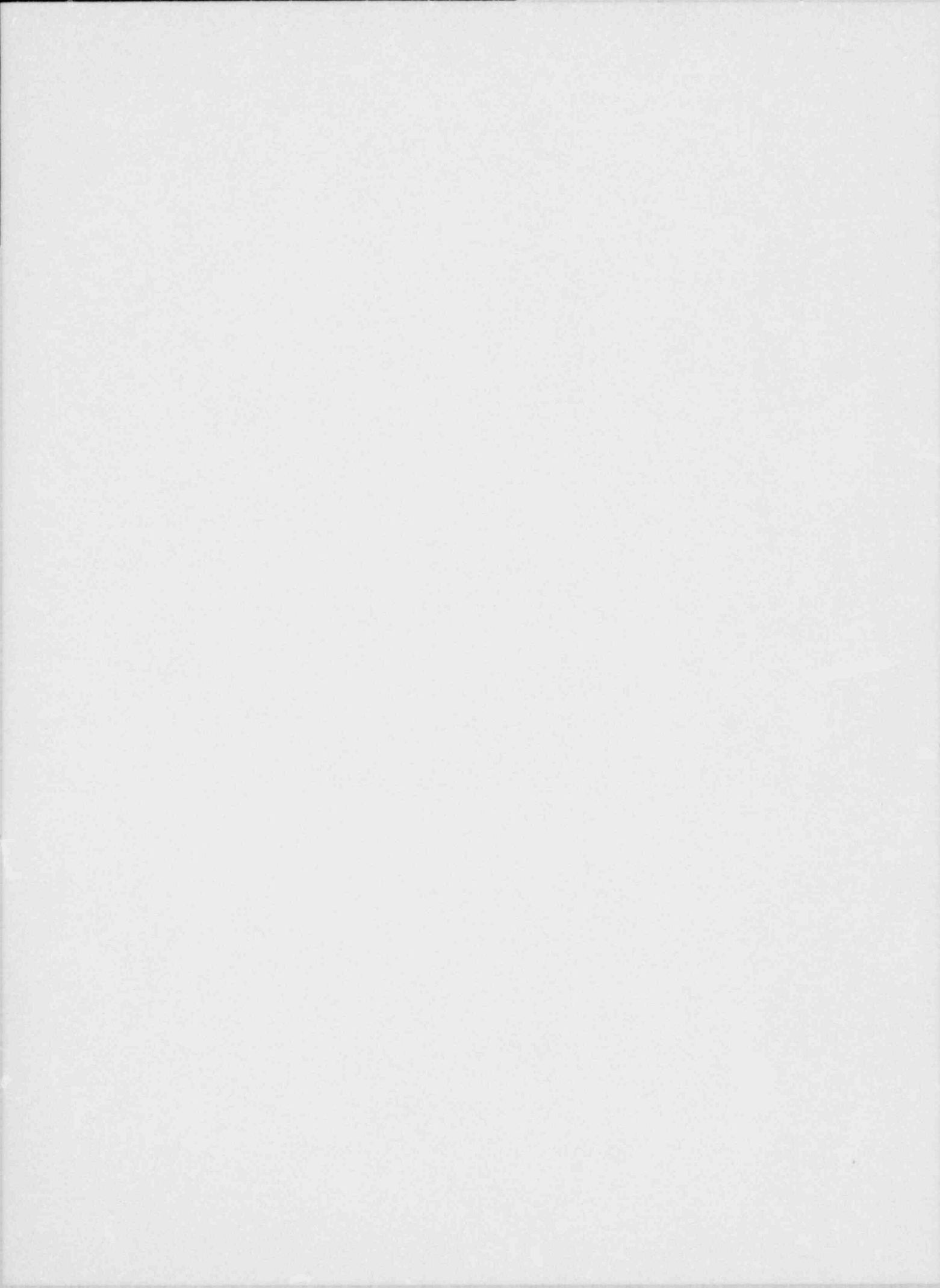
Figure 17

UPPER SUPPORT FORCE RESPONSE OF FIRST FUEL ASSEMBLY - CASE 2B



NRC SAMPLE PROB USING WEGAP - TOTAL DISP FA 1 G-3 NRC2B4F 05/30/80

Figure 18
 TOTAL DISPLACEMENT RESPONSE OF FIRST FUEL ASSEMBLY
 AT GRID NO. 3 - CASE 2B



Westinghouse Electric Corporation

Power Systems

PWR Systems Division

Box 355
Pittsburgh Pennsylvania 15230

March 30, 1979

NS-TMA-2057

Mr. John F. Stolz, Chief
Light Water Reactors Branch No. 1
Division of Project Management
Office of Nuclear Reactor Regulation
U. S. Nuclear Regulatory Commission
Washington, D.C. 20555

Dear Mr. Stolz:

Subject: Verification Testing and Analyses - 17 x 17 Optimized Fuel
Assembly

WCAP-9401 (P)

Enclosed are forty (40) copies of a report "Verification Testing and Analyses -
17 x 17 Optimized Fuel Assembly" (WCAP-9401 Proprietary).

To be provided later are twenty (20) copies of a report "Verification Testing
and Analyses - 17 x 17 Optimized Fuel Assembly" (WCAP-9402 Non-Proprietary).

The attached submittal is the partial result of the extensive testing and
development program which has been conducted during the development of the
improved fuel assembly design known as the Westinghouse Optimized Fuel
Assembly.

The testing and development program was discussed with you and other members
of DPM, DSS and DOR at a meeting held in Bethesda on March 21, 1978. The
presentation given at that meeting by Westinghouse representatives was
summarized by letter NS-CE-1729, C. Eicheldinger to yourself.

The status of the testing and development program and the licensing program
were summarized recently in letter NS-TMA-2022, T. M. Anderson to yourself.

The attached report is submitted to document the testing program and results
of the improved design. This report contains three sections. Section 1
contains information concerning the hydraulic flow tests and results of
fuel rod wear measurements. Section 2 summarizes the critical heat flux
testing and results. Section 3 contains the Safety Analyses of the optimized
fuel assembly for seismic and loss of coolant accidents.

NS-TMA-2057
March 28, 1979
Page 2

Please note that Section 3 does not contain results of the vertical blowdown analysis. This analysis is presently in progress and the results will be submitted as an Addendum to this submittal by June, 1979. For this particular transient the 17 x 17 optimized fuel assembly is expected to respond in a manner similar to the standard 17 x 17 fuel assembly, and the results are expected to give similarly acceptable results.

This submittal is background technical information for a future submittal, WCAP-9500 "Reference Core Report - 17 x 17 Optimized Fuel Assembly", to be submitted to you in June, 1979. Review and approval of both topical reports is needed no later than the third quarter of 1980 so as to minimize impact on individual plant docket.

This submittal is forwarded in advance of WCAP-9500 in order for you to commence your review of the improved fuel assembly design in a timely manner.

We are available to answer any questions or concerns you may have on this subject.

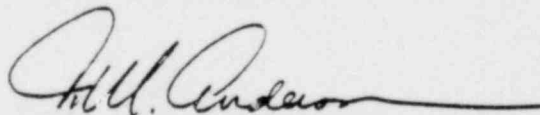
Also enclosed are:

One (1) copy of Application for Withholding, (Non-Proprietary).
One (1) copy of original Affidavit, (Non-Proprietary).

This submittal contains proprietary information of Westinghouse Electric Corporation. In conformance with the requirements of 10CFR2.790, as amended, of the Commission's regulations, we are enclosing with this submittal, an application for withholding from public disclosure and an affidavit. The affidavit sets forth the basis on which the information may be withheld from public disclosure by the Commission.

Correspondence with respect to the affidavit or application for withholding should reference AW-79-13 and should be addressed to R. A. Wiesemann, Manager of Regulatory and Legislative Affairs, Westinghouse Electric Corporation, P. O. Box 355, Pittsburgh, PA 15230.

Very truly yours,



T. M. Anderson, Manager
Nuclear Safety Department

CRT:pj
Enclosure



Westinghouse
Electric Corporation

Water Reactor
Divisions

Nuclear Technology Division
Box 355
Pittsburgh Pennsylvania 15230

August 22, 1980
NS-TMA-2293

Mr. James R. Miller, Chief
Special Projects Branch
Division of Project Management
U. S. Nuclear Regulatory Commission
Phillips Building
7920 Norfolk Avenue
Bethesda, Maryland 20014

SUBJECT: "Verification Testing and Analyses of the Westinghouse 17x17
Optimized Fuel Assembly" - WCAP-9401 (Proprietary) and WCAP-9402
(Non-Proprietary)

Dear Mr. Miller:

Enclosed are:

1. Forty (40) copies of responses to NRC Partial Question Set 1 on WCAP-9401, "Verification Testing and Analyses of the Westinghouse 17x17 Optimized Fuel Assembly" - WCAP-9401 (Proprietary)
2. Thirty-five (35) copies of responses to NRC Partial Question Set 1 on WCAP-9402, "Verification Testing and Analyses of the Westinghouse 17x17 Optimized Fuel Assembly" - WCAP-9402 (Non-Proprietary)

Also enclosed are:

1. One (1) copy of Application for Withholding (Non-Proprietary)
2. One (1) copy of original Affidavit (Non-Proprietary)

The attached is in response to a set of questions on the subject topical report sent to Westinghouse by the NRC via letter dated August 2, 1980 from J. R. Miller (NRC) to T. M. Anderson (Westinghouse).

This submittal contains proprietary information of Westinghouse Electric Corporation. In conformance with the requirements of 10CFR2.790, as amended, of the Commission's regulations, we are enclosing with this submittal an application for withholding from public disclosure and an affidavit. The affidavit sets forth the basis on which the information may be withheld from public disclosure by the Commission.

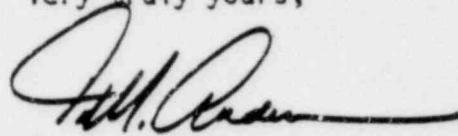
Mr. James R. Miller

-2-

August 22, 1980
NS-TMA-2293

Correspondence with respect to the affidavit or application for withholding should reference AW-80-49 and should be addressed to R. A. Wiesemann, Manager of Regulatory and Legislative Affairs, Westinghouse Electric Corporation, P. O. Box 355, Pittsburgh, Pennsylvania 15230.

Very truly yours,



T. M. Anderson, Manager
Nuclear Safety Department

/bek
Enclosures



UNITED STATES
NUCLEAR REGULATORY COMMISSION
WASHINGTON, D. C. 20555

JUN 23 1980

MEMORANDUM FOR: R. L. Tedesco, Assistant Director
for Licensing
Division of Licensing

FROM: L. S. Rubenstein, Assistant Director
for Core and Containment Systems
Division of Systems Integration

SUBJECT: PARTIAL FIRST ROUND QUESTIONS ON WCAP-9401

Report Title: Verification Testing and Analyses of the
17x17 Optimized Fuel Assembly

Report Number: WCAP-9401

Report Date: March 1979

Responsible Branch: Standardization and Special Projects Branch
and Project Manager: J. S. Berggren

Description of Review: Partial First Round Questions

Requested Completion Date: None

Review Status: Incomplete

We have reviewed a portion of the report described above and request that you forward the attached questions to Westinghouse so that this portion of the review may be completed. These questions cover the fuel assembly seismic and LOCA analysis in revised chapter 3; the Mechanical Engineering Branch is reviewing the parts of chapter 3 dealing with the reactor internals model. Chapters 1 and 2 are being reviewed by the Core Performance Branch Fuels Section and Thermal Hydraulics Section, respectively, and Q1's will be forthcoming as manpower permits.

L. S. Rubenstein, Assistant Director
for Core and Containment Systems
Division of Systems Integration

Attachment:
Questions

cc w/attachment:
D. Eisenhut W. Johnston
D. Ross J. Berggren
J. R. Miller R. O. Meyer

Response to
PARTIAL QUESTION SET 1
WCAP-9401 "Verification Testing and Analyses
of the 17x17 Optimized Fuel Assembly"

1. Lateral and vertical LOCA analyses are performed as well as a lateral seismic analysis. Please evaluate and discuss vertical seismic loads on the Optimized Fuel Assembly.

Response

The vertical seismic analysis was not included in the topical report because the vertical seismic responses are small compared to that from the vertical LOCA event and insignificant compared to the allowable. However, it was analyzed and the maximum dynamic forces at the top nozzle holddown spring and bottom nozzle are approximately []⁺ and [] of that of a vertical LOCA, respectively; or 21 % and 9 % of the allowable respectively. (a,c)

2. Please include a fatigue assessment, or reference documents which assess the 17x17 OFA fatigue predictions.

Response

The fatigue assessment on fuel components is not required for condition IV events. The faulted condition events are not expected to occur during the life of a fuel assembly, but are postulated to assure design conservatism. The plant would not be expected to return to normal operation, following a faulted condition event.

3. Combined motions in the horizontal and vertical directions may influence predictions based on independent analyses. Please evaluate and discuss beam-column coupling effects.

Response

The beam-column coupling effect in modeling is generally used for large deflection or deformation analysis. For the present type of structural analysis large deflections do not occur. The directions may be decoupled and linearly superimposed for the dynamic solution of a fuel assembly in a closely packed core due to the small and restrained lateral motion of the upper core plate. Therefore, the linear combination of decoupled motions of two perpendicular directions is justified.

4. Table 3-8 indicates different behavior in the vertical direction for reactors with stiff and soft vessel supports. What differences are expected in the lateral results for the stiff and soft Reactor Pressure Vessel supports?

Response

The effect of lateral stiffness variations was considered in the evaluations by parametric variations on lateral stiffness. Only the worst case response was presented in the topical report. The RPV support stiffnesses would influence the dynamic response of the core plate motions. As a result, the maximum grid load is also affected by the support stiffness variation. There is no direct relationship between the grid load and support stiffness due to the geometrical non-linearity in the core model and frequency contents in the transient forcing function.

The OFA core responses indicated that the vertical support stiffness [] to the maximum grid load. However, the soft lateral support stiffness tends to reduce the maximum grid load. The maximum grid load corresponding to a soft support stiffness for a RPV model is approximately []+ (a,c)

5. On page 3-26 it is stated that the spring stiffnesses were adjusted to include water mass. It is not clear what amount of adjustment was made or how this will affect the results. Provide a discussion of how the adjustment was made and include references. Include applicable experimental data (if taken) to support the adjustment of spring stiffness. (a,c)

Response

The adjustment for the fuel assembly submerged in water and at reactor operating conditions was accomplished in the detailed fuel assembly finite element model (FEM). The material properties and the connective mass correction at operating temperature were introduced in the input of the FEM in order to have both the connective mass and temperature effects. The experimental data indicates that the lowest fuel assembly fundamental frequency in water is approximately []+ lower than in air. (b,c)

The fuel assembly model for core safety analysis, as indicated in the topical report, was constructed based on the adjusted fuel assembly frequencies and total fuel assembly mass distribution.

Parametric studies have indicated that the grid impact forces are relatively insensitive to the fuel assembly frequency changes caused by water.

6. Please provide test data to support the values of in-grid stiffness and damping.

Response

The in-grid stiffness was not used in the core model, thus there was no experimental tests performed in this regard. The experimentally obtained thru-grid stiffness at operating temperature is given on page 3-26 of the topical report. The in-grid stiffness value is determined from analytical correlations with fuel assembly lateral impact tests.

7. Even though no permanent deformation is predicted in this analysis (with SRSS combination and 1.3 Factor on LOCA), the crushing behavior is of interest. Please include a picture of a crushed grid and discuss how the grid can fail in the innermost rows without disturbing the relative positioning of guide thimbles.

Response

The typical mode of failure for the Westinghouse zircaloy (OFA) grid is a []+ as seen in Figure 1. The distortion is primarily due to the []+. The control rod thimble diameter is not deformed. The relative control rod position may be displaced slightly. However, there would be no significant effect on control rod movement due to the sufficiently large clearance between the control rod and the guide thimble, and the structural flexibility of control rods. Also, the maximum grid loads under SSE and LOCA transients always occur []+ (b,c) (b,c) (a,c)

8. The heat treatment given to fuel components can significantly affect their lifetime performance. Please describe the final state of the Zircaloy grid material including amount of cold work and type of annealing. Other data desired are the initial spring loads and expected relaxation. Please discuss the effect of grid spring relaxation on fuel bundle stiffness and provide the estimated fuel bundle stiffness at Beginning-of-Life and End-of-Life.

Response

The cold finished grid strap material of controlled grain size is punched and stamped to form the basic unit of the grid cell consisting of dimples and springs. The final state of the grid strap is subjected to a relatively low temperature annealing process (about []+ for approximately []+ hours) to relieve the stresses due to forming. (a,c)

The initial spring preload at the beginning-of-life (BOL) hot condition is about []+ lbs. The loss of contact between the grid spring and fuel rod due to spring force relaxation is expected to occur at approximately []+ EFPH. []+ (a,c) (a,c)

9. What are the yield strength and ultimate strength that the allowable stresses are based on? What temperature do these values correspond to?]+ (a,c)

Response

Equations describing the Zircaloy-4 fuel cladding and thimble tubing uniaxial and biaxial strengths as a function of temperature for both unirradiated and irradiated material are given on pages 2-8 thru 2-10 of WCAP 9179, Revision 1, "Properties of Fuel and Core Component Materials". The equations given for

(b)(7)(C)

Figure 1 Typical Failure Mode for Dynamic Tests at 600°F

the yield strengths of the thimble tubing are applicable to the Zircaloy grids. Ultimate tensile strengths are not used in the design of the Zircaloy components of the fuel assembly.

For the Inconel-718 components of the fuel assembly (i.e., the top and bottom grids) the values for the ultimate tensile strength and tensile yield strength are given on pages 4-6 and 4-7 of WCAP 9179, Rev. 1.

For the 304 type stainless steel components of the fuel assembly (i.e., the top and bottom nozzles) the values for the ultimate strength and the yield strength are given on page 3-4 of WCAP 9179, Rev. 1.

For all components of the OFA, the unirradiated best estimate values at 600°F were used in design. The material strengths tend to increase under irradiated conditions.

10. Guide tubes are constructed with flow holes and are subject to significant wear where the control rods are parked. It appears that the values for guide tube stresses were based on nominal dimensions and did not include the effects of wear or stress concentration around the flow holes. Please account for these two effects on guide tube stresses.

Response

The thimble areas which exhibit slight wear are not highly stressed by the LOCA induced loads. Consequently, the thimble wear effects are usually evaluated for the handling condition which is more limiting.

The stress concentration effects around the guide tube holes were not evaluated for the faulted condition which is consistent with ASME stress evaluation procedures.

11. The axial model in Fig. 3-24 does not appear to have gap elements for fuel assembly lift and impact with core plates. Describe how the axial model predicts impacts.

Response

Although the gapped elements are not shown in the axial fuel assembly model, there are []+ gap elements for each group of fuel assemblies in the reactor vessel model to simulate the possible fuel assembly liftoff and impact with the core plates. [

(a,c)

]+

(a,c)

12. Comparisons between analytical models and experimental results are important. Although the models for conversion of strain and stress have not changed, the experimental fit of the model has. Please discuss the conversions of stress and strain, and compare experimental and predicted stresses for both the lateral and vertical models.

Response

The comparisons between analytical models and experimental results, in general, show excellent agreement with respect to the structural behavior under the applied load or deflection. Generally, the conversion of strain to stress uses the direct relationship of linear elastic analyses. The predicted stresses in various fuel assembly structural components are always based on the conservative values.

13. For comparison with the NRC audit code, please provide:

Clear full-page Plot of

- a) the time history of loads on the limiting grid
- b) the time history of vertical motions.

Masses

- a) Fuel rod
- b) Spacer grid
- c) End nozzles
- d) Guide and instrument tubes
- e) Total fuel assembly and center of gravity

Other measured quantities

- a) Axial gap between fuel nozzles and upper core plate
- b) Mode shapes (digital)
- c) Friction coefficients
- d) Axial holddown spring stiffness and preload
- e) Axial impact damping factor

Plots with experimental data

- a) Lateral force vs. deflection
- b) Vertical impact force vs. time
- c) Grid crush load (force) vs. velocity

Forcing Functions

- a) Core plate motions for SSE (digital)
- b) Core plate motions for LOCA (digital)

Response

Westinghouse has committed, via telephone conversation on April 16, 1980 with the Staff's Mr. G. Alberthal and their consultant Mr. R. Grubb (EG&G), to supply the necessary documentation to verify the general finite element computer code WEGAP which was used in the supporting analysis to WCAP 9401, Section 3.0 to calculate the dynamic structural response of the reactor core. Included in this documentation will be the results of the NRC's hypothetical fuel assembly problem analyzed with WEGAP. This submittal, scheduled for August 1980, will satisfy the NRC's need to evaluate the adequacy of WEGAP as a design code.

In addition, Westinghouse has performed an internal independent design verification of the WEGAP code consistent with the requirements of 10CFR50 Appendix B.

UNITED STATES
NUCLEAR REGULATORY COMMISSION
WASHINGTON, D. C. 20555

JAN 22 1981

Westinghouse Electric Corporation
ATTN: Mr. T. M. Anderson, Manager
Nuclear Safety Department
P. O. Box 355
Pittsburgh, Pennsylvania 15230

Dear Mr. Anderson:

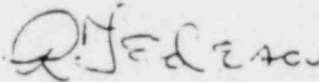
SUBJECT: REQUEST NUMBER 3 FOR ADDITIONAL INFORMATION ON WCAP-9401

We are currently reviewing Westinghouse Electric Corporation report WCAP-9401 entitled "Verification Testing and Analyses of the 17 x 17 Optimized Fuel Assembly".

The continuing reviews of the fuel assembly seismic and LOCA analysis of Section 3 of WCAP-9401 reveal the need for the additional information indicated in the enclosure.

This information is necessary to complete the review - its expeditious submittal will therefore be to the Westinghouse advantage. Please advise us as soon as possible of your planned submittal date to permit us, in turn, to develop a review schedule.

Sincerely,



Robert L. Tedesco, Assistant Director
for Licensing
Division of Licensing

Enclosures:
As stated

cc: Mr. Alex Ball
Westinghouse Electrical Corp.
Nuclear Safety Department
P. O. Box 355
Pittsburgh, Pennsylvania 15230

Westinghouse
Electric Corporation

Water Reactor
Divisions

Nuclear Technology Division
Box 1888
Pittsburgh, Pennsylvania 15200

February 13, 1981
NS-TMA-2384

Mr. James R. Miller, Chief
Special Projects Branch
Division of Project Management
U. S. Nuclear Regulatory Commission
Phillips Building
7920 Norfolk Avenue
Bethesda, Maryland 20014

Ref: NS-TMA-2293,
August 22, 1980

SUBJECT: Responses to "Request Number 3 for Additional Information on
WCAP-9401," NRC Letter from R. L. Tedesco to T. M. Anderson,
January 22, 1981

Dear Mr. Miller:

Enclosed are:

1. Twenty-five (25) copies of the proprietary responses to the NRC Request Number 3 for additional information on WCAP-9401 (Proprietary).
2. Twenty (20) copies of the non-proprietary responses to the NRC Request Number 3 for additional information on WCAP-9401 (Non-Proprietary).

Also enclosed are:

1. One (1) copy of Application for Withholding (Non-Proprietary).
2. One (1) copy of original Affidavit (Non-Proprietary).

This submittal contains proprietary information of Westinghouse Electric Corporation. In conformance with the requirements of 10CFR2.790, as amended, of the Commission's regulations, we are enclosing with this submittal an application for withholding from public disclosure and an affidavit. The affidavit sets forth the basis on which the information may be withheld from public disclosure by the Commission.

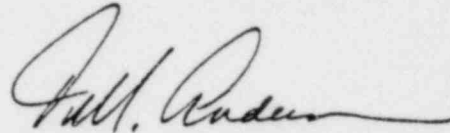
Mr. James R. Miller

-2-

February 13, 1981
NS-TMA-2384

Correspondence with respect to the affidavit or application for withholding should reference AW-81-13 and should be addressed to R. A. Wieseemann, Manager of Regulatory and Legislative Affairs, Westinghouse Electric Corporation, P. O. Box 355, Pittsburgh, Pennsylvania 15230.

Very truly yours,



T. M. Anderson, Manager
Nuclear Safety Department

/bek

Enclosures

QUESTION 1 Page 3-1;

What correlation exist between the spectra in Figure 3-1 and Figure 3-2:

RESPONSE

The design response spectra given in Figure 3-1 and Figure 3-2 were identical, but they were plotted on log-log and linear-linear scales, respectively. The response spectrum curve of the synthesized earthquake time history was also given in Figure 3-2 to show the conservative enveloping of the design response spectrum.

QUESTION 2 Page 3-6 and; Q1 question 12

Comparisons between analytical model and experimental results are important. Although the model has not changed, the experimental fit of the model has. Supply quantitative comparable experimental and analytical stress-strain results and a basis for comparison of these results.

RESPONSE

The strain data was obtained at selected thimble locations during the optimized fuel assembly lateral loading test. The test set-up as well as the gage locations is schematically shown in Fig.Q2.1. The thimble stresses derived from the strain reading are shown in Figure Q2.2.

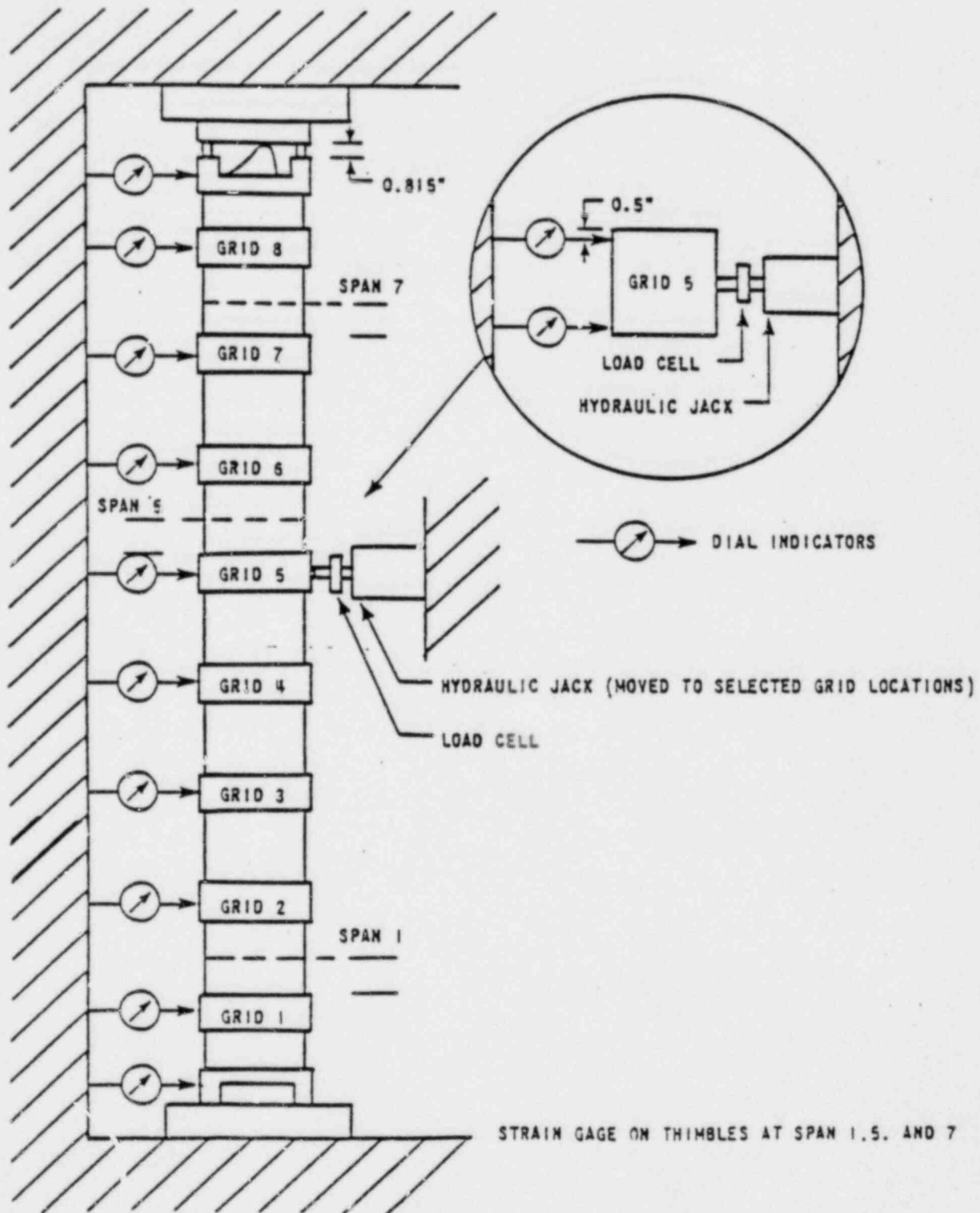


FIGURE Q2.1 17x17 OPTIMIZED FUEL ASSEMBLY LATERAL STIFFNESS TEST SETUP AND STRAIN GAGE LOCATIONS

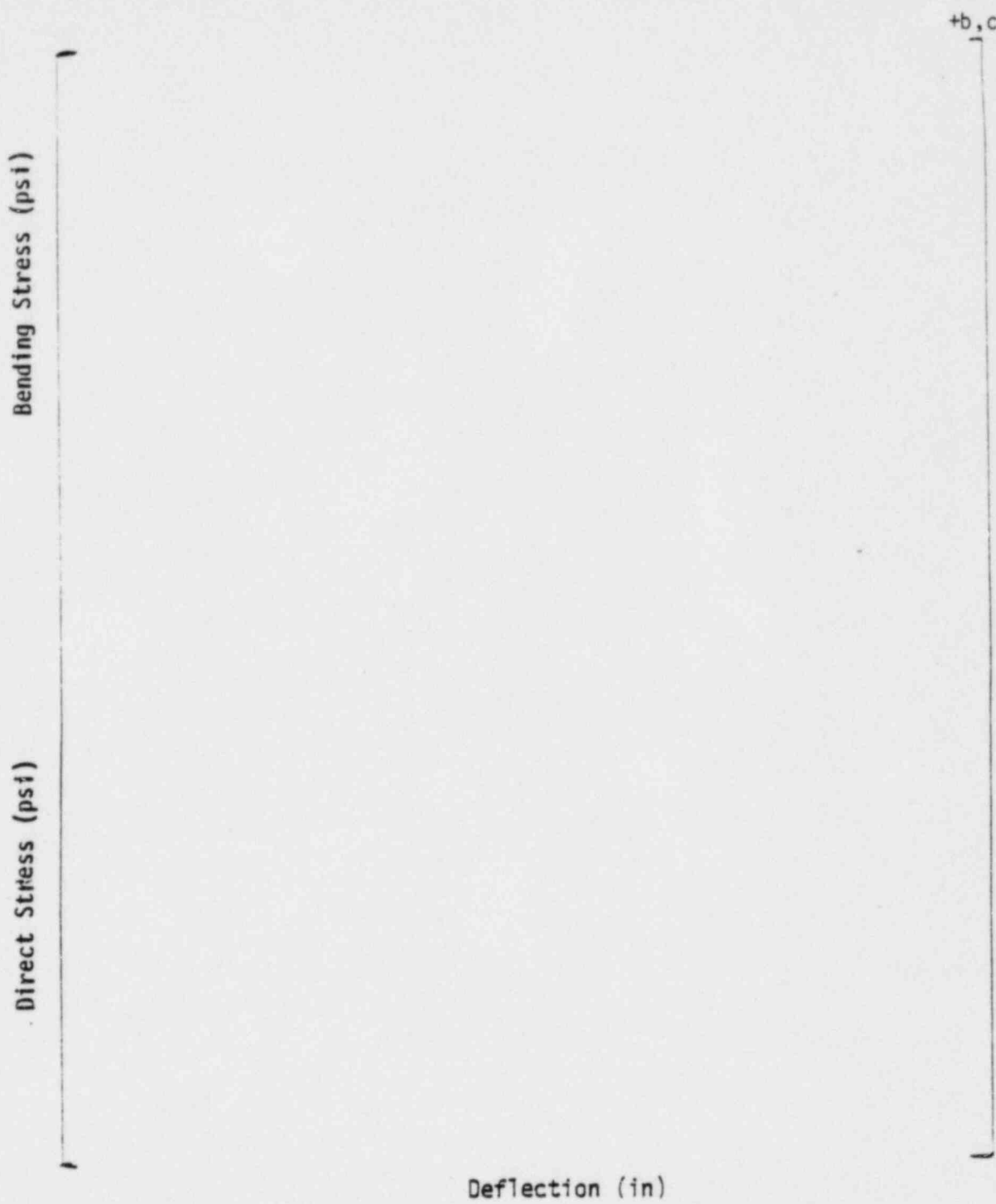


FIGURE Q 2.2 17x17 OPTIMIZED FUEL ASSEMBLY THIMBLE STRESS VERSUS LATERAL DEFLECTION
EOL COLD

QUESTION 3 Page 3-6;

The discussion concerning the model shown in Figure 3-4 is confusing. Please clarify.

RESPONSE

The lateral fuel assembly finite element model has been experimentally verified for the Westinghouse type fuel design. The discussion of the FEM is documented in WCAP-8236. A brief discussion of the lateral fuel assembly model is presented.

The fuel assembly model consists of the following structural modeling:

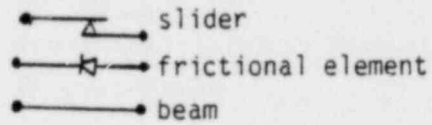
- 1) The fuel assembly skeleton structure which contains an array of twenty-four thimble tubes plus one instrumentation thimble, is represented by a pair of 2D-beam columns. The structural rigidity was established by properly spacing the vertical beams through the use of parallel theorem for calculating the equivalent moment of inertia.

The beam elements were used to simulate fuel nozzles and grid stiffnesses.

- 2) The fuel rods were modeled by two vertical beams. Since the fuel rod lateral deflections are independent of positions within the array, the summation of the individual fuel rod properties was used to simulate all of the rods.
- 3) The grid dimples and springs were modeled using friction elements, which are preloaded linear springs with out of plane friction to simulate the fuel rod lift-off within a grid. The functional elements were also used to model the axial fuel rod drag force in the grid cell.

The side dimples were represented by a slider type element to simulate the frictional effects caused by fuel rods sliding on the side dimple. The slider element is basically a simplified one dimensional frictional element.

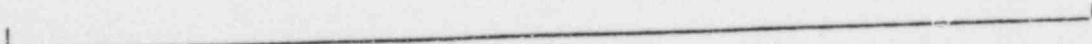
The legend for Fig 3-4 is



The element 5-11 in the text should be correctly read as 5-7.

- 4) A schematic representation of a portion of the fuel rod and the grid restraints is shown in Figure Q3.1.

+b, c



L-8

FIGURE Q3.1 SCHEMATIC OF A FUEL ROD WITH GRID RESTRAINTS

QUESTION 4 Page 3-8;

Provide analytical-experimental correlations for the fuel assembly lateral force-deflection response.

RESPONSE

The experimental-analytical correlations for the Westinghouse type fuel assembly design were documented in WCAP-8236. The fuel assembly lateral load versus deflection responses for the 17x17 OFA is shown in Fig Q4.1.

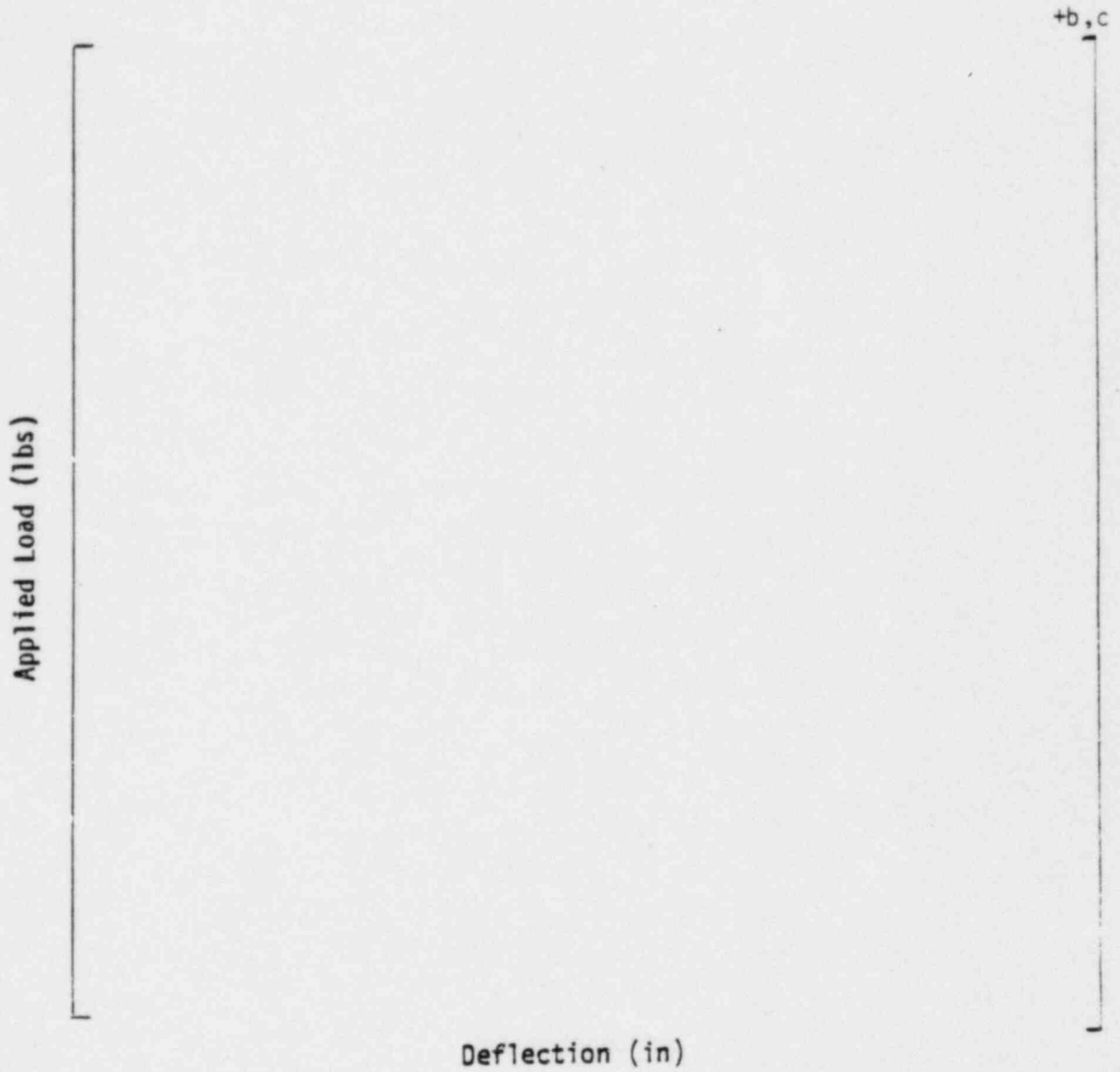


FIGURE Q4.1 17x17 OPTIMIZED FUEL ASSEMBLY LOAD VERSUS DEFLECTION -
LOAD APPLIED AT GRID NO. 5 - EOL COLD

QUESTION 5

[]⁺ is important in predicting core plate motion. Provide additional detail showing how this effect was implemented and what analytical-experimental justification exists for its use. Supply this information for both the lateral and vertical implementation. (a,c)

RESPONSE

[]⁺ is included for LOCA evaluation in the MULTIFLEX thermal hydraulic computer code. MULTIFLEX documentation is provided by Reference 5 of WCAP-9401. (a,c)

For seismic evaluation, []⁺ representation was included in the reactor vessel structural model to more accurately represent the reactor vessel structural dynamics in a []⁺. The outputs of the seismic analysis of the reactor vessel model are lateral core plate motions and fuel assembly vertical nozzle loads. (a,c)



+(a,c)

+(a,c)

+(a,c)

+(a,c)

$+(a, c)$

TABLE A

COMPARISON OF VERITICAL MODEL RESULTS WITH EXPERIMENTAL DATA



⁺(a,b,c)

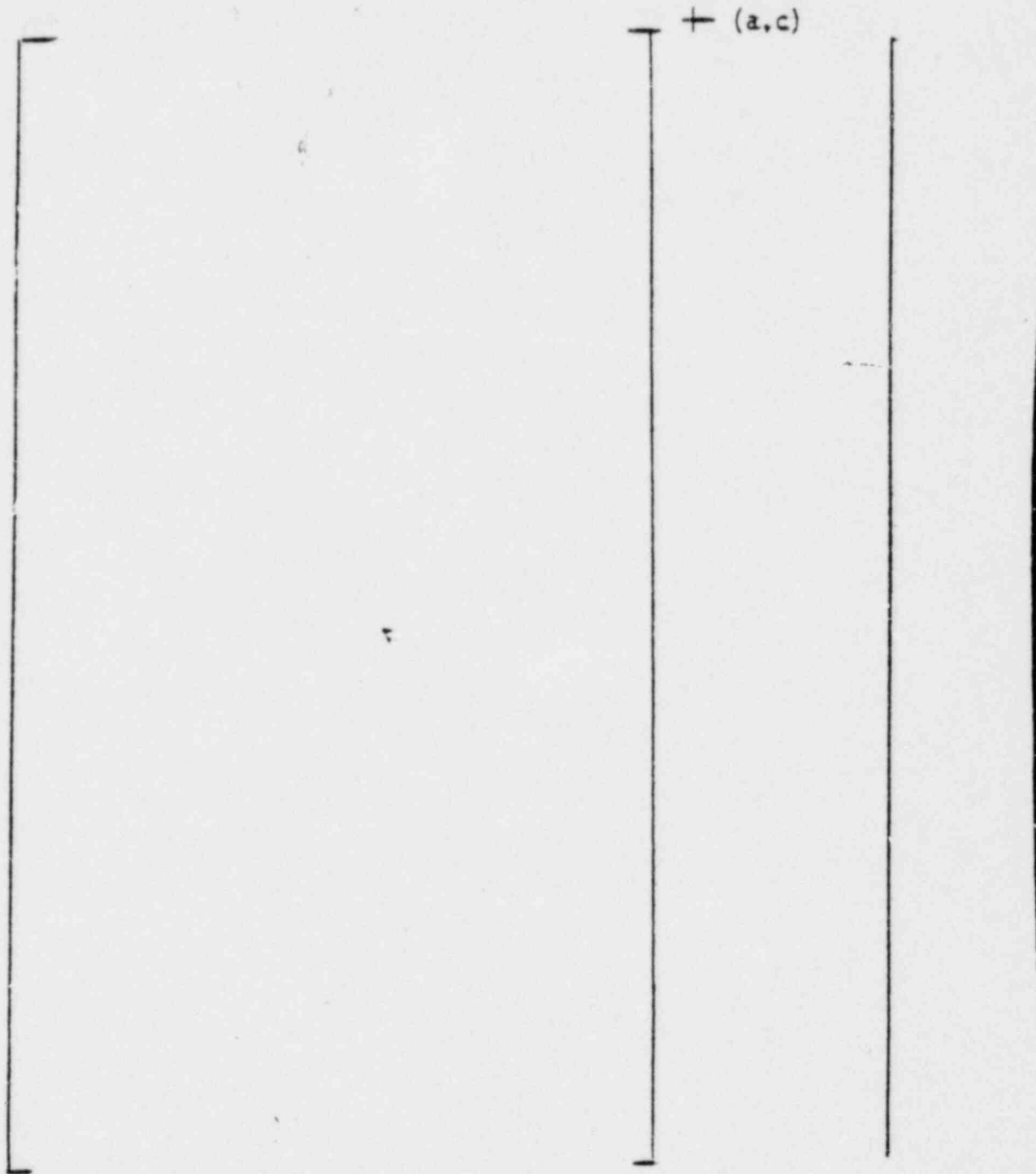


Figure 3-7(b) Reactor Core Barrel Model

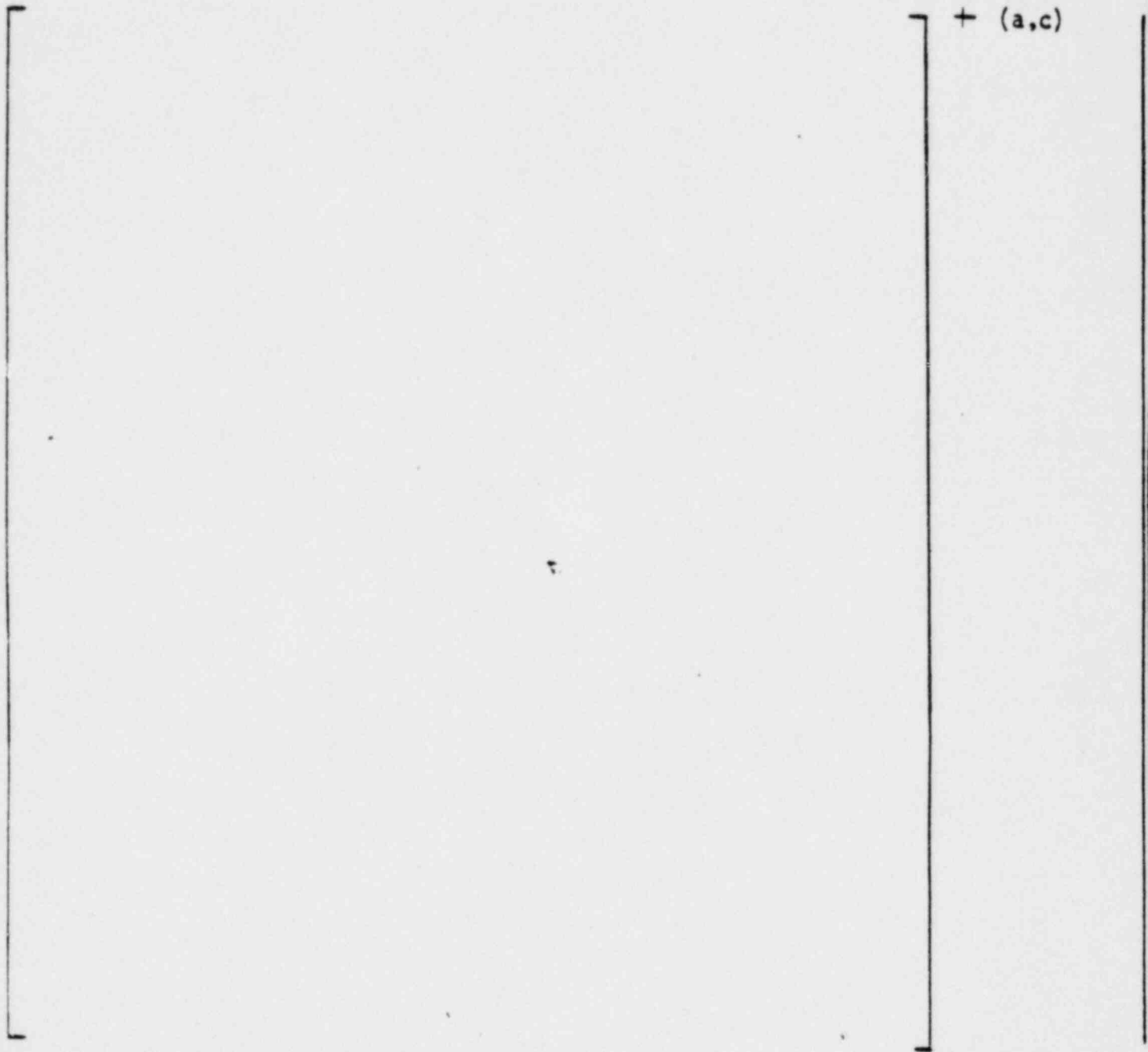


Figure 3-7(d) Vertical Hydrodynamics Model

QUESTION 6 Page 3-19;

Only one spectra is shown in Figure 3-1. Refer to question 1.

RESPONSE

The response spectrum curve given in Fig. 3-1 was developed by enveloping the response spectra for a number of typical Westinghouse four loop neutron panel plants. Since the spectrum presented in Fig. 3-1 is relatively severe, it is judged to be conservative in establishing the fuel capability. For plant designs which could exceed the given spectrum, specific analysis using the plant spectrum may be required.

QUESTION 7 Page 3-20 and; Q1 question 5

The response to Question Set 1 question 5 and the comment presented on page 3-20 concerning the importance of the fuel assembly fundamental mode of vibration to core region response appear to suggest different points of view. Explain.

RESPONSE

The peak grid impact response is, in general, dependent on the fundamental fuel assembly vibrational frequency. The answer to Question 5 of Q1 suggested that the added water mass tends to lower the fuel assembly fundamental frequency slightly.

Justify that []⁺ is a reasonable way to judge the worst case fuel system loading considering the fuel system response is nonlinear. Which []⁺ cases produced the largest impact forces and peak fuel assembly displacements in the system model? Do these cases correspond to the []⁺ case chosen?

a,c

a,c

a,c

RESPONSE

Seismic analyses using a number of different seismic waves have indicated that the [

]. The selected worst case wave corresponded to the []⁺ system. The fuel assembly grid maximum impact forces obtained from the Reactor Internals models generally occurred for the same input waves selected using the response spectra method.

a,c

a,c

The time history designated as case 2 was used to assess the Optimized Fuel Assembly seismic response. As shown in Figure Q8.1, the acceleration response spectrum obtained from the case 2 seismic time history envelopes the response spectra generated for the remaining six seismic waves in the [

] ⁺

a,c



FREQUENCY (HZ)

FIGURE Q8.1

FREQUENCY RESPONSE SPECTRA AT UPPER CORE PLATE

LEGEND

Case			
1	•••••	5	—•••—
2	————	6	—•—•—
3	-----	7	—••—
4	———		

QUESTION 9 Page 3-21;

Specify the break opening times used in the analyses. Provide additional data to support the break opening times selected.

RESPONSE

Reference 6 of WCAP 9401 specifies the standard break opening times used in Westinghouse LOCA analyses as instantaneous, []⁺ millisecond. a,c
This break opening time was the analytical basis used in WCAP 9401 which has been the NRC's accepted analytical basis.

What maximum percent error from the experimental values is associated with each analytical mode shape and analytical frequency?

RESPONSE

The mode shapes for the fuel assembly detailed model and the lumped mass-spring models were compared with the experimentally determined modes and indicated relatively good agreement. The lumped mass model used in the reactor core analyses is derived using an analytical procedure[

]⁺. The natural a,c

frequencies for the lumped mass model was based on experimental and finite element data with some minor adjustments to reflect operating conditions.

QUESTION 11 Page 3-26;

Are the analytical predictions presented in Figure 3-12 derived from the model values presented in Table 3-1? If not, discuss the differences.

RESPONSE

Yes.

QUESTION 12 Page 3-26 and; Q1, Question 6

The response given to Question Set 1 question 6 is somewhat confusing. The core region model presented in Figure 3-10 shows the definite inclusion of K_s and C_s values. Please supply a short explanation to resolve this situation.

RESPONSE

The in-grid and through-grid stiffnesses as defined by the NRC are associated with the method of grid impact testing. The in-grid dynamic stiffness is normally determined from tests in which a weighted grid is given an initial velocity and is impacted against a rigid or grid restraint. The through-grid stiffness is usually determined from tests in which a rigid mass impacts a stationary grid.

As shown in Fig. 3-10 the grid stiffness properties designated as K_g and C_g were obtained from through-grid impact tests at operating temperature. The local grid stiffness properties, K_s and C_s which represent the combined flexibility of the grid springs, dimples, and fuel rods, were determined from the fuel assembly lateral impact tests rather than from the in-grid impact tests.

The fuel assembly lateral impact properties such as impact duration, impact force, and rebound, together with the fuel assembly finite element model, were used to obtain K_s and C_s values.

QUESTION 13 Page 3-26 and;

The methods used for determining K_s , C_s , K_g , C_g , and the critical load (P_{crit}) have been discussed and information supplied supporting the values derived for the inconel spacer grids. The incorporation of Zircaloy grids in the fuel assembly design will effect the response of the fuel system and certain spacer grid allowable loads. To completely review this situation, the following information is requested:

- a. test data supporting the in-grid stiffness and damping values chosen,
- b. test data supporting the through-grid stiffness and damping values chosen, and
- c. test data supporting the value of P_{crit} chosen.

When discussing the above test data, discuss the velocities used in the impact test relative to those calculated analytically from the core region response. Discuss static and dynamic test values.

RESPONSE a.

The local grid flexibility (or in-grid stiffness damping values) K_s and C_s are derived from the fuel assembly lateral impact tests. The fuel assembly lateral impact test arrangement is shown in Fig. Q13.1. The impact duration obtained from these tests was approximately []⁺ sec. A correlation analysis was performed using the lumped mass-spring analytical model to verify the model by comparing the grid impact forces. These results are given in Table Q13.1. b,c

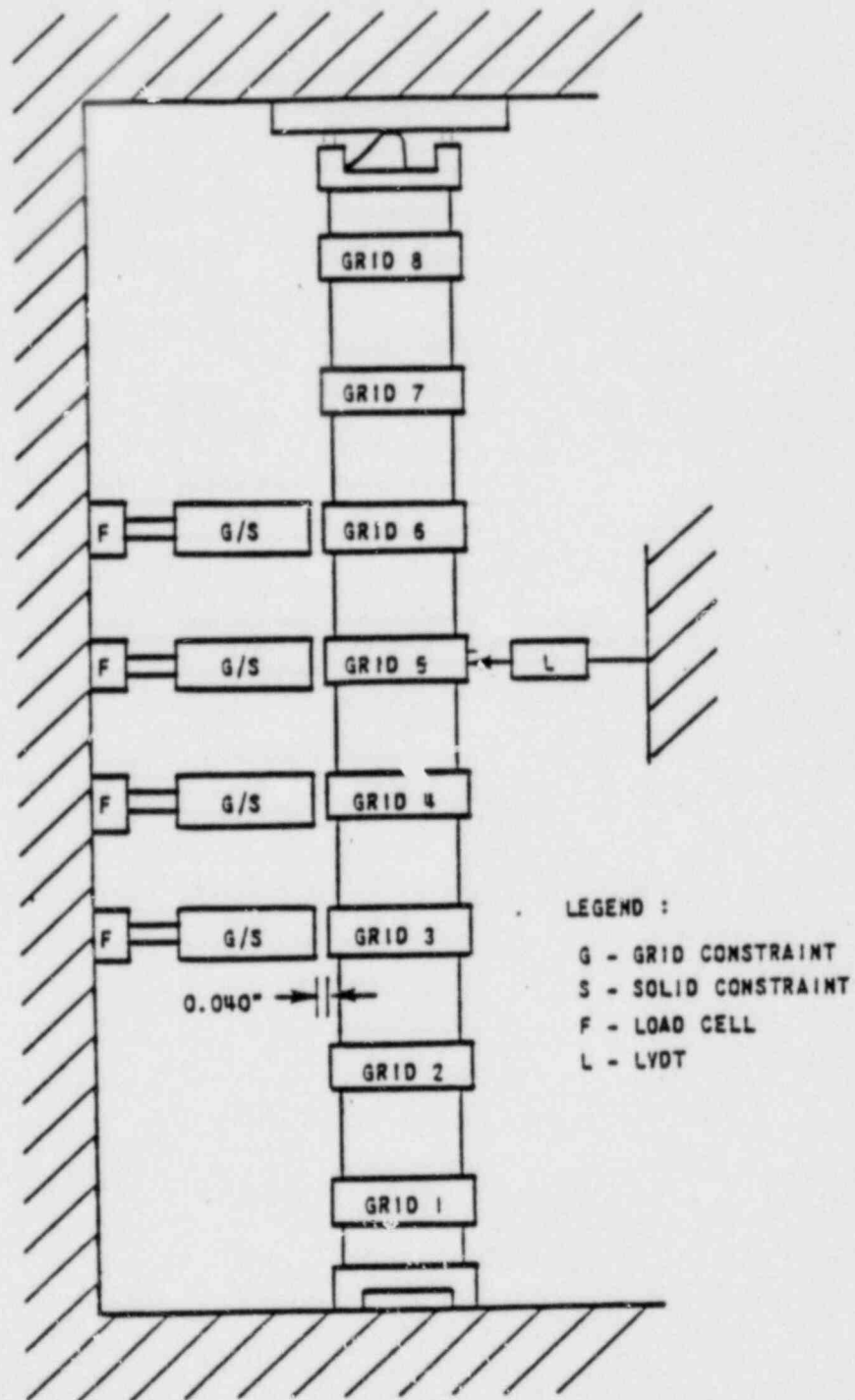


FIGURE Q13.1 17x17 OPTIMIZED FUEL ASSEMBLY LATERAL IMPACT TEST SETUP

TABLE Q13.1

COMPARISON BETWEEN FEM AND FA LATERAL IMPACT RESULTS

(Total Initial Deflection = []⁺ in.)

b,c

	FEM	Test	+
Time Duration (sec.)			
Rebound (in.)			
Max. Impact Force (lb)			

b,c

RESPONSE b.

The average dynamic through-grid stiffness for the zirc grids tested at []°F using the impact duration method was [][†] lb/in. b,c
This value was determined using energy methods in conjunction with the experimentally determined average impact duration of [][†] sec obtained b,c from the six test samples.

RESPONSE c.

The grid impact force as a function of impact velocity for the six Zircaloy grids tested at []°F is shown in Fig. Q13.2. The average crush strength value is [][†] lbs. with a standard deviation of [][†] lbs. b,c
The lower bound 95 percent confidence limit for the true mean crush strength using a one-tailed statistical analysis for the six samples is [][†] lbs. b,c

The relative fuel assembly velocity plot for grid 4 of a typical peripheral fuel assembly is given in Figure Q13.3. The relative fuel assembly velocity prior to the maximum impact force response is approximately [][†] in/sec, which is consistent with the testing impact velocity. b,c

b, c



IMPACT VELOCITY (IN./SEC)



IMPACT FORCE (LB)

FIGURE Q13.2 17x17 OFA ZIRCALOY GRID IMPACT FORCE AS A FUNCTION OF VELOCITY AT 600°F

L-33

VELOCITY (INCHES PER SEC)

FA NO. 1/GM
TIME (SEC)

+ b,c

FIGURE Q13.3 RELATIVE VELOCITY - GRID NO. 4 OF A TYPICAL PERIPHERAL FUEL ASSEMBLY

When presenting the above test data, discuss the velocities used in the impact test relative to those calculated analytically from the core region response. Discuss static and dynamic test values.

Supply the value of the friction force per grid which causes fuel rod slippage. Compare beginning-of-life friction values to end-of-life values and discuss the effect these values have on the axial dynamic response of the fuel assembly and resulting critical stresses.

RESPONSE

The average drag force required to cause fuel rod sliding at beginning-of-life (BOL) measured from the demonstration fuel assemblies was []⁺ lb. The grid spring force in the zircaloy grid cell is projected to be fully relaxed at end-of-life (EOL) with the drag force estimated to be approximately []⁺ lbs. b,c

The fuel assembly axial impact tests simulated the EOL condition and were performed with the internal grid cells pregapped. The test results indicated that the fuel assembly impact force did not exceed []⁺ lbs at a drop height up to []⁺ inches. The impact force was well below that obtained for a typical BOL fuel assembly, since the sliding of the fuel rod tends to mitigate the fuel assembly axial impact forces. Thus the BOL fuel assembly properties at temperature were incorporated in the reactor internal model for calculating the axial impact responses. b,c

QUESTION 15 Page 3-56;

Supply the fuel assembly location where the data in Figure 3-25 was obtained. How and at what location was the load applied?

RESPONSE

The curves presented in Figure 3-25 were obtained for an axially applied load at the top nozzle. The deflection were measured at the same location and in the same direction as the applied load.

QUESTION 16 Page 3-57;

Drop test data is particularly important in developing an axial dynamic impact model. Supply analytical-experimental drop test correlations and the experimentally derived constant "D" used to calculate the impact damping coefficient.

RESPONSE

A [

b,c

] was incorporated in the axial fuel assembly model. The finite element model was experimentally verified based on drop impact tests. The analytical-experimental correlations for a typical Westinghouse type fuel assembly is shown in Fig. Q16.1 and have been verified by a number of designs.

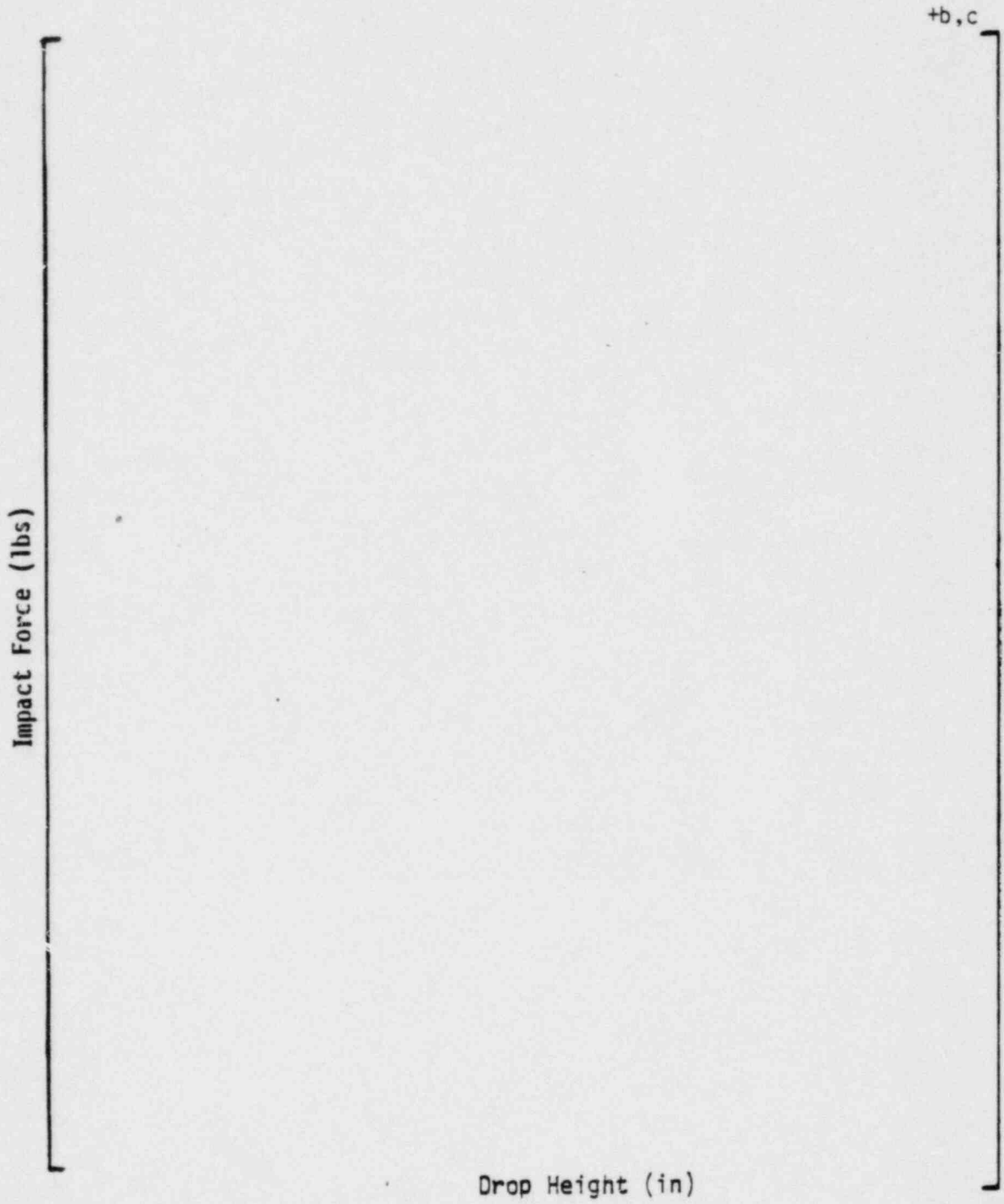


FIGURE Q16.1 17x17 OPTIMIZED FUEL ASSEMBLY AXIAL IMPACT FORCE VERSUS ROD HEIGHT

Question 17: Safe-Shutdown Earthquake (SSE) lateral core plate motions are presented in Figure 3-8, followed by lateral LOCA core plate motions in Figure 3-19. Supply similar information for the vertical applied loads (preferably in the form of pressure time histories at the core inlet and core outlet).

Response: Figures 17-1 through 17-5 represent the vertical forces which were applied to the RPV structural model at the core plates and fuel assemblies. These forces correspond to the [

]⁺

(a,c)

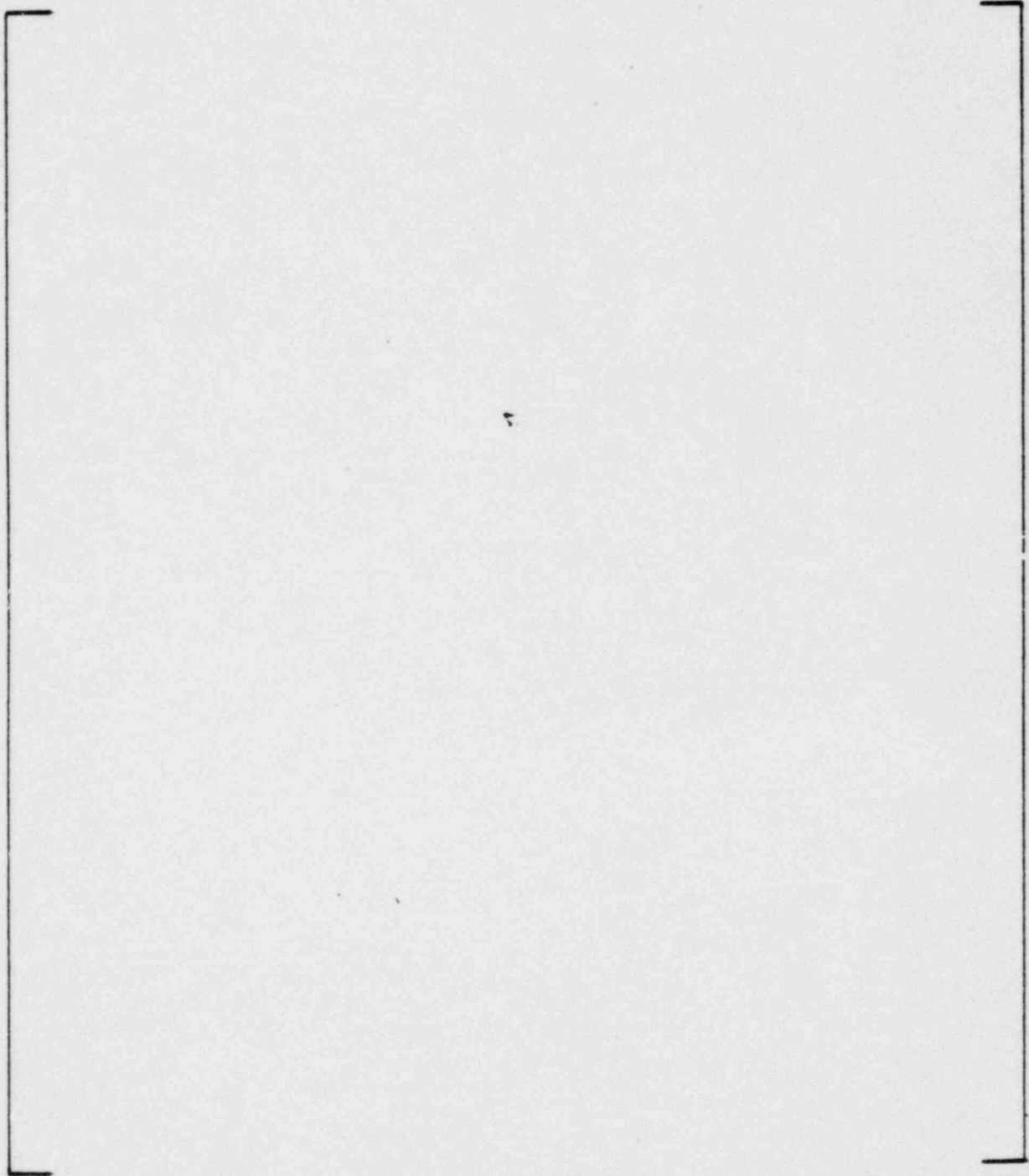


Figure 17-1. Total Vertical Force on Upper Core Plate
L-39

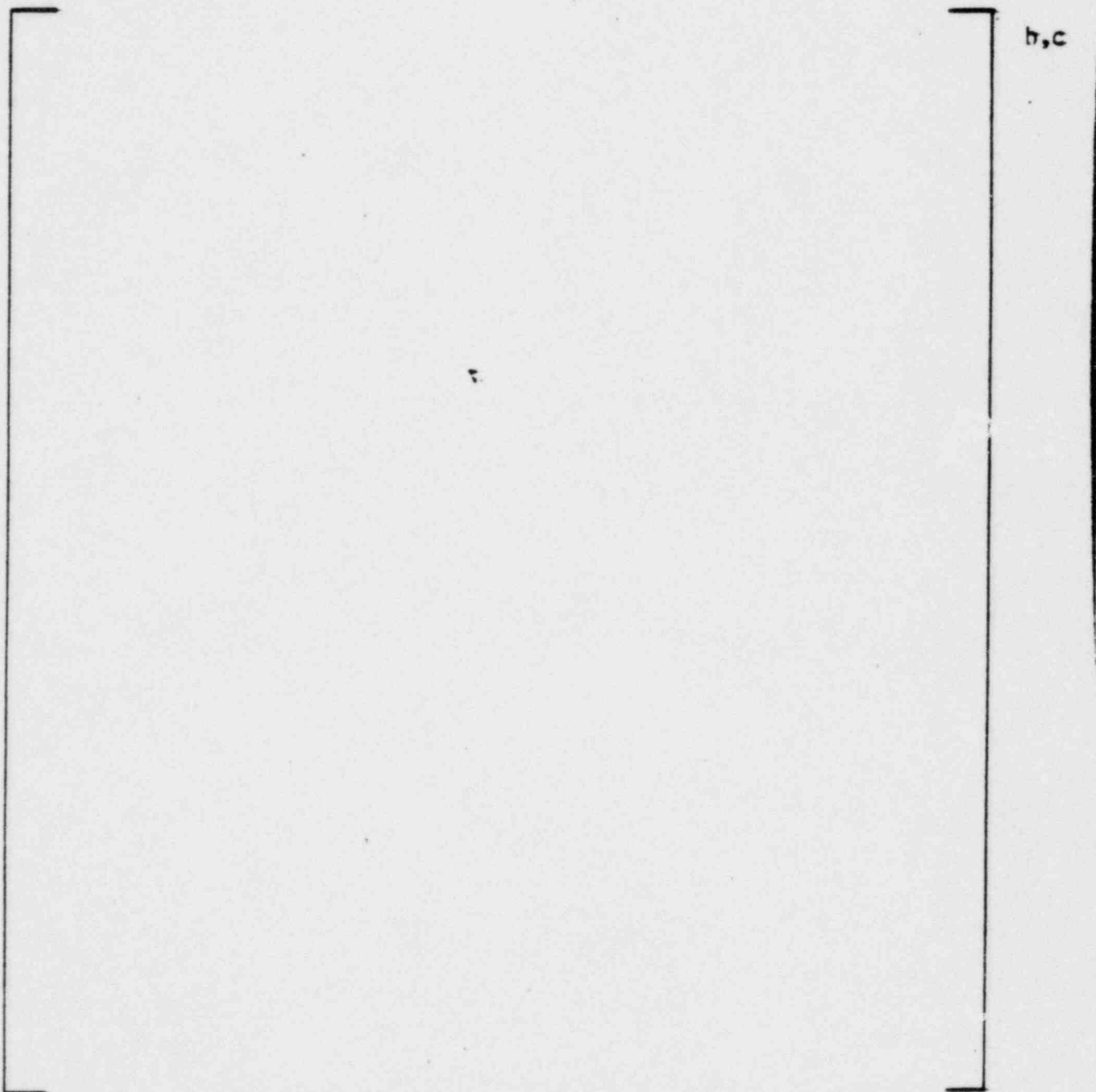


Figure 17-2. Total Vertical Force on Top Fuel Nozzle

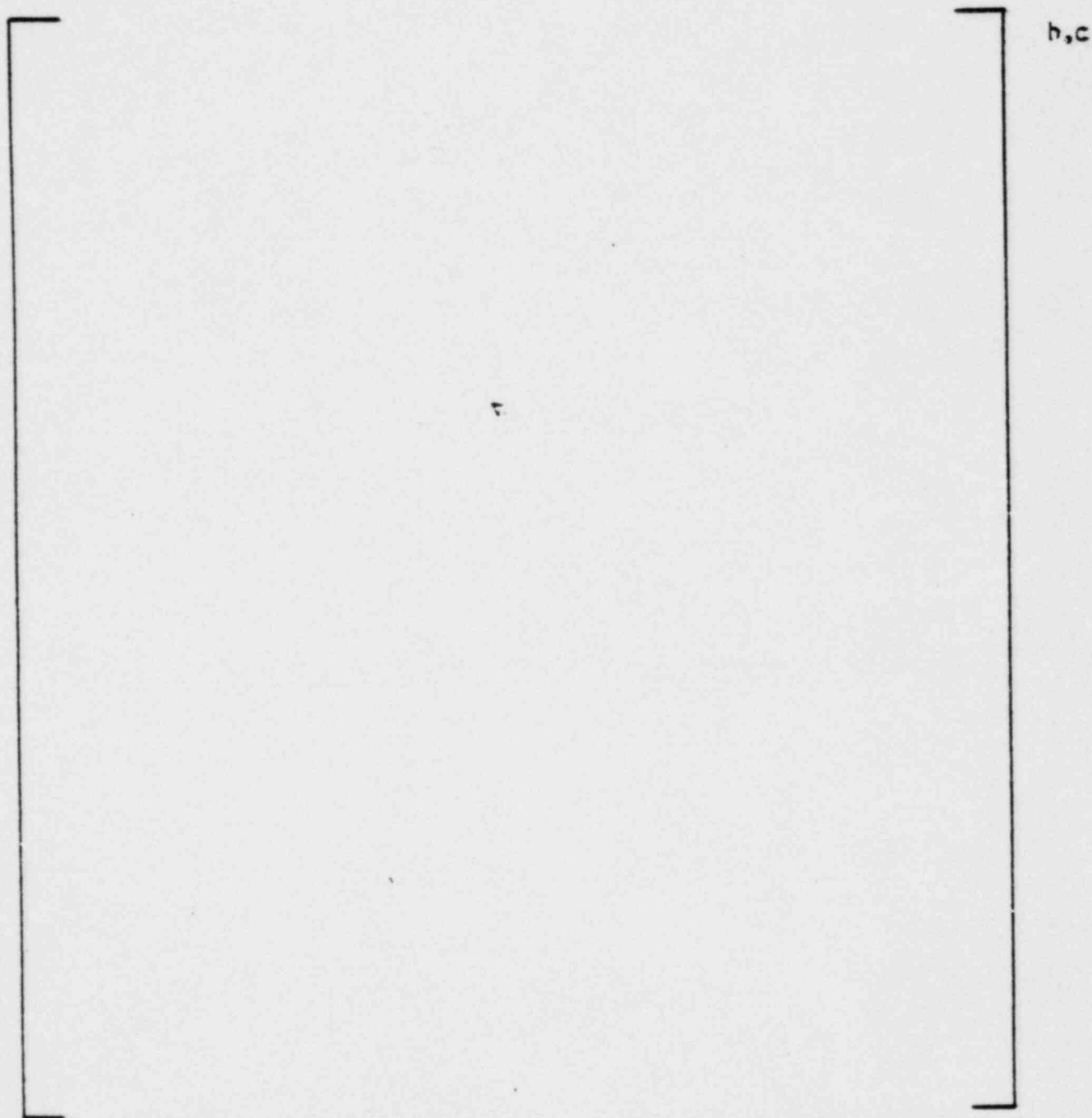


Figure 17-3. Total Vertical Force on Fuel Assembly C.G.

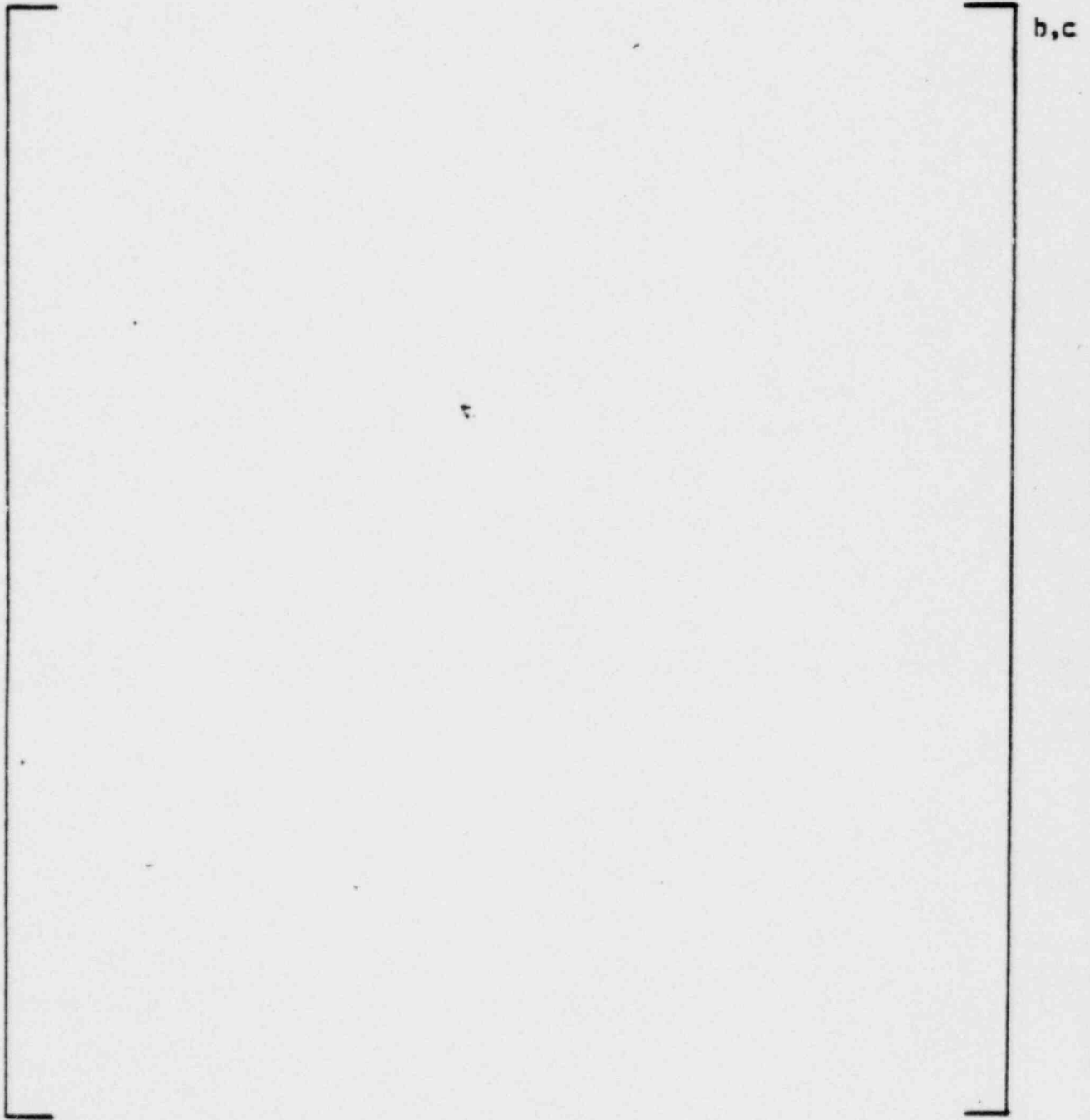


Figure 17-4. Total Vertical Force on Bottom Fuel Nozzle

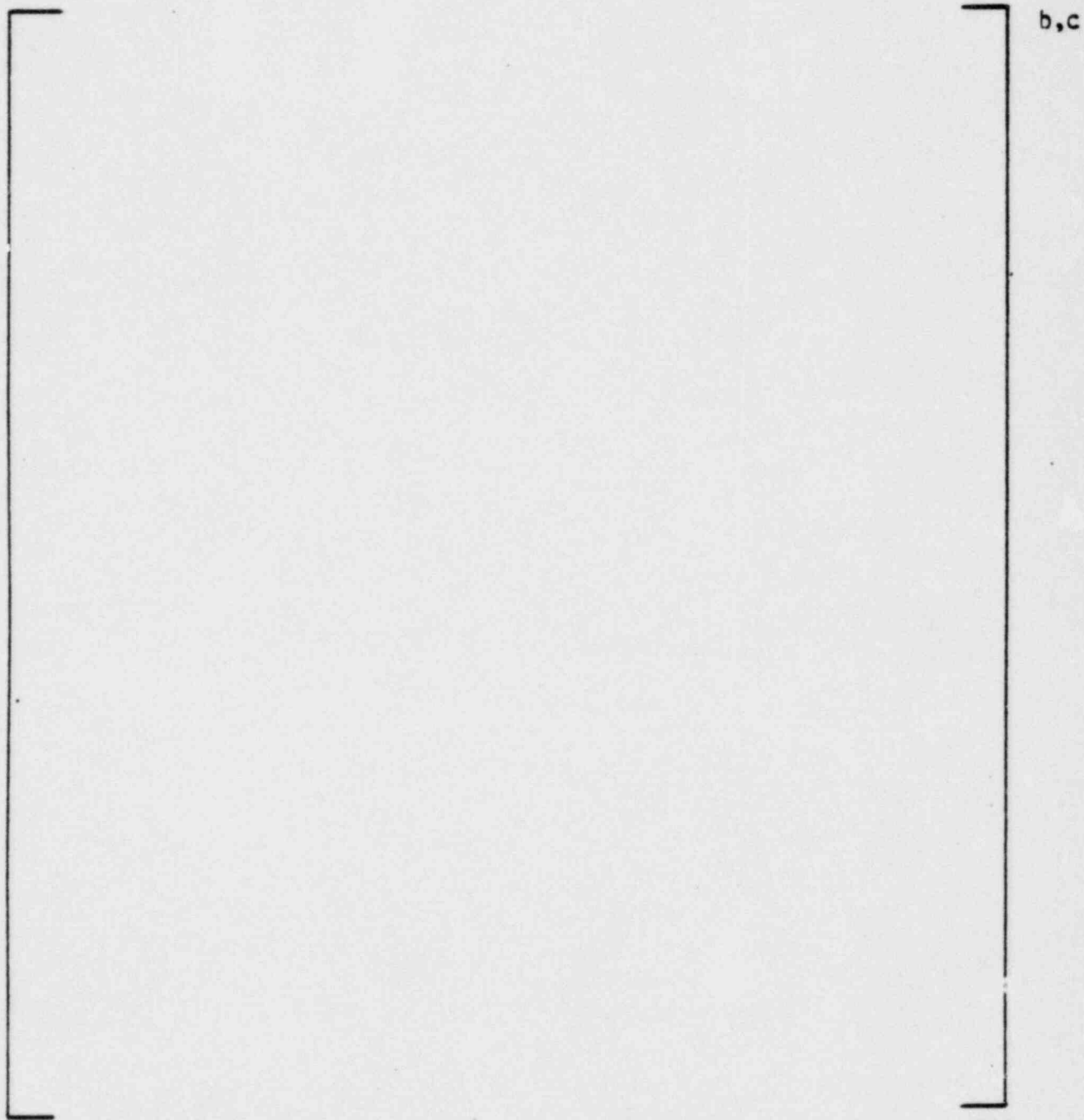


Figure 17-5. Total Vertical Force on Lower Core Plate

QUESTION 18 Table 3-7;

The maximum direct stress intensity for the guide thimble does not agree with the value presented in Tab' 3-6. Explain.

RESPONSE

The maximum direct stress value in Table 3-6 for guided thimble tube should read []⁺ instead of []⁺ which was a typographical error. | 1 a,c

QUESTION 19 Q1 question 3;

Combined motions in the horizontal and vertical direction were considered for beam-column effects in Reference 1. Has this type of assessment been performed for the optimized fuel assembly? If so, enclose the results. If not, why not? Explain.

RESPONSE

The beam-column effects were originally investigated in Ref. 1. The results of this study indicated that the higher order effects caused by the combination of axial and lateral deflections did not significantly alter the stress distribution. The test results as reported in Ref. 1 for an initially bowed assembly that was dropped from various heights indicated that the thimble stresses in the bowed assembly were slightly higher than those obtained for an initially straight assembly. Based on the fuel assembly axial impact tests as reported in Ref. 1, the effect of the fuel assembly bow resulted in an increase of approximately []%⁺ a,c in the maximum thimble stress. In view of the relatively large stress safety margin for the OFA design, the experimental and/or analytical investigations were not warranted.

*Ref. 1. WCAP-8236.

QUESTION 20 General;

Review of the fuel assembly models requires the following additional information:

a. Masses

1. Fuel rod
2. Spacer grid
3. End nozzles
4. Guide and instrument tubes
5. Fuel column
6. Total fuel assembly and center of gravity

b. Other measured quantities

1. Axial gap between fuel nozzles and upper core plate
2. Axial hold down spring stiffness and preload.

RESPONSE a.

The dry weight distribution for the Optimized Fuel Assembly components are tabulated below:

	+
	a,b,c

The center of gravity of the fuel assembly is approximately located at the geometrical center.

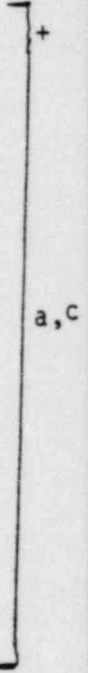
RESPONSE b.

1. The axial gap between the top fuel nozzle and upper core plate =
[]⁺ in. a,c

2. Axial holddown spring stiffness = []⁺ lb/in. b,c
Axial holddown spring preload = []⁺ lb. b,c

Table Q21.1

FUEL ASSEMBLY COMPONENT STRESSES AND LIMITS
(ksi)



QUESTION 22 General;

Discuss control rod insertability for both the SSE and the SSE-LOCA transients.

RESPONSE

Under the SSE and SSE-LOCA transients, there will be no grid distortion or thimble buckling as a result of maximum grid impact and fuel assembly deflection responses. Thus the insertion of the flexible control rod will not be hindered. It should also be noted that the maximum grid impact response, in general, occurred at the peripheral fuel assemblies which do not contain control rod assemblies.

Question 23: Define the cavity pressure load cases considered. Include break locations, areas and opening times considered.

Response: Prior to performing the analyses presented in WCAP 9401, a series of LOCA analyses were performed to select a representative cavity pressure load case. The plants of concern were reviewed and available cavity loads collected to determine variations in the magnitude and transient nature of the cavity loads. In addition, cavity load cases from other Westinghouse plants not covered by WCAP 9401 which demonstrated unique transient characteristics were considered. The plants for which these cavity pressure loads apply have undergone US NRC licensing review. No open items exist for the methods used in the calculation of the cavity pressure loads. The effect of variation in cavity design, plant operating conditions and the distribution of applied cavity loads on the reactor vessel are reflected in the transient variation of the cavity loads considered.

Three cases were selected with distinctly different transient variation (Figures 23-1 through 23-9). These cases were all based on a 144 square inch reactor vessel inlet nozzle break with a break opening time of 7 milliseconds. All three cases were ratioed so that the peak horizontal load was [][†]. This value is representative of (a,c) the peak horizontal cavity load applicable to any of the plants covered by WCAP 9401. Reactor vessel LOCA analyses were performed and fuel assembly impact loads were calculated for each of the three cases. The peak grid impact loads were [][†] (a,c)

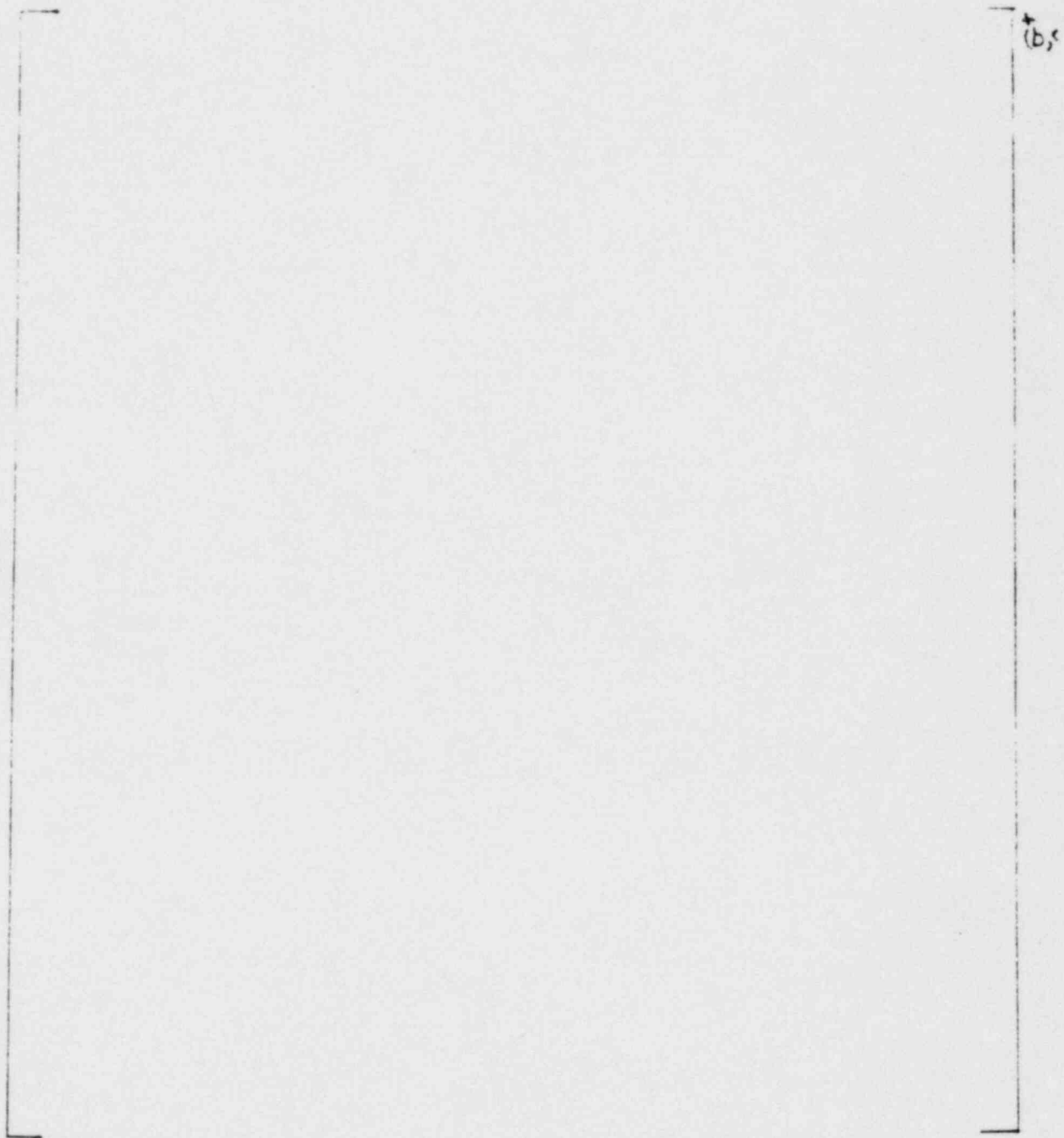


Figure 23-1. Cavity Load Case 1 Horizontal Force

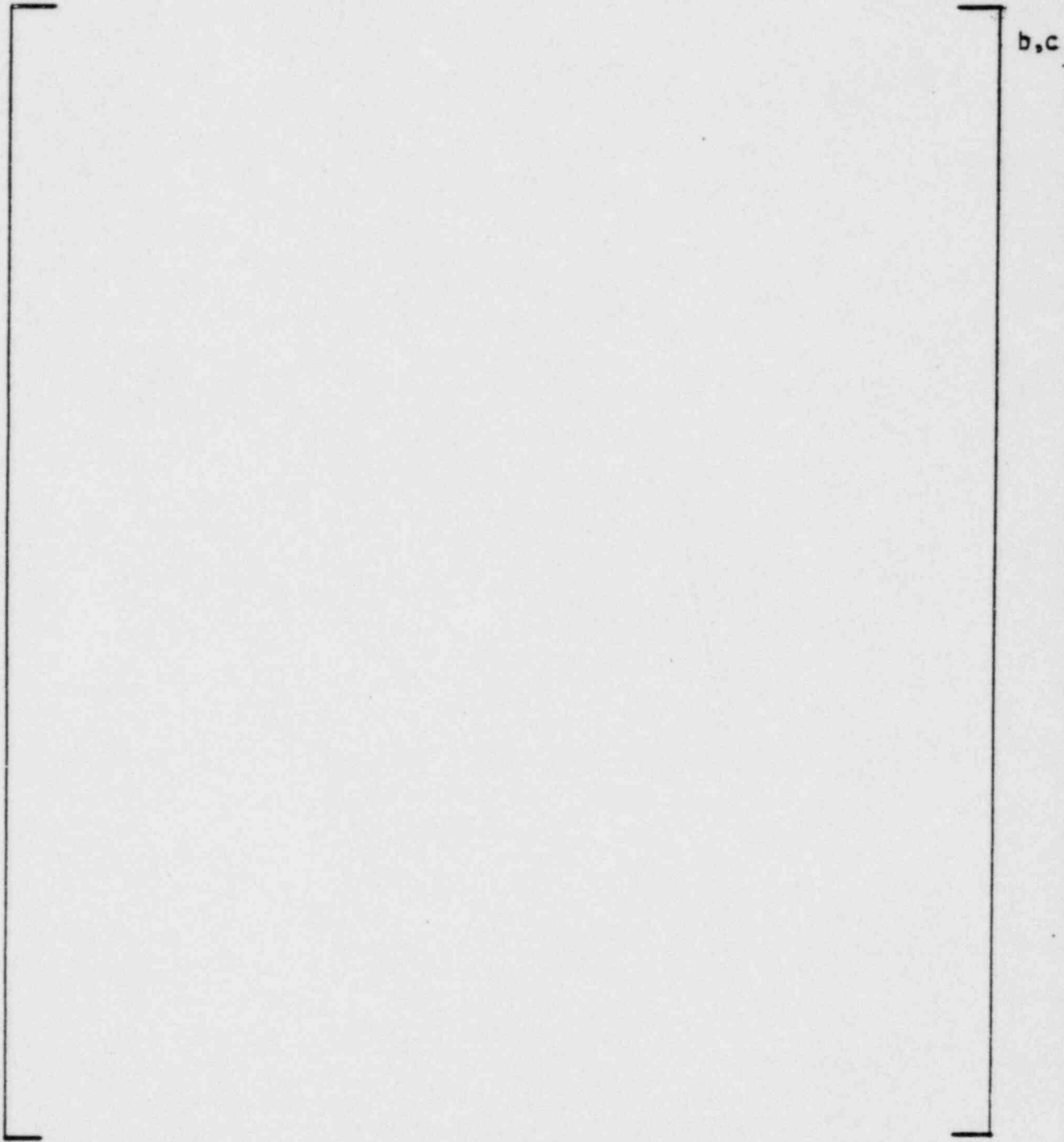


Figure 23-2. Cavity Load Case 1 Vertical Force

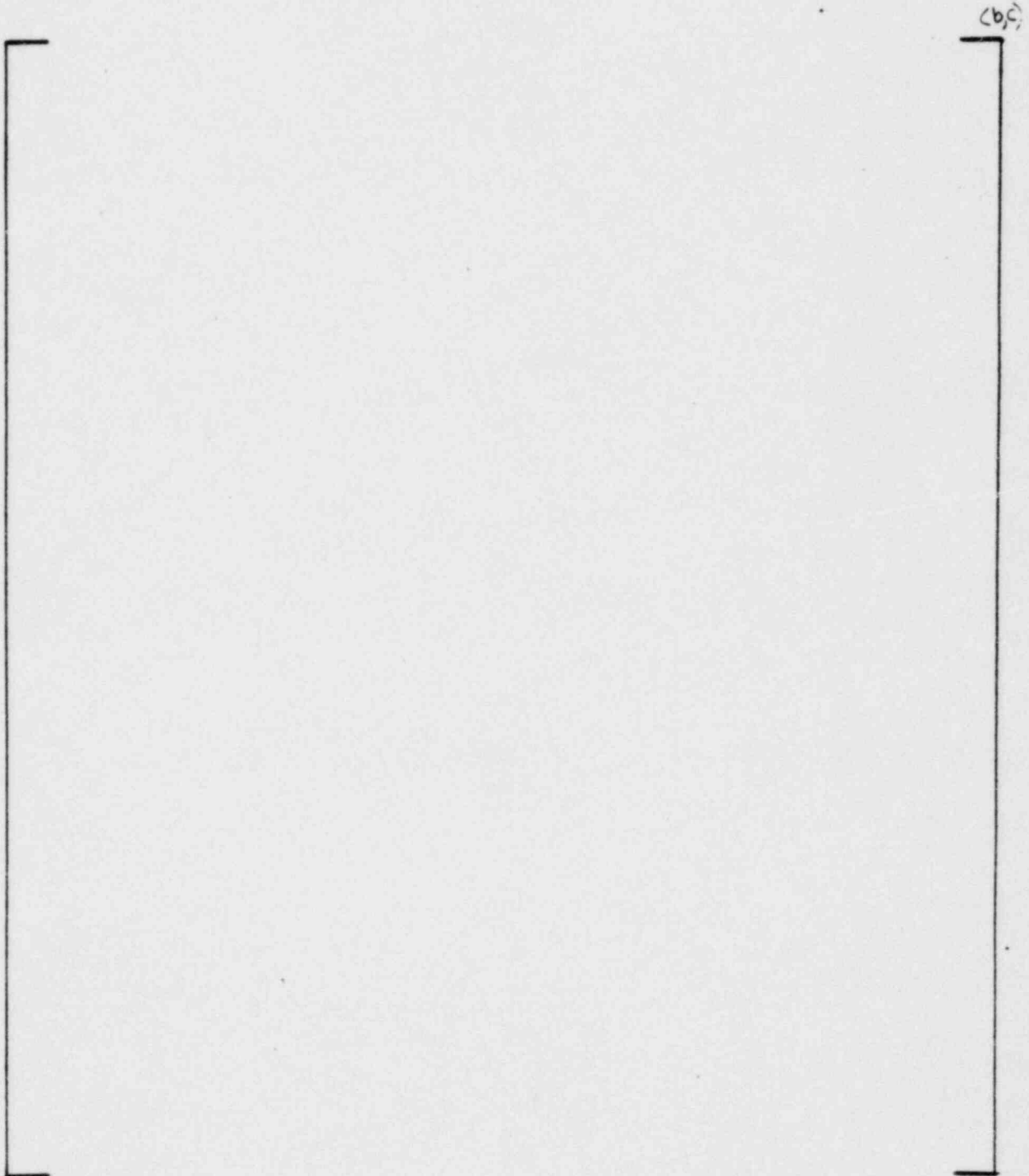


Figure 23-3. Cavity Load Case 1 Moment
L-54

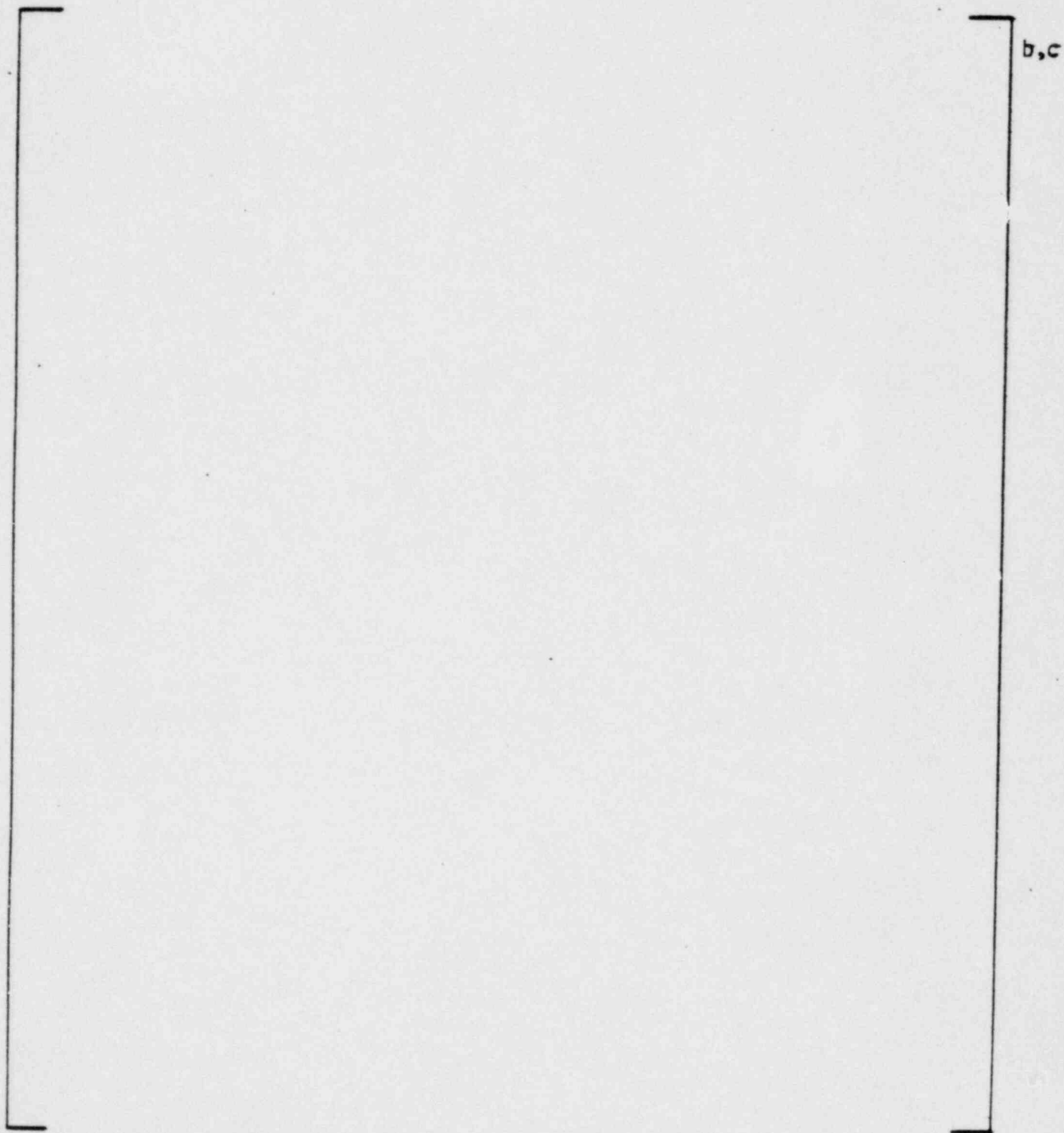


Figure 23-4. Cavity Load Case 2 Horizontal Force

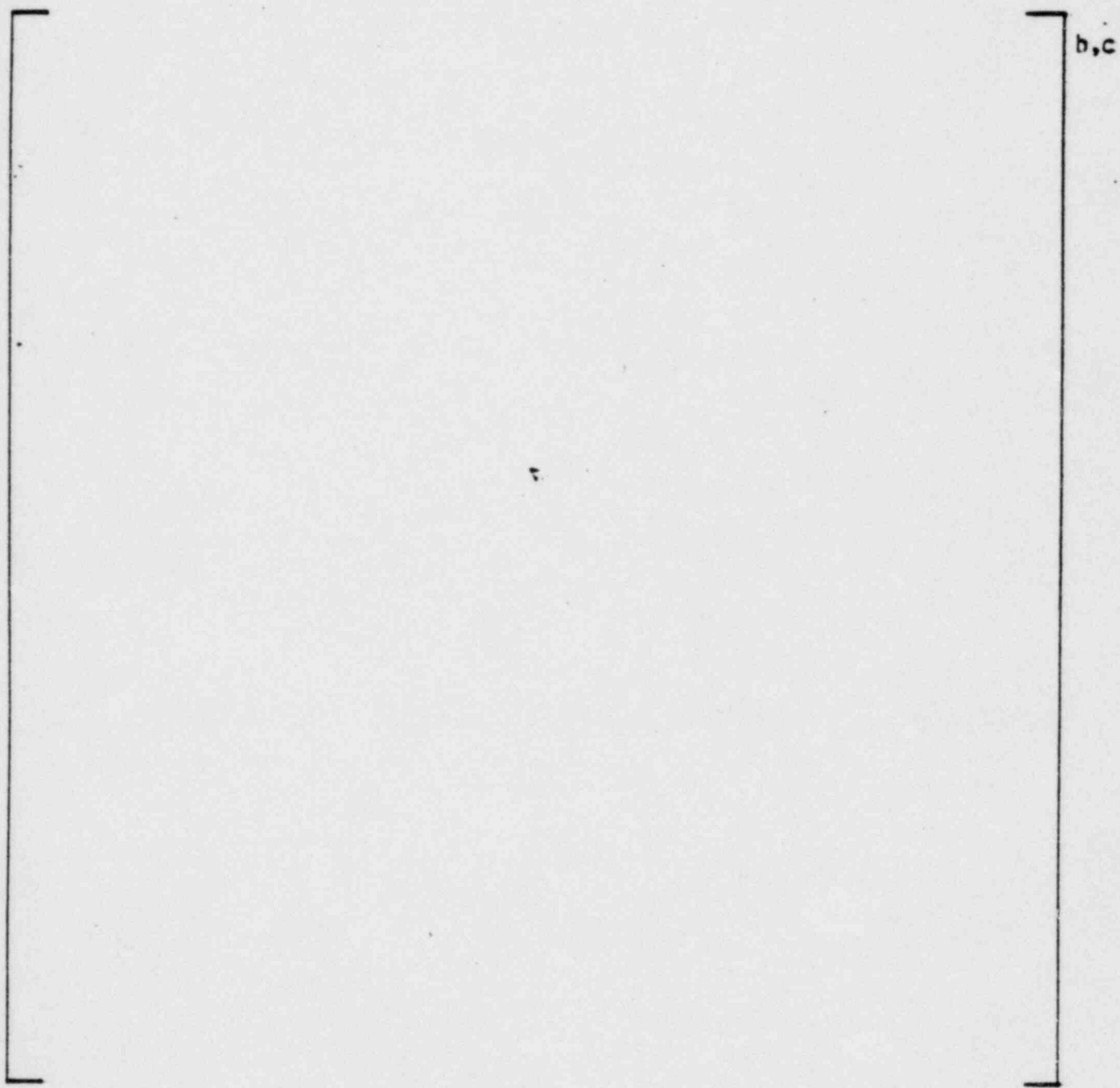


Figure 23-5. Cavity Load Case 2 Vertical Force

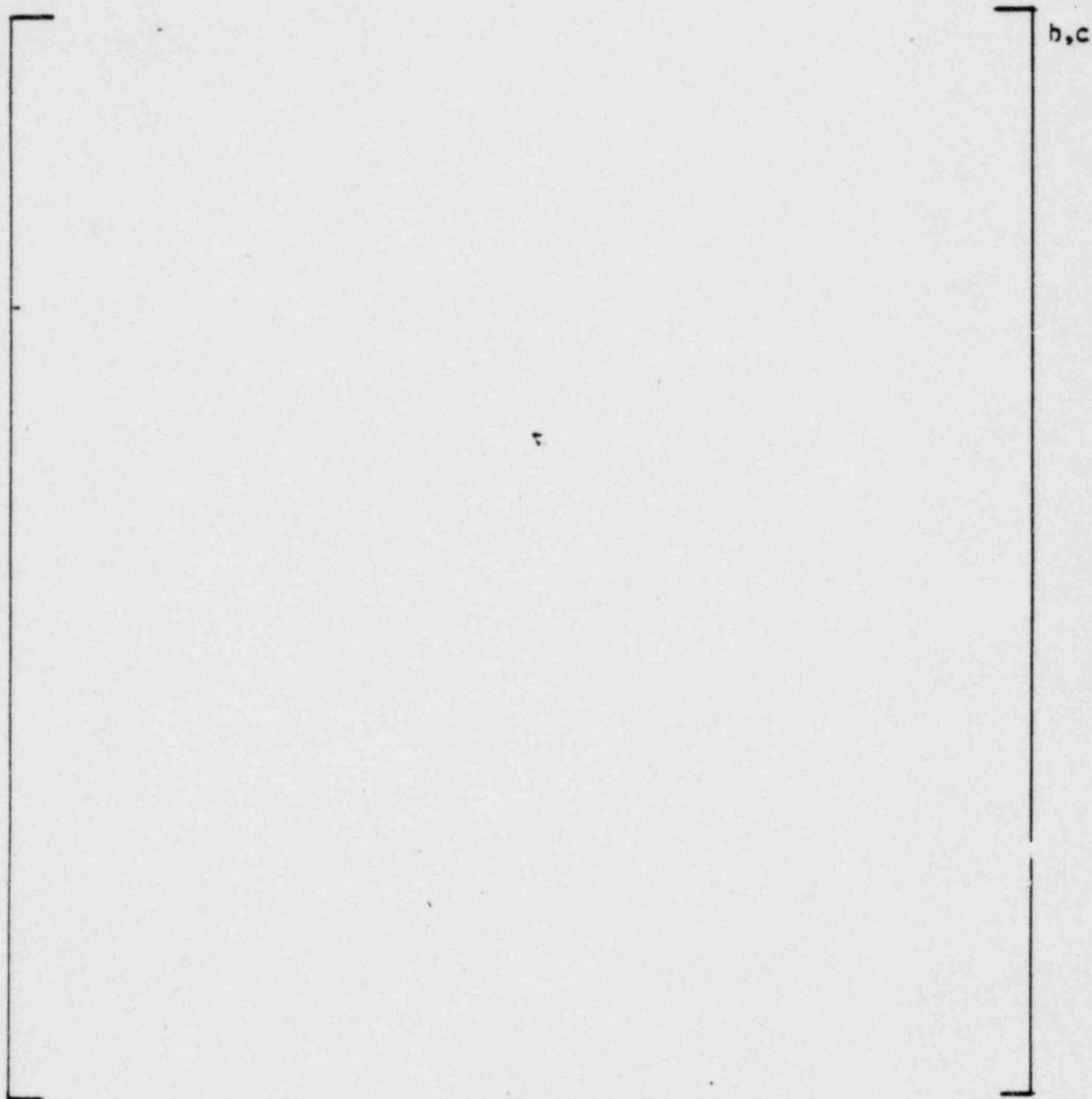


Figure 23-6. Cavity Load Case 2 Moment

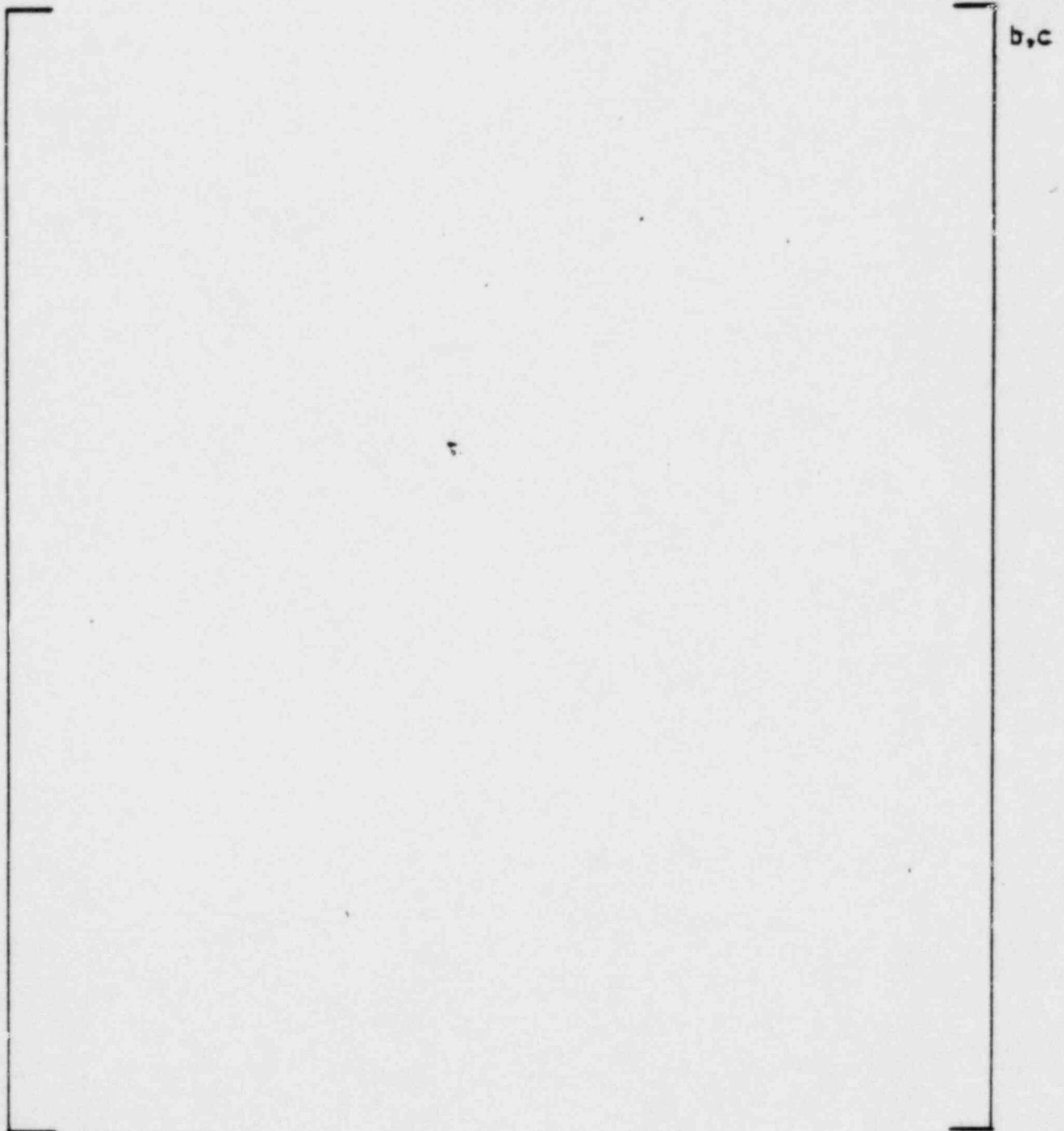
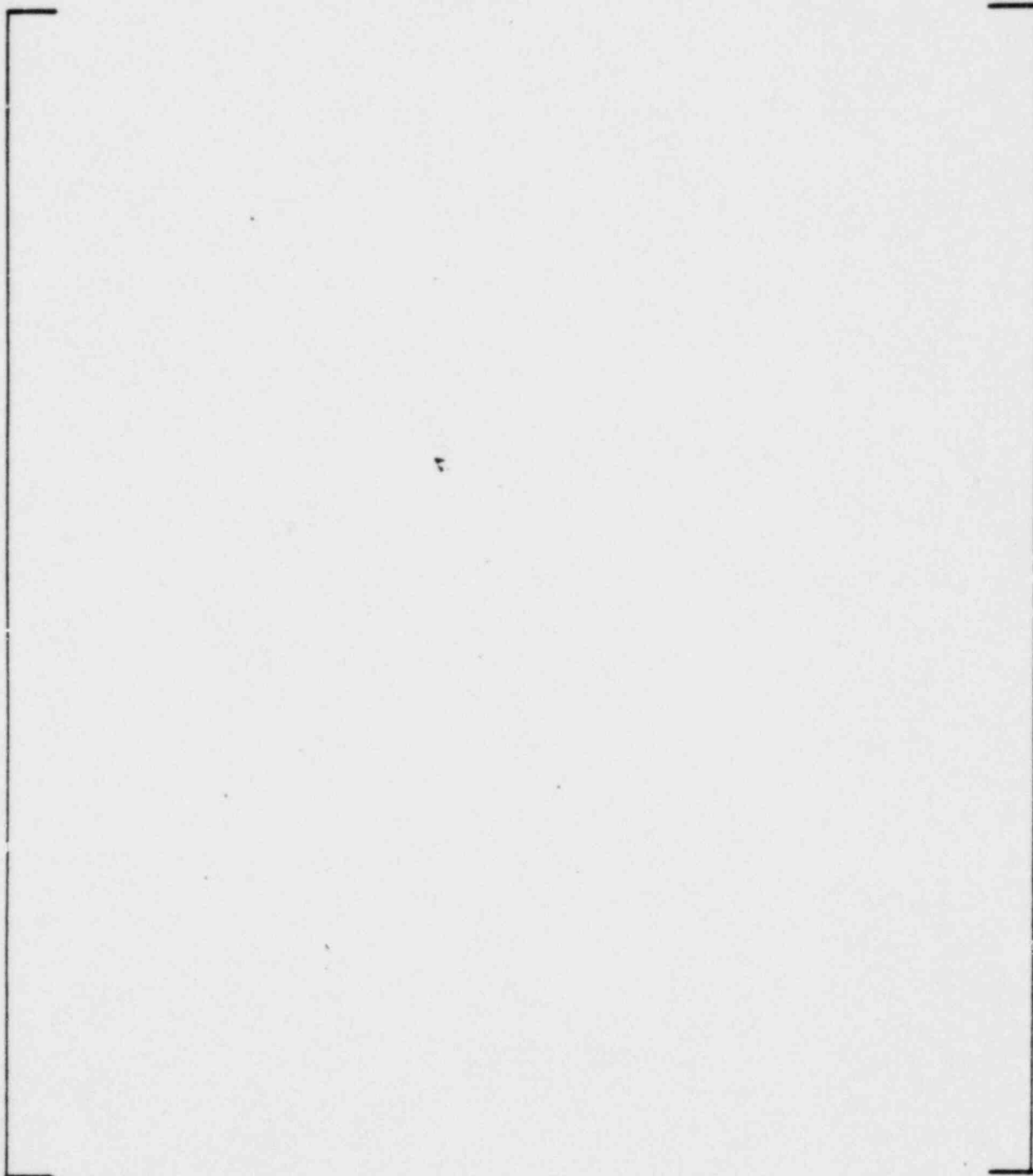


Figure 23-7. Cavity Load Case 3 Horizontal Force



b, c

Figure 23-8. Cavity Load Case 3 Vertical Force

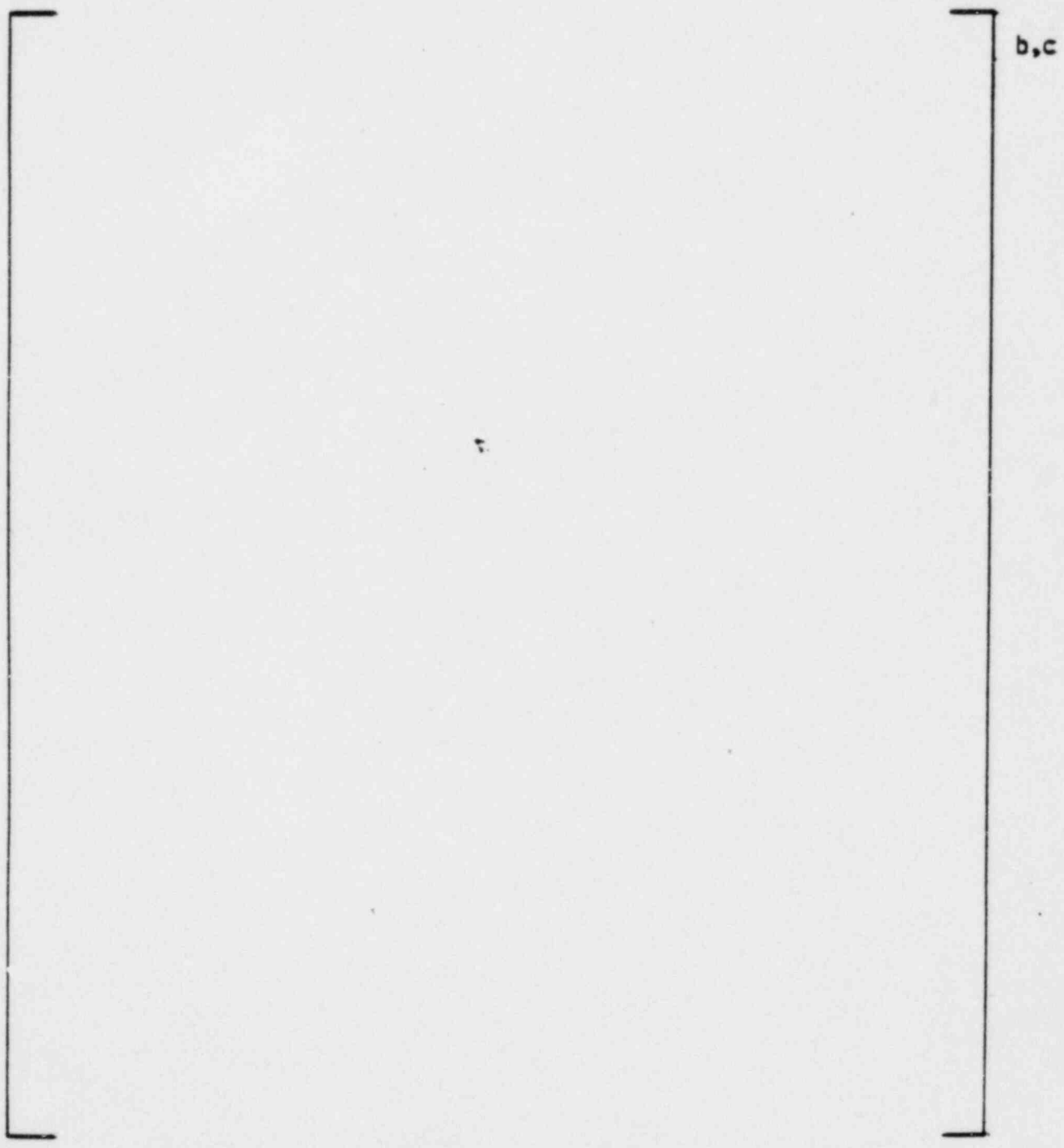


Figure 23-9. Cavity Load Case 3 Moment
L-60

REFERENCES

1. Gesinski, L. T. and Chiang, D., "Safety Analysis of the 17x17 Fuel Assembly for Combined Seismic and Loss-of-Coolant Accident," WCAP-8236, December 1973.
2. Cudlin, R., etal., "Methodology for Combining Dynamic Responses," NUREG-0484, September 1978.
3. Standard Review Plan PSRP-4.2, proposed Appendix A "Evaluation of Fuel Assembly Structural Response to Externally Applied Forces."



UNITED STATES
NUCLEAR REGULATORY COMMISSION
WASHINGTON, D. C. 20555

FEB 17 1991

Westinghouse Electric Corporation
ATTN: Mr. T. M. Anderson, Manager
Nuclear Safety Department
P. O. Box 355
Pittsburgh, Pennsylvania 15230

Dear Mr. Anderson:

SUBJECT: REQUEST NUMBER 4 FOR ADDITIONAL INFORMATION ON WCAP-9401

We are currently reviewing Westinghouse Electric Corporation report WCAP-9401 entitled "Verification Testing and Analyses of the 17 x 17 Optimized Fuel Assembly".

The continuing reviews of Sections 1 and 2 of WCAP-9401 reveal the need for the additional information indicated in the enclosure.

This information is necessary at the earliest possible date to complete the review - its expeditious submittal will therefore be to the Westinghouse advantage. Please advise us as soon as possible of your planned submittal date to permit us, in turn, to develop a review schedule.

Sincerely,

A handwritten signature in cursive script, appearing to read "R. L. Tedesco".

Robert L. Tedesco, Assistant Director
for Licensing
Division of Licensing

Enclosure: As stated

cc: Mr. Alex Ball
Westinghouse Electrical Corp.
Nuclear Safety Department
P. O. Box 355
Pittsburgh, Pennsylvania 15230



Westinghouse
Electric Corporation

Water Reactor
Divisions

Nuclear Technology Division

Box 355
Pittsburgh Pennsylvania 15230

March 2, 1981
NS-TMA-2400

Mr. James R. Miller, Chief
Special Projects Branch
Division of Project Management
U. S. Nuclear Regulatory Commission
Phillips Building
7920 Norfolk Avenue
Bethesda, Maryland 20014

Ref: NS-TMA-2293,
August 22, 1980

SUBJECT: Responses to "Request Number 4 for Additional Information on
WCAP-9401," NRC Letter from R. L. Tedesco to T. M. Anderson,
February 12, 1981

Dear Mr. Miller:

Enclosed are:

1. Twenty-five (25) copies of the proprietary responses to the NRC Request Number 4 for additional information on WCAP-9401 (Proprietary).
2. Twenty (20) copies of the non-proprietary responses to the NRC Request Number 4 for additional information on WCAP-9401 (Non-Proprietary).

Also enclosed are:

1. One (1) copy of Application for Withholding (Non-Proprietary).
2. One (1) copy of original Affidavit (Non-Proprietary).

This submittal contains proprietary information of Westinghouse Electric Corporation. In conformance with the requirements of 10CFR2.790, as amended, of the Commission's regulations, we are enclosing with this submittal an application for withholding from public disclosure and an affidavit. The affidavit sets forth the basis on which the information may be withheld from public disclosure by the Commission.

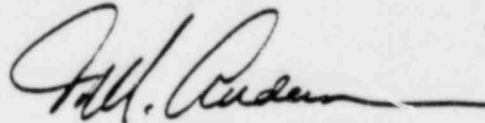
Mr. James R. Miller

-2-

March 2, 1981
NS-TMA-2400

Correspondence with respect to the affidavit or application for withholding should reference AW-81-15 and should be addressed to R. A. Wiesemann, Manager of Regulatory and Legislative Affairs, Westinghouse Electric Corporation, P. O. Box 355, Pittsburgh, Pennsylvania 15230.

Very truly yours,



T. M. Anderson, Manager
Nuclear Safety Department

/bek

Enclosures

QUESTION 492.1

What computer codes were employed to reduce experimental data and predict Critical Heat Flux (CHF)? What uncertainties are associated with them?

RESPONSE

The THINC subchannel analysis code is used in the reduction of DNS test data. Westinghouse does not attempt to evaluate any computational error that might be inherent in this code, but instead relies on statistical comparisons of measured to predicted critical heat fluxes for the total data sets.

QUESTION 492.2

The test data used to determine the DNBR limit is based on 19 standard and 2 OFA test series. This would tend to bias the limit towards the standard design. Since the WRB-1 correlation is empirical, provide the constants used for the OFA and standard fuel designs. Such parameters as F-factors and performance factors are dependent on D_e and D_n thus there should be a difference between the OFA and standard design. Discuss the differences in the values and how they affect CHF predictions.

RESPONSE

It should be clearly understood that WCAP-9401 does not claim that these standard and OFA test results were all alike; rather, it claims that the WRB-1 predicts these various data sets equally well. Stated another way: the WRB-1 correlation, using the appropriate performance factor and values of geometric parameters, predicts each run so well that the aggregates of the deviations of measured from predicted values are essentially random in nature, for all data sets, and that these statistical aggregates are thus indistinguishable from each other. Hence, the reduced data are in no way biased toward the standard design.

This is not to say that the results listed in Table 2-3 of WCAP-9401 are identical. They differ from each other due principally to irreducible experimental errors and, to a lesser extent, to mismatches in the correlation. These imperfections are allowed for by using, in the design process, a minimum DNBR of greater than unity: specifically, $(DNBR)_{MIN} = 1.17$ was shown in WCAP-8762 to be the appropriate value for the standard 17x17, and the results of WCAP-9401 showed that this value applies equally well to the OFA.

The form of the WRB-1 correlation, together with the numerical values of all constants, were given in the answers to the first round of questions on WCAP-9401. Note that most of the terms in WRB-1 are linear in nature, hence their effects on predicted CHF are readily discernable.

Finally, it should be noted that the Tong non-uniform F-factor and the performance factor are not dependent on D_e and D_h .

QUESTION 492.3

Provide a statistical analysis of the repeatability parameters for the standard and the GFA. Include a plot of the probability distribution function vs. repeatability parameters for both cases.

RESPONSE

This information is given in Figures 1 and 2.

t (b,c)



FIGURE 1. MODEL RESULTS (STANDARD DEVIATIONS)

PROPERTY TEST CJ 17417 C-THIRZED FIEL. TOPIC. 2-6-64

of ADV-

1964 OCT 10 10 10 AM '64

(b,c)



PERCENTILES (STANDARD DEVIATIONS)

PERCENTILES TEST OF 17417 OPTIMIZED CIRCUIT 2-G-01

FIGURE 2

PERCENTILES TEST OF 17417 OPTIMIZED CIRCUIT 2-G-01

QUESTION 492.4

Are the upper and lower end fittings the same for the OFA and standard fuel?

RESPONSE

Yes. The designs of the upper and lower end fittings (nozzles) are the same for the OFA and the standard fuel.

QUESTION 492.5

Table 2-2 on page 2-11 and 2-12 has data sets w2129 through w2158 missing. Why were these data omitted and how would this affect the overall thimble cell calculations? Are any other data excluded and if so, why?

RESPONSE

These runs were excluded, because the final data reduction showed critical heat fluxes higher than expected. For this reason, testing was interrupted so that the test section could be removed and inspected. This examination revealed that some of the copper/nickel electrical connectors (which attach to the bottom of the rods) had suffered partial collapse, probably due to thermal shock during the shut-down following run W-2128. The effect of this collapse would have been to loosen the seals which separate the mainstream from the electrical connector chamber, which is cooled by a separate flow. This cooling water is at about the same pressure as the mainstream, but is several hundred degrees cooler, hence a small leak through the seals would be possible and could lower the mainstream enthalpy enough to significantly increase the measured CHF. These failures of the connectors were probably due to a new design. Subsequently, the test section was rebuilt using connectors of the older design, and testing was resumed. The test conditions of runs 2129 through 2158 were repeated, hence the thimble cell calculations were not affected.

QUESTION 492.6

The standard deviation of the thimble cell CFA data is the lowest value listed in Table 2-3. A component of variance analysis for the CFA typical and thimble cells and the standard fuel data should be performed to account for variance due to the different geometry types.

RESPONSE

In analyzing these data to account for the variance due to different geometry types the M/P value determined for each datum point was considered as a random variable with the sets of M/P values obtained for each test being considered as random samples drawn from a population of M/P values.

Figures 1 and 2 in response to question 492.3 and Figures 3 and 4 in response to question 492.12 show that the R-grid data and each of the CFA data sets can be considered as being normally distributed. To test whether the CFA data sets can be considered as being from the same population as the standard R-grid data, the following analyses were carried out:

1. Analysis of Means

A procedure described in Reference 1 was used to determine 95 percent tolerance limits on the sample means of the three data sets. The values used and the resulting limits are given in the following table:

TABLE 1
ANALYSIS OF MEANS FOR WCAP-9401 DATA

	(b)
--	-----

As is indicated, the observed mean $\bar{M/P}$ values fall within the calculated tolerance limits, thus verifying that the OFA data are compatible with the standard R-grid data.

2. Comparison of Variances

A test of hypothesis that the sample variances for the OFA data and standard R-grid data are sample values from the same population was carried out using the F distribution. These results are given in the following table:

TABLE 2
COMPARISON OF VARIANCES FOR WCAP-9401 DATA

	(b)
--	-----

The information in the last two columns indicates that the hypothesis that the variances of the OFA typical cell and standard R-grid distributions are equal would not be rejected, whereas a similar hypothesis for the OFA thimble cell data would be rejected at a 5 percent significance level.

In summary, the results of the analyses given above confirm that the OFA typical cell data can be considered as being from the same population as the standard R-grid data. The same cannot be said for the thimble cell data because of the significantly smaller scatter of the OFA data about the mean as reflected in the relatively small standard deviation, indicative of higher quality data. Since the OFA thimble data base has been shown to exhibit normality and the mean of the data fall within the calculated tolerance limits, failure of the F-test because of relatively smaller variance should not be considered sufficient cause to reject use of the OFA thimble data. It is also of interest to note that the limit DNBR based on the OFA thimble cell data as requested in question 492.12 is 1.15 compared to the design limit of 1.17.

REFERENCES

1. L. S. Nelson, "Factors for the Analysis of Means," Journal of Quality Technology, Vol. 6, No. 4, Oct., 1974, p. 175.
2. P. G. Hoel, "Introduction to Mathematical Statistics," 4th Ed., John Wiley and Sons, Inc., New York, 1971, p. 139.
3. D. B. Owen, "Factors for One-Sided Tolerance Limits and for Variables Sampling Plans," SCR-607, Sandia Corp., March, 1963.

QUESTION: 492.7

The applicant should perform F-tests for each of the standard geometries and the total data population to support the hypothesis that the OFA data belongs to the total population. This should be done separately for the OFA typical and thimble cells. If it is determined that the OFA data does not fit certain standard data populations or the total population, justify using the standard data as a basis for calculating the DNBR limits.

RESPONSE

The following statistical data were used in performing F-tests:

[REDACTED] (b,c)

F-tests were carried out, leading to the following results (at the 10 percent rejection level):

[REDACTED] (b,c)

[REDACTED] (b,c)

QUESTION 492.6

For the test in Table 2-1 and 2-2, provide the inlet mass flow rates, and the measured and predicted values of pressure drop for each of a standard assembly tested under similar conditions. Provide a discussion of any effects due to individual pressure drops, what parameters affect these pressure drops and what uncertainties are inherent in the calculations.

RESPONSE

The inlet mass flow rates for the OFA are tabulated in Tables 2-1 and 2-2. The inlet mass flow values for the matching standard assembly runs are given in Tables A-5 and A-18 of reference 3 of WCAP-9401, as noted in WCAP-9401 (footnote, bottom of page 2-7). Pressure drop does not effect the CHF computations.

QUESTION 492.9

The pressure drop tests were performed with unheated rods and at temperature, pressures, and qualities, below normal operating conditions. Justify why these tests adequately simulate a reactor during steady-state operation and during anticipated transients.

RESPONSE

Pressure drop, ΔP , is given by

$$\Delta P = K \left(\rho \frac{V^2}{2g} \right)$$

where ρ = density
 V = flow velocity
 K = component loss coefficient
 g = gravitation constant

It is well known that K can be expressed as a function of Reynolds number only, and that a plot of K vs Reynolds number will be linear (in the log-log plane) over a very broad range of Reynolds number, allowing extrapolations to be made with confidence to reactor operating conditions. Since Reynolds number is independent of pressure, these experiments can be done at relatively low pressures.

The testing was conducted for flow rates 10 percent above the mechanical design flow rates and is representative of flows during anticipated transients.

QUESTION 492.10

Figure 2-1 from RESAR-414 is shown on the next page. Provide the same information for a core with 1/3 CFA and 2/3 standard fuel. Also provide a similar figure for the ΔP tests which were performed.

RESPONSE

The same information as shown on the next page for standard 17x17 fuel is given in WCAP-9500 Figure 4.2-1 for the 17x17 optimized fuel assembly. Also provided is a Figure to illustrate the ΔP test configuration.

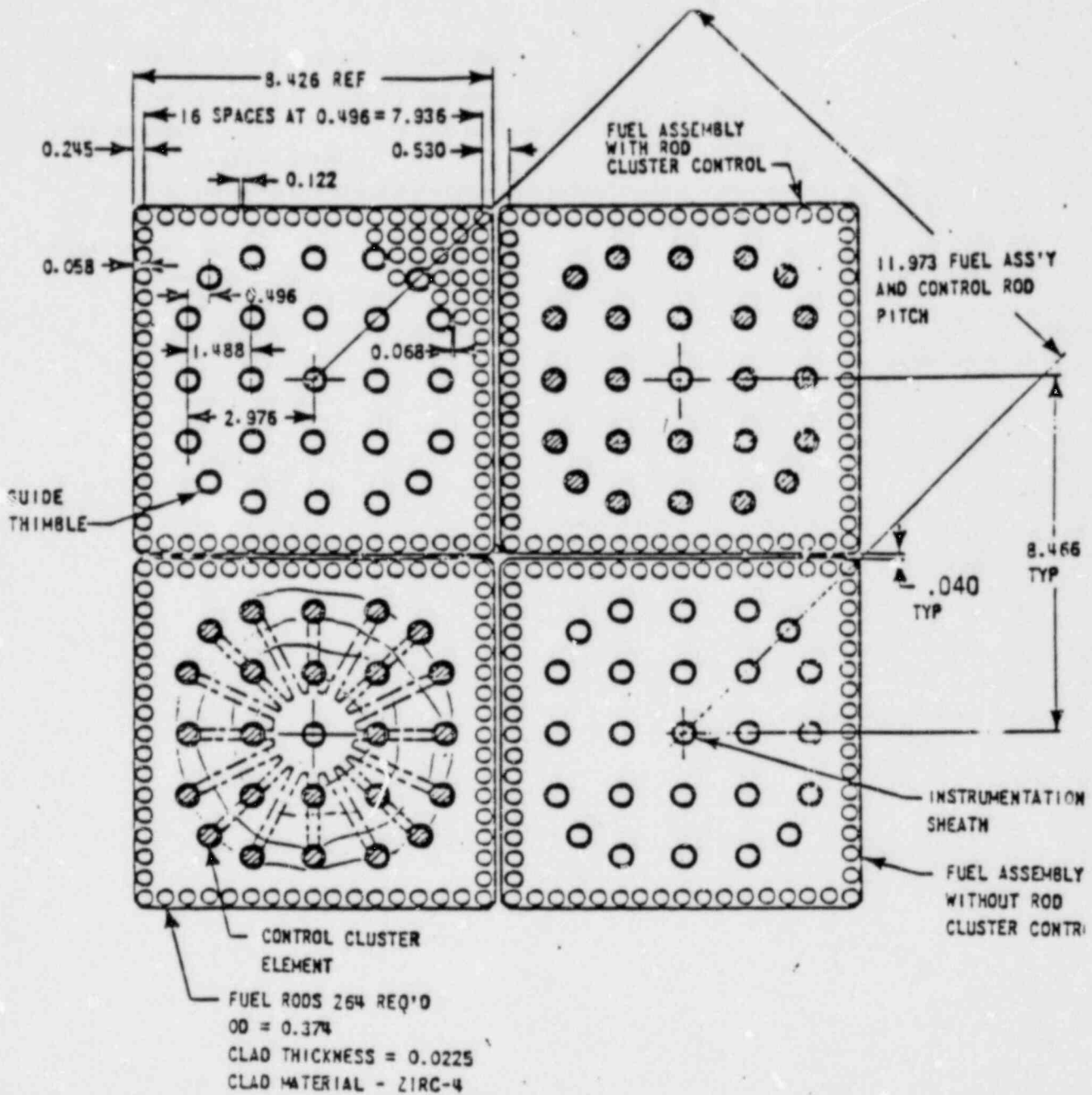
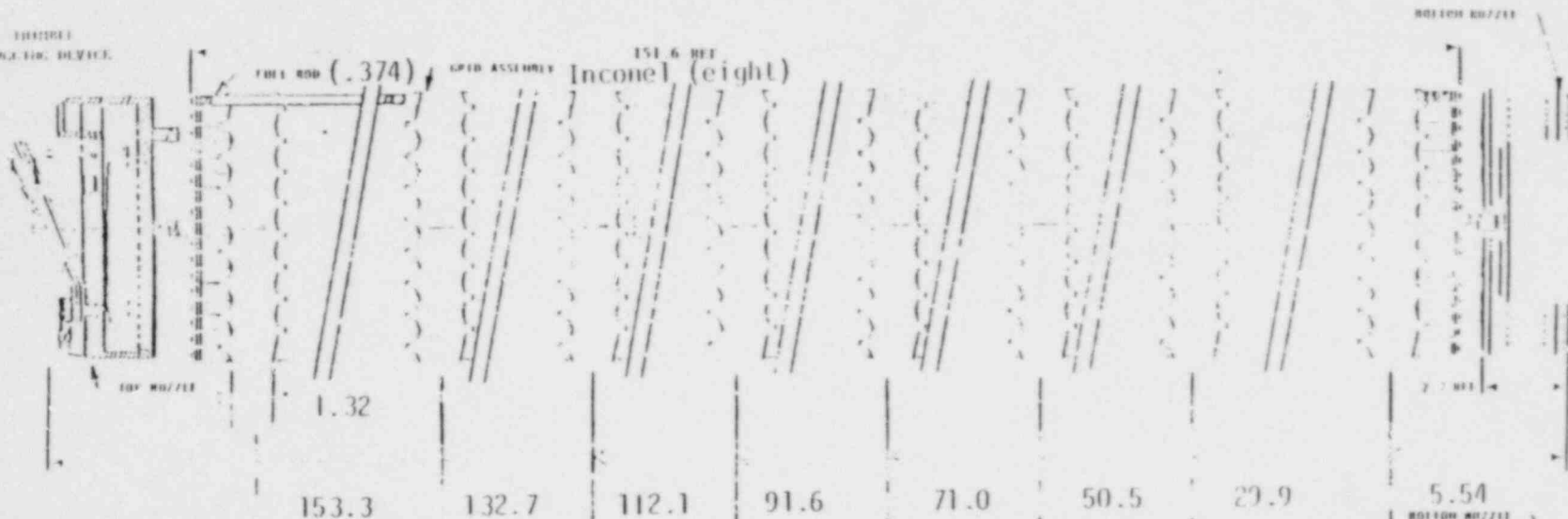


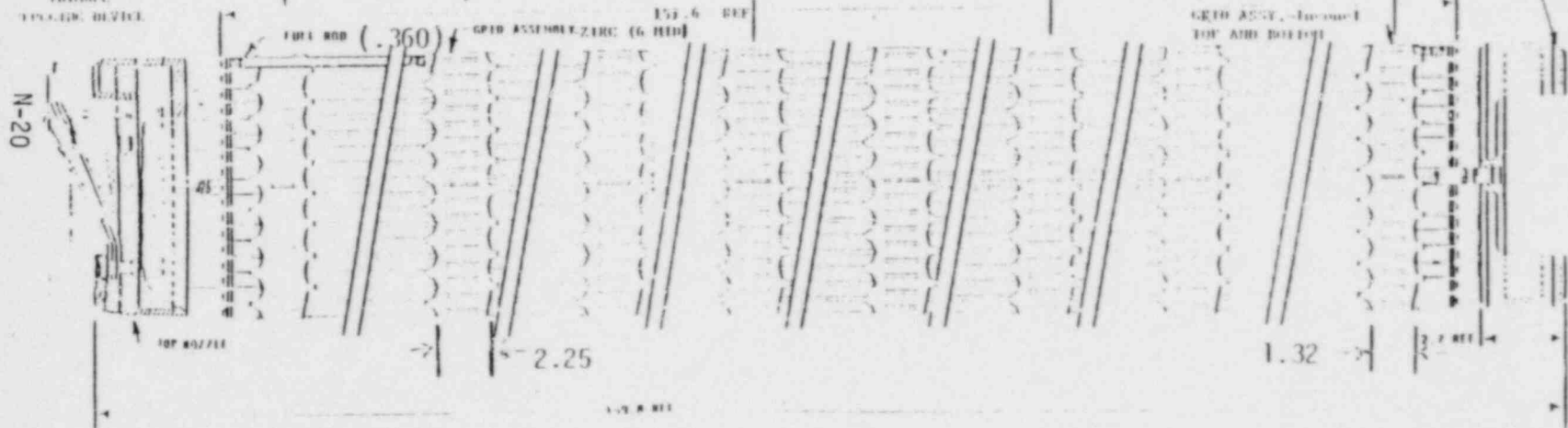
Figure 4.2-1. Fuel Assembly Cross Section 17 x 17

FIGURE 1
FRONT VIEW DEVICE



Standard
Fuel Assembly Outline 17-17

FIGURE 2
FRONT VIEW DEVICE



Optimized
Fuel Assembly Outline 17-17

FUEL ASSEMBLY AP FLOW TEST CONFIGURATION - PHASE II

QUESTION 429.11

Figure 1-7 on page 1-16 shows that at flow rates between 1700 and 2200 GPM the Phase I ΔP Measurement (STM Assem. and OFA) are below those ΔP s predicted. A statistical analysis should be performed to determine if any trends are present during each phase of testing.

RESPONSE

The line shown on this figure is a statistical fit not a predicted value. The expected error for fuel assembly pressure drop is on the order of []+ percent. As can be seen in Figure 1-7, all (b,c) the data fall well within that limit.

+ (b,c)

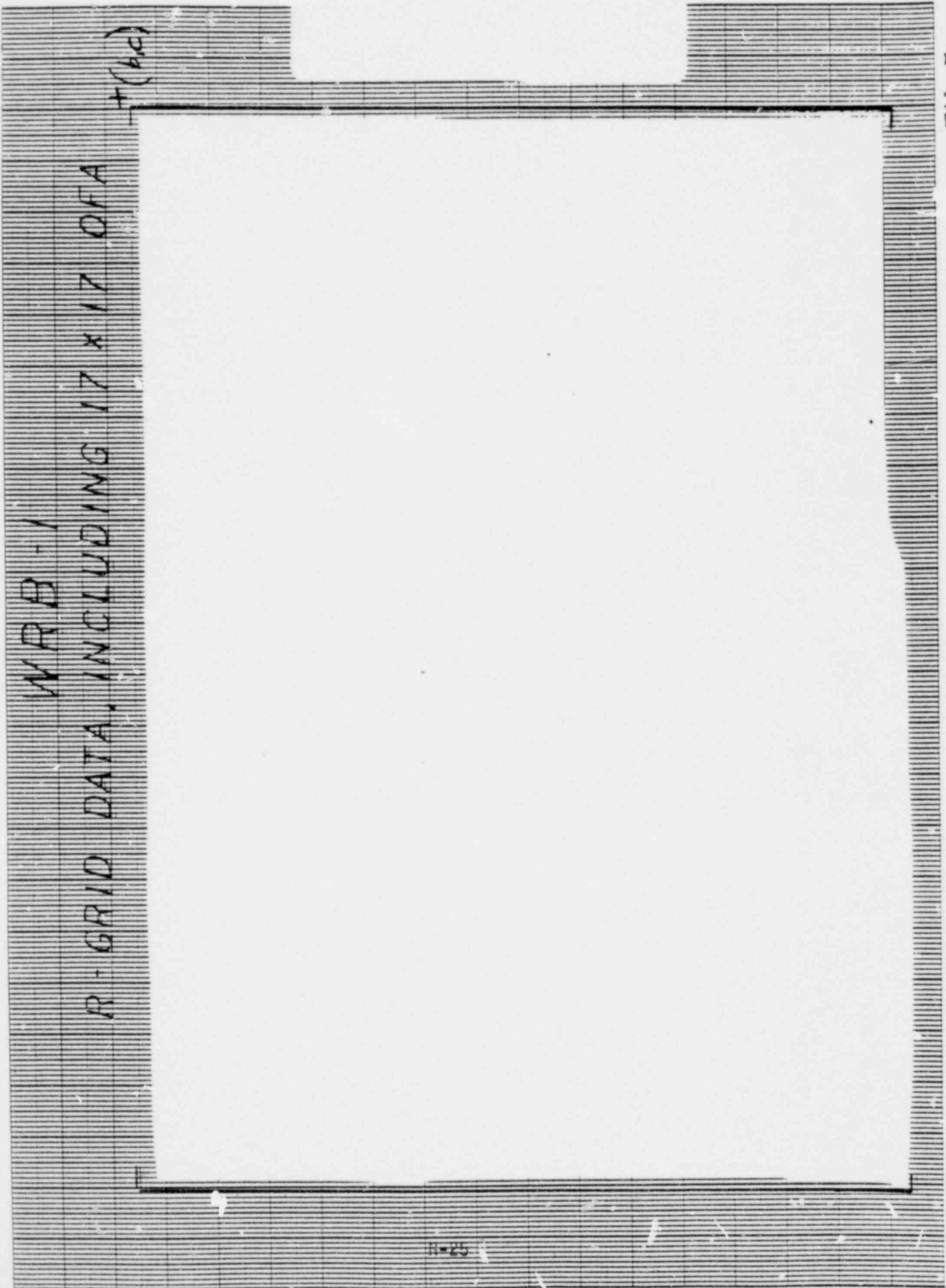


FIGURE 3
 RESOLUBLE ORBITALS
 LIQUIDITY TEST (E1/PP FIBER EEP-B02, TABLES A-1 THROUGH A-15)
 (TYPICAL CELL)

READY-01-015

01/01/01

FIG. 5



WRB-1

R-GRID DATA, INCLUDING 17 X 17 OFA

+ (b)(4)

QUESTION 492.13

What effects did the plugging of thimble cells have on the flow test performed to determine pressure drops?

RESPONSE

The plugging of the thimble tubes resulted in a reduction of fuel assembly flow rate on the order of []⁺ percent. This small (b,c) reduction in a bypass flow to the test assembly had no discernable effect on the pressure drop measurements.

QUESTION 492.14

What are the grid spacings for an OFA next to a standard assembly?
Since the OFA has wider grids, provide justification that the two grid types are compatible.

RESPONSE

The grid spacings for an OFA next to a standard assembly are identical to a standard assembly adjacent to a standard assembly. See Figure included in response to question 492.10.

The height of the grid has a negligible effect on the hydraulic compatibility of the grid, since the major hydraulic mismatch is due to the contraction and expansion losses thru the grid and not the additional frictional loss from the grid height. There are no elevation mismatches as stated previously, and the two grid types are therefore compatible, though there exists a difference in grid pressure loss coefficient. Further compatibility is justified by the negligible difference in over-all assembly pressure drop between the flow tested OFA and standard fuel assemblies.

QUESTION 492.15

How will the effects of crossflow between a OFA and standard assembly be accounted for in a "mixed" core loading?

RESPONSE

The effects of cross flow between an OFA and standard assembly are accounted for in a mixed core loading by inputting to the thermal analysis (THINC) the appropriate grid pressure loss coefficient and flow channel geometry associated with the standard and optimized fuel assemblies.